CIÊNCIA & TECNOLOGIA DOS MATERIAIS

REVISTA DA SOCIEDADE PORTUGUESA DE MATERIAIS | **2026** | **VOL.38** | **Nº1**

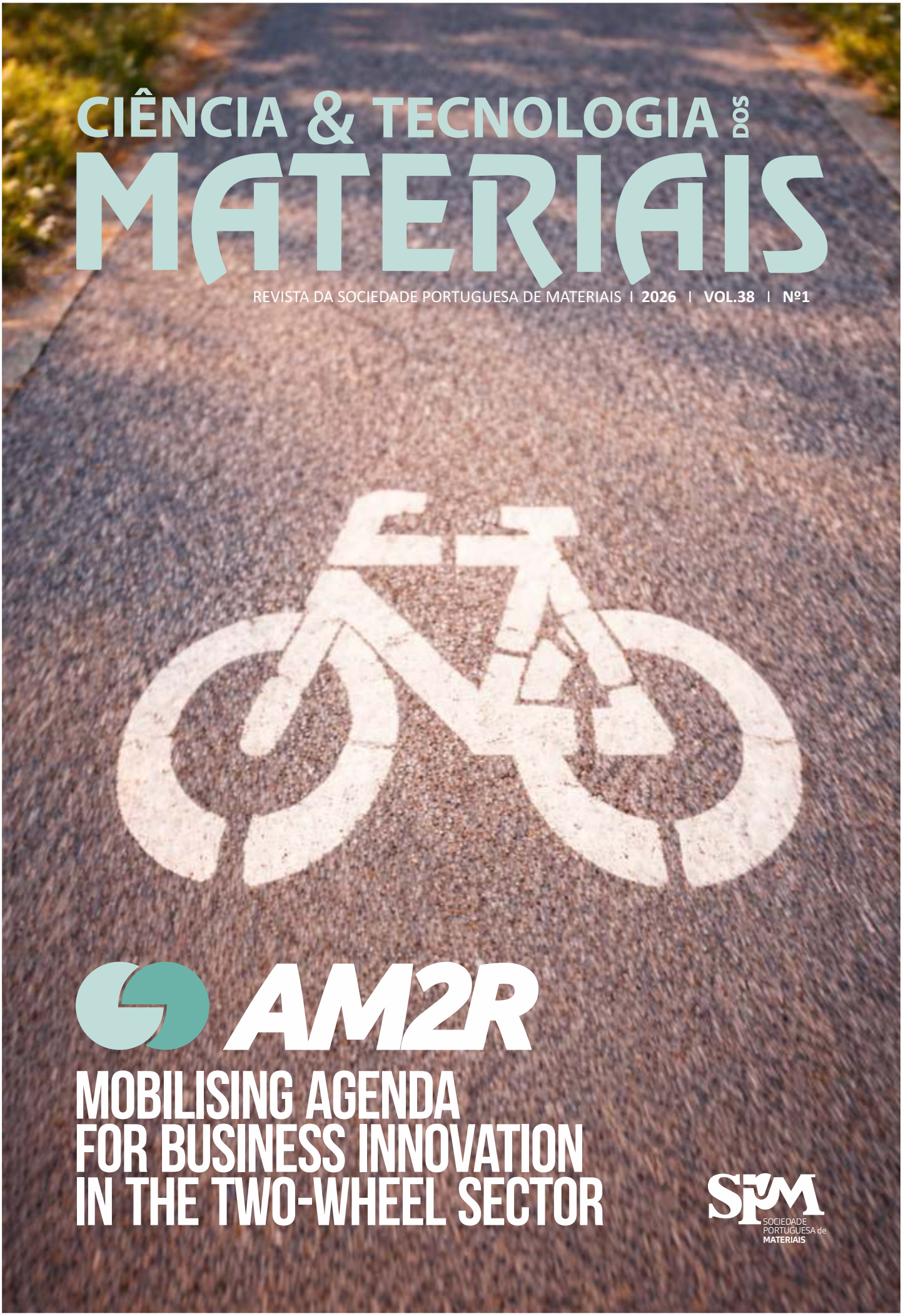

AM2R

MOBILISING AGENDA FOR BUSINESS INNOVATION IN THE TWO-WHEEL SECTOR

SPM SOCIEDADE PORTUGUESA de MATERIAIS

FICHA TÉCNICA

DIRETOR
Jorge Lino

DIRETOR ADJUNTO
Vitor Francisco

CONSELHO EDITORIAL
Manuela Oliveira
Joana Sousa

EDITORES CONVIDADOS
Ana Reis (FEUP/INEGI)
Rui L. Amaral (FEUP/INEGI)
Sara Pereira (ABIMOTA)
(DT de Materiais Estruturais)

PROPRIEDADE E REDAÇÃO
Sociedade Portuguesa de Materiais
Apartado 4538 EC
Carnide 1511-970 Lisboa

PAGINAÇÃO
Lemos design

DEPÓSITO LEGAS
nº 103503/96
ISSN
0870-8312
TIRAGEM
140 exemplares

A SOCIEDADE PORTUGUESA DE MATERIAIS

É MEMBRO DA...

EUROPEAN FEDERATION OF CORROSION (EFC)

IMPORTANTES BENEFÍCIOS DISPONÍVEIS PARA AS SOCIEDADES MEMBROS DA EFC (EUROPEIAS E INTERNACIONAIS) INCLUEM A OPORTUNIDADE DE:

- Nomear membros para os grupos de trabalho do EFC;
- Nomear candidatos para os comitês do EFC (Conselho de Administradores e Comité Consultivo de Ciência e Tecnologia);
- Nomear um representante para a Assembleia Geral anual do EFC (com direitos de voto);
- Nomear candidatos para os prémios da EFC;
- Organizar eventos e cursos com patrocínio e logotipo do EFC; com promoção especial no "Calendário de Eventos"do EFC, publicado no website da EFC e nas newsletters EFC;
- Obter descontos em conferências anuais da EUROCORR se desejar participar como expositor;
- Promoção gratuita dos eventos e atividades relacionados com a Divisão Técnica de Corrosão da SPM nos boletins da EFC;
- Disponibilidade de Afiliação Geral da Organização Mundial da Corrosão (WCO) sem custo adicional sujeito a solicitação formal e aprovação do Conselho de Administradores da WCO e da Assembleia Geral da WCO;
- Além disso, todos os que pertencem a uma Sociedade Membro do EFC usufruem de uma redução na inscrição em conferências anuais da EUROCORR; redução do registro em todos os eventos patrocinados pela EFC, se aplicável (com número de evento atribuído); acesso à área restrita contendo os procedimentos eletrônicos das conferências anteriores da EUROCORR; preços com desconto em todas as publicações da EFC;
- Sociedades membros europeias também são elegíveis para apresentar propostas de organização de conferências EUROCORR.

FEDERATION OF EUROPEAN MATERIALS SOCIETIES (FEMS)

IMPORTANTES BENEFÍCIOS DISPONÍVEIS PARA OS SÓCIOS DA SPM:

- Redução da Inscrição na conferência EUROMAT (15%);
- Uma voz mais forte na Europa como parte de uma organização de grande escala e que aglomera grandes sociedades europeias
- Divulgação dos eventos e atividades das sociedades membro FEMS;
- Capacidade de contribuir para a agenda europeia de materiais;
- Envolvimento direto em eventos organizados pela FEMS;
- Nas conferências da EUROMAT, os membros das sociedades nacionais serão identificados nos seus crachás como membros da sua sociedade - oportunidade para uma rede mais extensa entre os seus membros;
- Nomear membros para prémios FEMS e medalhas;
- A FEMS desenvolveu valiosas ligações à Comissão Europeia e a importantes Plataformas Tecnológicas Europeias, sendo membro da Alliance for Materials (A4M).

A SPM É TAMBÉM MEMBRO DA...

EUROPEAN POLYMER FEDERATION (EPF)

SPECIAL ISSUE AM2R AGENDA

ANA REIS
DEMec, FEUP

SARA PEREIRA
ABIMOTA

RUI L. AMARAL
FEUP/INEGI

The two-wheel sector in Portugal is not merely an industrial niche, it is a strategic pillar of national competitiveness, technological innovation, and sustainable mobility. Over the past decade, Portugal has consolidated its position as the leading bicycle producer in the European Union, a status underpinned by a long-standing industrial tradition, strong export capacity and a business ecosystem that combines engineering excellence, quality, and internationalization.

This European leadership translates into a significant economic impact. The two-wheel sector, encompassing bicycles, electric bicycles, motorcycles, and advanced components and accessories, generates close to one billion euros in annual turnover, employs thousands of skilled workers directly, and supports a broad value chain with a strong export orientation towards major European and international markets. The prominence of Portuguese products in global markets reinforces the country's reputation as a reliable and innovative manufacturing hub for mobility solutions.

It is within this context that the AM2R (Mobilising Agenda for Business Innovation in the Two Wheel Sector) plays a central role in shaping the sector's present and future. Funded by the Recovery and Resilience Plan (RRP) and led by Polisport Plásticos, with ABIMOTA acting as a key coordinating and sectoral hub, AM2R represents a collective and structured response to the challenges facing modern mobility.

The ambition of the AM2R Agenda is clear: to strengthen the international competitiveness of Portuguese companies, increase technological intensity along the value chain and reinforce collaboration between industry and the scientific and technological system. By bringing together 42 partners, including industrial companies, universities and research and technology organisations, AM2R promotes innovation in products, processes, and business models, with the goal of delivering 65 new market-ready solutions with high added value.

A defining feature of the AM2R Agenda is the governance role of its Scientific Committee, which ensures strategic coherence, scientific rigor and alignment with national and European innovation priorities. This committee brings together senior experts from key ENESII, including, BIKiNNOV, CeNTI, CITEVE, INEGI, IPCA, University of Aveiro and University of Coimbra, ensuring a close integration between industrial investment, applied research and public policy objectives. With a total investment exceeding €212 million, of which around €70 million is dedicated to research, development and innovation and approximately €139 million to productive investment, AM2R exemplifies a policy-driven approach that couples scientific excellence with industrial modernisation. This balanced investment model accelerates the industrialisation of knowledge, supports the delivery of the 65 market-ready solutions, strengthens technological autonomy and reinforces the international competitiveness of the Portuguese two-wheel sector, fully aligned with the objectives of the Recovery and Resilience Plan and the broader European agenda for sustainable and resilient mobility.

This transformation is particularly relevant in a global context marked by supply-chain disruptions, growing geopolitical uncertainty and increasing pressure for decarbonisation. Lightweight mobility solutions, electrification, digital manufacturing, advanced materials, and circular-economy principles are no longer optional, they are decisive factors for competitiveness. In this regard, the Portuguese two-wheel sector is

not merely adapting, it is actively shaping the future of sustainable mobility through innovation rooted in engineering and materials science.

The AM2R Agenda also reinforces Portugal international positioning by supporting the presence of national companies in major global trade fairs and innovation forums, fostering export growth and strengthening strategic partnerships worldwide. These initiatives contribute to reducing external dependencies, enhancing technological autonomy, and consolidating the "Made in Portugal" brand as a benchmark in quality, sustainability, and innovation.

For the scientific and industrial community, AM2R is more than a funding programme. It is a catalyst for industrial transition, promoting knowledge transfer, applied research and collaborative innovation. It demonstrates how coordinated action between industry, academia, and public policy can accelerate technological development while generating tangible economic and social value.

This special issue of the SPM Journal is dedicated to display the scope, ambition, and impact of the AM2R Agenda. The technical and scientific contributions gathered here reflect the diversity of research topics, industrial challenges, and technological solutions currently shaping the Portuguese two-wheel sector. Together, they offer a comprehensive picture of a dynamic ecosystem that combines tradition with forward-looking innovation.

We also wish to acknowledge the support of the Recovery and Resilience Plan (RRP), which has enabled the implementation of this Agenda, as well as the rigorous and constructive monitoring carried out by the "Recuperar Portugal" Mission Structure and by IAPMEI (Agency for Competitiveness and Innovation).

AM2R - MOBILISING AGENDA FOR BUSINESS INNOVATION IN THE TWO-WHEEL SECTOR

Soft mobility plays a key role in promoting health and quality of life, while also significantly contributing to environmental preservation and sustainable development on the planet.
In this context, it is becoming increasingly crucial to adopt an integrated and collaborative management of the value chain to create and maximise existing synergies, establishing Portugal as the largest European producer in the Two-Wheel sector.

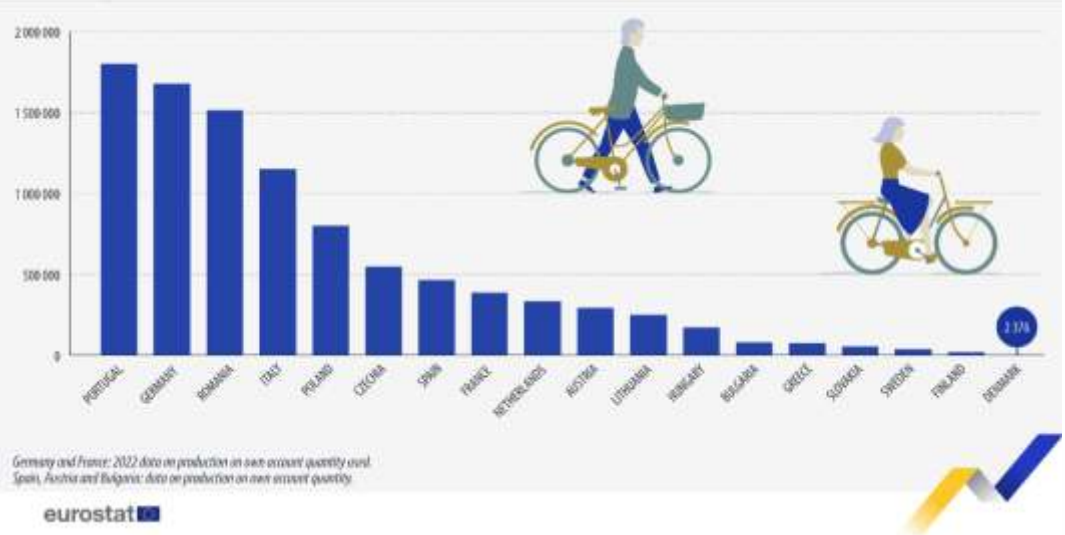

AM2R - Mobilising Agenda for Business Innovation in the Two-Wheel Sector aims to consolidate Portugal as an industrial and technological hub for the development of products and services within this sector. The aim is to create a consolidated image that highlights capabilities and competences of the current ecosystem, particularly those of the organisations that make up the consortium.

The Agenda is led by POLISPORT PLÁSTICOS and seeks to increase and differentiate the national productivity in the Two-Wheel sector, boosting the competitiveness and resilience of companies, based on sustainability and digitalisation.

The Mobilising Agenda intends to operationalise intervention in priority areas along the value chain, enabling the transformation of the national production profile and the development of a new specialisation in the sector. It is hoped that AM2R will boost Portugal's competitive position in the international market, with an emphasis on independence from the Asian market, by fostering and internalizing advanced knowledge around new products, processes, and services.

Started on October 1, 2021, AM2R is set to conclude on June 30, 2026. The project involves 42 organisations, including companies, scientific institutions, and a business association.

The close link between the business fabric and the scientific-technological system has proved to be an asset for the advancement of innovation. Through research, technological development and diversification of the production structure, an environment is created that encourages the development of disruptive and technologically mature solutions. At the same time, productive investment projects enable technology users to produce and implement them.

Therefore, with an investment of approximately 212 million euros, the Agenda aims to introduce significant product and process innovations in the Two-Wheel industry, with a high tradable profile. This will contribute to increasing the sector's exports, improving its scalability, and reducing imports. In short, the Agenda focuses on R&TD to develop new solutions that will be industrialised and economically valued.

The Agenda's five strategic axes are:
· Conception and endogenization of new knowledge and innovation
· Reindustrialisation and economic valorisation of the sector
· Certification and sustainability
· Training and qualification of the sector
· Internationalisation, promotion, and dissemination of the sector.

In addition to introducing 65 products, processes and services to the market, the Agenda provides for the publication of 116 technical-scientific articles and the organisation of 193 technological dissemination and technical-scientific promotion actions. The initiative is also supported by a plan for valuing and promoting results, ensuring a return on investment and a multiplier effect in the years following the Agenda conclusion.

The implementation of the Agenda is organised into Work Packages, reflecting the diversity of the Two-Wheel sector in Portugal. These packages include:
· Electric and conventional bikes
· Cargo Bikes
· Electric motorbikes
· Components, tools, and materials for the production of two-wheeled vehicles
· Frames and Rims/Wheels: Structural components for two-wheelers
· Accessories and support structures for two-wheelers
· Digitalisation, and integrated and sustainable management of the value chain
· Technology and Innovation Centre: BIKiNNOV - Bike Value Innovation Centre
· Training and promotion programmes for the sector and dissemination of the Agenda

The activity plan also covers interdependent strategic development actions for the sector, including:
· International participations to promote the Portuguese Two-Wheel industry and its R&D capacity
· Thematic meetings on Sustainability, Collaborative Logistics, and Innovation
· Visits to consortium organisations, promoting ongoing collaboration and knowledge sharing, with the aim of strengthening complementarity between members and promoting sustainable, long-term growth for the sector.

With this agenda, Portugal is building a stronger and more competitive future in the Two-Wheel sector, based on innovation, collaboration, and sustainability.

TOWARDS SAFE AND HEALTHY SMART CITIES: INNOVATIVE SOLUTION FOR AIR MONITORING IN BIKE LANES

João Pinheiro[1], Luis Caldas[1], Pedro Silva[2], William Soares[2], Nabiha Ben Sedrine[2], Paulo Mendes[2]

1 CeNTI - Centre for Nanotechnology and Advanced Materials, Vila Nova de Famalicão, Portugal
2 Castros S.A., Vila Nova de Gaia, Portugal

Poor air quality has been unequivocally proven to negatively impact the health of bicycle lane users. This article highlights the importance of monitoring air quality, focusing on the concentration of suspended particulate matter (PM2.5, PM10), ozone (O_3), and nitrogen dioxide (NO_2), along with their associated health implications. Additionally, it introduces a newly developed solution that provides users with real-time air quality data, designed for implementation in bicycle lanes. Practical comparisons are made between commercial sensors and the product developed to analyze variability within a defined time frame and explore strategies to address it. Furthermore, in the article is explained how the proposed solution will assist users in real time in interpreting air quality data and suggesting mitigation strategies.

KEYWORDS
SMART CITIES; AIR QUALITY; SENSOR; BIKE LANE.

INTRODUCTION

The European Environment Agency publishes an annual report on air quality and the exposure of European populations to harmful air pollutants. According to the 2024 report, one of the key findings is that 96% of the urban population in the European Union (EU) is exposed to dangerous concentrations of fine particulate matter (PM2.5). While improvements in air quality have been achieved through new regulation and monitoring efforts, long-term exposure to harmful air pollution remains a persistent issue. A comparison of PM2.5 concentrations between 2005 and 2021 (Figure 1) revealed a clear reduction in premature deaths attributed to this pollution. However, modern populations continue to be systematically exposed to harmful air pollution levels. Consequently, monitoring and controlling pollutant concentrations remain critical topics, with European institutions committed to mitigating these risks to ensure healthier and safer air quality [1].

Long-term exposure to poor air quality not only shortens life expectancy but also leads to severe health consequences. Individuals suffering from diseases linked to prolonged exposure to air pollution experience a reduced quality of life and represent a significant burden to the healthcare sector. In 2019, exposure to fine particulate matter (PM2.5) resulted in a total of 175,702 years lived with disability due to chronic obstructive pulmonary disease in 30 European countries. Additionally, NO_2 exposure accounted for 175,070 years with disability related to type 2 diabetes in 31 European countries, while ozone (O_3) exposure led to 12,253 hospital admissions due to respiratory infections [3].

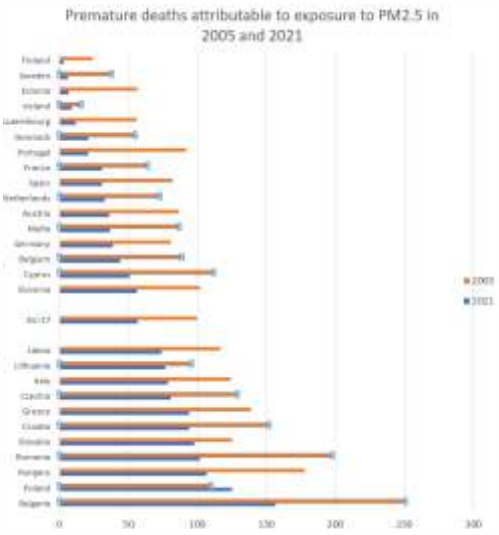

FIGURE 1
Premature deaths attributable to exposure to PM2.5 in 2005 and 2021, EU SDG 11_52, European Environment Agency (EEA) [2].

Children are among the most vulnerable to air pollutants. It is estimated that air pollution causes at least 1,200 premature child deaths annually across Europe. Beyond its direct effects, air pollution can have long-term consequences on children's development. The impact begins before birth, with studies relating air pollution with low weight in newborns and premature birth. Exposure to high levels of pollutants during childhood has been associated with impaired lung function, increased rates of asthma, pulmonary diseases, ear infections, higher allergies, and even restricted brain development, according to the most recent evaluation of air pollution by the Environmental Agency [4].

The harmful effects of air pollution disproportionately affect vulnerable individuals, yet as of the 2024 report, a large portion of the population remains exposed to hazardous levels of air pollution. Another affected group includes those who engage in outdoor physical activities near pollution sources. While some individuals are more susceptible than others, the adverse effects of air pollution have been observed in two different study cases: one analyzing marathon times in a specific race across different seasons and another comparing top performances in international marathons. These results were cross-referenced with local air quality and climate data. For instance, an increase of 10 µg/m³ of PM10 increased the race time by 1.4%, increase in race completion time among marathon runners. The more polluted the air, the more pronounced the effects. On a highly polluted day during the 2014 Beijing Marathon, the average runner took approximately 12 minutes longer to cross the finish line compared to a day with moderate air pollution [5].

Ground-level O_3 may have an even greater impact on athletic performance. Beyond reducing overall performance, high concentrations of O_3 increased the number of non-finishers by up to 50%. While low concentrations of O_3 have a less noticeable effect, it has been estimated that performance dropped 0.39% for every 20 µg/m³ increase in O_3 concentration [5].

The European Union enforces strict air quality standards, with safety thresholds for major pollutants. For PM2.5, the daily limit for healthy air quality is 25 µg/m³, while for PM10, the threshold is 50 µg/m³. Nitrogen dioxide (NO_2) has an annual average limit of 40 µg/m³, and ozone as an average 8-hour limit 120 µg/m³. These guidelines are applied across Europe and are monitored by a network of over 2,000 stations [6].

In Portugal, outdoor air quality stations measuring the pollutants NO_2, O_3 and PM are managed by the Commissions of Coordination and Regional Development (CCDR), with national-level coordination by the Portuguese Environment Agency (APA) [7].

Pollutant	Index level (based on pollutant concentrations in µg/m3)					
	Good	Fair	Moderate	Poor	very poor	Extremely poor
Particles less than 2.5 µm ($PM_{2.5}$)	0-10	10-20	20-25	25-50	50-75	75-800
Particles less than 10 µm (PM_{10})	0-20	20-40	40-50	50-100	100-150	150-1200
Nitrogen dioxide (NO_2)	0-40	40-90	90-120	120-230	230-340	340-1000
Ozone (O_3)	0-50	50-100	100-130	130-240	240-380	380-800
Sulphur dioxide (SO_2)	0-100	100-200	200-350	350-500	500-750	750-1250

FIGURE 2
European air quality index level according to pollutant concentration [7].

MATERIALS AND METHODS

In order to help mitigating health issues associated with urban air quality, it was developed a product (Figure 3) capable of monitoring air quality using commercial sensors that measure the concentration of various air pollutants, such as PM2.5, PM10, O_3 and NO_2. This product provides valuable information to bike lanes users. The main goal of this study was to evaluate the performance of these commercial sensors when integrated into the product, assessing the variability during the day along the bike lane. For

this study, the developed solution, a structure integrating commercial sensors, was implemented on September 8, 2024, that monitored air pollutants over a 10-day period, with data recorded every 10 seconds.

Beyond air quality monitoring, the product will incorporate additional features to enhance user safety, such as motion and presence detection. This functionality will help identify potentially hazardous interactions between cyclists and pedestrians, reducing the risk of accidents. Warnings can be made in real-time through a built-in light on via the mobile application, which will also provide information about potential hazards on bike lanes, such as poor air quality, traffic congestion, or roadwork.

FIGURE 3
Pilot monitoring station set up in the bike lane.

In the future, multiple modules will be distributed along bike lanes, providing detailed and real-time monitoring by zone. The collected data will be shared through a mobile application (Figure 4), enabling users to select the best route based on their destination and current air quality conditions along the bike lanes. The application will also allow users to customize their preferences by prioritizing one of the four air pollutants (PM2.5, PM10, O_3, or NO_2), tailoring recommendations accordingly.

The modules implemented will be strategically placed at 50 meter intervals along bike lanes, offering alternative route options to the user. It is important to note that air pollutant concentrations can vary due to several factors, including natural causes, construction work, and traffic conditions.

RESULTS AND DISCUSSION

Data collected from the pilot monitoring station (Figure 5) indicates notable fluctuations in the pollutant concentrations over short time intervals. Specifically, the levels of particulate

FIGURE 4
Mobile application demonstration.

matter, PM2.5 and PM10, exhibited clear daily periodic variations. These results suggest the presence of consistent patterns in the pollutant concentrations, likely influenced by factors such as traffic volume and weather conditions.

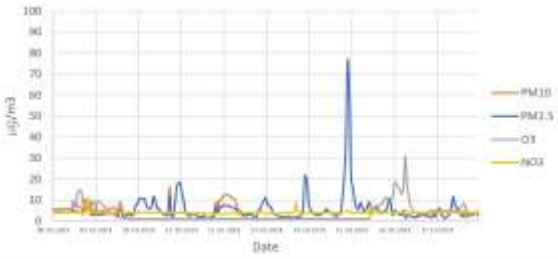

FIGURE 5
Measured pollutant concentrations between October 8 and 18, 2024.

During the monitoring period, a concerning peak in PM2.5 and PM10 was recorded on October 15, 2024 (as shown in Figure 6 and Figure 7, respectively). These short-term spikes reached levels categorized as extremely poor for PM2.5 and very poor for PM10, potentially posing significant health risks. Given the well-documented harmful effects of particulate matter on respiratory and cardiovascular health, these findings emphasize the importance of continuous air quality monitoring and targeted interventions to mitigate exposure.

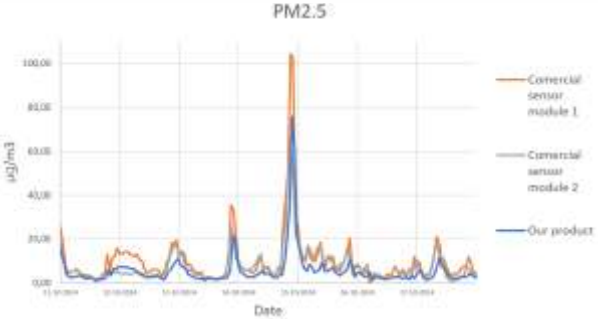

FIGURE 6
PM2.5 concentration measured between October 11 and 18, compared with two additional commercial systems.

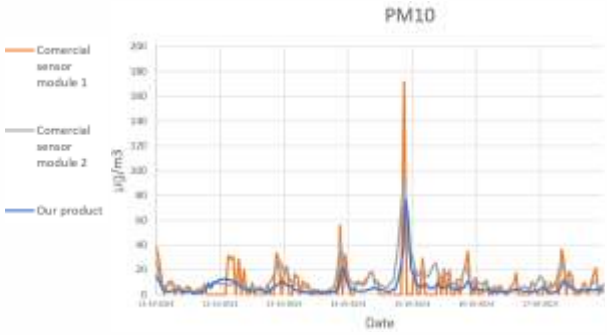

FIGURE 7
PM10 concentration measured between October 11 and 18, compared with two additional commercial systems.

The graphs depicted in Figure 6 and Figure 7 provide a comparative analysis of two commercial sensors and our developed product. The results demonstrate that the sensors included on our product perform similarly to commercial sensors, closely matching their behavior and accuracy. This indicates that our product not only provides reliable air quality data but is also competitive in terms of performance when compared to established commercial used market solutions.

CONCLUSION

Air pollution is a significant concern for public health and overall well-being, particularly in urban areas. The proposed solution aims to integrate air quality control and monitoring within bike lanes and, more broadly, into smart cities infrastructures. This product will contribute to public safety and health in three main ways:

1. Providing real-time air quality information to bike lane users, helping them identify the best times and routes to avoid areas with high pollutant concentrations.
2. Establishing a detailed air quality monitoring network in urban environments, particularly close to bike lanes, allowing monitoring of adverse effects and health issues probability on populations by the responsible authorities.
3. Maintaining a record of periodic tendencies in harmful concentrations pollutant spikes at different scales (daily, weekly, or annual) improving decision-making processes for urban planning and environmental policies.

The first pilot test implementation in real environment is set to begin in mid-2025 with the support of the Vila Nova de Famalicão city council. This initiative will allow us to evaluate the benefits for local populations and refine the system.

ACKNOWLEDGMENTS

The present study was developed in the scope of the Project "AM2R - Agenda Mobilizadora para a Inovação Empresarial do Setor das Duas Rodas" 02/C05-i01.01/2022.PC644866475-00000012 | Project nº 15], financed by RRP - Recovery and Resilience Plan under the Next Generation EU from the European Union.

REFERENCES

[1] E. C. o. t. E. Union, "European Council of the European Union," 30 1 2025. [Online]. Available: https://www.consilium.europa.eu/en/infographics/air-pollution-in-the-eu/#0.
[2] E. E. Agency, "European Environment Agency," 20 9 2024. [Online]. Available: https://www.eea.europa.eu/en/analysis/maps-and-charts/number-of-deaths-per-100?activeTab=265e2bee-7de3-46e8-b6ee-76005f3f434f.
[3] E. E. Agency, "European Environment Agency," 3 12 2024. [Online]. Available: https://www.eea.europa.eu/en/topics/in-depth/air-pollution/eow-it-affects-our-health.
[4] F. Harvey, "Support the Guardian," 24 4 2023. [Online]. Available: https://www.theguardian.com/environment/2023/apr/24/europe-failing-its-children-on-air-pollution-eea-says.
[5] V. Bougault, "The Conversation," 27 6 2024. [Online]. Available: https://theconversation.com/how-air-pollution-can-affect-athletes-227467.
[6] A. P. d. Ambiente, "Agência Portuguesa do Ambiente," [Online]. Available: https://apambiente.pt/ar-e-ruido/indices-de-qualidade-do-ar.
[7] A. P. d. Ambiente, "Agência Portuguesa do Ambiente," [Online]. Available: https://apambiente.pt/ar-e-ruido/redes-de-medicao.

USABILITY EVALUATION OF SMART BICYCLE GRIPS WITH INTEGRATED SAFETY TECHNOLOGIES

Rita Machado[1], Inês Calado[1], Patrícia Gonçalves[1], Marta Midão[1]; Beatriz França[2], Cristina Oliveira[2], Helena Silva[3], Pedro Silva[3]

1. CeNTI - Centre for Nanotechnology and Advanced Materials,
   2785 Fernando Mesquita St., 4760-034 Vila Nova de Famalicão, Portugal
2. CITEVE - Technological Centre for the Textile and Clothing Industries of Portugal,
   2785 Fernando Mesquita St., 4760-034 Vila Nova de Famalicão, Portugal
3. TMG Textiles,
   25 Comendador Manuel Gonçalves St., 4770-588 Vila Nova de Famalicão, Portugal

A bicycle grip with integrated technologies has been conceived to improve cyclist safety. It features a direction indicator activated by an encoder, allowing cyclists to signal their intentions without removing their hands from the handlebar. Additionally, also includes vibrational motors to alert cyclists to nearby obstacles or vehicles. Usability tests were conducted to evaluate materials, sizes, and grip comfort. Results indicated that the grip's functionality and comfort could be improved by adjusting the position of the encoder and enhancing vibrational feedback. Future developments will consider these factors to further improve ergonomics and safety.

KEYWORDS

BICYCLE GRIP; ENCODER; HAPTIC FEEDBACK; USABILITY; SAFETY; ERGONOMICS.

INTRODUCTION

Cyclists are the only road users whose fatalities have not decreased in recent years. The overall number of cyclist fatalities increased from 7% in 2011 to 10% in 2020 [1]. Many crashes between vehicles and cyclists occur when travelling in the same direction, with the vehicles approaching from behind the cyclist [2, 3]. Improving cyclists' perception of approaching vehicles could help to prevent such incidents.

Many cyclists rely on hand signals to communicate directional changes to other drivers, which can compromise their stability by requiring them to take their hands off the handlebars [4, 5]. An alternative solution is the use of flashing light signals to ensure the safety of cyclists and drivers. To address these challenges, different technologies were developed within the scope of PPS54, a component of the Two-Wheel Mobilizing Agenda (AM2R) project and later integrated into the bike's grip.

One key feature incorporated into the grip was the direction indicator, an encoder that the user interacts with to signal the intended change of direction, analogous to a car's direction indicators. This component is typically positioned on the driver's left side, supporting the encoder's location on the left grip. This also allows the right hand to operate essential functions, such as the gear shift. The grip is also equipped with side LEDs, ensuring the turn signals are clearly visible to other road users. As illustrated in Figure 1 (A), the upward and downward rotation indicates a change of direction to the right and left, respectively.

Currently, products with clip-on LED indicators are available on the market, which can be attached to the handlebar ends to signal a change of direction [6, 7]. However, these separate systems can compromise overall aesthetics and ease of use.

An additional feature is the vehicle/obstacle warning system, which includes a detection component integrated into another accessory developed within this project, and the grips that provide vibrational feedback. Vibration motors were strategically placed on the sides of the left and right grips, targeting the hypothenar area of the palm, Figure 1 (B). This area is more sensitive, allowing the motor to better transmit the vibrations, resulting in more immediate recognition by the user [8].

Warning systems for approaching vehicles have already been developed, using displays or smartphone apps to deliver visual, audible, and/or vibrational alerts [9, 10, 11]. However, these rely on the user's perception of signals from external devices, rather than integrated

haptic feedback in the bicycle grips. While vibration feedback incorporated into the grips is a promising concept, it is still largely limited to prototypes and research projects [12, 13, 14].

Enhancing safety through feedback systems may be a key component, however ergonomics also play an essential role in improving user experience. Cyclists often report chronic pain in their hands. With less adipose tissue and muscle mass, the hand has reduced protection and is more vulnerable to injuries. When the grip is not ergonomically designed, the hands deviate from the neutral position. To ensure a good grip, the bicycle grips are designed with a bigger contact area and with an extension, so-called "wings", supporting the natural curvature of the hand and allowing better upper body weight support [8, 15]. The currently available ergonomic grips aim to address the issues previously mentioned, but not all have demonstrated successful outcomes. The ones that have yielded better results served as the foundation for the grips' design. The grips developed are intended for use on city or hybrid bikes, specifically those with relatively straight handlebars that promote a slightly inclined torso, offering comfort and control in urban environments [16]. The grips' dimensions were restricted by the embedded electronics, allowing usability tests to occur at this stage of development.

The present research focusses on evaluating the technologies integrated into the bicycle grips based on usability criteria.

FIGURE 1
The developed grip and its features: (A) encoder and (B) vibrational motor.

MATERIALS AND METHODS

The evaluation of inserting an encoder into the left grip was conducted in two phases. The first stage, with the bike stationary, involved comparing two types of silicone: SmoothSill 960 and MoldStar16 with a shore hardness of A60 and A16, respectively, and two diameters (44 mm and 48 mm) to identify the best-performing option based on user preferences, while rotating the encoder. Next, each volunteer cycled a chosen route, making at least two directional changes while signaling with the encoder previously selected. In the second stage, participants assessed vibrational feedback on two routes: one on an even pavement and the other on an uneven pavement.

The participants selected for the usability tests had previous experience cycling in a road environment or on cycle paths. Data from 20 participants (n= 20; 11 males, 9 females) were collected (mean ± SD; age: 32.0 ± 9.1 years; weight: 70.9 ± 15.9 kg; height: 1.7 ± 0.1 m; left hand length: 180.7 ± 12.4 mm; left palm width: 79.6 ± 7.6 mm; left thumb length: 64.0 ± 5.9 mm).

RESULTS AND DISCUSSION

When asked about the most functional diameter of the silicone surrounding the encoder, 90% of the participants preferred the largest diameter, against 10% who preferred the smallest. Regarding the material, 85% of the participants said SmoothSill 960 (the hardest silicone) would be the most functional, while 10% chose MoldStar16, and 5% expressed indifference. Regarding tactile comfort, although half of the participants said that the softer silicone could be more comfortable, they said that functionality was a more important factor.

After testing the encoder while cycling, each participant was asked a set of questions to assess their experience with it. In the second stage, the participants were also asked to answer a set of questions regarding perceived vibration after cycling with the vibration on and off on different pavements. The results can be found in the Figure 2 and Figure 3, respectively.

Overall, the proposed solution to indicate a change in direction using an encoder was positive. The SmoothSill 960 silicone was preferred for its functionality and the larger diameter, highlighting these as key considerations for future developments. Participants found the solution more intuitive and safer compared to manual signalling. However, several participants suggested that the encoder should be farther along the grip's length, allowing the thumb to reach and rotate it more naturally without bending. This issue, affecting those with larger hands, was expected due to the single grip size. Future developments will address this issue and explore different grip sizes.

The majority of participants agreed that vibration could be a good method for warning approaching vehicles, but the intensity was

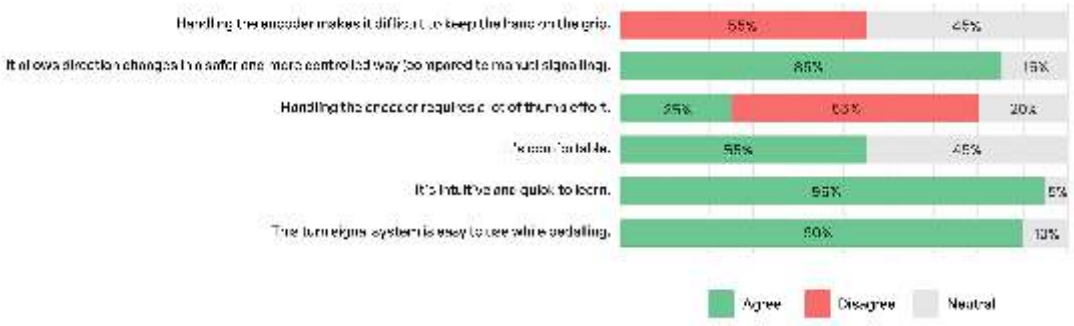

FIGURE 2
Results gathered from the encoder user experience survey, given as a percentage.

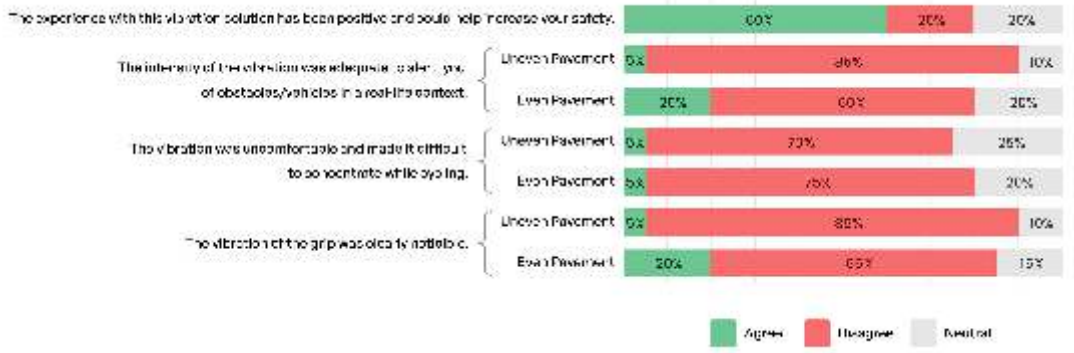

FIGURE 3
Results gathered from the vibration user experience survey, given as a percentage.

considered low on both pavements, so it might not be sufficient in a real-life context. Thus, increasing the vibration's intensity and then studying different modes (intermittent, continuous, duration, etc.) will be the next stage of development to enhance its effectiveness.
One aspect to consider is that although the participants have cycling experience, it is not a regular travelling mode for most of them, which may have influenced their perceptions, and the results observed.

As mentioned, future iterations will consider the development of bicycle grips in various sizes, considering user feedback on dimensions (length, width, and diameter) to ensure both comfort and functionality. Additionally, the wrist's comfort will be evaluated to prevent radial deviation or excessive extension, which could compromise the grip's ergonomics. The shape of the wings will also be studied for adequate palmar support, evenly distributing pressure, and reducing points of discomfort or fatigue. Research on grip materials will continue, considering their physical properties and impact on user comfort.

CONCLUSIONS

The developed grip features a direction indicator activated by an encoder, allowing the user to keep their hands on the handlebar. Simultaneously, a proximity system with haptic feedback alerts the user to nearby obstacles and/or vehicles. Although there is a wide variety of grips available on the market, this model stands out for its innovative technologies focused on enhancing user safety.

The next phase will focus on redesigning the grip based on participants feedback, with a particular emphasis on improving vibration perception and adjusting the encoder's positioning. Additionally, an in-depth analysis of the grip's shape will be conducted, taking into account user comfort with the integrated technologies and incorporating ergonomic insights from the literature.

ACKNOWLEDGEMENTS

This work was funded by the PRR - Recovery and Resilience Plan under the European Union's Next Generation EU programme and was carried out as part of the 'AM2R - Mobilising Agenda for Business Innovation in the Two-Wheel Sector' project [2022-C05i0101-02 | Project no. 15].

REFERENCES

[1] F. Slootmans, "European Commission (2023) Facts and Figures Cyclists. European Road Safety Observatory. Brussels, European Commission, Directorate General for Transport".

[2] P. Díaz Fernández, M. Lindman, I. Isaksson-Hellman, H. Jeppsson e J. Kovaceva, "Description of same-direction car-to-bicycle crash scenarios using real-world data from Sweden, Germany, and a global crash database,"*Accident Analysis & Prevention,* vol. 168, 2022.

[3] M.A.T.P.E.K.M.D.D.R.U.D.R.M.P.L.B.I.Z.A.T.A.Y.G.M. A.W. F. Brown L, "Investigation of accidents involving powered two wheelers and bicycles - A European in-depth study, "*Journal of Safety Research,* vol. 76, pp. 135-145, Feb 2021.

[4] O.A.H.P.A.C.A. &. S.D. Sinelnikov, "Bicycle Safety: Sport Education Style, "*Journal of Physical Education, Recreation & Dance*, vol. 76, no. 2, pp. 24-29, 2005.

[5] L. Alizadehsaravi e J. K. Moore, "Bicycle balance assist system reduces roll and steering motion for young and older bicyclists during real-life safety challenges, "*PeerJ*, vol. 11, 2023.

[6] "ulip Bicycle Turn Signals USB Rechargeable Direction Indicator Adjusta," [Online]. Available: https://ulipstore.com/products/ulip-bicycle-turn-signals-usb-rechargeable-direction-indicator-adjustable-diameter-blinkers-for-bikes-and-electric-scooters?pr_prod_strat=e5_desc&pr_rec_id=2b6787734&pr_rec_pid=8045845643577&pr_ref_pid=8055000531257&pr_seq=u. [Accessed 21 April 2025].

[7] "WingLights 360 Fixed turn signals for bicycles," [Online]. Available: https://cycl.bike/collections/best-sellers/products/winglights-360-fixed. [Accessed on 21 April 2025].

[8] L. Di Brigida, . I. Fiorillo, A. Naddeo and P. Vink, "Discomfort Threshold Evaluation for Hand and Elbow Regions: A Basis for Hand-Held Device Design, "*in Advances in Ergonomics in Design*, p. 649-657, 2021.

[9] "Garmin Varia™ RTL515: Radar de bicicleta com luz traseira," [Online]. Available: https://www.garmin.com/pt-PT/p/698001. [Accessed on 21 April 2025].

[10] "L508 Radar Tail Light," [Online]. Available: https://www.magene.com/en/bike-lights/55-l508-radar-tail-light.html?srsltid=AfmBOooaca03hsuW27kBM1EQNBo1cz7xZtIRIdPF7-ftBdFsWbDa3jNu. [Accessed on 21 April 2025].

[11] "Bryton Gardia R300L," [Online]. Available: https://global.brytonsport.com/pt/products/gardia-r300l. [Accessed on 21 April 2025].

[12] C. Johnsson e A. Muthumani, "HANDLE - High tech communication solutions for safer bicycles," [Online]. Available: https://trid.trb.org/View/2075230. [Accessed on 21 April 2025].

[13] J. Van Brummelen, B. Emran, K. Yesilcimen and H. Najjaran, "Reliable and low-cost cyclist collision warning system for safer commute on urban roads," Budapest, Hungary, 2016.

[14] C. Engbers, R. Dubbeldam, J. H. Buurke, N. Kamphuis, S. De Hair-Buijssen, F. Westerhuis, D. De Waard e J. S. Rietman, "A front- and rear-view assistant for older cyclists: evaluations on technical performance, user experience and behaviour," vol. 5, nº 4, pp. 257-276, 2018.

[15] W. E. Derman and M. Schwellnus, "Common injuries in cycling: Prevention, diagnosis and management," vol. 47, no. 7, pp. 14-19, August 2014.

[16] J. Pucher e R. Buehler, City Cycling, The MIT Press, 2012.

CHARACTERIZATION AND ANALYSIS OF A FORGED BICYCLE COMPONENT

Gonçalo Soares[1*], Rui L. Amaral[1], Sara Miranda[1], José A. Silva[2], Sérgio Silva[2], Ana Reis[1,3]
1 INEGI, Rua Dr. Roberto Frias, 4200-465 Porto, Portugal. E-mail: gsoares@inegi.up.pt
2 Ibérica S.A., Vale do Grou, 3750-064 Águeda, Portugal
3 FEUP, Rua Dr. Roberto Frias, 4200-465 Porto, Portugal

The production of forged components demands a high level of accuracy, from raw material selection to defining manufacturing parameters, especially for parts used in safety systems. This study analysed the forging process of a component for electric two-wheeled vehicles, using the aluminium alloys A356 and 357. Initially, a finite element method simulation was used to analyse the cavity filling considering the defined process parameters, including tool temperature, raw material preheating, required load capacity and preform geometry. This approach not only allowed for the verification of tool cavity filling but also provided a better understanding of the material behaviour during its shaping. Based on the simulation data, experimental trials were carried out to validate the forging process. The experimental tests demonstrated that the A356 alloy showed superior performance compared to the 357 alloy, evidenced by complete die filling and the absence of surface cracks. Concurrently, raw material analysis was conducted before and after heat treatment, including uniaxial tensile testing for mechanical characterisation, hardness measurements and microstructural observation.

KEYWORDS
FORGING; ALUMINIUM ALLOYS; ELECTRIC MOBILITY; NUMERICAL SIMULATION; EXPERIMENTAL VALIDATION.

INTRODUCTION

The development of forged components for safety systems in the electric two-wheeler sector requires a comprehensive approach to material selection and manufacturing parameters. A well-planned strategy is essential to meet the mechanical demands of these systems, ensuring reliability and compliance with safety regulations. Producing components with complex geometries through forging involves multiple stages, where successive preforms are shaped until the final configuration is achieved using different toolsets. This approach is necessary due to the standardised dimensions of initial geometries, such as round bars or plates, which difficult the direct forming.

In multi-stage forging, parameters such as stroke length, friction coefficient and raw material temperature significantly influence process feasibility. Additionally, each stage may require adjustments, increasing production costs [1, 2]. Studies have explored using cast preforms as an initial stage in forging, particularly for aluminium, magnesium, and steel alloys. Casting allows for preforms with near-final geometries, reducing additional forging steps and material waste, leading to cost savings [3-5]. The ideal preform ensures full cavity filling without defects, reducing forging forces, tool wear, and material waste [6]. For example, Chen et al. [7] demonstrated that cast steel preforms could achieve high-quality components with fewer operations, even for complex geometries. Similarly, Dziubinska [8] found that cast AlZn10Si8Mg preforms could reduce material waste by up to 30% compared to traditional forging.

Combining casting and forging processes offers a promising solution to manufacturing challenges. Hot forging and heat treatments refine the grain structure and improve mechanical properties such as fatigue resistance [9, 10]. Additionally, forging pressure eliminates micro-shrinkage and porosities, increasing material density [11].
This study evaluates the feasibility of using aluminium-silicon alloys A356 and 357 for forged components in the electric two-wheeler sector.

MATERIALS AND METHODS

To assess the feasibility of forging cast aluminium preforms, a multi-stage manufacturing strategy was adopted. This approach covered the casting of aluminium alloys to the heat treatment of

TABLE 1
Chemical composition of the aluminium alloys under study (% by mass).

Alloy	Al	Si	Fe	Mn	Mg	Ti	Sr
Ingot A356	92.6	6.82	0.13	0.001	0.26	0.11	0.022
A356	92.9	6.61	0.11	0.002	0.21	0.12	0.37
357	92.5	6.56	0.12	0.004	0.51	0.21	0.040

forged parts, ensuring precision at each stage. Preforms were cast using A356 and 357 alloys. The 357 alloy was produced by adding pure magnesium to A356 ingots. Both alloys suffered silicon modification (using strontium) and grain refinement (using TiB). The chemical compositions were analysed using optical emission spectrometry, with key differences shown in Table 1.

The main difference between A356 and 357 alloys is magnesium content, with 357 containing more than twice that of A356. Magnesium enhances mechanical strength as its percentage increases but reduces ductility.

FORGING PROCESS

The selected component was a lever for the safety system of electric bicycles (Figure 1a), chosen for its dimensions and forging simplicity. The required forging tools are shown in Figure 1b.

FIGURE 1
a) Safety system component of two-wheeler vehicles after forging; b) Tools (top and bottom dies) used in the forging process.

NUMERICAL SIMULATION

Numerical simulation was used to assess the feasibility of the forging process and predict material behaviour during deformation, allowing potential issues to be identified and mitigated before experimental trials. The finite element model was developed based on the component's tooling (Figure 2) and simulated using Abaqus/Explicit with a full 3D model. The tools were modelled as rigid surfaces, while the pin-shaped preform was a deformable body with a tetrahedral mesh (C3D4, 1 mm edges).

The material behaviour was described using the Johnson-Cook constitutive model, to account for strain hardening, strain rate sensitivity and thermal softening effects. The corresponding parameters are present in Table 2 for each alloy. Contact interactions between the tools and the billet were defined using a Coulomb friction model with a coefficient of 0.3, which is typical for hot forging conditions.

Simulation results showed overall acceptable cavity filling, though defects may occur in the central cylindrical region due to insufficient material flow.

RESULTS AND DISCUSSION

Due to the low ductility of the materials at room temperature, preheating was essential before forging. The raw material was heated in a gas furnace at 530 °C for 1 hour, then positioned in the die for forming. The lower die remained fixed, while the upper die moved via a mechanical press. Forging tools were preheated to 190 °C to reduce heat loss and graphite-based lubricant was applied to facilitate processing and part removal. The forged components (Figure 3) initially retained flash, later removed by mechanical trimming. Proper preform placement was crucial for cavity filling, as small misalignments caused uneven fills. The 357 alloy showed lower fluidity, leading to incomplete filling in some areas, particularly in the central cylindrical region.

TABLE 2
Johnson-Cook constitutive hardening model parameters for A356 and 357.

	A [MPa]	B [MPa]	n	C	m	e_0 [s^{-1}]	T_{room} [°C]	$T_{melting}$ [°C]
A356	84	138	0.21	0.0019	1.58	1.36E-3	22.1	610
357	107	155	0.26	0.0024	1.44	1.36E-3	22.1	610

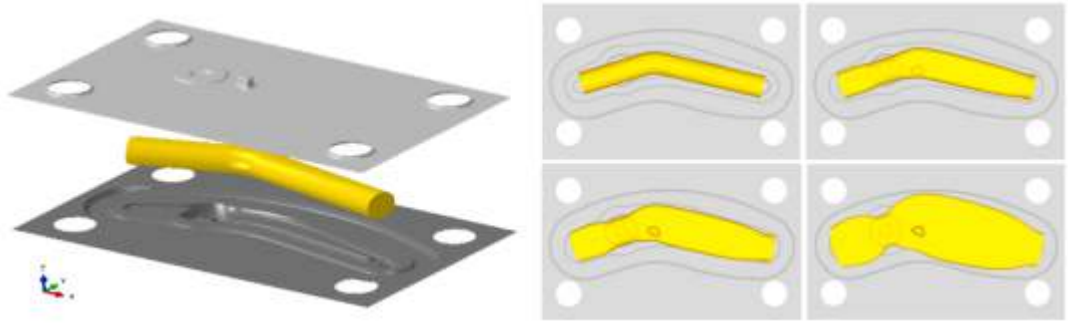

FIGURE 2
Stages of the forging process obtained through numerical simulation for A356.

Experimental observations closely matched the numerical simulations, especially in predicted possible defect zones. To assess heat treatment effects, some forged parts underwent T6 treatment (540 °C solutionising, water quen-ching, and 160 °C ageing).

FIGURE 3
Examples of parts obtained after the forging process: A356 (top); 357 (bottom).

HARDNESS MEASUREMENTS

The assessment of the properties of forged parts is essential to validate the efficiency of the forging process and the applied heat treatment. Hardness measurements help evaluate the resistance of alloys and the performance of parts under operating conditions. These measurements were performed on the raw material, as well as on parts with and without heat treatment for both alloys. Figure 4 contains the obtained results.

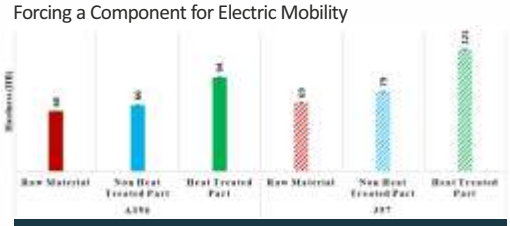

FIGURE 4
Hardness values obtained for alloys A356 and 357 with and without heat treatment.

The hardness values obtained after heat treatment fall within the specified range, however, these values are expected for parts made by gravity casting. The raw material shows the lowest hardness values, as its grain size is slightly larger than that of the forged parts. Due to the higher magnesium content in alloy 357, the hardness is higher compared to alloy A356, both before and after heat treatment. The hardness of A356 after heat treatment may increase if the heat treatment parameters, such as temperature and aging time, are adjusted. The response of this alloy to heat treatment may differ slightly from that of alloy 357, and thus, with the current parameters, alloy A356 may not have reached its peak hardness or may be in an over-aged state, which leads to a decrease in hardness.

MICROSTRUCTURE ANALYSIS

To compare the A356 and 357 alloys in terms of mechanical strength, hardness and microstructure, various tests were conducted to assess the effects of forging and heat treatment.

The Microstructural analysis was performed on raw material and forged components using a Leica optical microscope. The cast preform microstructure showed dendritic aluminium and eutectic silicon, which lacked a lamellar morphology due to strontium modification. However, some needle-like silicon formations remained, indicating incomplete modification. Although, no significant microstructural

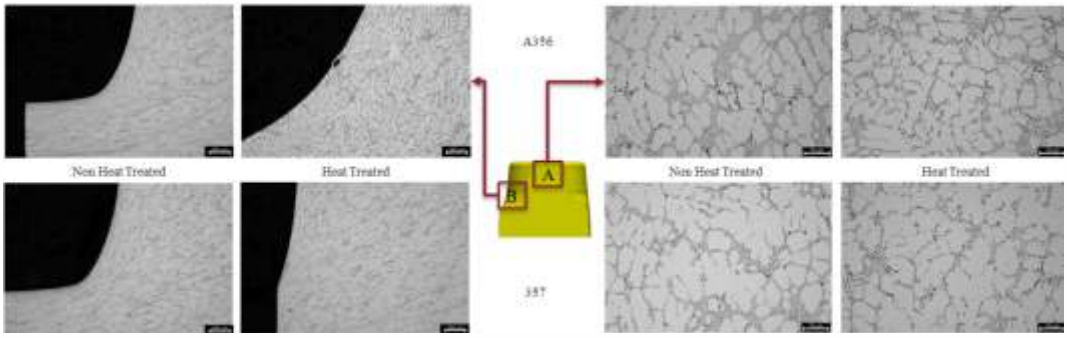

FIGURE 5
Microstructure obtained in different zone of the component for both alloys, with and without heat treatment.

differences were observed between the two alloys, as their chemical compositions were similar, except for magnesium content. The 357 alloy's higher magnesium concentration may have led to more Mg2Si phase formation, though its small size made optical identification difficult. After T6 heat treatment, eutectic silicon globulisation was more pronounced. This rounder morphology resulted from solution treatment, transforming the lamellar/acicular silicon into a globular form. Even in non-heat-treated samples, some silicon globulisation was present, likely initiated by preform preheating before forging.

Additionally, the analysis of different zones (Figure 4) revealed morphological variations across the section, highlighting the impact of forging and heat treatment on microstructural evolution and material properties. In Zone A (top part of the component), plastic deformation during forging was insufficient to alter the microstructure, leaving casting defects intact due to minimal forging effects. In Zone B, material flow effectively filled the cavity, causing grain orientation along the deformation direction, confirming successful cavity filling and proper forging execution.

MECHANICAL CHARACTERISATION

To ensure that the forged components meet mechanical performance requirements, uniaxial tensile tests were conducted for both alloys, following ASTM E8M standards under three different conditions. The test specimens were extracted from the inner section and along the length of the component. The specimens were tested at room temperature with a constant crosshead displacement speed of 2.5 mm/min until material failure. The tests were performed on an INSTRON 5900R universal testing machine equipped with a 5 kN load cell. An extensometer with an initial gauge length of 25 mm was used to measure deformations and elongation in the uniform section of the specimen. To ensure result consistency, a total of 7 tests were conducted for each alloy. The results are presented in Figure 6.

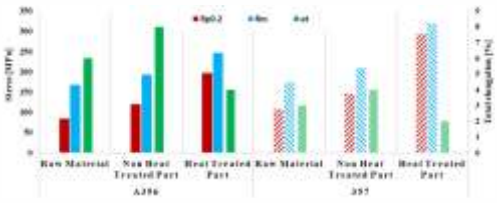

FIGURE 6
Yield stress (Rp0.2), ultimate tensile strength (Rm) and total elongation (et) of the A356 and 357 alloys.

Forging refines grain size and collapses defects present in cast preforms, resulting in higher mechanical properties compared to the raw material. The 357 alloy exhibits higher mechanical strength than A356 in all conditions due to its greater magnesium content, which also reduces its ductility.

The T6 heat treatment yielded expected results, improving mechanical strength in both alloys. Yield and ultimate strength increased by 64% and 28% for A356, while 357 saw greater gains of 102% and 52%. However, T6 treatment reduces ductility by half for both alloys, prioritising increased hardness and mechanical strength.

CONCLUSIONS

This study provided a detailed analysis of the forging process for aluminium alloys A356 and 357, aimed at producing safety components for electric two-wheelers. The combination of numerical simulation and experimental trials enabled a more precise understanding of the alloys behaviour throughout the process, from raw material preparation to the final mechanical property assessment.

Numerical simulation was crucial in predicting potential die cavity filling issues, some of which were later observed experimentally. Under the tested conditions, the A356 alloy demonstrated better cavity filling, resulting in fewer surface defects.

Microstructural analysis showed that forging led to a reorganisation of the grain structure. After heat treatment, eutectic silicon globulisation improved mechanical properties. Hardness measurements revealed that the 357 alloy, due to its higher magnesium content, exhibited greater hardness than A356 in both forged and heat-treated conditions. The T6 heat treatment enhanced mechanical properties, particularly strength and hardness. While the 357 alloy showed a significant increase in yield and ultimate strength, both alloys experienced reduced ductility, typical of this treatment. The higher mechanical strength of the 357 alloy makes it more suitable for components subjected to greater stresses.

ACKNOWLEDGEMENTS

The authors gratefully acknowledge the funding of AM2R - Agenda Mobilizadora para a Inovação Empresarial do Setor das Duas Rodas (02-C05-i01.01-2022.PC644866475-00000012), co-funded by the Plano de Recuperação e Resiliência (PRR), through financial support of the Portuguese Republic and the European Union's NextGenerationEU.

REFERENCES

[1] Kridli, G.T., P.A. Friedman, and J.M. Boileau, Chapter 7 - Manufacturing processes for light alloys, in Materials, Design and Manufacturing for Lightweight Vehicles (Second Edition), P.K. Mallick, Editor. 2021, Woodhead Publishing: p. 267-320.

[2] Kitayama, S., Technical review on design optimization in forging. The International Journal of Advanced Manufacturing Technology, 2024. 132(9): p. 4161-4189.

[3] Usrinus, J., et al. Hot forming of cast steel cylinders. in Conference Proceedings of the 28th International Conference on Metallurgy and Materials, METAL2019, Brno, Czech Rep. 2019.

[4] Böhmichen, U., et al., From casting to forging-The combined simulation for a steel component. Engineering Reports, 2022. 4(7-8): p. e12400.

[5] Kodippili, T., et al., Multi-objective optimization of a cast-preform shape for a magnesium alloy forging application. The International Journal of Advanced Manufacturing Technology, 2023. 129(7): p. 3221-3232.

[6] Biba, N., et al., Closed Die Forging Preform Shape Design Using Isothermal Surfaces Method. Procedia Manufacturing, 2020. 47: p. 268-273.

[7] Chen, H.Q., Q.C. Wang, and H.G. Guo, Research on the casting-forging precision forming process of alternator poles. Journal of Materials Processing Technology, 2002. 129(1): p. 330-332.

[8] Dziubinska, A., The New Technology of Die Forging of Automotive Connecting Rods from EN AB-71100 Aluminium Alloy Cast Preforms. Materials, 2023. 16(7): p. 2856.

[9] Perrier, F., C. Desrayaud, and V. Bouvier. Microstructural and mechanical evolutions during the forging step of the COBAPRESS, a casting/forging process. 2016. Cham: Springer International Publishing.

[10] Azqadan, E., et al., Hardness variation in cast-forging process of AZ80 magnesium alloys and its data-driven prediction. Materials Today Communications, 2023. 36: p. 106833.

[11] Liu, Y., et al., Surface micromorphology and strength formation mechanisms of steering knuckles produced by casting-forging technology. Journal of Materials Research and Technology, 2023. 24: p. 6279-6292.

[12] Mallapur, D.G., et al., Studies on Wear Properties of Forged A356 Alloy with Addition of Grain Refiner and/or Modifier. Procedia Materials Science, 2014. 5: p. 130-136.

[13] Loong, C.A., et al., Semi-Solid Casting and Forging of A357 Aluminum Alloy Components, in Proceedings of the 7th International Conference on Semi-Solid Processing of Alloys and Composites 2002.

BIKiNNOV / bikevalueinnovationcenter association

From Sketch to Prototype

- Market Studies
- Design
- Finite Elements Analysis
- Advanced Material Characterization
- Advanced Chemical Characterization (Reach & RoHS)
- Accelerated Aging Studies
- Coatings Characterization

Development, Performance and User-Experience

- Dynamic Imaging Studies
- Product Sensorization
- Power and Electronic Systems
- Prototyping
- Aerodynamic and Cooling Studies
- Crash Tests
- Vibration Performance

www.bikinnov.pt

More info: https://recuperarportugal.gov.pt/

PRR Plano de Recuperação e Resiliência

REPÚBLICA PORTUGUESA

Financiado pela União Europeia NextGenerationEU

DESIGN OF A BICYCLE FRAME BY LOW-PRESSURE DIE CASTING IN ALUMINIUM ALLOY

Filipe Monteiro[1*], Rui Madureira[1], Gonçalo Soares[1], Rui Amaral[2], António Esteves[2]
1 INEGI, Rua Dr. Roberto Frias 400, 4200-465, Porto, Portugal. E-mail: fmonteiro@inegi.up.pt
2 FAB, Parque Industrial Sobreposta, Lugar da Alagoa, Este (São Pedro e São Mamede), 4715-533 Braga, Portugal

The low-pressure die casting process is a technique that is increasingly being adopted by the industry to produce high-performance components using light alloys (aluminium/magnesium). In the world of mobility, particularly two-wheel mobility, there has been greater demand for the use of lightweight materials, leading to a reduction in the weight of components and, in the case of electric mobility, increasing the autonomy of bicycles and their comfort for the user.

This work developed the design of a bicycle frame for an electric city bike model. During the development of this model, the main objective was to create a design that would bring ample advantages in terms of the final assembly process of the equipment, with the proposed solution substantially reducing the number of welding operations traditionally required by incorporating elements such as the steering and saddle tubes directly into the as-cast part.

The frame was modelled using SolidWorks® software, with the gating targeting the low-pressure die casting process being subsequently designed. The geometry and the casting system were validated using ProCAST® software, where numerical simulations were carried out and proved to be satisfactory, showing that this manufacturing process can be a great ally of the two-wheels industry in the ceaseless search for higher quality and reduced weight components.

KEYWORDS
LOW-PRESSURE DIE CASTING; ALUMINIUM; LIGHTWEIGHT MOBILITY; NUMERICAL SIMULATION.

INTRODUCTION

Urban mobility is undergoing significant transformations, driven by environmental challenges and the search for more sustainable solutions. These dynamics are prompting people to seek out efficient alternatives for their daily journeys, with the adoption of personal vehicles such as electric bicycles being encouraged. The increased environmental awareness is a strong catalyst for the transition to greener ways of transport [1]. This transition is evidenced by the steady growth in the electric bicycle market, as demonstrated by the substantial increase in sales within the European Union, as illustrated in Figure 1.

FIGURE 1
Sales projection of bicycles and electric bicycles in the European Union [2].

Electric bicycles represent a compelling option when contrasted with conventional commuting alternatives, such as public transport or private cars. The escalating proliferation of vehicles on the road, consequent to an increase in population density, has precipitated a rise in journey times. This has led to an increasing number of individuals opting for two-wheeled mobility solutions. Electric bicycles offer their users a high degree of flexibility, reducing commuting times and facilitating issues such as parking, while also offering significantly lower maintenance costs than a car [3,4]. Concerns regarding battery autonomy and overall equipment weight have been identified as primary considerations for

potential e-bike buyers. It is crucial to acknowledge that e-bikes tend to be heavier than conventional bicycles due to the incorporation of components such as the motor and the battery. This increase in weight is not solely attributable to these components, but also to the structural reinforcements necessary to ensure their safe integration. Consequently, there is a necessity to develop electric bicycles that maintain minimal weight while ensuring the structural integrity necessary for the safety and durability of the equipment [3,5]. The low-pressure casting process is a technique that is increasingly being adopted in the industry to produce high-performance components from light alloys such as aluminium and magnesium. This technique offers several advantages over the traditional gravity casting process, most notably the precise control of the filling process, which allows the liquid metal to flow in a laminar regime, thus minimising air entrapment and, consequently, internal defects in the castings. The aforementioned characteristics of the low-pressure casting process have led to its widespread recognition for its ability to produce components with very good quality [6]. The schematic in Figure 2 presents a representation of the primary components that constitute the low-pressure die casting process.

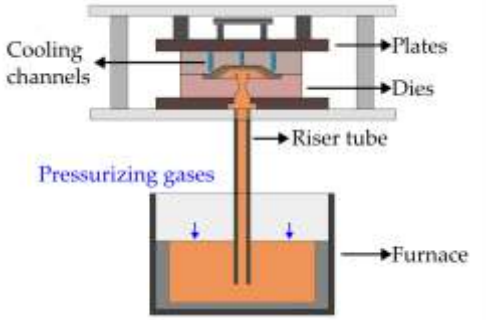

FIGURE 2
Schematic representation of the low-pressure die casting process.

MATERIALS AND METHODS

Initially, a benchmark was made of existing solutions on the market, which culminated in the preliminary concept shown in Figure 3. The following prerequisites for the final equipment were taken into account when drawing up the concept:

- City-type bicycle;
- Step-through frame;
- Central motorisation;
- Removable battery integrated in the frame;
- Front suspension;
- Design compatible with the casting process.

This concept underwent a series of iterations,

FIGURE 3
Preliminary concept of the frame.

culminating in the proposed solution, depicted in Figure 4. The primary objective of the frame's modelling process was to formulate a solution that would not only be compatible with the casting process, but would also enhance the efficiency of the frame's production. To this end, the proposed solution involves the incorporation of the steering and saddle tubes, the motor coupling and the internal battery supports into the casted part, thereby substantially reducing the number of welding operations that would conventionally be required for their production. The casted part's dimensions are approximately 650x565x100 mm, with an average wall thickness of 4.5 mm and a total mass of 4.35 kg.

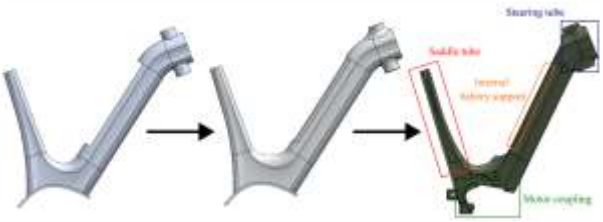

FIGURE 4
Frame design iterations.

Considering the last iteration, the gating system was modelled to accommodate the low-pressure die casting process. The proposed gating system utilises two sprues to fill the part, which is achieved via two blades that directly engage the part, as illustrated in Figure 5, with the objective of ensuring uniform filling of the part. The proposed solution also involves the use of a sand core to create the interior details of the frame.

To assess the feasibility of the geometry and the gating system, numerical simulations of filling and solidification were then carried out using the ProCAST® software.

For these simulations, all the elements of the mould were modelled, as shown in Figure 6.

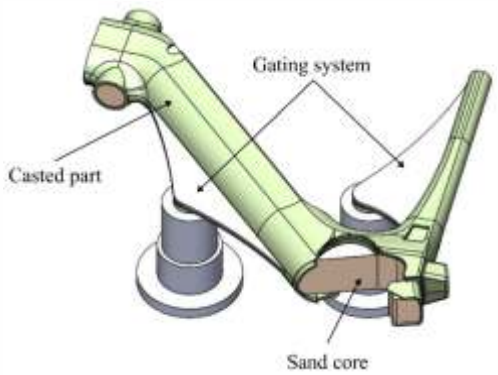

FIGURE 5
Proposed gating system for the low-pressure die casting process.

Twenty thermal cycles (solidification simulation) were conducted to realistically determine the thermal gradient of the mould during steady-state operation, and subsequently a single-cycle simulation of filling and solidification was performed, the latter being the object of analysis in this article.

The material utilised for the frame was an aluminium alloy (AlSi7Mg0.3), and an H13 steel tool was considered.

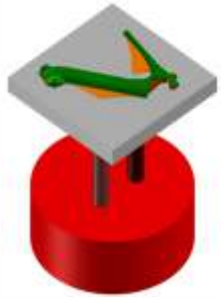

FIGURE 6
Geometry of the numerical simulation model of the frame.

RESULTS AND DISCUSSION

FILLING SIMULATION

The simulation of the filling process revealed that the filling occurred in a laminar regime, with temperatures consistently above the metal's liquidus temperature (613 °C), as illustrated in Figure 7.

FIGURE 7
Filling analysis of the frame; a) beginning of filling b) end of filling,

SOLIDIFICATION SIMULATION

In relation to the solidification simulation, the final sections of the component to solidify have been determined, along with a prediction of the sections most susceptible shrinkage porosities, as illustrated in Figure 8. These sections offer a potential for enhancement through optimising the utilisation of the cooling channels incorporated within the model. There is considerable scope for eliminating the sections exhibiting the highest propensity for shrinkage porosities to a virtually complete extent.

FIGURE 8
Solidification analysis of the frame: a) Last sections to solidify; b) shrinkage pososity prediction.

CONCLUSIONS

The validity of the geometry of the proposed frame was confirmed through the utilisation of numerical simulation tools, thereby substantiating its viability for production. The filling process occurred in a laminar regime, with the temperature consistently maintained above the liquidus temperature of the metal. In instances where shrinkage porosities were identified, it was found to occur in regions that were not critical to the part's functionality. This observation suggests that the shrinkage porosities could potentially be mitigated by optimising the cooling channels present within the mould. The outcomes of this study demonstrate the efficacy of the low-pressure casting process as a viable method for advancements and innovations within the two-wheel industry.

ACKNOWLEDGEMENTS

The authors gratefully acknowledge the funding of AM2R - Agenda Mobilizadora para a inovação empresarial do setor das Duas Rodas (02-C05-i01.01-2022.PC644866475-00000012), cofinanced by Plano de Recuperação e Resiliência (PRR), through the financial support of the Portuguese Republic and NextGenerationEU from European Union.

REFERENCES

[1] Mina, G., et al., How to improve the attractiveness of e-bikes for consumers: Insights from a systematic review. Journal of Cleaner Production, 2024. 442: p. 140957.

[2] European Cyclists' Federation. Get ready for the cycling boom: Experts predict 30 million bicycle sales by 2030. Retrieved November 18th, 2024, from https://ecf.com/news-and-events/news/get-ready-cycling-boom-experts-predict-30-million-bicycle-sales-2030

[3] Frizziero L, Freddi M, Bucchi G, Coltelli L, Leon-Cardenas C. Electric Bike Product Conception and Styling According to Design Trends. Designs. 2022; 6(3):42.
[4] Tozluolu Ç., et al. (2024). "Potential of e-bikes to replace passenger car trips and reduce greenhouse gas emissions." Journal of Cycling and Micromobility Research 2: 100043.
[5] Kapousizis, G., et al. (2024). "User acceptance of smart e-bikes: What are the influential factors? A cross-country comparison of five European countries." Transportation Research Part A: Policy and Practice 185: 104106.
[6] Dong, G., et al. (2023). "Process optimization of A356 aluminum alloy wheel hub fabricated by low-pressure die casting with simulation and experimental coupling methods." Journal of Materials Research and Technology 24: 3118-3132.

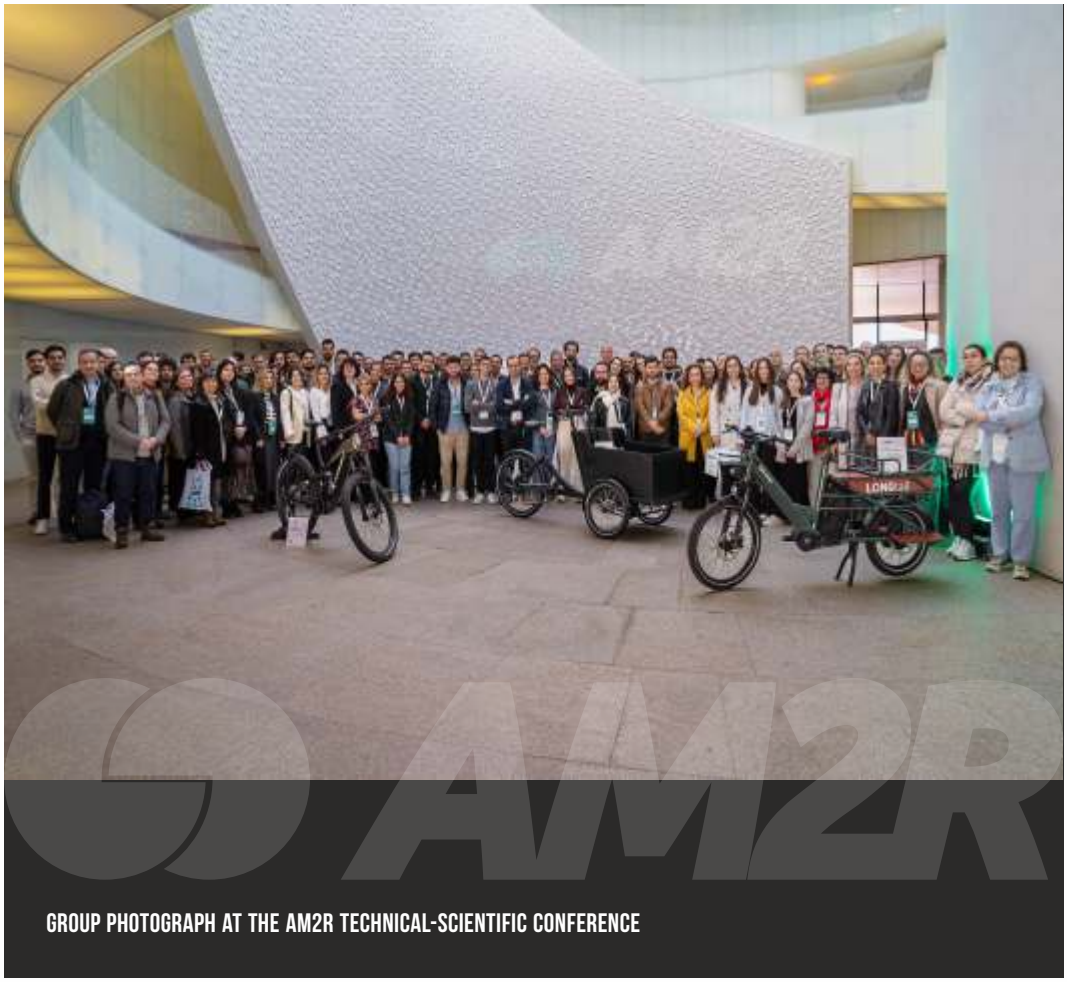

GROUP PHOTOGRAPH AT THE AM2R TECHNICAL-SCIENTIFIC CONFERENCE

STRUCTURAL VALIDATION OF A BICYCLE FRAME BY NUMERICAL SIMULATION

Duarte Cachulo[1*], Gonçalo Soares[1], Rui Amaral[1], António Esteves[2]
1 INEGI, Rua Dr. Roberto Frias 400, 4200-465, Porto, Portugal. E-mail: dcachulo@inegi.up.pt
2 FAB, Parque Industrial Sobreposta, Lugar da Alagoa, Este (São Pedro e São Mamede), 4715-533 Braga, Portugal

Urban electric mobility has become a prominent and rapidly evolving sector within the two-wheel industry. This study focuses on the structural development of an aluminum frame for an electric bicycle, achieved by numerically replicating the tests required by the ISO 4210 and EN 15194 standards. The frame was designed to be aesthetically appealing, modern, and innovative. It was developed using low-pressure and gravity casting processes, which eliminate traditional production steps such as welding and the extrusion/shaping of profiles, thereby streamlining the manufacturing process.

KEYWORDS
NUMERICAL SIMULATION; ALUMINUM; LIGHTWEIGHT MOBILITY; FATIGUE; IMPACT.

INTRODUCTION

Numerical simulation is an indispensable tool in product optimization, particularly in industries where efficiency and innovation are paramount. By replacing traditional trial-and-error manufacturing methods, this tool enables the exploration and refinement of different designs prior to the creation of physical prototypes, significantly reducing development time and avoiding costly, unforeseen adjustments during production.

Unlike conventional methods that rely on physical prototypes and extensive experimental testing cycles, numerical simulation, allows for the recreation of physical phenomena and facilitates detailed analysis. Compared to traditional physical prototyping methods, numerical simulation offers clear advantages, such as the ability to test multiple scenarios, quickly adjust parameters, and optimize geometries, providing a more comprehensive understanding of a product's structural behavior. Moreover, numerical simulation reduces costs by eliminating the need to produce physical prototypes for every iteration. This approach is particularly valuable in industries like transportation. However, it is crucial to strike a balance in the complexity of numerical models to avoid excessively long computational times.

As part of the AM2R - Mobilizing Agenda for Business Innovation in the Two-Wheel Sector, the finite element method was used to perform a structural assessment of an aluminum alloy

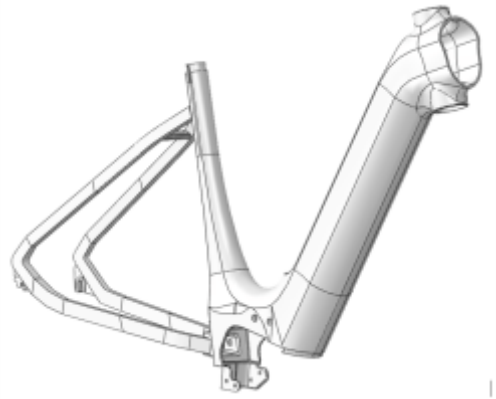

FIGURE 1
CAD representation of bicycle frame (dimensions: 1250 x 630 x 165 mm).

electric bicycle frame. A CAD representation of the analyzed geometry can be seen in Figure 1. The goal was to validate the frame design by numerically replicating the mechanical tests required by ISO 4210 [1] and EN 15194 [2] standards, which require impact and fatigue assessments. Through computer simulations, impact tests predicted the frame's behavior in collision scenarios and under impulsive forces applied over short time intervals. Meanwhile, fatigue tests predicted the frame's lifespan under cyclic loading conditions.

Based on the simulation results, the frame's geometry was optimized by addressing structural weaknesses before producing physical prototypes. This approach not only increases confidence in the mechanical performance of the manufactured frames but also significantly

reduces costs by minimizing the need for adjustments during later stages.

Additionally, by incorporating numerical simulation into their manufacturing processes, companies in the two-wheel sector can produce bicycles that are lighter, more efficient, and safer. This enables more agile development with new materials and designs, accelerating innovation and offering a clear competitive advantage in an increasingly globalized market.

MATERIALS AND METHODS

The development of the frame was conducted in two distinct phases. During the first phase, the design process focused on the initial concept, ensuring compliance with key requirements. These included ergonomic dimensions, seamless integration of accessories and components necessary for assembling a bicycle, and optimal conditions for producing a high-quality cast part in A356 aluminum alloy with uniform thickness (average thickness of 4.5 mm) and rounded edges to avoid stress concentrations.

In the second phase, the frame design underwent structural validation through numerical simulations in Abaqus software. The elements used were 3D tetrahedral elements (C3D4) with a size varying between 5 and 15 mm in the critical region. The material was assumed to have a linear elastic behavior with the following elastic properties, $E = 70$ GPa and $\nu = 0.3$. The finite element method was employed to evaluate the frame of the aluminum alloy electric bicycle. The objective was to structurally validate the frame design by virtually replicating the rigorous mechanical tests required by the ISO 4210 and EN 15194 standards. These standards mandate impact and fatigue testing, which respectively allow for the prediction of the frame's behavior in collision scenarios, where impulsive forces are applied over short time intervals, and the assessment of the frame's durability under cyclic loading conditions.

The phenomena to be captured by the simulation are complex, making it essential to strike a balance between the complexity of the numerical models and the need for reliable information, in order to avoid excessive computational time. To achieve this, the initially outlined models incorporated conservative simplifications, which allowed for preliminary results and the identification of areas requiring more detailed analysis. Subsequently, the model was gradually refined, increasing its complexity as needed to better understand the structure's behavior.

One of the main simplifications applied was to consider the fork of the structure (whose geometric definition is outside the scope of this work) as a rigid body that transmits all forces to the bicycle frame. This conservative simplification avoided the need to model an additional body and its interactions, and enabled the use of a mesh with fewer elements, significantly reducing computational time. Furthermore, if the structure is validated under this conservative condition, it will also be validated for a scenario where the fork partially absorbs the applied forces. Furthermore, the geometric model was simplified for the simulation, accurately representing the load bearing components, but reducing on uninfluential details that would complicate on the elaboration of a finite element mesh.

The intrinsic characteristics of the numerical model were adjusted according to the type of test conducted. To capture the dynamic phenomena associated with the impact test, an explicit dynamic simulation was performed. In contrast, for the fatigue tests, where the inertia of the structure plays a less significant role, an implicit static simulation was chosen. Additionally, boundary conditions, body interactions, and force applications were adapted as necessary for each specific scenario.

RESULTS AND DISCUSSION

The results obtained from these simulations enabled the identification and implementation of geometric adjustments to the bicycle frame. Based on the results obtained, it was possible to optimize the frame geometry by addressing structural weaknesses and validating geometric modifications before the production of physical prototypes.

The results obtained from these simulations allowed for the identification of areas with stress concentrations, which were addressed by applying small geometric adjustments. It is presented in Figure 2 and Figure 3 the von Mises equivalent stress field obtained during the falling mass and falling frame test required by ISO 4210, respectively. The falling mass test consists on dropping a weight on the top of the bicycle fork while holding the frame vertically, and the falling frame consists on dropping the frame with weights attached to designated locations and understanding how the structure reacts. Since these tests are dynamic, the images show the stress field at a selected time step, which is considered representative of the test results.
It is possible to observe that the 'U'-shaped notch is one of the most critical geometric details and, therefore, has been subjected to a

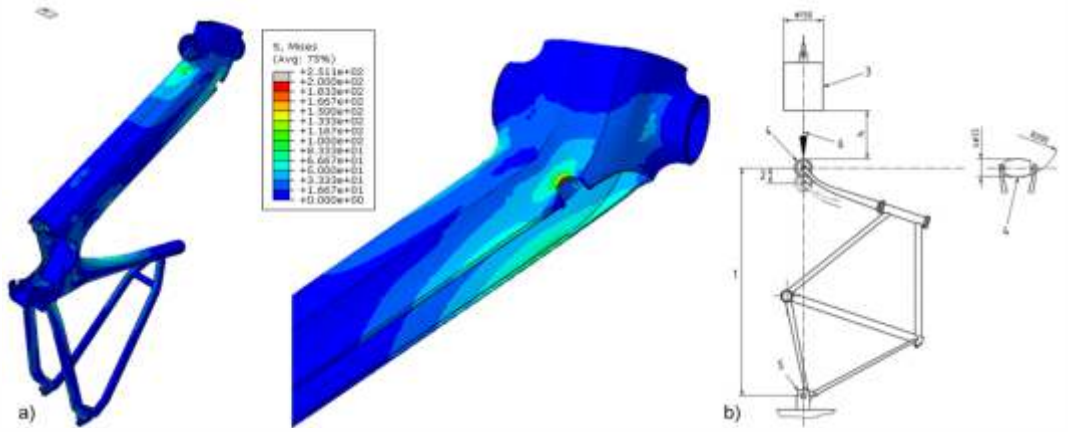

FIGURE 2
Falling mass test. a) Impact test results according to ISO 4210; b) Assembly presented in ISO 4210.

FIGURE 3
Falling frame - Impact test results according to ISO 4210.

geometric alteration to introduce reinforcement. Additionally, these simulations also demonstrate how the transition from the zone coupling with the fork to the zone storing the battery is subjected to high loads and so, it has been modified to become smoother.

The fatigue tests were performed, and the elastic stress fields for each cycle to which the structure was subjected were obtained. The stress values at the critical points, along with the use of S-N curves of the material, allowed for estimations of the number of cycles the structure would endure, which were then compared to the standard requirements. Satisfactory results were obtained.

CONCLUSIONS

Numerical simulation provides the capability to virtually replicate the structural tests required for the certification of a bicycle frame, offering a powerful tool for assessing the performance of a design before physical testing. By using this approach, engineers can simulate various real-world conditions and ensure that the frame meets all necessary safety and performance standards. However, in certain cases, it may be necessary to apply a set of simplifications to the model in order to find an optimal balance between the computational time required for the simulation and the accuracy of the results. These simplifications are carefully chosen to ensure that the key aspects of the frame's behavior are accurately represented without overburdening the computational resources.

The ability to perform these simulations not only accelerates the development of new products but also reduces costs by eliminating the need for producing multiple physical prototypes. This efficiency enables a faster, more cost-effective design process while ensuring that the final product meets the required standards. By relying on numerical simulation, manufacturers can achieve a higher level of precision and confidence in their designs, leading to improved quality and reduced time-to-market for new bicycle frames.

ACKNOWLEDGEMENTS

The authors gratefully acknowledge the funding of AM2R - Agenda Mobilizadora para a inovação empresarial do setor das Duas Rodas (02-C05-i01.01-2022.PC644866475-00000012), cofinanced by Plano de Recuperação e Resiliência (PRR), through the financial support of the Portuguese Republic and NextGenerationEU from European Union.

REFERENCES

[1] International Organization for Standardization (ISO). ISO 4210:2014 - Cycles - Safety requirements for bicycles. Geneva: ISO; 2014.

[2] European Committee for Standardization (CEN). EN 15194:2017 - Electrically power-assisted cycles - EPAC bicycles - Requirements and test methods. Brussels: CEN; 2017.

Polisport GROUP

SINCE 1978

KLICKfix

NEXT-LEVEL DESIGN STARTS HERE.

BRING HRP INTO YOUR PRODUCT – UNLOCK INFINITE POSSIBILITIES.

DESIGN FREEDOM. DESIGN INTEGRATION. BUILT-IN PERFORMANCE.

Eurobike GOLD WINNER AWARD 2025

GERMAN DESIGN AWARD WINNER 2025

HRP®

TECHNOLOGY

HOLLOW REINFORCED PARTS

MADE IN EUROPE.

- RELIABLE, RESILIENT, RESPONSIVE SUPPLY CHAIN.
- SHORT LEAD TIMES. LESS INVENTORY.
- **CUSTOMIZABLE** – MODULAR OPTIONS & COLORS FOR OEM FLEXIBILITY.

PREMIUM FINISHING.

- NO SINK MARKS. NO WELDING. NO PAINTING. JUST READY-TO-ASSEMBLE.
- CLEAN AESTHETICS, INTEGRATED DESIGNS – LIGHTS, RAILS, DROPOUTS - ONE-SHOT TECHNOLOGY.
- SUSTAINABLE BY DESIGN – RECYCLABLE, LEAN PROCESS, NO TOXIC COATINGS.

BUILT LIGHT. PROVEN STRONG.

- LIGHTER, YET STRONGER -STATIC TESTED UP TO 200KG
- CERTIFIED FOR 27KG - ISO11243: 2016 / 2023

OPTIONAL MIK CLICK GO

SCAN TO DISCOVER OUR TURNKEY SOLUTIONS

DON'T JUST FOLLOW INNOVATION. BUILD WITH IT.

OEM@POLISPORT.COM

DEVELOPMENT OF ROAD SAFETY SUPPORT APPLICATION FOR ELECTRIC SCOOTERS

Ronaldo Ferreira[1,3*], José Santos[1,3], António Pereira[1,3], Lucilene Mouzinho[1,4], Margarida C. Coelho[2,3], M.S. Henriques[5]

1 Department of Mechanical Engineering, Centre for Mechanical Technology and Automation Center (TEMA), University of Aveiro, Campus de Santiago, Aveiro 3810-193, Portugal
2 Department of Environment and Planning, Centre for Mechanical Technology and Automation (TEMA), University of Aveiro, Campus Universitário de Santiago, 3810-193 Aveiro, Portugal
3 LASI - Intelligent Systems Associate Laboratory, Campus Azurém, Guimarães 4800-058, Portugal
4 Instituto Federal do Maranhão - Campus Monte Castelo, Avenida Getúlio Vargas nº4, Monte Castelo, São Luís/MA- 65030-005, Brasil
5 Grupo MHS - Estrada Nacional, Travanca do Mondego, Penacova - Coimbra 3360-312, Portugal
* E-mail: ronaldoferreira@ua.pt

The increasing adoption of electric scooters in urban mobility faces safety challenges to efficiently detect obstacles and pedestrians. This study proposes a mobile driving assistance application for electric scooters using computer vision based on Convolutional Neural Networks (CNNs). The model, trained on a large set of images and optimized for mobile devices, showed high accuracy and low latency in hazard detection. This work validates the predictions of ADAS systems for micromobility, contributing to road safety and confidence in the use of electric scooters.

KEYWORDS
E-SCOOTERS; SAFETY; MICROMOBILITY.

INTRODUCTION

The increasing integration of electric scooters in urban mobility, although beneficial for sustainability and congestion reduction [1-5], has introduced pressing road safety challenges [6-9]. Scientific literature and technical reports point to a significant increase in accidents, often attributed to the difficulty of drivers in detecting obstacles such as pavement anomalies [10-15], and pedestrians [16-18] in a timely manner, a situation aggravated by inadequate infrastructure [12].

To mitigate these risks, this work explores the application of computer vision and Convolutional Neural Networks (CNNs) [19], technologies that have demonstrated high efficiency in real-time object detection [10-18]. The ability of these algorithms to operate on devices with limited computing resources, such as smartphones, makes it feasible to implement them as a driver assistance system (ADAS) for scooters [11, 14].

Therefore, we propose the development of a mobile application that uses CNNs to identify hazards and issue alerts in real time, with the aim of increasing the safety of drivers and pedestrians [19, 20] and, consequently, strengthening confidence in micromobility as a sustainable urban transport [19, 20].

METHODOLOGY

The development methodology of the driving assistance application for electric scooters comprised three main steps: (a) data collection and preparation, (b) training the object detection model, and (c) application development and operation.

DATA COLLECTION AND PREPARATION

A dataset of 600 frames was constructed, divided equally into two classes: C_1= {"People" ~ ("Pessoas")} and C_2= {"Potholes" ~ ("Buracos")}. The collection was performed using a smartphone positioned at a height of 1.2 m, simulating the perspective of a scooter driver. For class C_1, frames of people crossing roads were captured at a linear distance of 5.0 m. For class C_1, potholes with diameters between 0.10 and 0.30 m and depths of 0.05 to 0.10 m were filmed at a linear distance of 5.0 m.

Variations in distance and viewing angle were intentionally modified during collection to simulate different obstacle approach scenarios, as illustrated in Figure 1. All illustrations were

made under good lighting conditions. After collection, the frames were carefully annotated for each class, making the dataset available for model training.

FIGURE 1
Schematic Representation of the Data Collection Process and Parameter Variation.

OBJECT DETECTION MODEL TRAINING

The object detection model was trained using the YOLOv8-tiny architecture, selected for its balance between accuracy and computational efficiency, crucial for mobile devices. Training was performed on a laptop with a 6th Gen Intel® Core i7 processor and 16 GB of RAM. The annotated data was split into training, validation, and test sets.

During training, hyperparameters such as learning rates, number of epochs, and batch size were optimized to maximize model performance. The trained model was then exported to a format optimized for inference on mobile devices.

APPLICATION DEVELOPMENT AND OPERATION

The application was developed for the Android 13 operating system (or higher), integrating the trained object detection model. The application architecture consists of a basic operational cycle of four blocks: start/stop, real-time classification, result display, and state control.

The application processes video frames in real time, performs object detection (people and potholes), and displays the results visually to the user. The application's operating logic is detailed in Pseudocode 1 and its flow is visualized in Flowchart 1 (Figure 2).

After presenting the detailed algorithmic logic in Pseudocode 1, the application's operational flow is visualized more intuitively through a flowchart. Flowchart 1 illustrates the sequence of events and interactions between the main modules of the system, from detection initialization and control to processing and displaying the results in real time.

This graphical representation complements the

Pseudocode 1

```
Algorithm: RoadSafetySupportAppForScooters
Var boolean active = false
When classifier.ready:
   Display "ready."
When button.clicked:
   If active is false:
     Start classifier.processvideo
     Active = true
Else:
     Stop Classifier.processvideo
     Active = FALSE
End if
When Classifier.datareceived(results):
   Clear Display
   For each item in results:
     Display item.label + ": " + item.confidence
   End for
End algorithm
```

End pseudocode

FIGURE 2
Flowchart 1: Operation Flow of the Driving Assistance App for Electric Scooters.

pseudocode, providing a clear understanding of the application's functional architecture.

RESULTS

The results obtained allowed the detection of the objects for which the models were trained. The mobile device used was a smartphone of the brand Samsung Galaxy A50's, processor 4x2.3 GHz Cortex-A73 + 4x 1.7 GHz, chipset Samsung Exynos 9611, RAM 4GB, memory 128GB.

The application was able to detect the objects of the class C_1= {"People"} and C_2= {"Potholes"}. For this work, only 6 records of the detections will be presented (due to a space limitation). In Fig. 3, the records of 3 detection images are shown. Of these, 2 are C_1, and the other is C_2.

FIGURE 3
Detected objects - (a) people detected. (b) pothole in the street pavement detected.

These images were captured and are part of the results generated by the application. The other numerical results of the detection are shown in Table 1.

TABLE 1
Accurancy and average detection accuracy.

Classes (C_i)	Accuracy (%)						Mean accuracy
C_1	100	99	100	100	89	99	97.8%
C_2	96	98	99	99	100	100	98.7%

The percentage values of detection obtained for C_1 Were C_1={100,99,100,100,89,99}. For C_2 The percentage values of detection obtained were: C_2={96,98,99,99,100,100}. For C_1, the average per-centage of accuracy was 97.5%, with a 2.5% = p < 5% (p - value). Already for C_2, The average percentage obtained was 98.7%, com 1.3% = p < 5% (p - value).

The values obtained for p associated with C_1 and C_2, respectively were obtained from the subtraction between the values obtained by the model YOLO TINY v8, analyzing the same frames, running on the notebook and the values obtained, recorded by the application running on the smartphone. These percentage values of precision for C_1 and C_2, as well as their respective p - values, show a high accuracy, with no considerable latency observed for the set.

CONCLUSION

The application developed for mobile devices was designed to use computer vision capabilities of low-cost smartphones for real-time detection of obstacles on urban roads, specifically people and potholes, with the aim of increasing the safety of electric scooter drivers. The mobile device used, a Samsung Galaxy A50s with limited processing capabilities, was able to perform the detection task effectively.

The results obtained in object detection for the classes "People" (C_1) and "Potholes" (C_2) were promising. The average detection accuracy for class C_1 was 97.8%, while for class C_2 it was 98.7%. The difference between the percentage detection accuracy values obtained by the YOLO TINY v8 model running on a notebook and the values recorded by the application running on the smartphone was described by a p-value between 1.3% and 2.5% in both cases. These percentage accuracy values, together with their respective p-values, indicate high accuracy, and no specific latency was observed during the obstacle detection task.

Despite the success in validating the concept, this work presents some limitations that may affect the generalization of the results. The number of frames used for training was not extensive, and the quality of the frames employed may have influenced the performance. In addition, simplification measures were adopted to improve computational efficiency and reduce costs, which may have an impact on robustness in more complex scenarios.

A more in-depth analysis of external variables, such as lighting conditions (e.g. day/night, shadow) or different road types (e.g. smooth asphalt, cobblestones, dirt), was not the focus of this study and represents an important limitation. Consequently, the current results may not be directly extrapolated to all usage conditions in varied urban environments.

This work represents an innovative and low-cost solution that differentiates itself from existing approaches by exclusively using the computer vision capabilities inherent to smartphones. It contributes significantly to the lack of driver assistance systems for electric scooters, being a scalable, efficient and viable technology.

As future work, it is expected that the application will be able to detect more complex obstacles and that it will be possible to integrate the measurement of internal signals from the driver to infer their safety, in addition to expanding the tests to include a wider range of environmental conditions and road surface types to assess the generalizability of the model.

ACKNOWLEDGEMENTS

This work was developed within the scope of the Center for Mechanical Technology and Automation (TEMA) through the projects UIDB/00481/-2020 and UIDP/00481/2020. This study was also funded by the PRR - Plano de Recuperação e Resiliência and by the NexGenerationEU funds at University de Aveiro, through the scope of the

Agenda for Business Innovation "AM2R - Agenda Mobilizadora para a inovação empresarial do setor das Duas Rodas" (Project no. 15 with the application C644866475-00000012).

REFERENCES

[1] Dias, M. M. de O., da Silva, R. C. C. F. de M., & de Castro, J. P. de L. F. de C. (2023). The role of e-scooters in the future of urban mobility: A review. Sustainability, 15(13), 10476. https://doi.org/10.3390/su151310476

[2] Nikiforiadis, A., Ayfantopoulou, G. A., & Vlahogianni, E. I. (2024). A systematic review of the performance of shared e-scooter services. Transportation Research Part D: Transport and Environment, 127, 103683. https://doi.org/10.1016/j.trd.2024.103683

[3] Al-Ayyad, M., & Al-Odat, M. (2024). The Environmental and Economic Impacts of E-Scooters: A Case Study in Amman, Jordan. Energies, 17(1), 238. https://doi.org/10.3390/en17010238

[4] Schepers, J. P., Fishman, M., & van Wee, P. G. M. (2023). The safety of electrically assisted bicycles and electric scooters: A systematic literature review. Accident Analysis & Prevention, 192, 107255. https://doi.org/10.1016/j.trd.2024.103683

[5] Leal, G. L. de A. e S., de Castro, J. P. de L. F. de C., & da Silva, R. C. C. F. de M. (2024). E-scooter safety: An analysis of risk factors. Journal of Safety Research, 88, 243-252. https://doi.org/10.1016/j.jsr.2023.12.011

[6] European Transport Safety Council (ETSC). (2022). Safety of E-scooters (PIN Flash Report 41). ETSC. https://etsc.eu/pin-flash-41-safety-of-e-scooters/

[7] Silva, R. M. G. da, da Silva, J. C. M., & de Andrade, L. M. T. (2023). E-scooter safety: A study on the factors influencing the severity of accidents. Transportation Research Procedia, 73, 259-268. https://doi.org/10.1016/j.trpro.2023.12.015

[8] de Silva, D. P. K. T. de S., da Silva, R. C. C. F. de M., & de Castro, J. P. de L. F. de C. (2024). The influence of road infrastructure on e-scooter accidents. IATSS Research, 48(1), 108-116. https://doi.org/10.1016/j.iatssr.2023.08.002

[9] Ahmed, S. S., Bhuiyan, M. A. H., & Hoque, M. M. (2024). Pothole and crack detection using deep learning: a review. Journal of Engineering and Applied Science, 71(1), 43. https://doi.org/10.1186/s44147-024-00367-9

[10] Bade, S. K., Budhkar, S. S., & Shinde, S. S. (2024, April). Real Time Pedestrian Detection and Tracking using YOLOv8 for Advanced Driver Assistance Systems. In 2024 2nd 28. https://doi.org/10.1007/s11042-023-15233-y

[12] Smith, S. J., & Johnson, L. M. (2024). A review of computer vision techniques for ADAS. IEEE Transactions on Intelligent Transportation Systems, 25(1), 1-15. https://doi.org/10.1109/TITS.2023.3312056

[13] Vu, V. T., Nguyen, T. D., & Nguyen, H. T. (2022, October). An Advanced Driver-Assistance System for E-Scooters Based on a Deep Learning Approach. In 2022 14th International Conference on Knowledge and Systems Engineering (KSE) (pp. 1-6). IEEE. https://doi.org/10.1109/KSE56042.2022.9946221

[14] Maeda, Y., & Kawano, T. (2024). Real-time pothole detection using a lightweight network and transfer learning. Sensors, 24(4), 1234. https://doi.org/10.3390/s24041234

[15] Al-Azzawi, M. A. K., & Al-Janabi, A. A. A. (2023, August).Pothole Detection and Road Condition Monitoring System Using Deep Learning. In 2023 International Conference on Communication, Computing, and Big Data (CCBD) (pp. 1-6). IEEE. https://doi.org/10.1109/CCBD58339.2023.10214010

[16] Wang, Y., Li, Z., & Liu, J. (2023). A Real-Time Pedestrian Detection Method for Embedded Systems. Electronics, 12(4), 945. https://doi.org/10.3390/electronics12040945

[17] Raut, S. S., Shingte, P. P., & Sakhare, S. R. (2023, May). Real time Obstacle Detection and Avoidance for Visually Impaired People using YOLO and Deep Learning. In 2023 4th International Conference for Emerging Technology (INCET) (pp. 1-6). IEEE. https://doi.org/10.1109/INCET57972.2023.10170428

[18] Chen, R., & Wang, F. (2024). Lightweight CNNs for Real Time Object Detection on Mobile Devices: A Survey. ACM Computing Surveys, 56(1), 1-36. https://doi.org/10.1145/3624771

[19] Leal, J.A.C. de A. e S., de Castro, J.P. de L.F. de C., & daSilva, R. C. C. F. de M. (2024). Promoting safe and sustainable micromobility: A review of policy and technology. Transport Policy, 148,10-20. https://doi.org/10.1016/j.tranpol.2024.01.008

[20] Jones, P. J., Smith, D. A., & Brown, L. M. (2024). Building Trust in Micromobility: The Role of Safety Technology. Journal of Urban Technology, 31(1), 4562. https://doi.org/10.1080/10630732.2023.2235836

SMART E-BIKE SYSTEMS: INTEGRATING OWN RIDER INFORMATION FOR IMPROVING RIDING EXPERIENCE

Syed Tahir Ali Shah [1,3,*], José Maria Fernandes [2,3], José Paulo Santos [1,3], Gabriel Constantinescu [1,3], António Bastos Pereira [1,3], Ana Horovistiz [1,3], Margarida Isabel Coelho [3,5], Mário Sousa Henriques [4]

1 TEMA - Centre for Mechanical Technology and Automation, Department of Mechanical Engineering,
2 Department of Electronics, Telecommunications and Informatics (DETI) / IEETA,
University of Aveiro, Campus Universitário de Santiago, 3810-193 Aveiro, Portugal.
3 LASI - Intelligent Systems Associate Laboratory, Guimarães, Portugal
4 MHSi, Lda Factory Hub - Estrada Nacional 228, n.19, Covais, Coimbra, 3360-312, Portugal
5 Department of Environment and Planning, Centre for Mechanical Technology and Automation (TEMA),
University of Aveiro, Campus Universitário de Santiago, 3810-193 Aveiro, Portugal.
* E-mail: syedtahiralishah@ua.pt

This paper presents a smart E-bike system that fuses real-time physiological, environmental, and bike-status data to enhance rider safety. A Random Forest model classifies current fatigue with 80.5 % accuracy (recall 0.88), while an LSTM predicts imminent fatigue at 84.1 % accuracy (recall 0.90). Benchmarking demonstrates up to a 19.4 percentage points (pp) accuracy gain over prior methods. The system issues context-aware alerts based on these predictions.

INTRODUCTION

The Internet of Things (IoT) has revolutionized various sectors, including transportation, enabling smarter and more efficient mobility solutions [1,2]. Electric bicycles (E-bikes) have gained popularity as eco-friendly transportation, enhanced by IoT features like real-time tracking and adaptive control systems [3]. However, current E-bike systems mainly focus on environmental data, neglecting critical psychophysiological metrics such as fatigue and stress, which are essential for safety and user experience [4]. Existing IoT-enabled E-bike systems lack real-time physiological monitoring, limiting their ability to adapt to rider states. This gap increases risks related to fatigue and stress and restricts personalized safety interventions and comfort enhancements. This study introduces an IoT-integrated E-bike system incorporating sensors for heart rate to monitor rider states.

The Machine Learning (ML) models used in this study, Random Forest (RF) and Long Short-Term Memory (LSTM) networks, classify current states and predict future ones, enabling dynamic recommendations for enhanced safety and comfort.

The key objectives include:

- Sensor Integration: Develop a pipeline combining environmental and physiological data.
- ML Models: Implement models for state classification and prediction.
- Real-Time Recommendations: Create a recommendation engine for personalized alerts.
- Field Testing: Validate the system through real-world testing.

This scalable system contributes to sustainable and safe urban mobility. The system offers personalized recommendations, such as rest alerts for fatigued riders or safe route suggestions for stressed users, ensuring a proactive and user-centric riding experience.

METHODOLOGY

This section outlines the methodology employed to integrate a physiological layer into IoT networks, specifically within the context of an E-bike eco-commuting system. The approach leverages quantified self-concepts to create personalized and adaptive responses based on user-specific data and environmental factors.

The proposed system includes environmental sensors, physiological sensors, and E-bike status sensors (Figure 1). Environmental sensors monitor the rider's surroundings, such as tem-

perature, humidity, and light intensity, to ensure comfort and safety. Physiological sensors track the rider's physical state, such as heart rate. E-bike status sensors monitor the bike's operational parameters, such as speed, GPS, and battery status, to ensure optimal performance and safety. These components work together to provide real-time recommendations to the user.

FIGURE 1
Sensor choice and placement.

SENSOR VARIABLES AND UNITS

Physiological data (heart rate) were collected via a wearable smartwatch equipped with a photoplethysmography sensor, which streamed measurements in real time to the E-bike's onboard processor.

TABLE 1
List every signal recorded, the sensor type, unit.

Variable	SensorType	Unit
Heart rate	Photoplethysmography	beats min^{-1}
Temperature	Thermistor	°C
Humidity	Capacitive hygrometer	% RH
Light intensity	Ambient light sensor	lux
Speed	Wheel encoder	km h^{-1}
GPS coordinates	GNSS receiver	(lat, lon)
Battery status	Voltage monitor	V

The training data for the models is gathered from controlled E-bike commutes, involving participants who provide physiological and environmental data under different conditions, including heart rate, temperature, humidity, light intensity, speed, location, battery status, and user state labels.

The system architecture (Figure 2) aims to facilitate data flow from sensor collection to real-time user recommendations. It comprises modules like sensor placement, data collection module, and data transmission module. The data collection module synchronizes sensor inputs and handles discrepancies, while the data transmission module uses the ESP32 microcontroller for wireless data transmission using Bluetooth protocols.

The data processing and analysis module is a tool that performs preprocessing steps like data

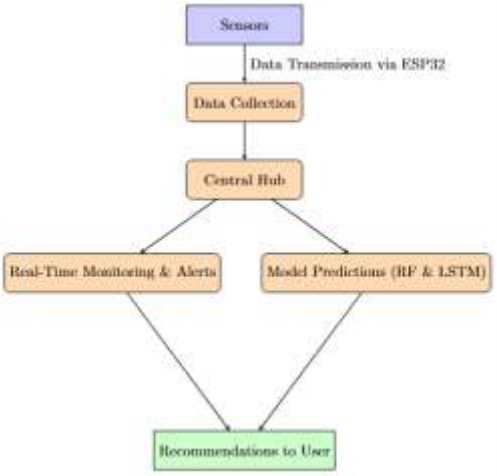

FIGURE 2
System architecture flowchart.

cleaning, normalization, and feature extraction using three ML algorithms: RF, LSTM, and Linear Regression (LR). RF analyzes sensor data to classify rider's current state, LSTM predicts future states, and LR computes an overall score by weighing sensor inputs, to refine classification and prediction outcomes.

RECOMMENDATION ENGINE

The recommendation engine creates personalized recommendations for users to optimize rider safety and system efficiency by addressing detected states like fatigue. Data processing is crucial for the system's accuracy and reliability (Figure 3). Key steps include normalization techniques, feature extraction, and ML models. Normalization rescales data to a mean of 0 and a standard deviation of 1, while feature extraction calculates statistical measures like mean, standard deviation, and variance from time-series data.

The system uses two ML models: RF, for real-time rider state classification, and LSTM, for predicting future states based on historical data. RF is robust to noise and overfitting, providing insights into influential features and offering versatility for classification and regression tasks. LSTM excels at temporal pattern recognition, memory retention, and sequential data hand ling, making it ideal for processing time-series data from physiological sensors. To ensure the models' effectiveness, a meticulous training and validation process is required. The dataset is divided into training (70%), validation (20%), and test (10%) sets, with model selection based on performance metrics and hyperparameter tuning. K-fold cross-validation is implemented to ensure model generalizability across different data subsets, and time windows are considered to account for temporal dependencies in the data.

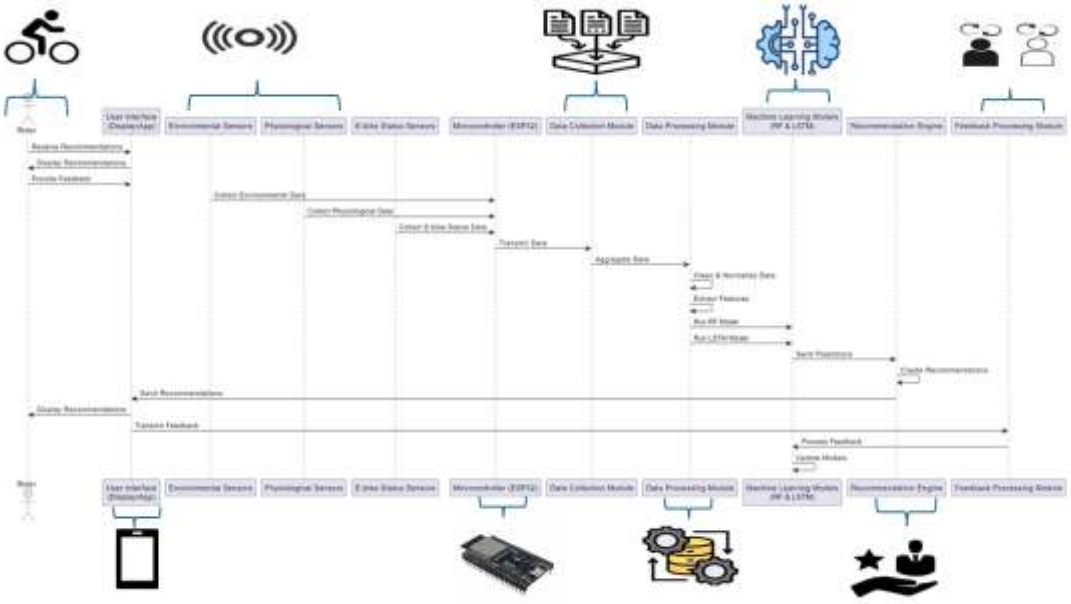

FIGURE 3
Unified Modeling Language (UML) sequence diagram for sensor data collection and ML processing.

The system uses a decision-making layer to integrate and analyze data from various sources, enabling informed and adaptive recommendations. Data fusion combines environmental, physiological, and E-bike sensor data into a unified dataset, while ML integration uses RF and LSTM models to identify patterns and make predictive assessments.

MODEL INTEGRATION AND ROLE CLARITY

In our proposed method, we have three models that work to make actionable recommendations: the LSTM model is for future state prediction, the RF model is for current state classification, and the LR model calculates an overall continuous score S from sensor inputs. At the same time, the RF and LSTM models yield categorical outputs.

The LR model provides a quantitative measure that reflects the overall physiological state of the rider by incorporating variables such as heart rate, environmental temperature, and humidity. The thresholds T_1 (140 bpm) and T_2 (160 bpm) were empirically determined based on an analysis of physiological data collected from a pilot study involving ten riders. Specifically, these thresholds correspond to the 75th and 90th percentiles of measured physiological exertion levels, representing meaningful transition points from normal physiological states to moderate and high-stress or fatigue conditions. These percentiles were selected to reflect clinically accepted ranges that differentiate comfortable riding conditions (Normal) from moderate physiological stress indicating onset of fatigue (Fatigued), and critical stress conditions that demand immediate intervention (Stressed). This percentile-based approach ensures thresholds are data-driven, representative, and applicable across typical rider profiles.

To ensure clarity in the decision-making process, the overall score S is subjected to threshold-based classification:

Normal: *if* $S \leq T_1$
Fatigued: *if* $T_1 < S \leq T_2$
Stressed: *if* $S > T_2$

The integration process is as follows:
RF Output: Provides an immediate, categorical assessment of the rider's current state.
LSTM Output: Predicts the near-future state by estimating how soon fatigue may set in.
Overall Score (S): Acts as a complementary measure that refines these predictions by quantifying the degree of deviation from the rider's normal state.

In scenarios where the RF and LSTM outputs may conflict when the overall score falls near threshold boundaries, the system employs a weighted fusion of these outputs to determine the final recommendation.

Suppose the RF model indicates a "Normal" state, yet the overall score is marginally above T1. In that case, the system may adopt a more cautious recommendation than one based solely on the RF output.

This integrated approach ensures that the decision-making process is robust and accounts for immediate observations and anticipated changes in the rider's condition, enhancing overall safety and system performance.

RECOMMENDATION GENERATION

Based on the model predictions, the system generates tailored recommendations aimed at enhancing the rider's safety and comfort. These recommendations are dynamically adjusted based on real-time data to ensure optimal system performance and rider safety.

DECISION RULE FORMULA

Let:

- RF be the prediction from the Random Forest model.
- LSTM be the prediction from the Long Short-Term Memory model.

The possible outputs from the RF model are:
RF = *"Normal"*
RF = *"Fatigued"*
RF = *"Stressed"*

The possible outputs from the LSTM model are:
LSTM = *"Normal"*
LSTM = *"Fatigue in 20 minutes"*
LSTM = *"Fatigue in 10 minutes"*

The recommendations based on these outputs can be defined as follows:
Recommendation = *f(RF, LSTM)*

Based on these combined outputs, the system applies decision rules to generate recommendations, as shown in Table 2 below.

The system calculates the overall score S by assigning weights to various sensor readings, using the LR model trained on labeled data. The weights are determined by calculating the relationship between sensor inputs and the user's physiological state. The overall score S is calculated as:
$S = w_{HR} \cdot HR + w_{Temp} \cdot Temp + w_{Humid} \cdot Humid$, where
w_{HR} is the weight for the heart rate, *HR.*
w_{Temp} is the weight for the environmental temperature, *Temp.*
w_{Humid} is the weight for the humidity, *Humid.*
To accurately determine the weights w_{HR}, w_{Temp}, w_{Humid}, a LR model was employed, in which a linear relationship between the sensor readings (independent variables) and the user's state (dependent variable) was established.

MODEL FORMULATION

The LR model for S is defined as:
$S = b_0 + b_1 HR + b_2 Temp + b_3 Humid + e$, where: $b0$ = intercept term, b1, b2, b3 = coefficients representing the weights for each sensor, and e = error term capturing variance not explained by the model.

The study collected sensor readings and user state labels from participants during E-bike commutes under different conditions. Data preparation involved data cleaning, normalization, and feature selection. The LR model was trained using the prepared dataset, which was divided into training, validation, and testing subsets. The model was fitted by minimizing the Mean Squared Error (MSE) between predicted scores and actual user states. Hyperparameter tuning was employed to ensure model robustness, as LR has minimal hyperparameters. The training process aimed to evaluate model performance and prevent overfitting.

The LR model's coefficients b*1,* b*2,* b*3* represent the weights for each sensor reading, quantifying their contribution to the overall score S.

MODEL SUMMARY

Table 3 compares our three ML approaches in terms of purpose, inputs, outputs, advantages, limitations and key hyperparameters.

WEIGHT DETERMINATION

All sensor inputs were first normalized to zero mean and unit variance. We then determined weights as follows:

Linear Regression coefficients (bi):

The LR model was fitted by ordinary least squares on the training set, yielding
b*1=0.5,* b*2=0.3,* b*3=0.2,*
Thus, the continuous exertion score is computed as
S=0.5·HR_norm+0.3·Temp_norm+0.2·Humid_nor

TABLE 2
Decision rules and recommendations.

RF Prediction	LSTM Prediction	Recommendation	Justification
Normal	Normal	Continue Ridind	Rider is in a stable state with no immediate concerns
Normal	Fatigue in 20 mins	Take a Short Break	Early signs of fatigue detected; preventing escalation
Normal	Fatigue in 10 mins	Immediate Rest	High likelihood of fatigue shortly; ensuring safety
Fatigued	Normal	Continue Ridind	Current fatigue is manageable; continue with caution
Fatigued	Fatigue in 20 mins	Take a Short Break	Rides is already fatigued; prevent further exhaustion
Fatigued	Fatigue in 10 mins	Immediate Rest	Critical fatigue state requiring immediate action
Stressed	Normal	Take a Short break	Stress detected; a break can help alleviate it
Stressed	Fatigue in 20 mins	Take a Short Break	High stress combined with potential fatigue; proactive break
Stressed	Fatigue in 10 mins	Immediate Rest	Elevated stress and inninent fatigu; ensure rider safety

TABLE 3
Summary of modeling approaches: purpose, input features, outputs, advantages, limitations, and key hyperparameters for the Random Forest, LSTM, and Linear Regression models used in this study.

Model	Function	Inputs	Outputs	Advantages	Limitations	Key Hyperparameters
RF	State classification	All sensors (HR,Temp, Humid, Light, Speed, GPS, Battery status)	State label (Normal / Fatigue / Stressed)	Noise-robust; interpretable; fast	Overfits small data; ignores temporal order	trees = 100; depth = 10; criterion = gini
LSTM	Fatigue prediction	Seq windows (len=50 of all sensors)	Continuous fatigue risk score	Captures temporal patterns; handles sequences	Data-heavy; slow; complex tuning	units = 64; dropout = 0.2; lr = 0.001; epochs = 100
LR	Exertion estimation	Avg HR; Avg Temp; Avg Humid	Continuous exertion score S	Simple; interpretable; fast	Linear: sensitive to outliers	L2 regularization (l = 0.01)

m

These coefficients quantify each sensor's relative contribution to the score.

Model-fusion weights (a_j)**:**

To combine the RF, LSTM and LR outputs into a single recommendation decision, we performed a grid search over weights

a_{RF}, a_{LSTM}, a_{LR} on the validation set. The combination that maximized F1-score was $a_{RF}=0.4, a_{LSTM}=0.4, a_{LR}=0.2$.

IMPLEMENTATION

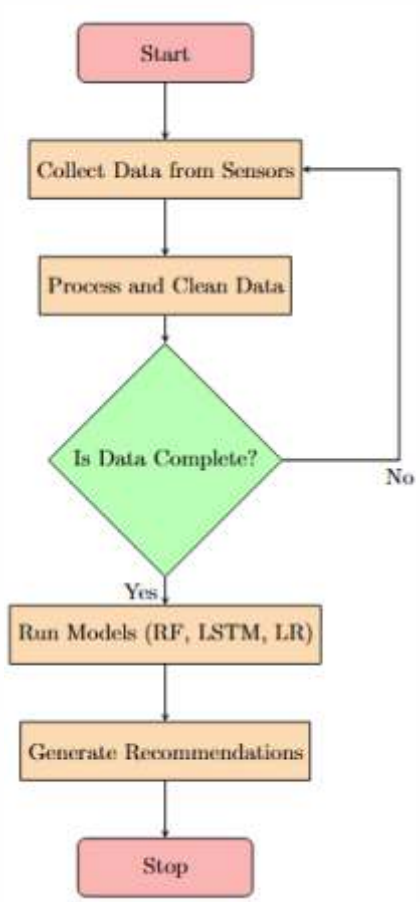

FIGURE 4
Data processing and model implementation flowchart

The LR model assumes a linear relationship between independent and dependent variables, applying independence, homoscedasticity, and normality (Figure 4).

However, the model may not capture complex nonlinear relationships in psychophysiological data. The overall score S is used to classify user states into Normal, Fatigued, or Stressed, with thresholds T1 and T2 applied to facilitate this classification.

$$\text{State} = \begin{cases} \text{Normal, if } S \leq T_1 \\ \text{Fatigued, if } T_1 < S \leq T_2 \\ \text{Stressed, if } S > T_2 \end{cases}$$

REAL-TIME ADJUSTMENTS AND FUTURE PREDICTION

The system continuously samples all sensors at 1 Hz and updates fatigue and exertion estimates every 10 s using a sliding-window approach. Based on the latest model outputs and environmental readings, it issues context-aware recommendations. For example:

- Rising fatigue on uphill segments: if heart rate exceeds T_1 (140 bpm) while GPS-derived elevation gain > 5 m over the last 30 s, the system alerts "Uphill fatigue detected - consider reducing speed".
- Heat stress management: when temperature > 30 °C and humidity > 70 % coincide with a fatigue risk score > 0.8, it prompts "High heat stress - hydrate and slow down".
- Battery-aware guidance: if battery status drops below 20 % on a planned long route, it advises "Low battery - seek charging or shorten route."
- Imminent fatigue prediction: the LSTM forecasts > 80 % probability of fatigue within the next 5 min, prompting "Fatigue predicted - prepare to rest soon".

RESULTS

QUANTITATIVE EVALUATION

We evaluated each model on the held-out test set (10 % of the data). For the Random Forest (RF) and LSTM classifiers we report accuracy and

TABLE 4
Performance metrics on test data. Computed on continuous exertion scores from the LR model (see Module formulation).

Model	Accuracy	Precision	Recall	F1-score	AUC	MSE
RF	**0.805**	**0.82**	**0.88**	**0.85**	**0.9**	**-**
LSTM	**0.841**	**0.87**	**0.9**	**0.88**	**0.93**	**-**
LR	**-**	**-**	**-**	**-**	**-**	**0.012**

recall; for the Linear Regression (LR) estimator we report mean squared error (MSE). Table 4 summarizes these metrics for fatigue detection.

To contextualize our results, we compare ourselves with Luo et al. [5], who reported physical-fatigue detection using an RF classifier at 71.85% accuracy and 0.72 average recall, and cognitive-fatigue detection at 64.69% accuracy and 0.65 recall. Our RF model improves physical-fatigue accuracy to 80.50% (+8.65 pp) and recall to 0.88 (+0.16), while our LSTM model improves cognitive-fatigue accuracy to 84.10% (+19.41 pp) and recall to 0.90 (+0.25).

These results confirm that our LSTM delivers the strongest cognitive fatigue discrimination, the RF provides robust physical fatigue classification, and the LR model yields accurate continuous exertion estimates.

E-BIKE ECO-COMMUTING SYSTEM PROOF-OF-CONCEPT

To demonstrate the practical application of the proposed methodology, a proof-of-concept system is implemented within a prototype E-bike eco-commuting scenario. This scenario involves a typical user commuting in an urban environment, utilizing the E-bike equipped with the integrated sensors suite.

SCENARIO DEFINITION

User Profile and Recommendation Purpose.

We target urban commuters aged 18-65 in general good health but with varying fitness levels, who rely on the E-bike for daily trips of 5-20 km. The system continuously monitors rider physiology and environmental conditions to issue context-aware guidance-specifically: "Continue Riding" when no fatigue or stress is detected, "Take a Short Break" at early signs of fatigue or stress, "Immediate Rest" when imminent or critical fatigue is predicted, "Low battery - seek charging or shorten route" when battery runs low. These personalized prompts help maintain safe exertion levels, prevent sudden fatigue or stress escalation, and enhance overall comfort and trip confidence.

IMPLEMENTATION STEPS

Sensor Deployment: Install environmental, physiological, and E-bike status sensors on the E-bike and wearable devices.
Data Collection Framework: Develop a system to aggregate real-time data from all sensors, ensuring data integrity and synchronization.
Data Processing Pipeline: Implement preprocessing algorithms to clean, normalize, and extract features from the collected data.
Model Integration: Deploy RF and LSTM models to analyze the processed data and generate predictions.
Recommendation Engine Deployment: Integrate the recommendation engine to provide actionable suggestions based on model outputs.

IoT-Based E-bike Monitoring & Recommendation System Algorithm:

Require: Environmental, Physiological, and E-bike sensor data
Ensure: Real-time alerts, state classification, future predictions, and recommendations
Procedure Initialize_System():
1. Initialize sensors, microcontroller (ESP32), Bluetooth, ML models (RF, LSTM), and UI.
End Procedure
Procedure Main_Loop():
While system is running:
1. Collect & preprocess sensor data (clean, normalize, filter).
2. Extract features, fuse data, detect anomalies.
3. Predict state (RF) and future fatigue (LSTM).
4. Generate & display recommendations based on predictions.
5. Collect & process user feedback.
6. If (feedback > 50) > Retrain models.
7. If (negative feedback) > Adjust model parameters.
End While
End Procedure

CONCLUSIONS AND FUTURE WORK

In this work, we demonstrated a smart E-bike system that fuses physiological, environmental, and bike-status data to detect and predict rider fatigue-achieving 80.5% accuracy for current fatigue detection and 84.1% accuracy for imminent fatigue prediction. Real-time recom-

mendations based on fused model outputs were shown to improve safety and rider comfort.

Building on this prototype, future work will:

- Explore advanced modeling techniques,such as polynomial regression and deep learning architectures, to boost predictive accuracy.
- Integrate additional psychophysiological sensors (skin conductance, EEG) for richer state estimation.
- Conduct long-term field trials across diverse riding conditions to assess real-world usability, gather user feedback, and quantify energy-efficiency impacts.

ACKNOWLEDGEMENTS

This work was developed within the scope of the Centre for Mechanical Technology and Automation (TEMA) through the projects UIDB/00481/-2020 and UIDP/00481/2020. This study was also funded by the PRR - Plano de Recuperação e Resiliência and by the NextGenerationEU funds at Universidade de Aveiro, through the scope of the Agenda for Business Innovation "AM2R - Agenda Mobilizadora para a inovação empresarial do setor das Duas Rodas" (Project no. 15 with the application C644866475-00000012).

REFERENCES

[1] C. Gheorghe and A. Soica, "Revolutionizing Urban Mobility: A Systematic Review of AI, IoT, and Predictive Analytics in Adaptive Traffic Control Systems for Road Networks," Electro-nics, vol. 14, no. 4, art. 719, Feb. 2025, doi:10.3390/electronics14040719.

[2] S. Mukhopadhyay, A. Kumar, J. Gupta, A. Bhatnagar, M. V. V. Prasad Kantipudi, and M. Singh, "A Review and Analysis of IoT Enabled Smart Transportation Using Machine Learning Techniques," Int. J. Transport Dev. Integration, vol. 8, no. 1, pp. 61-77, Mar. 2024, doi:10.18280/ijtdi.080106.

[3] E. G. Avina-Bravo, F. A. S. de Sousa, C. Escriba, P. Acco, F. Giraud, J.-Y. Fourniols, and G. Soto-Romero, "Design and Validity of a Smart Healthcare and Control System for Electric Bikes," Sensors, vol. 23, no. 8, art. 4079, Apr. 2023, doi:10.3390/s23084079.

[4] E. G. Avina-Bravo et al., "Smart Electrically Assisted Bicycles as Health Monitoring Systems: A Review," Sensors, vol. 22, no. 2, art. 468, 2022, doi:10.3390/s22020468.

[5] H. Luo, P. A. Lee, I. Clay, M. Jaggi, and V. De Luca, "Assessment of fatigue using wearable sensors: a pilot study," Digital Biomarkers, vol. 4, no. 1, pp. 59-72, 2020.

BACKPACK

Made from textile waste and equipped with a smart add-on featuring **sensors for signaling direction changes**, **sudden braking**, and **proximity alerts**, with **light-based feedback** for enhanced safety.

CeNTI . TMG Têxtil . Citeve

SAFOOS

Risk detection and real-time alert system, with sensors, smart signage, and network communication to **improve safety** in mixed-traffic areas.

CeNTI . Castros . MatGlow

BICYCLE GRIPS

Ergonomic integration of sensors and actuators that enable signaling of **direction changes, falls, vehicle proximity, and sudden braking.**

CeNTI . TMG Têxtil . Citeve

BATTERIES

Wireless power transfer for e-bike charging, complemented by a diagnostic station for **battery monitoring.**

CeNTI . edmtech

CeNTI

CeNTI is a Technology and Innovation Centre (CTI) with expertise and technologies in the fields of applied **Nanotechnology, Advanced and sustainable Materials, and Smart Systems**, supporting companies in technological development and prototyping of new materials and products.

Find out more at
centi.pt

AM2R
centi Centre for Nanotechnology and Advanced Materials
PRR Plano de Recuperação e Resiliência
REPÚBLICA PORTUGUESA
Financiado pela União Europeia NextGenerationEU

CARBURISED AND NITRIDED STEELS FOR BICYCLE FREE-WHEEL HUB GEARS

Jorge Santos[1*], Samuel E. Pereira[1], Bernardo L. Tavares[1], César Cardoso[2], João Bastos[2], António B. Pereira[3], F. J. Oliveira[1]

1 Department of Materials and Ceramic Engineering, CICECO Aveiro Institute of Materials, University of Aveiro, Portugal
2 RODI Industries, S.A., Portugal
3 Department of Mechanical Engineering, TEMA - Centre for Mechanical Technology and Automation, University of Aveiro, Portugal

In this study, the wear performance of carburised and nitrided steels was compared to that of hard chromium-coated steel using a counter body DIN 100Cr6 steel ball. The ball-on-disc wear tests indicated that the carburised and nitrided discs showed no measurable wear under the conditions tested. In contrast, the hard chromium-coated discs showed an average specific wear rate of $1.5x10^{-6}$ $mm^3/N.m$ for a sliding distance of 1000 m. The results obtained suggest that carburising and nitriding thermochemical treatments can offer alternative solutions for improving the wear performance of bicycle rear hub gears.

KEYWORDS
CARBURISING; NITRIDING; WEAR; GEARS; FREEHUB.

INTRODUCTION

Bicycle rear freehubs are critical components for transmitting movement from the pedal to the wheel through a system of gears [1]. To increase the longevity of gears, it is common practice to apply coatings, the most common being hard chromium electroplating [1]. Hard chromium electroplating of gears improves corrosion resistance and wear performance. Despite the performance benefits of hard chromium electroplating, there is an environmental and public health risk resulting from the use of hexavalent chromium-based solutions to obtain these coatings [2]. Thermochemical treatments involve a change in the chemical composition of the steel's surface through the interstitial diffusion of carbon or nitrogen atoms in the metal's crystal lattice, increasing hardness and fatigue resistance [3]. This work aims to evaluate the wear performance of carburised and nitrided steels as alternatives to hard chromium coating for bicycle rear freehub gears.

MATERIALS AND METHODS

40CrMnNiMo 8-6-4 and 16MnCr5 steel rods were obtained in the tempered and annealed states, respectively. The average chemical composition of each steel is shown in Table 1.

TABLE 1
Chemical composition of the steels used in this study (wt.%)

Elements	16MnCr5	40CrMnNiMo 8-6-4
C	**0.17**	**0.38**
Si	**0.27**	**0.32**
Mn	**1.29**	**1.37**
Cr	**1.10**	**1.94**
Ni	**-**	**1.00**
Mo	**-**	**0.18**
Fe	**bal.**	**bal.**

Test discs, Ø50 mm x 6 mm thick, were machined from each steel rod. The 16MnCr5 steel was carburised in an industrial furnace with a controlled atmosphere at a temperature of 900°C, followed by quenching in oil and tempering at 200°C. The ALLNIT® low-pressure nitriding thermo-chemical treatment was carried out at 540°C in a gaseous atmosphere consisting of NH^3, N^2 and NO^2 on 40CrMnNiMo 8-6-4 steel. After the thermochemical treatments, all the discs were ground to remove the oxidation layer present after carburising and to reduce the roughness induced by machining. Some of the thermochemically carburised discs were sent for hard chromium electroplating after surface grinding. After hard chromium deposition, the discs were heat treated at 130°C for 8 hours to reduce the steel's susceptibility to hydrogen embrittlement [4]. The roughness parameters obtained using a Sensofar S Neox

optical profilometer in interferometric mode for the discs after grinding and hard chromium electroplating are shown in Table 2.

TABLE 2
Roughness of the discs' surfaces after grinding and hard chrome coating.

	Sa [mm]	Sq [mm]
Discs after grinding	**0.12 ± 0.03**	**0.16 ± 0.05**
Discs after hard chromium deposition	**0.16 ± 0.02**	**0.22 ± 0.04**

The microstructure of the samples was analysed by optical and scanning electron microscopy after cross-cutting, polishing and etching with 2% Nital solution. Knoop microhardness was measured using INNOVATEST FALCON 600G2FAO5 equipment with a load of 0.098 N applied for 10 s, and Vickers microhardness was carried out using Wilson VH1102 equipment with a load of 0.980 N applied for 10 s. Ball-on-disc tribological wear tests were carried out on an Anton Paar model TRB3 equipment in an unlubricated regime following the ASTM G99 standard, with a constant applied force of 3 N, a constant linear speed of 0.25 m/s and sliding distances of 500 and 1000 m. A DIN 100Cr6 steel ball with a Ø of 6 mm was used as a counter-body, and the tests were repeated 3 times for each condition. The wear volume of the balls was obtained from the diameter of the wear scar, and for the discs, a 3D optical profilometer, Sensofar S-neox, was used under white light interferometry.

RESULTS AND DISCUSSION

Figure 1 shows the microstructures obtained of the 16MnCr5 steel discs after carburising, after hard chromium electroplating, and from the 40CrMnNiMo 8-6-4 steel after nitriding. In Figure 1 (A), it is observed that the 16MnCr5 steel disc, after carburising, shows internal oxidation in the surface layer of the disc [5,6]. Therefore, this internal oxidation layer was removed by grinding after carburising and before the hard chrome coating was applied. Figure 1 (B) shows the microstructure of the 40CrMnNiMo 8-6-4 steel disc after nitriding, which consists of most probably a compound layer of nitrides ε-$Fe_{2-3}N$ and γ'-Fe_4N on the surface, followed by a diffusion layer of nitrogen-saturated ferrite and dispersed nitrides (probably CrN), as can be seen in Figure 1 (C) [3]. The thickness of the compound layer was 7.5 ± 1.8 µm. Figure 1 (D) shows the microstructure of the 16MnCr5 steel disc after hard chromium coating, in which no internal oxidation can be detected, and the hard chromium layer can be observed. The thickness of the hard chromium layer determined by the ball-cratering Calotest method was 3.8 ± 0.5 µm [7].

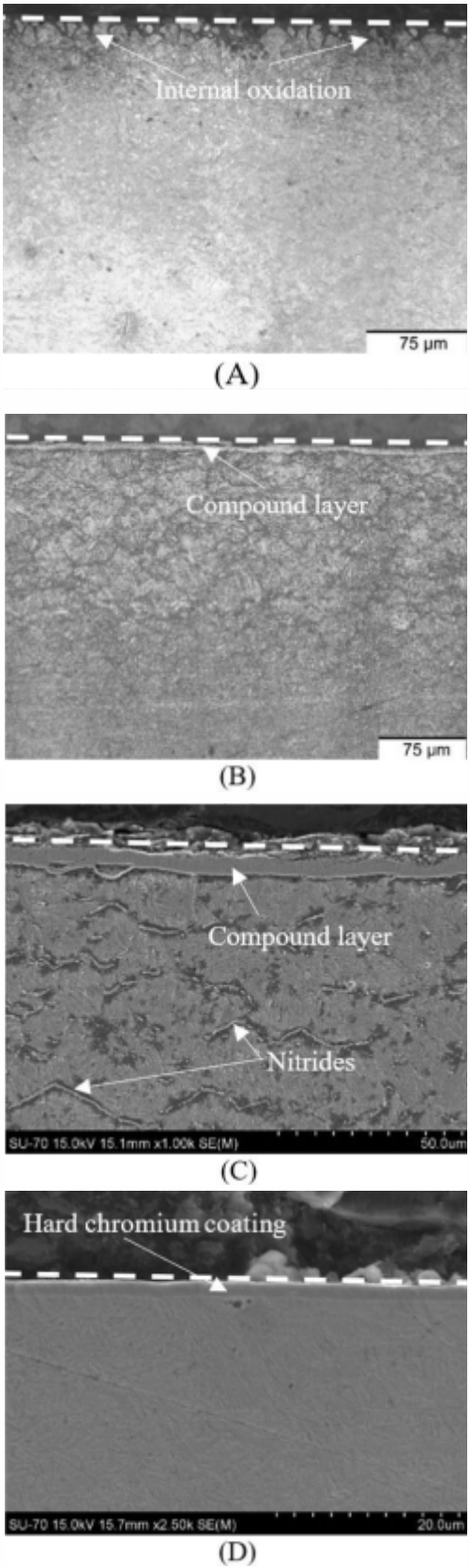

FIGURE 1
Microstructures obtained by optical microscopy of the cross-section of the discs of (A) 16MnCr5 steel after carburising and (B) 40CrMnNiMo 8-6-4 steel after nitriding. Secondary electron images were obtained by scanning electron microscopy on the cross-section of the discs of (C) 40CrMnNiMo 8-6-4 steel after nitriding and (D) 16MnCr5 steel after carburising and hard chromium electroplating. The white dashed lines indicate the position of the disc surface.

Figure 2 shows the Vickers microhardness profiles as a function of distance from the surface for the various treated steels. After nitriding, 40CrMnNiMo 8-6-4 steel had higher microhardness up to 50 µm from the surface than carburised 16MnCr5 steel. As the distance from the disc surface increases, the microhardness of 40CrMnNiMo 8-6-4 steel after nitriding decreases sharply. After carburising, the 16MnCr5 steel shows a much more gradual decrease in microhardness with increasing distance from the surface compared to the nitrided 40CrMnNiMo 8-6-4 steel, showing a case-hardened layer depth of around 550 µm, as can be seen in Figure 2. The Vickers microhardness profile obtained from 16MnCr5 steel after hard chromium electroplating was slightly lower compared to 16MnCr5 steel without hard chromium electroplating. The microhardness obtained for hard chromium was 1308 ± 51 HK 0.01.

Figure 3 shows the coefficients of friction (µ) and specific wear rate (Ws) of the balls, calculated for the different ball-on-disc pairs and sliding distances of 500 and 1000 m. The coefficients of friction for the tribological pair consisting of the hard chromium-coated disc and the DIN 100Cr6 steel ball were significantly higher than those of the tribological pairs consisting of the carburised and nitrided steels and the DIN 100Cr6 steel ball. It is thus interesting to note that the specific wear rates of the balls used on the 16MnCr5 discs after carburising and 40CrMnNiMo 8-6-4 after nitriding were higher than those of the 16MnCr5 steel disc with hard chromium electroplating, as shown in Figure 3.

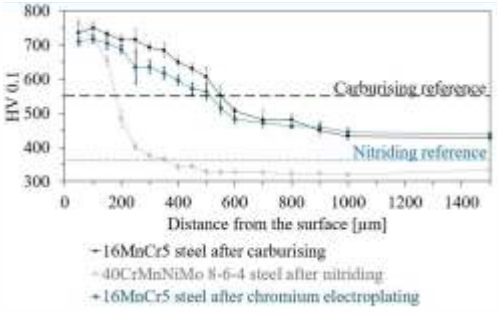

FIGURE 2
Vickers microhardness variation as a function of distance from the surface. The horizontal dashed lines indicate the reference value for determining the case hardening layer depth for carburising and nitriding according to the standard EN ISO 18203:2016.

Figure 4 shows the specific wear rates obtained for the hard chromium-coated 16MnCr5 steel discs for different sliding distances. It was found that the wear on the discs of 16MnCr5 steel after carburising and 40CrMnNiMo 8-6-4 after nitriding was negligible under the selected test conditions, while the 16MnCr5 steel disc after carburising and hard chromium electroplating had a measured wear track. The specific wear rate of the hard chromium-coated disc increased slightly with increasing sliding distance, as shown in Figure 4.

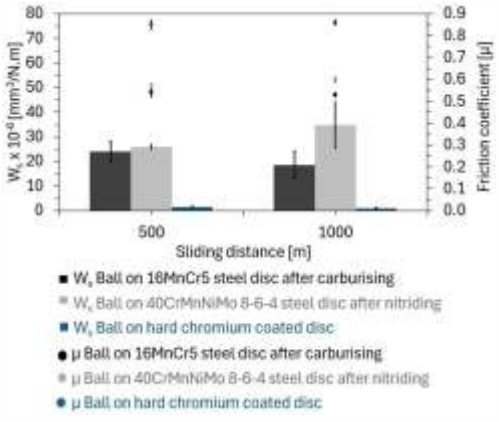

FIGURE 3
Friction coefficients (µ) for the ball-disc set and specific wear rate (Ws) obtained for the DIN 100Cr6 steel balls tested on the different discs for sliding distances of 500 and 1000 m.

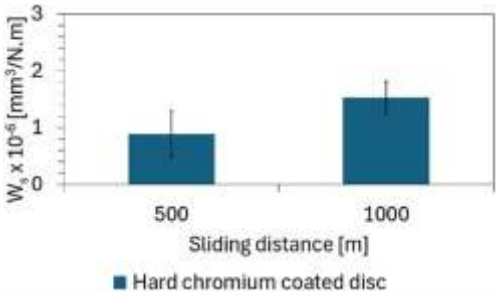

FIGURE 4
Specific wear rates obtained for the 16MnCr5 steel discs with hard chromium coating tested for sliding distances of 500 and 1000 m.

CONCLUSIONS

The thermochemical treatments of carburising and nitriding increased the surface hardness of the 16MnCr5 and 40CrMnNiMo 8-6-4 steels, respectively. The uncoated steel discs showed no measurable wear under the test conditions in this study, while the hard chromium-coated steel discs showed distinct wear tracks. Furthermore, the friction coefficients of the tribological pairs made up of the carburised and nitrided steels and the DIN 100Cr6 steel ball were significantly lower than those of the hard chromium coating and steel ball pair. The results obtained suggest that the thermochemical treatments of carburising and nitriding steels may be viable alternatives for the wear performance of bicycle rear hub gears.

ACKNOWLEDGEMENTS

This work was developed within the scope of the project CICECO-Aveiro Institute of Materials,

UIDB/50011/2020 (DOI 10.54499/UIDB/50011/2020), UIDP/50011/2020 (DOI 10.54499/UIDP/50011/2020) & LA/P/0006/2020 (DOI 10.54499/LA/P/0006/2020), financed by national funds through the FCT/MCTES (PIDDAC) and the Centre for Mechanical Technology and Automation (TEMA) through the projects UIDB/00481/2020 and UIDP/00481/2020. This study was also funded by the PRR - Plano de Recuperação e Resiliência and by the NextGenerationEU funds at Universidade de Aveiro, through the scope of the Agenda for Business Innovation "AM2R - Agenda Mobilizadora para a inovação empresarial do setor das Duas Rodas" (Project no. 15 with the application C644866475-00000012).

REFERENCES

[1] T.J. Mackin, N. Anderson, S. Aguilar, G. Beemiller, B. Copsey, D. Draper, E. Eckberg, L. Herbert, D. Layton, Fatigue failure of a star-ratchet gear, Eng Fail Anal 32 (2013) 334-347. https://doi.org/10.1016/j.engfailanal.2013.03.00

[2] ECHA - European Chemical Agency, Chromium (VI), 2024. https://echa.europa.eu/pt/substance-information/-/substanceinfo/100.132.559 (accessed December 15, 2024).

[3] E.J. Mittemeijer, M.A. Somers, Thermochemical Surface Engineering of Steels, Woodhead Publishing, 2014.

[4] EN ISO 9588:2007, Metallic and other inorganic coatings - Post-coating treatments of iron or steel to reduce the risk of hydrogen embrittlement, 2007.

[5] K.J. Winkler, T. Tobie, C. Guntner, Stefan Schurer, Material Properties and Tooth Root Bending Strength of Shot Blasted, Case Carburized Gears with Alternative Microstructures, Gear Technology (2021).

[6] L. Song, X. Gu, F. Sun, J. Hu, Reduced internal oxidation by a rapid carburizing technology enhanced by pre-oxidation for 18CrNiMo7-6 gear steel, Vacuum 160 (2019) 210-212. https://doi.org/10.1016/j.vacuum.2018.11.006.

[7] EN ISO 1071-2:2002 Advanced technical ceramics - Methods of test for ceramic coatings - Part 2: Determination of coating thickness by the crater grinding method, 2002.

GROUP PHOTOGRAPH AT THE AM2R TECHNICAL-SCIENTIFIC CONFERENCE

TRIBOLOGICAL SOLUTIONS FOR BIKE CHAINS

Diogo Cavaleiro[1], Susana Devesa[1], Pedro Santos[2], Albano Cavaleiro[1,3], Sandra Carvalho[1]

1 Department of Mechanical Engineering, CEMMPRE, ARISE, University of Coimbra, Rua Luis Reis Santos, 3030-788, Coimbra, Portugal

2 SRAMPORT Lda., Rua António Sérgio 15, 3025-041, Coimbra, Portugal

3 Laboratório de Ensaios, Desgaste e Materiais (LED&MAT), Instituto Pedro Nunes, Rua Pedro Nunes, Coimbra 3030-199, Portugal

In cycling, chains play a vital role in transferring power from pedal motion to the wheels, significantly influencing overall bike performance. Historically, hard chromium has been used to enhance chain performance. However, growing environmental concerns and stricter regulations surrounding the release of toxic hexavalent and trivalent chromium have driven the search for sustainable coating alternatives. This work focused on the deposition of ZrCN, WSC and DLC-Si-O coatings, onto bike chain components using magnetron sputtering. The aim was to evaluate their friction and wear behavior, as an eco-friendly substitute for hard chromium. The produced coatings exhibited hardness values of 6 to 14 GPa and compact and dense morphologies. Tribological tests involved reciprocating sliding motion and a comparison to a commercially used hard chromium coating. The results displayed that the magnetron sputtered coatings all showed significantly improvements in the friction coefficients. Specific wear rates were also shown as an improvement with the WSC and DLC-Si-O coatings showing lower wear rates than the reference. Some coatings exhibit promising results, suggesting they could serve as a superior alternative to the current use of hard chromium.

KEYWORDS

TRIBOLOGY; SPUTTERING; ZrCN; WSC; DLC-Si-O_2; BIKE CHAINS.

INTRODUCTION

Cycling has become increasing popular as the preferred way to encourage the practice of healthy lifestyles, environmental awareness, and for the need of sustainable modes of transportation [1]. From an environmental perspective, the European Cyclists' Federation reports that cycling generates €150 billion in benefits annually across the EU, with over €90 billion attributed to environmental protection, public health, and mobility [2]. Considering this, when it comes to smooth movement, the bicycle chain plays a crucial role, as a key component in transmitting power from the pedals to the wheels through interconnected links that engage with gears and sprockets [3]. A malfunctioning chain hinders movement, reduces power efficiency, and affects gear shifting. Excessive wear can also lead to costly repairs. Regular maintenance and awareness of chain wear help extend its lifespan and prevent unnecessary expenses [4]. To further address the issue of wear, considerable attention has been devoted by researchers over the years to developing modern surface modification techniques. These methods aim to prevent and control wear-related problems effectively [5]. Traditionally, industries have, for nearly a century, extensively utilized hard chromium (Cr) in numerous applications across the manufacturing, production, and consumer goods industries [6, 7] due to its high hardness [8], outstanding corrosion resistance, [9] and excellent anti-wear performance [10]. Despite the benefits of hard electroplated chromium coatings, concerns over the plating process have increased in the past decade. Hexavalent chromium (Cr^{+6}), commonly used in electroplating, poses significant safety, health, and environmental risks [11]. Due to its widespread use in metallurgy, electroplating, leather production, and stainless steel manufacturing, chromium is classified as a highly hazardous metal by the Toxic Substances and Disease Registry (TSDR) [12] and the International Agency for Research on Cancer (IARC) [13]. In response to these environmental and health concerns associated with the release of hexavalent, interest in other hard coatings has surged over the past decade. Over the last 50 years, various coating deposition and diffusion techniques have been developed to enhance surface hardness, each suited to specific materials and applications [14]. More recently, research has focused on creating durable, wear-resistant coatings that significantly improve the

physical properties of different surfaces [15]. Over the past three decades, several families of these coatings have been developed, including various carbon-based films, carbides, borides, nitrides, oxides, and metal nitrides [16, 17]. These coatings are widely used in hard coating applications due to their superior mechanical and tribological properties. In addition to their high hardness and wear resistance, they also offer excellent oxidation resistance and chemical stability in extreme environments [18, 19]. To add to this, the advancement of 'clean' physical vapour deposition (PVD) technologies in industrial manufacturing is a crucial task in depositing these high-performance coatings and more specifically magnetron sputtering [20]. This technique is well known for being extensively versatile in the materials it can deposit [21] and by the huge control one can have over the process [22]. Moreover, this is a process that can be considered "clean" with low carbon footprint that aligns well with environmental legislation protections [23]. In this context, this work focuses on the deposition of three different coating systems (ZrCN, DLC-Si-O and W-S-C) by magnetron sputtering into inner plates parts of a commercial bike chain followed by a tribological analysis of the friction and wear to assess the feasibility of its viability as a replacement for hard chromium in bike chains.

EXPERIMENTAL PROCEDURE

For this work, all three different coating systems were deposited by normal DC magnetron sputtering. Prior to the start of all the depositions, the chamber was evacuated to a pressure of $6x10^{-4}$ Pa. After and before starting the final deposition of the coating, the substrates and targets were sputter cleaned using argon plasma, by applying a substrate bias voltage of 600 V through a pulsed DC power supply followed by the deposition of a chromium interlayer and gradient layers to promote the adhesion of the coatings. During the depositions, the working pressure was around 0.5 Pa for the ZrCN, DLC-Si-O and W-S-C systems. For the ZrCN system, reactive mode was used with the introduction of nitrogen (N_2) and methane (CH_4) with partial pressures of 0.03 Pa and 0.14 Pa, respectively. For the DLC-Si-O system, reactive mode was also used with the introduction of oxygen (O_2) gas with a partial pressure of 0.08 Pa. Note that, for the ZrCN coating, the nomenclature of ZrN 75C is used, where 75C refers to the amount of carbon in the coating (in this case, 75 at.%). The substrates used to deposit the coating systems were (111) silicon wafers and commercial inner plates of a bike chain. To achieve complete deposition of the complex geometry of the small inner plates, a carousel with a double-fold rotation planetary system was used, as shown in Fig. 1.

FIGURE 1
Deposition chamber and sample mounting example.

The surface and cross-section morphology of coatings were analyzed using a field emission scanning electron microscope (Hitachi SU3800), and coating thickness was obtained from micrographs of the fractured cross-sections in the silicon wafers. The elemental composition was measured using an energy dispersive spectroscopy (EDS, Bruker Nano) analyzer, operated at an accelerating voltage of 10 kV. The

TABLE 1
Deposition parameters and main properties of the deposited coatings.

	ZrN 75C	DLC-Si-O	W-S-C	Reference
Traget power (W)	**550 (Zr)**	**1750 (C)** **580 (Si)**	**1300 (W)** **2 x 1600 (C)**	-
Working pressure (Pa)	**0.5**	**0.5**	**0.5**	-
Bias (V)	**50**	**50**	-	-
Thickness (mm)	**~2**	**~2**	**~2**	**~10**
Hardness (Gpa)	**~8**	**~14**	**~6**	**~12**
Reduced elastic modulus (Gpa)	**~75**	**~160**	**~65**	-
Structure	**FCC (ZrN)**	**Amorphous**	**Amorphous**	-
Color	**Blackish**	**Black**	**Dark grey**	**Metallic grey**

crystal structure was assessed by X-ray diffraction (X'pert PRO MRD, Panalytical) in conventional mode on bragg-brentano configuration using Co K radiation (= 0.178901 nm). The hardness and reduced elastic modulus were measured by nanoindenation (Nanotest, Micromaterials), using a pyramidal Berkovich diamond indenter using a maximum load of 10 mN in a total of 16 indentations. More details on the experimental procedure and the characterization and analysis of some of the properties of the coatings can be seen on Table 1.

The tribological behavior of the films was evaluated on a reciprocating sliding tribometer RTec Instruments. The tribology tests were performed against 100Cr6 balls and were carried out at room temperature (RT) under a normal load of 5 N (ZrCN, reference and DLC-Si-O) and 20N (W-S-C), a constant linear speed of 0.1 ms^{-1} for 5000 cycles. The specific wear rate of the coatings was determined through the evaluation of the cross-section area of the 2D profiles obtained in 4 different zones of the wear track, using a 2D profilometer, followed by an estimation of the wear volume.

The surface morphology, wear mechanisms and chemical composition of the wear tracks and wear debris were analyzed by scanning electron microscopy (SEM) integrated with energy dispersive x ray spectroscopy (EDS) using an accelerating voltage of 10 kV.

RESULTS

The coefficient of friction and the corresponding specific wear rates for the tested coatings can be seen in Figure 2 and 3, respectively. As displayed, the reference exhibits a considerably high friction coefficient of around 0,75, which is typical for these types of materials when in contact with other similar materials (such as chrome steels). However, the introduction of carbon into the films, as expected, leads to a significant decrease in the friction coefficient, most likely due to the presence of graphite at the contact interface, which provides a lubricating effect and consequently results in low friction coefficients. Indeed, the ZrN 75C coating shows a steep decrease of the friction to values around 0.2 while the DLC-Si-O and W-S-C coatings go even further with a reduction in friction to around 0.1. This could suggest that wear resistance for these coatings is very high.

However, when analyzing Figure 3 and the calculated specific wear rates, this was not the case for the ZrN 75C coating. In fact, this coating shows the lowest wear resistance of all the tested samples (even than the reference) while

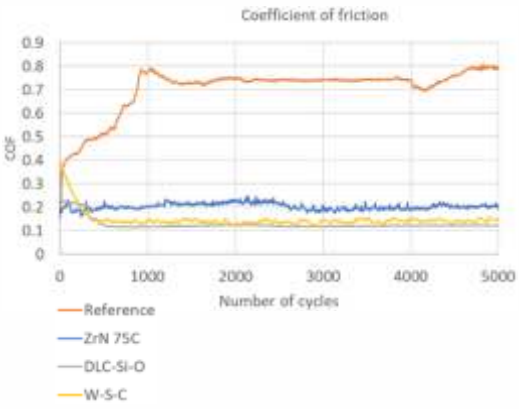

FIGURE 2
Coefficient of friction for the tested coating.

the DLC-Si-O and the W-S-C coatings show a considerable decrease in the wear rate, showing clear improvements in the wear resistance when compared to the reference. To understand better the wear behavior and the mechanisms, analysis of the wear tracks was conducted.

For the reference sample it was found that most of the wear was adhesive. The combination of its relatively high hardness (~12 GPa), which "protects" against abrasion, and the followed formation of a protective tribo-film of chromium oxide, explains the good wear resistance of this sample, despite the high coefficient of friction observed. Typically, the carbon phase introduction (for the other tested coatings) is the main contribution towards the reduction in friction during ambient air sliding through friction-induced graphitization. In fact, such is the case for all the coatings although, the ZrN 75C coating shows a decrease in the wear resistance. Analysis of the wear track shows only slight signs of abrasion which suggest that the combination of its low hardness (~8 GPa) and the presence of the small and very hard ZrN crystallites (~25 GPa) are the culprit for the abrasive signs. Although high hardness typically suggests superior wear resistance, hard coatings can often suffer from the issue of small particle and/or debris detachment from the coating itself which then act as a third body within the contact interface and lead to an extreme increase in contact pressure. This, in turn, can cause a sharp rise in the wear rate and consequently a reduction in wear resistance. In the case of DLC-Si-O, the wear track looks smooth with no signs of abrasion. Thus, the increased wear resistance can be attributed to the combined effect of the presence of the lubricious carbon tribolayer, like in a pure DLC coating, the presence of Si-O which is also known to provide low friction and wear values and the relatively high hardness (~14 GPa) that protects against plastic deformation. Finally, the W-S-C shows the best wear resistan-

ce of all the tested samples, due to the very well-known low friction combinations that can be achieved through the graphitization and formation of the lubricious WS2 tribolayers in the contact. As soon as the tribolayer is formed, the friction behavior is quite similar to that of DLC-Si-O and thus, most of the wear processes, very likely occur before the formation of the lubricious tribofilms (as seen by the high initial COF present in Figure 2 for this coating). Usually, for this type of coatings the tribological response is guided by the S/W ratios, with higher ratios yielding better responses. Very low S/W ratios can result in reduced toughness and hinder the formation of the lubricious tribolayer. Since this coating has a high S/W ratio of around 1.5, the efficient formation of the tribofilm explains why the coating possesses such good wear resistance.

All in all, the significant reduction in friction and wear achieved for some of the coatings tested in this study show their potential as a promising solution to replace the commercially used hard chrome.

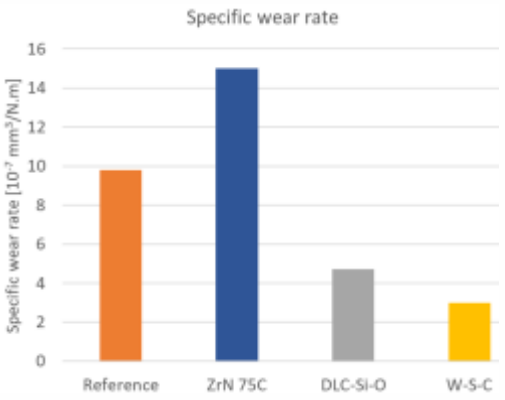

FIGURE 3
Specific wear rate calculated for the tested coating.

CONCLUSIONS

This study investigated the tribological performance of ZrCN, W-S-C, and DLC-Si-O coatings as potential eco-friendly alternatives to hard chromium coatings for bicycle chains. The coatings were deposited via magnetron sputtering and analyzed in terms of their friction and wear behavior. The results showed that all tested coatings exhibited significant reductions in the coefficient of friction compared to the commercially used hard chromium reference. The DLC-Si-O and W-S-C coatings demonstrated the lowest friction values, attributed to their ability to form lubricious tribolayers. DLC-Si-O and W-S-C coatings also displayed superior wear resistance compared to the reference, whereas the ZrN 75C coating, despite its friction reduction, exhibited higher wear rates due to abrasive wear mechanisms.

Overall, the findings highlight the potential of W-S-C and DLC-Si-O coatings as promising candida-tes for replacing hard chromium coatings in bicycle chains. The combination of reduced friction and enhanced wear resistance positions them as viable solutions for improving chain durability and performance.

ACKNOWLEDGMENTS

This research is sponsored by national funds through FCT-Fundação para a Ciência e Tecnologia, under projects UIDB/00285-Centre for Mechanical Engineering, Materials and Processes and ARISE Associated Laboratory LA/P/0112/2020.

This research is financed by PRR - Recovery and Resilience Plan and by the Next Generation EU Funds, following NOTICE N.º 02/C05-i01/2022, Component 5 - Capitalization and Business Innovation - Mobilizing Agendas for Business Innovation under the AM2R project "Mobilizing Agenda for business innovation in the Two-Wheel sector" (reference: 7253).

REFERENCES

[1] W.H.O. (WHO), Health economic assessment tool (HEAT) for walking and for cycling: methods and user guide on physical activity, air pollution, injuries and carbon impact assessments, in, 2021.

[2] E.C.F.E.C. Federation, Cycling facts & figures.

[3] J. Waite, Bicycle chains: How efficient are they, The Physics Teacher, 62 (2024) 534-535.

[4] Y.W. Liew, O. Matthews, D.V. Dao, H. Li, Power Transmission Mechanism and Tribological Performance of Modern Bicycle Drivetrains-A Review, in: Machines, 2025.

[5] G.A. El-Awadi, Review of effective techniques for surface engineering material modification for a variety of applications, AIMS Materials Science, 10 (2023) 652-692.

[6] J.M. Tyler, Automotive applications for chromium, Metal Finishing, 93 (1995) 11-14.

[7] J.O. Nriagu, E. Nieboer, Production and uses of chromium, Chromium in the natural and human environments, 20 (1988) 81-104.

[8] Z. Zeng, L. Wang, L. Chen, J. Zhang, The correlation between the hardness and tribological behaviour of electroplated chromium coatings sliding against ceramic and steel counterparts, Surface and Coatings Technology, 201 (2006) 2282-2288.

[9] S. Han, J.H. Lin, S.H. Tsai, S.C. Chung, D.Y. Wang, F.H. Lu, H.C. Shih, Corrosion and tribological studies of chromium nitride coated on steel with an interlayer of electroplated chromium, Surface and Coatings Technology, 133-134 (2000) 460-465.

[10] M.H. Sohi, A.A. Kashi, S.M.M. Hadavi, Comparative tribological study of hard and crack-free electrodeposited chromium coatings, Journal of Materials Processing Technology, 138 (2003) 219-222.

[11] M. Shahid, S. Shamshad, M. Rafiq, S. Khalid, I. Bibi, N.K. Niazi, C. Dumat, M.I. Rashid, Chromium speciation, bioavailability, uptake, toxicity and detoxification in soil-plant system: A review, Chemosphere, 178 (2017) 513-533.
[12] H. Abadin, M. Fay, L. Ingerman, B. Tencza, D. Yu, S.B. Wilbur, Toxicological profile for chromium, (2012).
[13] F. Lyon, IARC monographs on the evaluation of carcinogenic risks to humans, World health organization, International agency for research on cancer. availble at publication@ iarc. fr, (2014).
[14] M. Ramezani, Z. Mohd Ripin, T. Pasang, C.-P. Jiang, Surface Engineering of Metals: Techniques, Characterizations and Applications, in: Metals, 2023.
[15] B. Fotovvati, N. Namdari, A. Dehghanghadikolaei, On Coating Techniques for Surface Protection: A Review, in: Journal of Manufacturing and Materials Processing, 2019.
[16] T. Hoornaert, Z.K. Hua, J.H. Zhang, Hard Wear-Resistant Coatings: A Review, in: J. Luo, Y. Meng, T. Shao, Q. Zhao (Eds.) Advanced Tribology, Springer Berlin Heidelberg, Berlin, Heidelberg, 2010, pp. 774-779.
[17] D.K. Devarajan, B. Rangasamy, K.K. Amirtharaj Mosas, State-of-the-Art Developments in Advanced Hard Ceramic Coatings Using PVD Techniques for High-Temperature Tribological Applications, in: Ceramics, 2023, pp. 301-329.
[18] I.P. Okokpujie, L.K. Tartibu, H.O. Musa-Basheer, A.O.M. Adeoye, Effect of Coatings on Mechanical, Corrosion and Tribological Properties of Industrial Materials: A Comprehensive Review, Journal of Bio- and Tribo-Corrosion, 10 (2023) 2.
[19] P. Gao, Q. Guo, Y. Xing, Y. Guo, Structural, Mechanical, and Tribological Properties of Hard Coatings, in: Coatings, 2023.
[20] P.J. Kelly, R.D. Arnell, Magnetron sputtering: a review of recent developments and applications, Vacuum, 56 (2000) 159-172.
[21] M. Stueber, H. Holleck, H. Leiste, K. Seemann, S. Ulrich, C. Ziebert, Concepts for the design of advanced nanoscale PVD multilayer protective thin films, Journal of Alloys and Compounds, 483 (2009) 321-333.
[22] A. Inspektor, P.A. Salvador, Architecture of PVD coatings for metalcutting applications: A review, Surface and Coatings Technology, 257 (2014) 138-153.
[23] B. Navinšek, P. Panjan, I. Milošev, PVD coatings as an environmentally clean alternative to electroplating and electroless processes, Surface and Coatings Technology, 116-119 (1999) 476-487.

Sustainable Biotechnologies for Industrial Wastewater Treatment

Key Objectives

- Promote economically viable and environmentally sustainable solutions
- Develop bacterial biopolymers with high capacity for metal removal from wastewater
- Identify and apply bacterial strains capable of reducing COD wastewater

Bacterial Biopolymers for Metal Removal

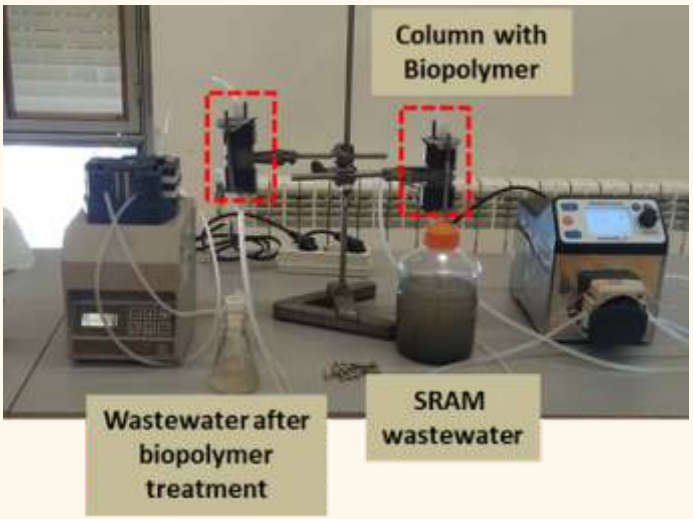

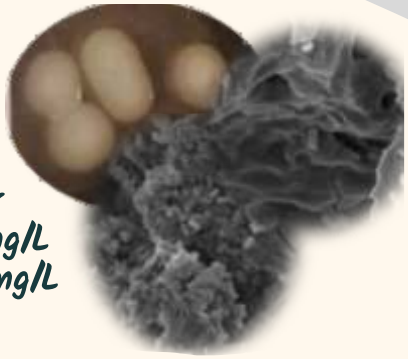

SRAM Wastewater
Iron (Fe)-14,6-20,7 mg/L
Nickel (Ni)-6.2-40.4 mg/L

Removal Efficiency
Fe: 50-80%
Ni: 40-75%

Synthetic Water
Iron (Fe)-55,8 mg/L
Nickel (Ni)-57.8 mg/L

Removal Efficiency
Fe: 55-60%
Ni: 40-45%

Biological COD Removal

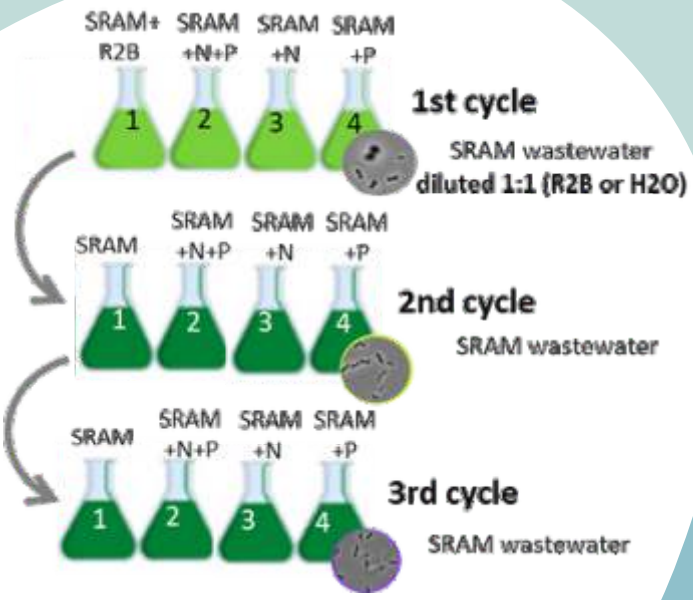

Cycles of bacterial adaptation to SRAM wastewater

SRAM wastewater
COD-1945 mg/L

COD in the 3rd adaptation cycle (< 1000 mg/L)

- Strain B2A2W2: 707.0 mg/L
- Strain M47T1: 991.6 mg/L
- Strain UCCCB20: 932.1 mg/L

Involved Partners

1290 UNIVERSIDADE D COIMBRA

SRAM

PRR Plano de Recuperação e Resiliência
REPÚBLICA PORTUGUESA
Financiado pela União Europeia NextGenerationEU

DOUBLE-LAYERED BLACK NICKEL COATINGS ON STEEL: IMPROVING COLOUR AND PERFORMANCE

Gabriel Santos[1], Susana Devesa[1], Diogo Cavaleiro[1], Pedro Santos[2], Sandra Carvalho[1], Albano Cavaleiro[1]

1 Department of Mechanical Engineering, CEMMPRE, ARISE, University of Coimbra, Rua Luís Reis Santos, 3030-788, Coimbra, Portugal
2 SRAMPORT Lda., Rua António Sérgio 15, 3025-041, Coimbra, Portugal

Electrodeposition poses as a cost-effective technique for the coating industry. Its wide range of compatible materials include black nickel coatings, which are applied to a plethora of applications, from functional to decorative ones. However, progress in its research is often constrained by lack of adhesion and poor properties. Pertaining to this, the following study focuses on the deposition of an undercoating of dull nickel on C35 steel, and a subsequent black nickel coating. Indeed, the use of an undercoating, as well as the pre-treatment of the substrate, play an important role when it comes to both coating adhesion and particular properties. As a result, amorphous black nickel coatings with promising brightness and coefficient of friction (COF) values were successfully deposited. The findings highlight the potential of these black coatings for both decorative and functional applications, as well as the need for further investigation.

KEYWORDS
ELECTRODEPOSITION; NICKEL COATINGS; BLACK NICKEL; COF; BRIGHTNESS.

INTRODUCTION

Within the field of coating deposition, electrodeposition stands out not only by its straightforwardness, versatility, and low-cost, but also by its potential for scaling and manufacturability. Moreover, nickel coatings are widely studied and used in this regard, as applications range from functional to decorative and protective ones.

Concerning this study, most of the challenges were directly related to the adhesion of the coatings, especially the black coatings. In this regard, various approaches were carried out to solve it, among which, the use of HCl, resorting to an immersion of the substrate for several minutes, and the deposition of an undercoating of dull/semi-bright nickel. The undercoating was a crucial step on this matter, improving the adhesion of the subsequent black coatings.

In fact, the deposition of black coatings combined with bright/dull nickel undercoatings is frequently described in the literature. Specifically, black nickel coatings have weak corrosion and wear resistance, which limits their use in the absence of an undercoating [1-3].

Accordingly, this study focuses on the adhesion, colour, uniformity, and wear resistance of black nickel coatings deposited over dull nickel underlayers.

METHODOLOGY

Depositions were conducted within a polyethylene cell, coupled with a power supply and a multimeter installed as an ammeter, respectively an EA-PSI 9360-15 (Elektro-Automatik) and a 2831E digital multimeter (B&K Precision). Concerning the electrodes, a pretreated C35 steel plate with a deposition area of 3 cm² and 1 mm of thickness was used as substrate (cathode), and a rectangular piece of nickel (99.99%, Test-bourne Ltd) as anode. A schematic representation of the electrodeposition process is given in Fig. 1.

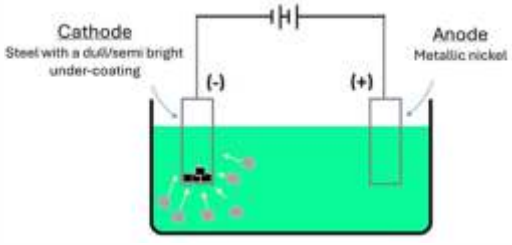

FIGURE 1
Schematic representation of the electrodeposition process.

As for the black coatings, deposition times of 5 and 10 minutes were carried out, resulting in two different samples, BC5 and BC10. Additionally, the substrate pre-treatment consisted of its immersion in a 25% V/V aqueous solution of HCl (Panreac), for 20 min. The deposition parameters and electrolytes composition for both undercoating and black coating are outlined in Table 1.

X-Ray Diffraction (XRD) investigation was performed on a PANalytical X'Pert PRO diffractometer (PANalytical), according to set operation parameters: Cu Ka (l = 1.54060 Å) radiation, 45 kV, 40 mA, and an incidence angle of 2°. The tests employed a parallel beam geometry with the following parameters: exposure time of 1 s per step, a step size of 0.025°, and 2q parameter ranging from 30° to 120°.

Surface and cross-section characterisation were undertaken by Scanning Electron Microscopy (SEM), with a SU3800 microscope (Hitachi) and a Zeiss-Merlin microscope (Zeiss), respectively, both in secondary electrons mode.

TABLE 1
Deposition parameters and electrolytes composition for the undercoating and black coatings.

	Undercoating	Black Coating
Reagents	Concentration (g/L)	
$NiCl_2$ $6H_2O$	75.33	75.33
NaCl	30.00	30.00
H_3BO_3	26.67	-------
Deposition parameters		
T (°C)	Room temperature	
t (min)	5	5 and 10
J (mA/cm^2)	27	3
w (rpm)	200	200
pH	4.83-4.93	6.40-6.50

The chemical composition of the coatings was investigated by Energy Dispersive X-ray Spectroscopy (EDS), on a Bruker Nano equipment, at an accelerating voltage of 10 kV.
Atomic Force Microscopy (AFM) micrographs over an area of 10 × 10 m² unveiled the surface topography. After levelling and applying polynomial background filters, 2D and 3D images were generated. Overall, this analysis employed tapping mode, as well as a SiN tip with tip radius below 8 nm.

Tribological investigation covered both the study of friction and wear of the coatings. For this purpose, a reciprocating ball-on-slab tribometer (SRV™ 2, Optimol Instruments) and an upper counter body consisting of a 10 mm diameter 100Cr6 bearing steel ball, chrome plated by SRAMPort. The investigation parameters were set as: 2 N load, 20 cycles, 1 Hz for oscillating frequency, and a 4 mm stroke.

RESULTS

Pertaining to the XRD diffractograms (Fig.2), the black coatings present peaks that match those of the undercoating (UC), confirming their amorphous nature.

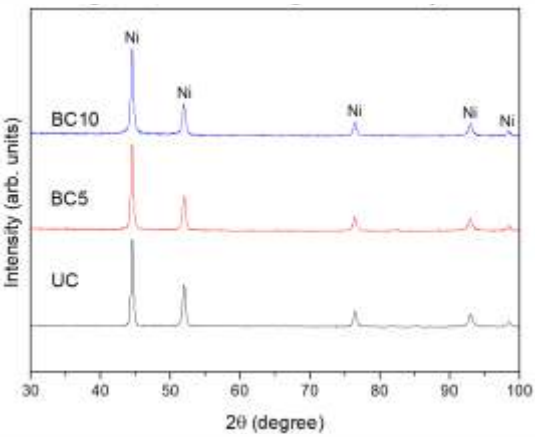

FIGURE 2
XRD diffractograms of the black coating and undercoating.

Moreover, regarding SEM analysis (Fig.3) of the undercoating, there is a clear nodular morphology with round superficial features and well-defined boundaries. A SEM cross section was used to measure thickness, which was (2.8 ± 0.1) m, corresponding to a deposition rate of ~0.6 m/min. The SEM cross section shows that the nickel film has a columnar grain structure, consistent with dull/semi-bright nickel deposits found in the literature [4]. SEM analysis of the black coatings, BC5 and BC10 (Fig.4), revealed a compact, homogeneous surface with no visible pinholes or significant porosity. Similarly, the SEM cross section was used to measure thickness, which was (0.5 ± 0.1) m for the BC5 sample and (1.1 ± 0.1) m for the BC10 sample, corresponding to a deposition rate of ~0.1 m/min. EDS analysis (Table 2) found a consistent Ni:O ratio, but it could not be associated to specific compounds like NiO or Ni_2O_3.

The average roughness (Sa) was obtained through the roughness subroutine of the AFM apparatus from six independent measurements. AFM analysis showed substantial roughness (Fig.5), decreasing with longer deposition times. BC10 had lower roughness values, indicating better surface stability and reduced heterogeneities.

The COF results, represented in Fig.6 (a), show that BC10 has lower values, which may suggest the best COF. Additionally, it has the smoother

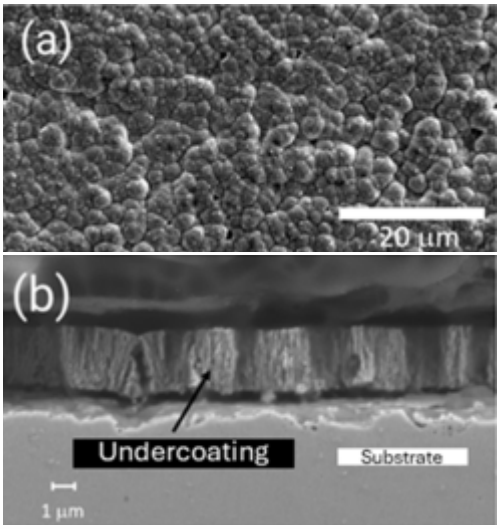

FIGURE 3
SEM micrographs of the undercoating: (a) surface and (b) cross section.

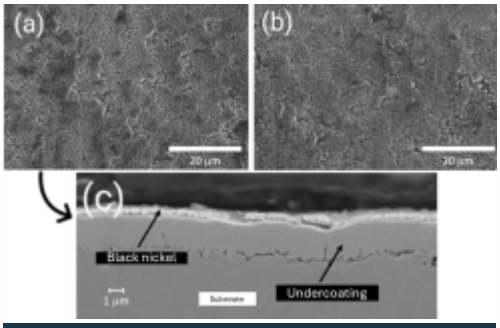

FIGURE 4
SEM micrographs of the black nickel surface (a) B 5 and (b) BC10; (c) cross section of BC5.

TABLE 2
Atomic concentration of Ni and O, obtained by EDS analysis of the coatings.

Sample	Atomic concentration (%)	
	Ni	**O**
Bc5	**67 ± 2**	**33 ± 2**
Bc10	**64 ± 2**	**36 ± 2**

curve, regarding stabilisation, which is in accordance both with its lower roughness heterogeneity, studied previously. The reference values for mild steel (COF Î [0.5;0.6]) and pure nickel (COF Î [0.55;0.80]) allows to infer that the wear did not reach the substrate [5]. Specifically, BC5 and BC10 might have slightly better COF values than mild steel.

Nevertheless, the measurement of specific wear rates was constrained by different factors, namely the low thickness and considerable roughness of the coatings. Indeed, the order of magnitude of the latter is similar to the depth of tracks, which might explain this problem. On the other hand, SEM analysis disclosed the fish-like appearance of the coatings' plastic deformation, with BC5 presenting a more heterogeneous track surface and some signs of delamination wear (Fig.7) [6]. Once again, these findings could be attributed to the thinner nature of the coatings, as well as the higher hardness of the ball. Additionally, complementary EDS analysis settles the absence of material from the ball and similar compositions between the tracks and that of the coatings, confirming that the undercoating layer was not exposed.

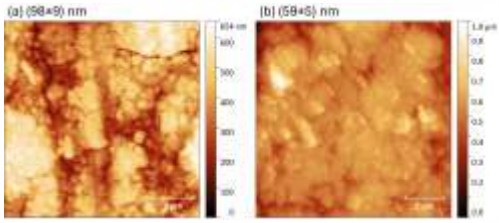

FIGURE 5
2D AFM images of (a) Bc5 and (b) Bc10.

Brightness (L*) analysis (Fig.6 (b)) showed that UC had the highest values (similar to chromium coatings) [7, 8], while BC10 was the darkest, nearing absolute black (0).

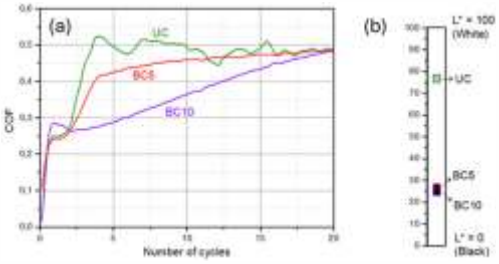

FIGURE 6
(a) Coefficient of friction and (b) brightness of the undercoating and black coating.

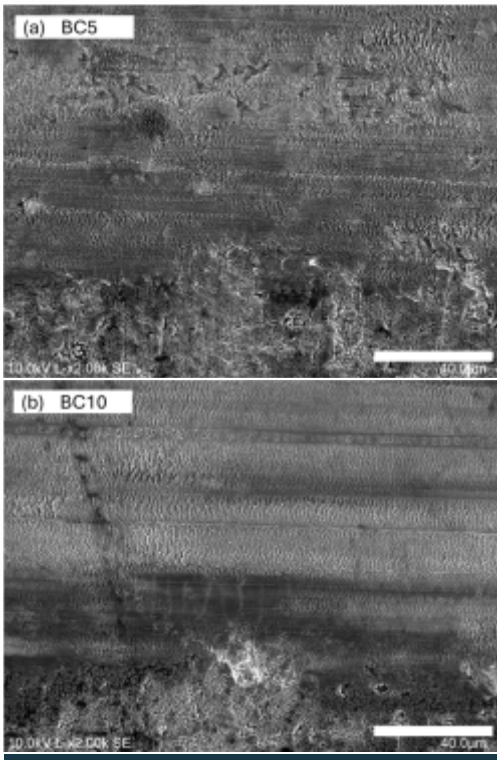

FIGURE 7
Surface SEM micrographs of wear tracks on coating (a) BC5 and (b) BC10.

Aligned with the goals of this study, the optimization of the pre-treatment of the substrate and the dull nickel undercoating resulted in a black coating with enhanced adhesion, as well as promising brightness and coefficient of friction.

CONCLUSION

A double layered black nickel coating was obtained with electrodeposition. In fact, the dull nickel undercoating was a key factor in the improvement of the black nickel coating adhesion. As for the characterisation, the XRD analysis unveiled the amorphous nature of both black coatings. Concerning this, the black coating deposited for 10 min, BC10, showed an overall higher performance. It presented the lowest L*, the closest to absolute black, the least heterogeneous and least rough surface, and a lower COF.

These findings indicate that double-layered black nickel coatings, particularly BC10, offer a promising route for applications where dark appearance and low friction are desirable, such as in decorative hardware or sliding components.

The optimization of deposition parameters presented in this study offers a clear path for improving coating performance while maintaining cost-effectiveness in large-scale production.

Future work will focus on studying the aging process of these coatings to assess their long-term stability and performance under varying environmental conditions.

ACKNOWLEDGEMENTS

This research was sponsored by national funds through FCT - Fundação para a Ciência e Tecnologia, under projects UIDB/00285 - Centre for Mechanical Engineering, Materials and Processes and LA/P/0112/2020. This research was also financed by PRR - Recovery and Resilience Plan and by the Next Generation EU Funds, following NOTICE N.º 02/C05-i01/2022, Component 5 - Capitalization and Business Innovation - Mobilizing Agendas for Business Innovation under the AM2R project "Mobilizing Agenda for business innovation in the Two-Wheel sector" (reference: 7253).

REFERENCES

[1] M. A. Estrella-Gutiérrez, F. I. Lizama-Tzec, O. Arés-Muzio, and G. Oskam, 'Influence of a metallic nickel interlayer on the performance of solar absorber coatings based on black nickel electrodeposited onto copper', Electrochimica Acta, vol. 213, pp. 460-468, Sep. 2016, doi: 10.1016/j.electacta.2016.07.125.

[2] B. P. Kafle et al., 'Optical, structural and thermal performances of black nickel selective coatings for solar thermal collectors', Sol. Energy, vol. 234, pp. 262-274, Mar. 2022, doi: 10.1016/ j.solener.2022.01.042.

[3] J.K. Dennis, T.E. Such, Nickel and Chromium Plating, 2nd edn. (Butterworth-Heinemann, London, 1986).

[4] Nickel Institute. Nickel Plating Handbook-Knowledge for a Brighter Future; Nickel Institute: Toronto, ON, Canada, 2022.

[5] M. Surender, B. Basu, and R. Balasubramaniam, 'Wear characterization of electrodeposited Ni-WC composite coatings', Tribol. Int., vol. 37, no. 9, pp. 743-749, Sep. 2004, doi: 10.1016/ j.triboint.2004.04.003.

[6] X. Li, Q. Shen, Y. Zhang, L. Wang, and C. Nie, 'Wear behavior of electrodeposited nickel/graphene composite coating', Diam. Relat. Mater., vol. 119, p. 108589, Nov. 2021, doi: 10.1016/ j.diamond.2021.108589.

[7] M. Leimbach, C. Tschaar, D. Zapf, M. Kurniawan, U. Schmidt, and A. Bund, 'Relation between Color and Surface Morphology of Electrodeposited Chromium for Decorative Applications', J. Electrochem. Soc., vol. 166, no. 6, pp. D205-D211, 2019, doi: 10.1149/2.0871906jes.

[8] F. Ponte, P. Sharma, N. M. Figueiredo, J. Ferreira, and S. Carvalho, 'Decorative Chromium Coatings on Polycarbonate Substrate for the Automotive Industry', Materials, vol. 16, no. 6, 2023, doi: 10.3390/ma16062315.

EFFECT OF FILLET RADIUS ON THE FRACTURE STRENGTH OF HARDMETALS WITH INCREASING CO CONTENTS

M. Pinto[1*], J. Almeida[1], F. J. Oliveira[1], P. Pereira[2], J. Sacramento[2], L. F. Malheiros[3]

1 Department of Materials Engineering and Ceramics, CICECO Institute of Materials of Aveiro, University of Aveiro, Portugal
2 DURIT Metalurgia Portuguesa do Tungsténio, Lda., Portugal
3 INEGI, Faculty of Engineering, University of Porto, 4200-465 Porto, Portugal

Hardmetals are widely employed in wear-resistant components and metal-forming tools due to their exceptional properties. The geometry of these tools significantly influences their wear behaviour and performance, potentially leading to shortened service life or catastrophic failure under stress. This study shows that smaller fillet radii decrease the fracture strength of hardmetals. The binder content and WC grain size have a non-monotonic effect on the fracture strength, whereas wear resistance decreases with increasing binder content and WC grain size. The findings offer insights into optimizing durability of hardmetal components through an adequate design and changes in the composition of the hardmetal.

KEYWORDS
HARDMETAL; MECHANICAL CHARACTERIZATION; METAL FORMING; FILLET RADIUS.

INTRODUCTION

Hardmetal is a composite material composed of high-hardness tungsten carbide (WC) particles and a ductile metal binder, usually cobalt (Co). These materials have an excellent combination of properties, namely better toughness than ceramic materials and higher hardness than most metal alloys. Their properties can be adjusted to specific requirements by altering the grain size of the WC and the content and composition of the binder phase. The versatility of hardmetals is reflected in their wide range of applications, which includes drilling and mining tools, structural components, wear components, and metal cutting and forming tools [1-4].

Metal forming tools are indispensable in the manufacturing processes of most industries. During the forming and cutting operation, hardmetal tools withstand high cyclic loads and are subject to considerable wear. The geometry of the tools has a significant impact on their wear behaviour and performance, affecting the tool service life. Edges and corners are stress concentration zones with increased wear stresses, that can lead to the catastrophic failure of metal forming tools, requiring early replacement and resulting in decreased productivity [5-7].

This work studies the influence of the fillet radius, at the transition between two distinct cylindrical diameters, on the flexural fracture strength of different hardmetal grades, and the influence of WC grain size and increasing binder content on their wear resistance in unlubricated reciprocating sliding ball-on-flat tests.

MATERIALS AND METHODS

Table 1 presents the composition of the five industrial grades of hardmetal studied, with Co contents between 10 wt.% and 27 wt.% and different WC particle sizes. Sintering methods are also indicated, as well as the physical and magnetic characterization of samples of each composition and the nominal values of the transverse rupture strength (TRS, type C specimens, ISO 3327 standard). All sintered samples showed a microstructure free of defects or porosity (A00B00C00). The designation of the samples indicates their cobalt content in wt. %, followed by the first letter of the classification of the initial FSSS WC powder particle size (F- fine, M- medium, C- coarse).

Table 2 summarizes the methods, standards and equipment used in the characterization of

TABLE 1
Composition and characterization of industrial hardmetal grades.

Grade	Sintering Method	Co content		WC FSSS (μm)	r (g/cm³)	HC Coercive Force (Oe)	FG Ferrite Content (%)	S_m Magnetic Saturation (emu/g)	TRS (Mpa)
		wt.%	vol.%						
10M	SinterHIP	10.0	16.4	2.5 (medium)	14.49	164	8.6	138	3473±81
15F	SinterHIP	15.0	23.8	0.8 (fine)	13.99	165	11.6	143	3216±216
15M	SinterVAC	15.0	23.8	2.5 (medium)	14.01	125	14.3	140	3903±104
18C	SinterVAC	18.0	28.0	4.0*(coarse)	13.81	85	17.7	135	3400±241
27C	SinterVAC	27.0	39.6	4.0*(coarse)	13.05	71	25.2	136	3456±41

* 25% WC x 2.5 μm + 75% WC x 6 μm

TABLE 2
Microstructural and mechanical characterization methods.

Property	Method/Test	Standard	Equipment/Software
Grain size, dwc	Mean Linear Intercept technique	ISO 4499-2	Hitachi SU70 SEM
Hardness, HV	Vickers hardness	ISO 6507	Buehler Wilson VH3300 durometer
Young's modulus, E	Impulse excitation technique	ASTM C 1259	Grindo Sonic Mk5i
Shear modulus, G			
Poisson's ratio, υ			
Fracture strength	Cantilever bending test	-	Zwick/Roell Z020 Load cell: 20 kN (0.033 mm/s)
	FEM simulation		Fusion360 software
Coefficient of friction, CoF	Linear reciprocating ball-on-flat sliding	ASTM G133	Anton Par TRB3 tribometer
Wear rate, k – **Flat specimens**	Vertical Scanning Interferometry (VSI)		SensoFAR S Neox 3D optical profilometer SensoMAP software
Wear rate, k – **Ball specimens**	-		LEICA EZ4HD optical microscope Image J software

hardmetal compositions. The WC grain size was obtained according to ISO 44992 [8], and the mechanical characterization included the determination of the Vickers hardness, the Young's modulus, the shear modulus, and the Poisson's ratio.

The effect of the fillet radius (R) in the fracture strength, determined by a cantilever bending test, was evaluated in specimens with the geometry shown in Figure 1a, for radii of 0.10 mm, 0.25 mm, 0.50 mm, 1.00 mm, and 3.0 mm. These increasing radii correspond to stress concentration factors (Kt) of, respectively: 2.72, 1.94, 1.52, 1.30 and 1.00, calculated based on [9]. For each radius and composition, 10 specimens were tested, and the load was applied at 5 mm from the end of the specimens. These tests were simulated in the Fusion 360 software through the Finite Element Method (FEM), based on the values of the mechanical properties obtained experimentally. An example of the mesh used for simulation is presented in Figure 1b.

Tribological wear tests were carried out in non-lubricated reciprocating sliding contact using DIN 100Cr6 steel balls, with a load of 12 N, for 100 m and 200 m. The parameters of the wear tests are summarized in Table 3 and for each condition, three repetitions were performed. After testing, the wear tracks of the hardmetal samples and the steel balls were analysed to evaluate the wear mechanisms and to calculate the wear volume.

Fig. 1 Technical drawing of the specimens of the fracture tests (a), with a 1 mm fillet radius (R1), and the respective mesh used in the FEM simulation in the Fusion 360 software (b).

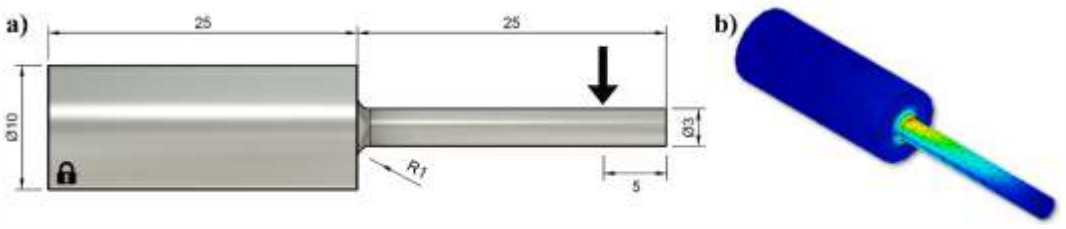

FIGURE 1
Technical drawing of the specimens of the fracture tests (a), with a 1mm fillet radius (R1), and the respective mesh used in the FEM simulation in the Fusion 360 software (b).

TABLE 3
Wear test parameters in non-lubricated linear reciprocating sliding contact.

Ball Specimen	Load (N)	Amplitude (mm)	Frequency (Hz)	Total Sliding Distance (m)	Time (min:s)	Severity (N.m)
DIN 100Cr6 (869 8 Hv2)	**12**	**10**	**5**	**100**	**16:40**	**1200**
				200	**33:20**	**2400**

RESULTS

The results of the microstructural and mechanical characterization of hardmetal compositions are presented in Table 4. The volume-weighted average grain size (dV) [10] is also presented because it represents the contribution of the volume of each grain to the strength of the material more accurately than the average value, dWC. As expected, the binder mean free path strength [11] increases with increasing binder content and grain size, resulting in a decrease in hardness. The remaining properties generally follow the same hardness trend, i.e., decrease with the increase of binder content and grain size, except for the 15M composition which has the highest Young's modulus and the lowest Poisson's ratio.

Table 5 shows the microstructure and the fracture strength results of the different compositions for the various fillet radii, as well as the respective graphical representations, including the simulation results.

In general, the fracture strength increases considerably with the increase of the fillet radius, due to the stress concentration effect, especially between 0.10 mm and 0.5 mm. For the same radius, the fracture strength tends to decrease with increasing cobalt content and tungsten carbide grain size, i.e. in the order: 10M > 15F > 15M > 18C > 27C. For a fillet radius of 0.1 mm, the 18C composition has the highest fracture strength, followed by the 15F composition, that has the highest average fracture strength values for fillet radii up to 0.5 mm. For higher radii (1 mm and 3 mm), the 10M and 15M compositions have higher fracture strengths. The 27C composition has the lowest fracture strength values for all fillet radii.

Note that for the same radius, the variation in the fracture strength between specimens decreases with the increase in binder content and grain size, i.e., the coarser grain grades (18C and 27C) have a better reproducibility of results. This is probably due to their greater fracture toughness, which also results in a lower susceptibility to the fillet radii. Namely, the average fracture strength of the 18C composition is the less dependent on the fillet radius, with an amplitude of 184 N. The remaining compositions have amplitudes of fracture strength between the smallest and the largest radius of 226 N (27C), 240 N (15F), 267 N (15M) and 273 N (10M).

The 15F composition presents the fracture strength values closest to the simulation results. The difference between the simulation results and the experimental results increases with increasing grain size and binder content. The simulation values are closer to the experimental ones in the grades produced in SinterHIP furnaces, presumably due to the elimination of defects and residual closed porosity during the application of external pressure in the HIP treatment. The TRS values were obtained with specimens produced from different batches, which may also contribute to these differences.
Table 6 presents the steady state friction coefficients (CoF) and the specific wear rates of hardmetal samples in sliding contact with steel balls. The CoF decreases with the increase of the binder content, but mainly with the increase of the grain size, as seen by comparing the 15F and 15M compositions. This is probably due to the metallic nature of the binder, with a higher ductility than the WC phase, which better accommodates plastic deformation during sliding wear contact. Higher binder contents represent a larger continuous metallic phase, which contributes to a lower overall friction coefficient. Furthermore, coarser WC grains

TABLE 4
Microstrutural and mechanical charecterization of industrial hardmetal grades.

Composition	Co Content (wt. %)	dwc	dv	l	Hardness (Hv30)	E	G	u
		(mm)				(Gpa)		
10M	10.0	0.87 ± 0.55	2.71	0.38	1414 ± 8	518	265	0.24
15F	15.0	0.52 ± 0.29	1.18	0.30	1313 ± 9	538	215	0.25
15M	15.0	0.82 ± 0.49	2.18	0.47	1191 ± 9	588	237	0.23
18C	18.0	1.15 ± 0.81	3.00	0.76	1019 ± 7	523	212	0.26
27C	27.0	1.15 ± 0.81	3.26	1.02	873 ± 5	514	204	0.26

TABLE 5
Fracture strength for different hardmetal grades with increasing fillet radii.

Microstructure	Fracture Strength	Average FEM Simulation Max-min Range	R (mm)	Fracture Strength (N) Average	Max.	Min.	Simulation
10M		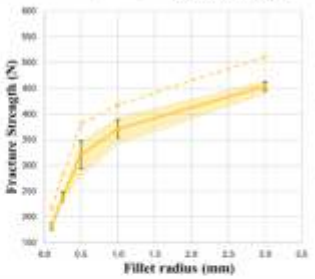	0.10	181 ± 6	190	170	217
			0.25	239 ± 9	252	230	282
			0.50	321 ± 27	346	275	381
			1.00	371 ± 17	395	340	418
			3.00	454 ± 9	464	438	511
15F		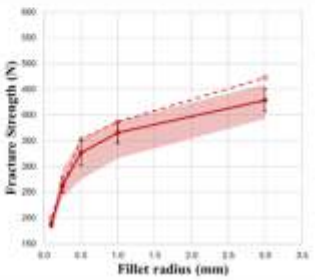	0.10	189 ± 7	197	172	201
			0.25	264 ± 15	293	239	262
			0.50	327 ± 24	355	274	353
			1.00	366 ± 21	388	316	387
			3.00	429 ± 22	459	392	473
15M		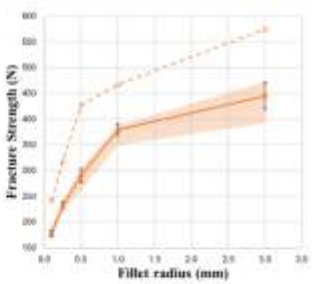	0.10	178 ± 6	188	166	242
			0.25	232 ± 8	245	219	317
			0.50	290 ± 13	306	263	427
			1.00	380 ± 12	388	349	467
			3.00	445 ± 25	473	394	574
18C	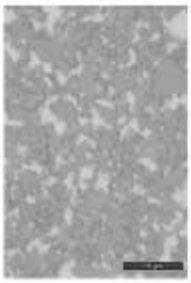	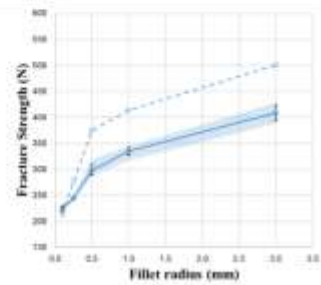	0.10	225 ± 5	232	219	214
			0.25	245 ± 3	249	241	277
			0.50	298 ± 9	317	287	375
			1.00	335 ± 8	343	316	414
			3.00	409 ± 14	427	387	501
27C		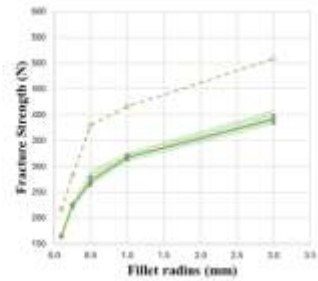	0.10	165 ± 4	170	157	217
			0.25	224 ± 5	230	217	282
			0.50	271 ± 9	292	262	380
			1.00	318 ± 6	327	307	416
			3.00	391 ± 8	408	381	509

TABLE 6
Friction coefficient and wear rate of hardmetal grades in reciprocating sliding contact with steel balls.

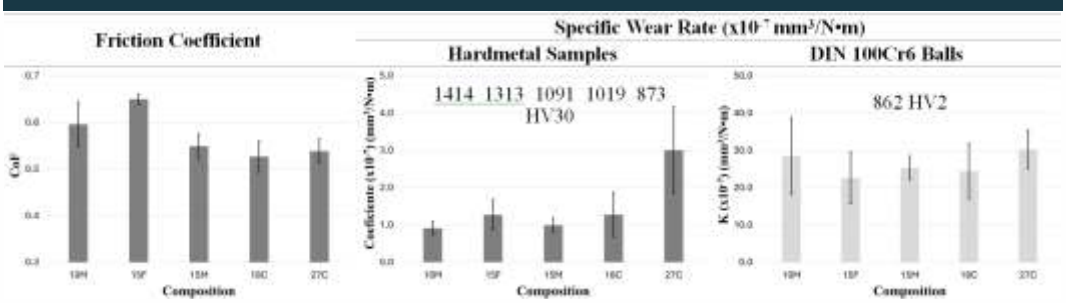

result in fewer WC/Co interfaces, a larger binder mean free path, a lower hardness, and presumably a higher ductility [6, 12].
The CoF values observed for the 15M, 18C and 27C compositions are close to those for non-lubricated steel-on-steel sliding contacts [13]. Under the tested conditions, the specific wear rate increases with increasing cobalt content, due to the decrease of the hardmetals' hardness.

The 27C composition has a much higher wear rate than the remaining hardmetals, possibly due to its lower hardness, closer to that of 100Cr6 steel balls. The specific wear rate of the balls is an order of magnitude higher than that of the hardmetal counter samples and similar for all compositions, including in contact with 27C samples, most likely due to the abrasive effect of the hard WC grains.

CONCLUSIONS

The fracture strength increases with the increase of the fillet radius, and for the same radius, the fracture strength tends to decrease with increasing cobalt content and WC grain size (10M > 15F > 15M > 18C > 27C). The fracture strength of the grades with high binder contents and coarse grains (18C and 27C) shows a lower deviation between specimens than the others and less susceptibility to the fillet radii. The difference between the simulation results and the experimental results increases with the increase of grain size and binder content and is smaller in the grades sintered in SinterHIP furnaces.

The friction coefficient decreases with the increase of WC grain size, and the wear rate of hardmetal samples increases with the increase of cobalt content.

ACKNOWLEDGMENTS

This work was developed within the scope of the projects AM2R - Agenda Mobilizadora para a inovação empresarial do setor das Duas Rodas (Project n. 15 with application number C644866475-00000012), financed by PRR - Plano de Recuperação e Resiliência and by NextGenerationEU funds and CICECO-Aveiro Institute of Materials, UIDB/50011/2020 (DOI 10.54499/UIDB/50011/2020), UIDP/50011/2020 (DOI 10.54499/UIDP/50011/2020) & LA/P/0006/2020 (DOI 10.54499/LA/P/0006/2020), financed by national funds through the FCT/MCTES (PIDDAC).

REFERENCES

1. G. S. Upadhyaya, "1. Introduction", Cemented Tungsten Carbides - Production, Properties, and Testing: William Andrew Publishing/Noyes, 1998.
2. B. Straumal and I. Konyashin, "WC-Based Cemented Carbides with High Entropy Alloyed Binders: A Review", Metals vol. 13, no. 1, pp. 171-171, 2023, DOI: 10.3390/met13010171.
3. I. Y. Konyashin, "Cemented Carbides", Concise Encyclopedia of Self-Propagating High-Temperature Synthesis - History, Theory, Technology, and Products, I. P. Borovinskaya, A. A. Gromov, E. A. Levashov, Y. M. Maksimov, A. S. Mukasyan, and A. S. Rogachev Eds.: Elsevier, 2017, pp. 56-57.
4. J. García, V. Collado Ciprés, A. Blomqvist, and B. Kaplan, "Cemented hardmetal microstructures: a review", International Journal of Refractory Metals and Hard Materials, vol. 80, pp. 40-68, 2019, DOI: 10.1016/J.IJRMHM.2018.12.004.
5. H. Klaasen, J. Kübarsepp, and R. Eigi, "Peculiarities of hardmetals wear in blanking of sheet metals", Tribology International, vol. 39, no. 4, pp. 303-309, 2006, DOI: https://doi.org/10.1016/-j.triboint.2005.01.041.
6. L. Prakash, "1.02 - Fundamentals and General Applications of Hardmetals", Comprehensive Hard Materials, vol. 1, V. K. Sarin Ed. Oxford: Elsevier, 2014, pp. 29-90.
7. I. Velkavrh et al., "Using a standard pin-on-disc tribometer to analyse friction in a metal forming process", Tribology International, vol. 114, pp. 418-428, 2017, DOI: https://doi.org/10.1016/-j.triboint.2017.04.052.
8. Hardmetals - Metallographic determination of microstructure - Part 2: Measurement of WC grain size, ISO 4499-2:2020, I. O. f. Standardization, 2020. [Online]. Available: https://www.iso.org/-standard/74884.html
9. W. D. Pilkey, D. F. Pilkey, and Z. Bi, "Shoulder Fillets", Peterson's Stress Concentration Factors, 4th ed.: John Wiley & Sons, 2020, p. 198.
10. P. Lehto, H. Remes, T. Saukkonen, H. Hänninen, and J. Romanoff, "Influence of grain size distribution on the Hall-Petch relationship of welded structural steel", Materials Science and Engineering: A, vol. 592, pp. 28-39, 2014, DOI: https://doi.org/10.1016/j.msea.2013.10.094.
11. B. Roebuck and E. G. Bennett, "Phase size distribution in WC/Co hardmetal", Metallography, vol. 19, no. 1, pp. 27-47, 1986, DOI: https://doi.org/10.1016/0026-0800(86)90005-4.
12. M. G. Gee, A. J. Gant, B. Roebuck, and K. P. Mingard, "1.12 - Wear of Hardmetals", in Comprehensive Hard Materials, V. K. Sarin Ed. Oxford: Elsevier, 2014, pp. 363-383.
13. W. F. Gale and T. C. Totemeier, "25 Friction and wear", Smithells Metals Reference Book (8th Edition): Elsevier, 2006, pp. 25-24.

Urban Commute: Redefining Two-Wheel Mobility with Advanced Textile-based Products

URBAN COMMUTE

Functional, interactive, and textile-based smart solution to improve safety for two-wheeled vehicles mobility on urban settings

Garment's active lighting, backpack's modularity and sensor integration, and handles' unobtrusive control electronics

Sustainable textile-based composites engineered from recycled polyester fibres and bi-component materials

www.citeve.pt

Product development is conducted under PPS48, a component of the Two-Wheel Mobilizing Agenda (AM2R) project.

AM2R

TMG TEXTILES

citeve TEXTILE TECHNOLOGY

centi

PRR Plano de Recuperação e Resiliência

REPÚBLICA PORTUGUESA

Financiado pela União Europeia NextGenerationEU

ADJUSTING THE CHARACTERISTICS OF LIGHT ALLOYS FOR THE PRODUCTION OF FORGINGS

Rui Madureira[1], Gonçalo Soares[1], Rui L. Amaral[1], José A. Silva[2], Sérgio Silva[2], Ana Reis[1,3]
1 INEGI, Rua Dr. Roberto Frias, 4200-465 Porto, Portugal. Email: rdmadureira @inegi.up.pt
2 Ibérica S.A., Vale do Grou, 3750-064 Águeda, Portugal
3 FEUP, Rua Dr. Roberto Frias, 4200-465 Porto, Portugal

Since forged parts are used in safety components, a rigorous selection of the alloys is required. In this work, two aluminium alloys that are commonly used in casting were used: A356 and 357. To assess the feasibility of using these alloys in forging, preforms were produced using gravity die casting. These preforms were then used to produce forgings. The microstructures and mechanical properties of both alloys were analysed in the preforms and in the parts with and without T6 heat treatment. The 357 alloy forgings showed higher mechanical properties than the A356 alloy forgings in both the untreated and treated states. Microstructure analysis revealed that forging leads to a reorientation of the grains.

KEYWORDS
ALUMINIUM ALLOYS; A356; 357; FORGING.

INTRODUCTION

The production of forged components for safety systems requires special care in the choice of preforms and alloys.

When producing complex geometries through forging, several steps are required before the preform reaches the desired final geometry. This is due to the fact that preforms are usually regular and therefore do not allow for direct forming [1].

With casting, it is possible to obtain preforms with geometries very close to the final shape of the part, and intermediate forging operations can be avoided, which translates into savings in wasted material and a reduction in costs related to the production of the components.

Combining the casting and forging processes is therefore a solution that allows the challenges underlying each process to be overcome [2, 3].
For this work the A356 and 357 alloys from the Al-Si alloy family were chosen, which are widely used in casting and have also been explored in limited forging applications. These alloys are widely used in industrial applications thanks to their good casting properties, good resistance to corrosion, low tendency to hot cracking, low coefficient of thermal expansion and because they are resistant to wear [4, 5].

MATERIALS AND METHODS

Cylindrical preforms were produced by gravity die casting in the A356 and 357 alloys. Alloy 357 was produced by adding pure magnesium to the A356 alloy ingot. Al10Sr and Al5Ti1B master alloys were added after degassing to the bath of both alloys to modify the silicon and refine the grain, respectively.

The preforms were used to produce forgings with the geometry presented in Figure 1. The preforms had to be preheated to 530°C for 1 hour in order to undergo a bending process before forging. The forging dies were heated to 190°C and graphite-based lubricant was used between each clamping of the dies.

FIGURE 1
Forged component used in the safety system.

Part of the produced forgings were subjected to T6 heat treatment - solution treatment at 540°C for 6 hours, quenching in water and artificial ageing at 160°C for 6 hours.

TABLE 1
Chemical composition of the alloys under study (% wt).

Alloy	Si	Fe	Cu	Mn	Mg	Zn	Ti	Sr	Cr	Al
A356	6.61	0.11	0.001	0.002	0.21	-	0.12	0.037	0.001	92.90
357	6.56	0.12	0.001	0.004	0.51	0.002	0.21	0.040	0.001	92.50
A356 Ingot	6.82	0.13	0.001	0.001	0.26	-	0.11	0.022	0.003	92.60

The following analyses were performed: chemical composition (Table 1) by optical emission spectrometry, only on the ingot and preforms, Brinell hardness (HB10) on 16 samples (8 preforms and 8 parts), microstructure using an optical microscope and tensile tests according to standard ISO 6892-1:2019 using 48 specimens.

RESULTS AND DISCUSSION

The hardness values obtained are shown in Figure 2.

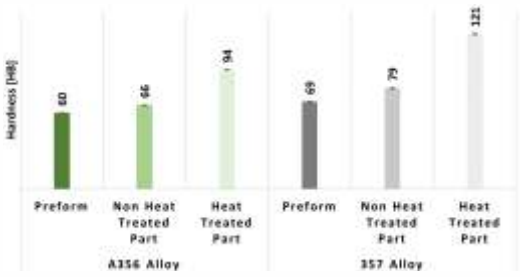

FIGURE 2
Hardness of A356 and 357 preforms and forgings with and without heat treatment.

According to the values in the EN1706:2020 standard shown in Table 2, the hardnesses obtained after heat treatment are in line with the stipulated value. However, it is important to emphasise that the hardness indication given in the standard is for parts obtained by gravity casting.

TABLE 2
Hardnesses presented in standard EN1706:2020.

Standard	Alloy	Hardness [HB]
EN1706:2020	A356-T6	> 90
	357-T6	> 100

The hardness of alloy 357, before and after heat treatment, is higher than that of alloy A356 due to the higher percentage of magnesium. This alloying element is responsible for forming the phases (e. g.: Mg2Si) that give the alloy increased hardness and mechanical strength. The response of the A356 alloy to the heat treatment that was carried out may be different to that of the 357 alloy, and therefore it may not have reached peak hardness or may be in an overaged state, characterised by a decrease in hardness.

The microstructure of the preforms (Figure 3) is characterised by the dendritic aluminium phase and the non-lamellar eutectic silicon. Modification with strontium was not enough to eliminate some acicular morphologies.

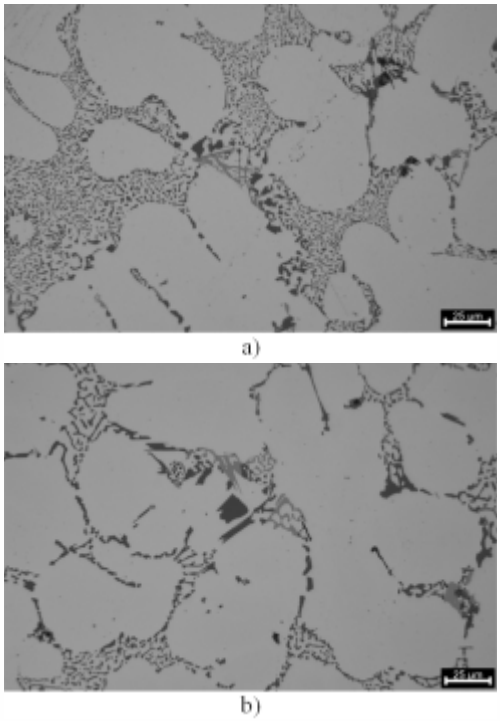

FIGURE 3
Microstruture of the preforms: (a) A356 alloy; (b) 357 alloy.

In the microstructures of the forgings (Figure 4) it is not possible to observe any difference between the two alloys. In the samples subjected to the T6 heat treatment (figures (b) and (d)) it is possible to observe the globulisation of the eutectic silicon. This morphology is due to the solution treatment where there is a transformation of the non-lamellar/acicular silicon morphology into a globular morphology, which enhances ductility. However, in the samples that have not been heat-treated, partial globularisation of silicon is also observed, probably initiated during preheating. Preheating the preform before bending may have caused this onset of globulisation.

When comparing Figures 3 and 4, it is possible to see that with forging there is a reorientation of the grains caused by the forces exerted during the process.

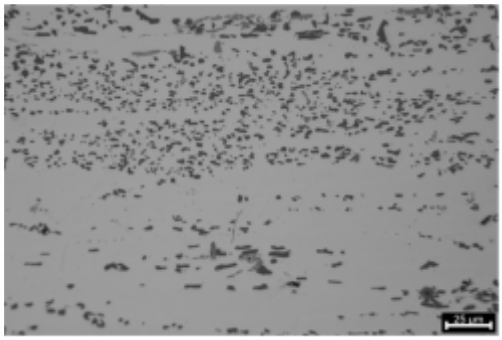

(a)

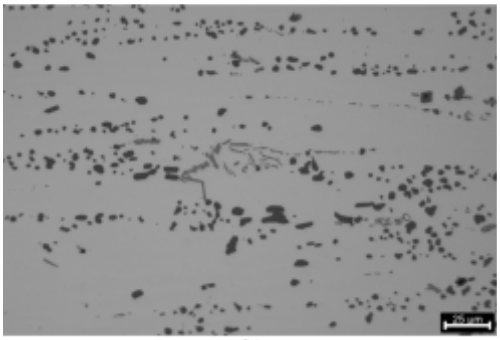

(b)

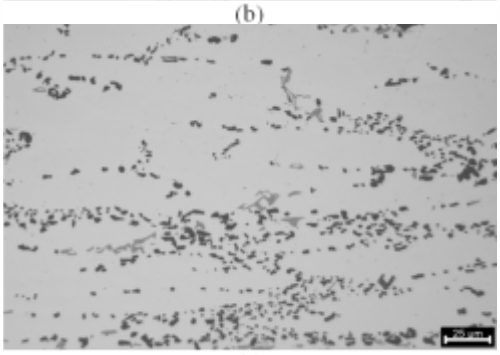

(c)

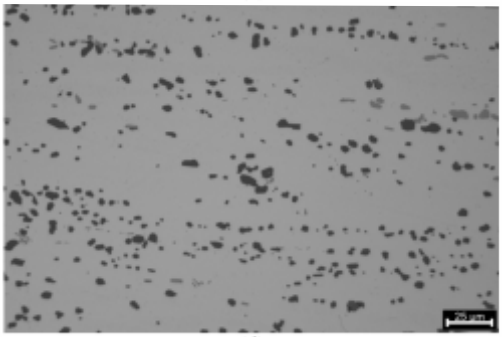

(d)

FIGURE 4
Microstructures of the forgings under study: (a) A356 alloy w/o HT; (b) A356 alloy w/ HT; (c) 357 alloy w/o HT; (d) 357 alloy w/ HT.

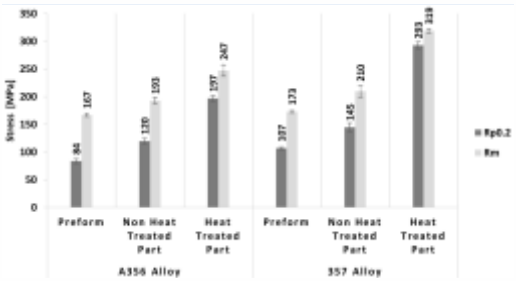

FIGURE 5
Yield stress (Rp0.2) and ultimate tensile strength (Rm) of the A356 and 357 alloys.

As can be seen from the graph in Figure 5, the mechanical properties of the forgings are superior to those of the preforms. With the T6 heat treatment there is an increase of 64% and 28% in the yield and tensile strength, respectively, for the A356 alloy, while for the 357 alloy these increases were higher, 102% and 52% respectively.

CONCLUSIONS

After carrying out this work, the following conclusions can be drawn:

- Forging results in a reorientation of the grains;
- Due to the higher percentage of magnesium in the 357 alloy, it has higher hardness values than the A356 alloy, both in the forged condition and after heat treatment;
- The T6 heat treatment led to an improvement in the mechanical strength and hardness of both alloys. 357 alloy showed higher mechanical strength than A356 alloy, making it the main choice for components subjected to high loads.

ACKNOWLEDGEMENTS

The authors gratefully acknowledge the funding of AM2R - Agenda Mobilizadora para a Inovação Empresarial do Setor das Duas Rodas (02-C05-i01.01-2022.PC644866475-00000012), co-funded by the Plano de Recuperação e Resiliência (PRR), through financial support of the Portuguese Republic and the European Union's NextGenerationEU.

REFERENCES

[1] Kitayama, S., Technical review on design optimization in forging. The International Journal of Advanced Manufacturing Technology, 2024. 132(9): p. 4161-4189. https://doi.org/10.1007/s00170-024-13593-w.

[2] Kodippili, T., et al., Multi-objective optimization of a cast-preform shape for a magnesium alloy forging application. The International Journal of Advanced Manufacturing Technology, 2023. 129(7): p. 3221-3232. https://doi.org/10.1007/s00170-023-12478-8.

[3] Usrinus, J., et al. Hot forming of cast steel cylinders. in Conference Proceedings of the 28th International Conference on Metallurgy and Materials, METAL2019, Brno, Czech Rep. 2019. https://doi.org/10.37904/metal.2019.820.

[4] Loong, C.A., et al., Semi-Solid Casting and Forging of A357 Aluminum Alloy Components, in Proceedings of the 7th International Conference on Semi-Solid Processing of Alloys and Composites 2002. 2002.

[5] Mallapur, D.G., et al., Studies on Wear Properties of Forged A356 Alloy with Addition of Grain Refiner and/or Modifier. Procedia Materials Science, 2014. 5: p. 130-136. https://doi.org/10.1016/j.mspro.2014.07.250.

MATERIAIS 2027

Materials for a Better Future

22 A 24 DE MARÇO

ISEP . INSTITUTO SUPERIOR DE ENGENHARIA DO PORTO

A conferência MATERIAIS 2027, que integra o XXIII Congresso da Sociedade Portuguesa de Materiais e o XIV International Symposium on Materials. O evento reunirá estudantes, investigadores e profissionais da área dos materiais, proporcionando um fórum de excelência para a apresentação e discussão dos mais recentes avanços científicos e tecnológicos em Ciência e Engenharia de Materiais, com especial enfoque na **sustentabilidade e reciclabilidade.**

O MATERIAIS 2027 contará com um programa técnico-científico de elevada qualidade, que incluirá:
ESCOLA + PALESTRAS PLENÁRIAS E CONVIDADAS + COMUNICAÇÕES ORAIS, SELECIONADAS + SESSÕES DE POSTERS

materiais2027@isep.ipp.pt **https://congressomateriais.pt/**

ALUMINIUM ALLOYS 6XXX IN THE BICYCLE INDUSTRY: AA6061 AND POSSIBLE ALTERNATIVES

Fábio Vidal[1], César Coutinho[1], Luís Mota[2]
1 BIKiNNOV - Bike Value Innovation Center Association, Rua da Indústria, 369, Covão, 3750-792, Águeda, Portugal
2 Hydro Aluminium Extrusion Portugal, Travessa das Alheiras, 216, 4415-272, V.N. Gaia Pedroso

The 6xxx series aluminium alloys, particularly AA6061, are extensively used in bicycle frames due to their high strength, corrosion resistance, fatigue performance, and weldability. Maximize mechanical properties through heat treatment and alloying strategies remains a challenge. This work evaluates the response of AA6061 and alternative 6xxx series alloys to different heat treatment conditions, aiming to enhance their mechanical properties. Hardness measurements (HBW 2,5/62,5), chemical composition analysis through optical emission spectroscopy (OES) and uniaxial tensile testing examinations were performed. Results demonstrate correlations between the heat treatment parameters and the alloys mechanical and microstructural characteristics.

KEYWORDS
ALUMINIUM 6XXX ALLOYS; HEAT TREATMENT; MGSI; PRECIPITATION HARDENING.

INTRODUCTION

The aluminium alloys 6xxx (Al-Mg-Si alloys) had a considerable employment in the bicycle industry over the years. The AA6061 is predominant, especially in bicycle frames, but the search for alternative alloys is continuous [1]. The AA6xxx series alloys are valued for their tensile properties, corrosion resistance, fatigue strength, weldability, formability, extrudability and resistance to stress-corrosion cracking [2].

The aluminium is extracted from bauxite, a residual rock present in Earth's crust [3]. From bauxite to aluminium, the 2 main processes comprise the Bayer process, where alumina (Al2O3) is produced from bauxite, and the Hall-Héroult process, that involves the electrolysis of alumina and the conversion to primary liquid aluminium [4]. After this, normally follows a remelting in a furnace where alloying elements are added in the desired concentrations, ending with the product being casted in ingots or billets [4, 5]. Temperature is a key factor in extrusion, influenced by billet temperature, heat transfer, and frictional heating [2].

Pressure loads, related to flow stress, internal shearing, and friction, also play a crucial role [2]. Higher billet temperatures lower extrusion pressures by reducing flow stress, easing deformation, and benefiting post-extrusion quenching. Lower billet temperatures reduce friction but have less impact on lowering pressures. The choice depends on the desired mechanical properties and surface finish. Extrusion speed affects cooling rates, influencing mechanical properties and surface quality, making controlled speeds essential [2].

Post-extrusion heat treatments are crucial for defining the mechanical properties of AA6xxx alloys, influencing precipitation kinetics, phase distribution, and microstructural stability [6]. The interaction between extrusion-induced dislocations and heat treatment affects strength, ductility, and surface quality [6]. Alloys like AA6082 rely on precipitation hardening, where solution treatment dissolves alloying elements, quenching prevents premature precipitation, and aging controls phase formation [7]. Processes such as T4 and T6 treatments regulate the precipitation of strengthening phases like Mg and Si clusters [7]. MgSi is the key strengthening phase in 6xxx aluminium alloys, enhancing mechanical properties through precipitation hardening [8]. Heat treatment induces a sequence starting with a supersaturated solid solution (SSSS), followed by Guinier-Preston (GP) zones and the primary strengthening phase, (coherent MgSi), which significantly increases hardness and strength [8, 9]. With aging,transitions to (semi-coherent) and finally to -MgSi (equilibrium phase) [8, 9] phase effectively

TABLE 1
Key differences between b'', b', and b-Mg_2Si Phases.

Phase	Size & Shape	Strengthening Effect	Formation Stage
β'' (Beta Double Prime)	Very fine, needle-like, <10 nm	Most effective for strengthening	Early artificial aging (T6 treatment)
β' (Beta Prime)	Larger rods (~20-50 nm)	Moderate strengthening	Intermediate stage, after β''
β-Mg_2Si	Coarse precipitates (>100 nm)	Weak strengthening	Over aging or equilibrium phase

hinders dislocation movement, while the coarser phase reduces ductility and may act as a stress concentrator, limiting strengthening [8, 9, 10]. Table 1 presents key characteristics of each one of these phases.

The precipitation of MgSi is influenced by temperature, time, and alloying elements like Cu, Mn, Cr, and Fe. To refine its distribution and size, two heat treatments are commonly used: solution treatment + natural aging (T4) and solution treatment + artificial aging (T6). Solution treatment at 530-550 °C dissolves Mg and Si into the matrix, forming a homogeneous solid solution. Rapid quenching retains these elements, while artificial aging at 160-180 °C for several hours initiates the precipitation sequence [9, 10].

The morphology of MgSi precipitates depend on cooling rates and alloying elements. In as-cast alloys, it forms dendritic structures, while equilibrium solidification produces polyhedral or octahedral shapes. During heat treatment, MgSi typically appears as needle or plate-like precipitates [10, 11].

Solution treatment and artificial aging ensure optimal distribution for peak performance [9]. However, heat treatment effectiveness depends on prior extrusion, as dislocations and solute distribution influence precipitation kinetics, affecting strength and ductility [6]. Understanding factors that control MgSi morphology and stability is key to developed aluminium alloys with improved properties.

METHODS AND EXPERIMENTAL PROCEDURES

ALLOY SAMPLES

HYDRO conducts research for alternative alloys to AA6061, enhancing mechanical performance and formability. Even within the same alloy range, minor composition variations affect microstructure and production processes [12]. This study characterized 4 HYDRO-supplied alloys, widely used in the bicycle industry: AA6061 (1 Rod and 2 hollow profiles), HHS400 (Rod), HHY320 (Hollow), and Recycled300/R300 (Hollow).

HEAT TREATMENTS CONDITIONS

Samples underwent heat treatments to maximize mechanical properties, with parameters based on literature [13, 14, 15, 16] and internal trials. They were heated to 550 °C for 45 minutes, then water-quenched and naturally aged (considered the T4 stage). One batch was stored at 18-25 °C and environmental humidity before artificial aging (170 °C for 12 hours), while the other was submitted to artificial aging just one hour after solution heat treatment, to perform the T6.

TABLE 2
Chemical composition results.

Chemical element	Chemical Composition (wt.%)					
	6061 ROD	HHS400 ROD	6061 A (1196)	6061 B (1589)	HHY320	R300
Si	0,53 ±0,061	1,0 ±0,12	0,51 ±0,059	0,50 ±0,058	0,65 ±0,076	0,59 ±0,069
Fe	0,26 ±0,033	0,29 ±0,037	0,23 ±0,029	0,22 ±0,027	0,26 ±0,033	0,26 ±0,033
Cu	0,26 ±0,040	0,43 ±0,067	0,20 ±0,031	0,20 ±0,031	0,11 ±0,020	0,22 ±0,034
Mn	0,051 ±0,015	0,63 ±0,10	0,045 ±0,015	0,045 ±0,015	0,030 ±0,014	0,071 ±0,017
Mg	0,73 ±0,11	0,79 ±0,13	0,69 ±0,11	0,73 ±0,11	0,83 ±0,13	0,63 ±0,095
Cr	0,044 ±0,017	0,089 ±0,041	0,048 ±0,019	0,049 ±0,019	0,013 ±0,0048	0,020 ±0,0072
Ni	0,0047 ±0,0017	0,0044 ±0,0011	0,0039 ±0,00095	0,0037 ±0,00089	0,0031 ±0,00078	0,0042 ±0,0010
Zn	0,036 ±0,0089	0,055 ±0,014	0,17 ±0,044	0,17 ±0,044	0,0066 ±0,0017	0,046 ±0,011
Ti	0,017 ±0,0039	0,022 ±0,0051	0,015 ±0,0035	0,015 ±0,0034	0,015 ±0,0034	0,017 ±0,0040

CHEMICAL COMPOSITION, HARDNESS AND TENSILE STRENGTH TESTS

Sample characterization included chemical and mechanical analyses. Optical emission spectroscopy (OES) identified elemental composition, while Brinell hardness (HBW 2,5/62,5) and uniaxial tensile tests evaluated mechanical strength.

RESULTS AND DISCUSSION

CHEMICAL COMPOSITION ANALYSIS

Table 2 resumes the chemical composition of the tested alloys.

HHS400 shows the highest elemental variation, with elevated Si, Cu, Mn and Cr, which contributes to solid solution strengthening, grain refinement, and increased hardness [17]. HHS400's higher Mn and Cr levels suggest superior hardness and strength, with limited ductility impact [17]. R300, HHY320 and 6061 alloys, with moderate Si and Mg levels, rely primarily on MgSi precipitation hardening and Si for solid solution strengthening and microstructural refinement [17, 18], although higher zinc content in 6061 A and B alloys may contribute to improve mechanical properties through precipitation hardening [8, 17]. Lower Fe, Mn, and Cr and higher Mg/Si in HHY320 levels suggest reduced density compared to 6061. Despite similar Mg/Si ratios, HHY320's higher absolute Mg and Si content may enhance hardness and strength after T6 due to increased MgSi precipitation [13, 15, 19].

HARDNESS TESTS

Comparing alloys with different compositions and geometries is usually challenging due to variations in microstructure, properties, and processing. Nevertheless, hardness tests were performed at key stages: as-received (F state); post-T4 heat treatment (550 °C for 45 min); and post-T6 heat treatment after T4 (170 °C for 12h). To ensure accurate comparison, samples were classified into hollow and rod profiles. The hardness results for the F state are presented in Figure 1.

Hardness in the as-fabricated (F) condition is influenced by solid solution strengthening, extrusion-induced work hardening, and alloy composition [6]. R300 and 6061 Rod exhibit the highest hardness, attributed to strong MgSi precipitation potential. 6061 Hollow shows slightly lower hardness, likely due to extrusion strain retention [2, 6]. HHY320, despite higher Mg and Si content, has lower Mn and Cr levels, which reduces grain boundary strengthening and promotes dynamic recovery during extrusion, leading to greater ductility in F condition, while HHS400 records the lowest hardness, indicating that its Mn and Cr content enhances aging response rather than immediate strengthening in extruded state [15]. HHY320's lower hardness in extruded state indicates higher ductility, making it suitable for forming prior to artificial aging [6].

T4 and T6 heat treatments followed different approaches. T4 solubilization was applied, and

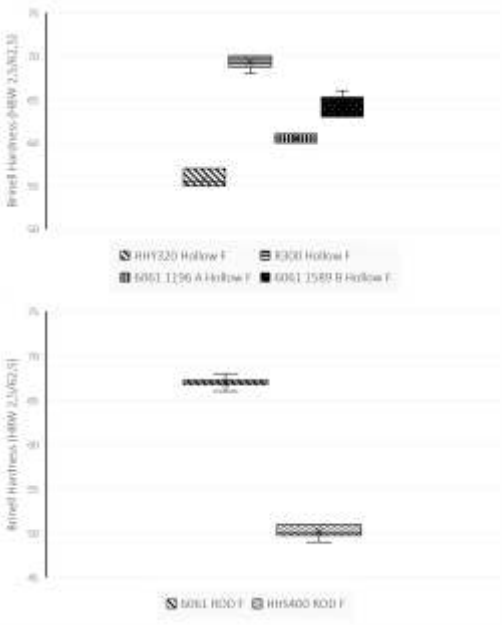

FIGURE 1
Hardness comparation between HHY320, R300, 6061 A, 6061 B (Hollow), and HHS400, 6061 (ROD), on F state.

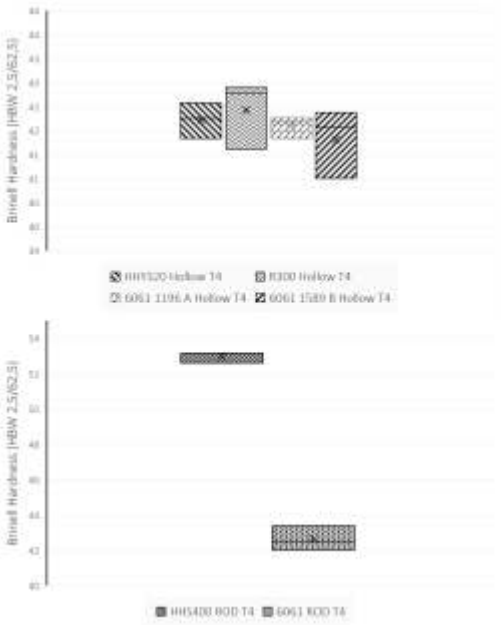

FIGURE 2
Hardness comparation between HHY320, R300, 6061 A, 6061 B (Hollow), and HHS400, 6061 (ROD), after T4 state.

hardness was measured post-treatment (Figure 2). Results deviate from F-state values, indicating that extrusion variables influence final microstructure differently than solubilization treatment.

After T4 treatment, all alloys except HHS400 showed hardness between 40 and 44 HBW, while HHS400 exceeded 50 HBW. This variation is attributed to extrusion effects, elemental composition, and precipitation kinetics. Initial hardness in the as-fabricated (F) condition resulted from solid solution strengthening, work hardening, and residual strain. During T4, MgSi precipitates dissolve to homogenize the microstructure, reducing hardness. However, HHS400's higher hardness may result from higher Mn content, which refines grains, stabilizes the microstructure, and limits recrystallization, allowing retention of some strength even after solution treatment [15]. Cu could also have had an important role in enhancing hardness and refining the microstructure by influencing the precipitation sequence, facilitating the formation of Cu containing precipitates [15].

For artificial aging, the study assessed the effect of natural aging on final properties. One set of samples underwent T6 after a 1-hour gap (T4-1hour-T6), while another had an 8-day gap (T4-8days-T6). Both sets were tested using machined specimens, with results presented in Figure 3.

Figure 3 shows that shorter intervals between solution treatment and artificial aging lead to higher hardness, while longer delays reduce the

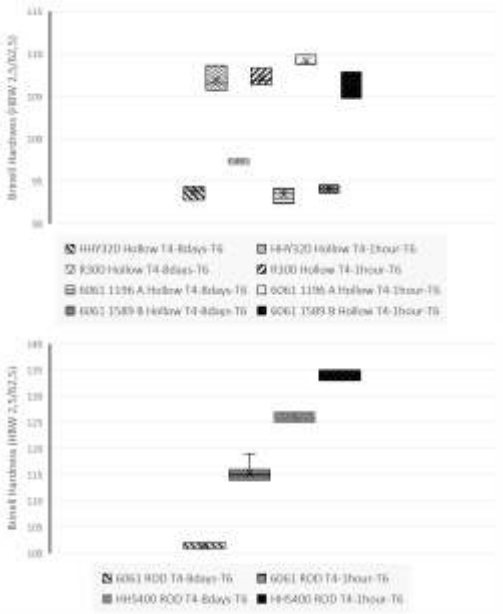

FIGURE 3
Hardness comparation between HHY320, R300, 6061 A, 6061 B (Hollow), and HHS400, 6061 (ROD), after T4+T6 state.

T6 strengthening effect. Immediate artificial aging after solution treatment retains more solute for precipitation, maximizing hardness. In contrast, extended intervals allow partial precipitation before artificial aging, reducing solute supersaturation and limiting formation, leading to lower peak hardness [7]. HHS400 exhibits the highest hardness post-T6, likely due to its higher Si, Cu, Mn and Cr content. 6061, HHY320, and R300 exhibit similar MgSi precipitation behaviour in the T6 condition.

TENSILE TESTS

Following the hardness tests, specimens underwent uniaxial tensile testing in two conditions, both post-T6. As in previous tests, one set was tested after a 1-hour gap between solution treatment and artificial aging (T4-1hour-T6), while the other had an 8-day gap (T4-8days-T6). Ultimate tensile strength (UTS) and 0.2% offset yield strength (Rp0.2%) were measured for each alloy, with results presented in Figure 4.

The uniaxial tensile test results aligned with the hardness measurements for the same sample sets. Ultimate tensile strength (UTS) and 0.2% offset yield strength (Rp0.2%) strongly correlated with the aging interval between solution treatment and artificial aging. The 1-hour gap between solution treatment and artificial aging maximized mechanical properties, confirming that immediate artificial aging enhances precipitation and strengthens 6xxx aluminium alloys [7].

HHS400 exhibited the highest UTS and Rp0.2%, highlighting the role of alloying elements in 6xxx series alloys, particularly compared to AA6061. HHY320 and R300 maintained a balanced strength-ductility ratio but showed no significant improvements over AA6061. Adjusting aging time, temperature, or introducing additional treatments could improve precipitation distribution and mechanical performance in these alloys [6, 16, 18].

CONCLUSIONS AND FUTURE PERSPECTIVES

This study analysed the effects of heat treatment parameters on the mechanical properties and microstructure of AA6061 and alternative 6xxx-series aluminium alloys used in the bicycle industry. Chemical composition analysis, hardness testing, and tensile testing established correlations between heat treatment conditions and material performance, aligning with the expected precipitation sequence (SSSS GP zones -MgSi). Solution heat treatment and quenching, followed by artificial

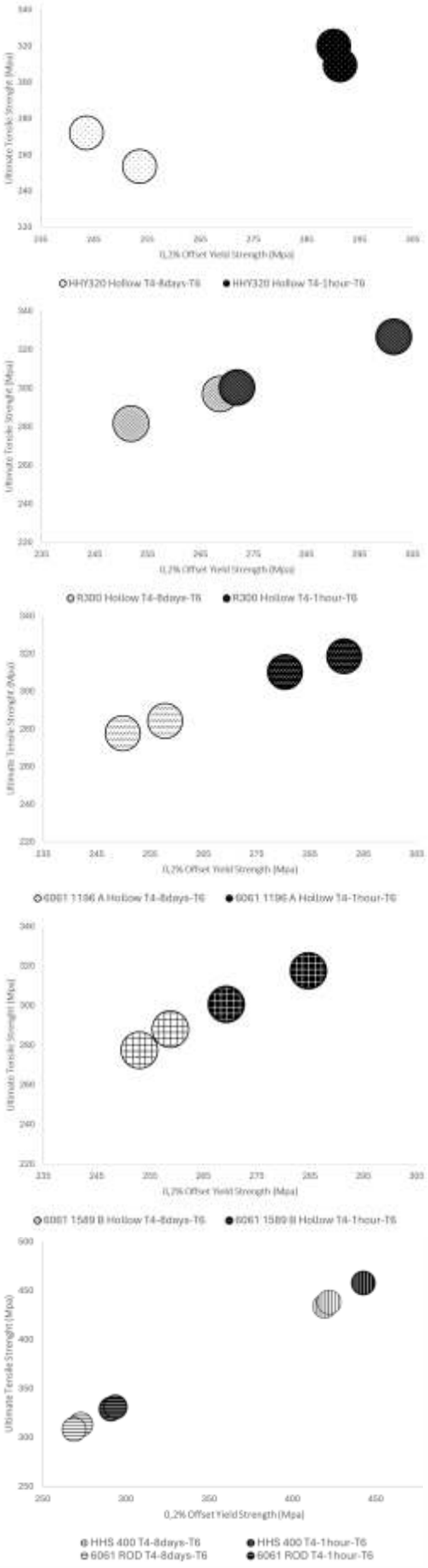

FIGURE 3
Hardness comparation between HHY320, R300, 6061 A, 6061 B (Hollow), and HHS400, 6061 (ROD), after T4+T6 state.

aging with shorter intervals led to higher hardness and strength, due to precipitates distribution.

The influence of alloying elements, like Si, Cu, Mn and Cr, was evident, with HHS400 exhibiting the highest hardness. HHY320 show potential to be a viable alternative to AA6061 for applications requiring greater formability. R300 demonstrated competitive mechanical properties, supporting its potential for sustainable fabrication. HHY320 and R300 did not achieve optimal results with this heat treatment sequence, indicating that alternative temperatures and aging times should be explored.

The strong correlation between tensile strength and hardness confirms hardness as a reliable predictor of mechanical performance.

Future research should incorporate advanced microstructural characterization techniques (SEM, STEM, TEM) to distinguish from and phases, providing critical insights into their morphology and interaction with the aluminium matrix. Additionally, further studies precipitation kinetics, extrusion parameters, and alternative alloy compositions could facilitate the development of next-generation materials with improved performance and sustainability for bicycle frame applications.

REFERENCES

[1] R. Bansal and B. Altaf, "Lightweight, Cost-Effective, and Environmentally Friendly Materials for a Mountain Bicycle Frame during High-Impact Riding: A Comparative Analysis of Traditional Aluminum, Aluminum 6013, and a BioMid FiberTM Composite," 2023, doi: 10.35702/msci.10022.

[2] K. Delijic, V. Asanovic, and D. Radonjic, "The influence of the extrusion process and heat treatment on the properties of some AA6XXX extruded profiles, "*Materiali in tehnologije (MTAEC9)*, vol. 39, no. 4, pp. 101-106, 2005.

[3] F. M. Meyer, "Availability of Bauxite Reserves, "*Natural Resources Research*, vol. 13, no. 3, Sep. 2004.

[4] H. Alamdari, "Aluminium production process: Challenges and opportunities,"Apr. 11, 2017, *MDPI AG*. doi: 10.3390/met7040133.

[5] K. Dhoska et al., "Manufacturing Process of the Aluminum Alloy AA6063 for Engineering Applications,"*Journal of Integrated Engineering & Applied Sciences*, vol. 1, no. 1, pp. 1-13, 2023, doi: 10.5281/zenodo.10655539.

[6] P. Mukhopadhyay, "Alloy Designation, Processing, and Use of AA6XXX Series Aluminium Alloys, "*ISRN Metallurgy*, vol. 2012, pp. 1-15, Apr. 2012, doi: 10.5402/2012/165082.

[7] T. A. Baser, "Effect of aging parameters on the mechanical properties of naturally aged Al-Mg-Si alloy,"*Materwiss Werksttech*, vol. 46, no. 8, pp. 829-834, Aug. 2015, doi: 10.1002/mawe.201500342.

[8] S. J. Andersen, C. D. Marioara, J. Friis, S. Wenner, and R. Holmestad, "Precipitates in aluminium alloys," Jan. 01, 2018, *Taylor and Francis Ltd*. doi: 10.1080/23746149.2018.1479984.

[9] R. Kahlenberg, T. Wojcik, G. Falkinger, A. L. Krejci, B. Milkereit, and E. Kozeschnik, "On the precipitation mechanisms of -MgSi during continuous heating of Aa6061,"*Acta Mater*, vol. 261, Dec. 2023, doi: 10.1016/j.actamat.2023.119345.

[10] G. Asghar, L. Peng, P. Fu, L. Yuan, and Y. Liu, "Role of MgSi precipitates size in determining the ductility of A357 cast alloy,"*Mater Des*, vol. 186, Jan. 2020, doi: 10.1016/j.matdes.2019.108280.

[11] C. Li, Y. Y. Wu, H. Li, and X. F. Liu, "Morphological evolution and growth mechanism of primary MgSi phase in Al-MgSi alloys,"*Acta Mater*, vol. 59, no. 3, pp. 1058-1067, Feb. 2011, doi: 10.1016/j.actamat.2010.10.036.

[12] E. H. Bartawi, C. D. Marioara, G. Shaban, C. Hatzoglou, R. Holmestad, and R. Ambat, "Atomic Structure of Hardening Precipitates in Al-Mg-Si Alloys: Influence of Minor Additions of Cu and Zn,"*ACS Nano*, vol. 17, no. 23, pp. 24115-24129, Dec. 2023, doi: 10.1021/acsnano.3c09129.

[13] N. M. Siddesh Kumar, Dhruthi, G. K. Pramod, P. Samrat, and M. Sadashiva, "A Critical Review on Heat Treatment of Aluminium Alloys,"*Mater Today Proc*, vol. 58, pp. 71-79, Jan. 2022, doi: 10.1016/j.matpr.2021.12.586.

[14] D. Maisonnette, M. Suery, D. Nelias, P. Chaudet, and T. Epicier, "Effects of heat treatments on the microstructure and mechanical properties of a 6061 aluminium alloy,"*Materials Science and Engineering: A*, vol. 528, no. 6, pp. 2718-2724, Mar. 2011, doi: 10.1016/j.msea.2010.12.011.

[15] E. Tan and B. Ogel, "Influence of Heat Treatment on the Mechanical Properties of AA6066 Alloy, «*Turkish Journal of Engineering and Environmental Sciences*, vol. 31, pp. 53-60, 2007.

[16] F. Ozturk, A. Sisman, S. Toros, S. Kilic, and R. C. Picu, "Influence of aging treatment on mechanical properties of 6061 aluminum alloy, "*Mater Des*, vol. 31, no. 2, pp. 972-975, Feb. 2010, doi: 10.1016/j.matdes.2009.08.017.

[17] R. S. Rana, R. Purohit, and S. Das, "Reviews on the Influences of Alloying elements on the Microstructure and Mechanical Properties of Aluminum Alloys and Aluminum Alloy Composites,"*International Journal of Scientific and Research Publications*, vol. 2, no. 6, 2012, [Online]. Available: www.ijsrp.org

[18] K. Pal and S. Chauhan, "Influence of Heat Treatment on the Mechanical Properties of Aluminium Alloys (6xxx Series): A Literature Review,"*International Journal of Engineering Research & Technology (IJERT)*, vol. 6, pp. 386-389, Mar. 2017, [Online]. Available: www.ijert.org

[19] J. Buha, R. N. Lumley, and A. G. Crosky, "Microstructural Development and Mechanical Properties of Interrupted Aged Al-Mg-Si-Cu Alloy,"*Metallurgical and Materials Transactions A*, vol. 37, pp. 3119-3130, Oct. 2006.

PHOSPHORESCENT FIBRES FOR PASSIVE LIGHTING IN EQUIPMENT FOR TWO-WHEELED VEHICLES

Cíntia Martins[1], Marta Midão[1]; Beatriz França[2], Cristina Oliveira[2]; Helena Silva[3], Pedro Silva[3].

1 CeNTI - Centre for Nanotechnology and Advanced Materials, 2785 Fernando Mesquita St. 4760-034 Vila Nova de Famalicão
2 CITEVE - Technological Center for the Textile ans Clothing Industries of Portugal, 2785 Fernando Mesquita St., 4760-034 Vila Nova de Famalicão
3 TMG Textiles

Two-wheel mobility has contributed to a sustainable future by reducing global carbon emissions.

In this scope, there is a growing demand for the adoption of environmentally friendly processes and materials in the production of mobility components.

A key requirement for two-wheel vehicle users is safety, which emphasizes the need for high-visibility garments, that ensure the user's presence to prevent accidents. Current commercial solutions include, mainly, reflective and fluorescent materials, which typically involve the incorporation of functional particles in fossil-based polymers. The present project focuses on the development of sustainable light-emitting textile fibre solutions, by incorporating phosphorescent pigments in a biopolymer Polylactic acid (PLA). These fibres will be integrated in clothing and accessories tailored for two wheels vehicle users, offering a sustainable alternative while maintaining safety and functionality.

KEYWORDS
PASSIVE LIGHTING; PHOSPHORESCENT FIBRES; SUSTAINABLE POLYMERS.

INTRODUCTION

Phosphorescence is a physical phenomenon that involves the retransmission of absorbed visible light over a period, ranging from minutes to hours, during which it has been exposed to a light source. Examples of applications of this type of technology are mainly found in the scope of safety-related products and anti-counter feiting measures. This functionality can be achieved in textiles through the incorporation of phosphorescent pigments using extrusion compounding, followed by melt-spinning [1]. The incorporation of these additives into fibres through the melt-spinning process has been reported for fossil-based thermoplastic materials, such as Polyethylene Terephthalate (PET) [2] and Polyamide 6 (PA6) 5 %w/w of pigment with a similar chemical base to the studied pigments were incorporated. PET fibres achieved a luminance and an average tenacity of 3.0 cN/dtex. PA6 fibres exhibited Light Intensity, i.e. Relative Intensity, values between 250 and 500. To develop more sustainable and functional solutions, the present work focused on studying the influence of phosphorescent pigments on the production of phosphorescent textile fibres and their final properties, using Polylactic acid (PLA) through the melt-spinning process. A key objective is to determine the maximum pigment amount that can be incorporated without compromising the fibre's compliance with safety standards and its compatibility with textile manufacturing processes.

MATERIALS AND PROCEDURE

For the phosphorescent effect, two pigments were studied regarding their performance and final properties in fibre spinning. The properties of the pigments are represented in Table 1, and they were incorporated into PLA by extrusion compounding, using a twin-screw extruder. The

TABLE 1
Properties of the selected phosphorescent pigments.

Pigment	Emission colour	Excetation Peak Wavelength (nm)	Emission Peak Wavelength (nm)	Time for Luminance of 0.32 mcd/m² (min)
Pigment 1	Green	350	518	900
Pigment 2	Blue	375	492	1932

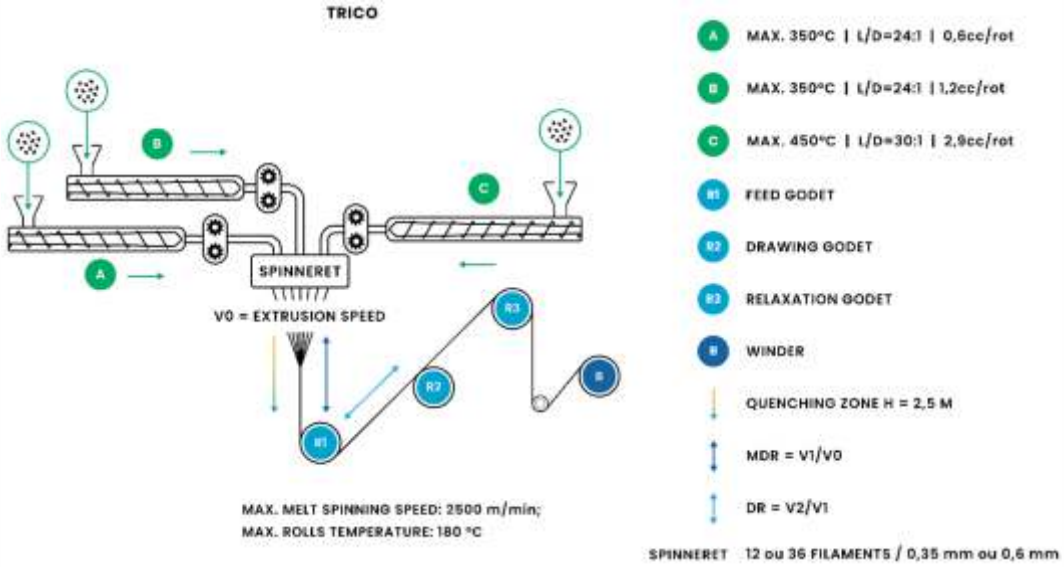

FIGURE 1
Representation of melt-spinning technique.

fibres were obtained by melt-spinning, as represented in Figure 1.

Melt-spinning is a processing technique used to produce textile fibres, where the raw material is fed into extruders (represented by A, B and C), melted, and transported to the spinneret, where it acquires the shape of a fibre. After extrusion, the fibres pass through the quenching zone and onto the Feed godet. The ratio between the extrusion speed (V0) and the Feed Godet (R1) speed corresponds to the Melt Draw Ratio (MDR). The Draw Ratio (DR) - cold drawing - is defined as the ratio between the Feed Godet speed (R1) and the Drawing Godet (R2) speed (R2). The process ends with the fibre being wound onto the winder (B).

The parameters influencing the processability of phosphorescent PLA fibres were studied using a standard and flexible Response Surface Methodology (RSM). Variables and their levels were defined based on preliminary tests. The selected variables included: (i) the type of pigment (identified in Table 1); (ii) mass of pigment, (% w/w: 10 % and 15 %); and (iii) Draw Ratio (DR: between 1.0 and 1.6) from the melt-spinning process. After determining the pigment with better phosphorescence performance (an indication of Light Intensity, i.e. Relative Light Intensity), its processing limits were studied, establishing the maximum pigment mass that could be incorporated and the maximum achievable DR.

This methodology employs Analysis of Variance (ANOVA) to identify the variables with the greatest impact on the process, as well as their interactions, using a Two-Factor Interaction (2FI) model. The model responses were Light Intensity, i.e. phosphorescent performance, and Tenacity, i.e. mechanical performance. Light Intensity was measured using a fluorimeter, in phosphorescence mode, where the samples were excited at the wavelength of the excitation peak (Table 1). The fibres were compared based on the obtained Light Intensity corresponding to the wavelength of the emission peak. Tenacity was determined through tensile tests, based on ASTM D3822 standard.

RESULTS AND DISCUSSION

The results were analysed using ANOVA, employing a 2FI model as the process to evaluate the factors and/or interactions with the greatest impact on the model responses-Light Intensity and Tenacity. The responses produced Model F-values of 73 and 21, respectively, indicating that the studied factors have a statistically significant effect on these responses. The RSM of Light Intensity is represented in Figure 2. Tenacity was also analysed, and the statistical values will also be presented.

Light intensity is strongly influenced by the type of pigment used, confirmed by the F-value of 405 ($p < 0.0001$), followed by the mass of Pigment (% w/w), with a F-value of 4.14 ($p = 0.0460$). DR or the interaction between factors is not significant. Figure 2 shows this tendency, since Light Intensity values, in average, corresponds to 6602 and 2580 for Pigment 1 and Pigment 2, respectively. Additionally, for Tenacity, the significant model terms are DR, mass of Pigment (% w/w) and the interaction between type of pigment and mass of Pigment (% w/w).

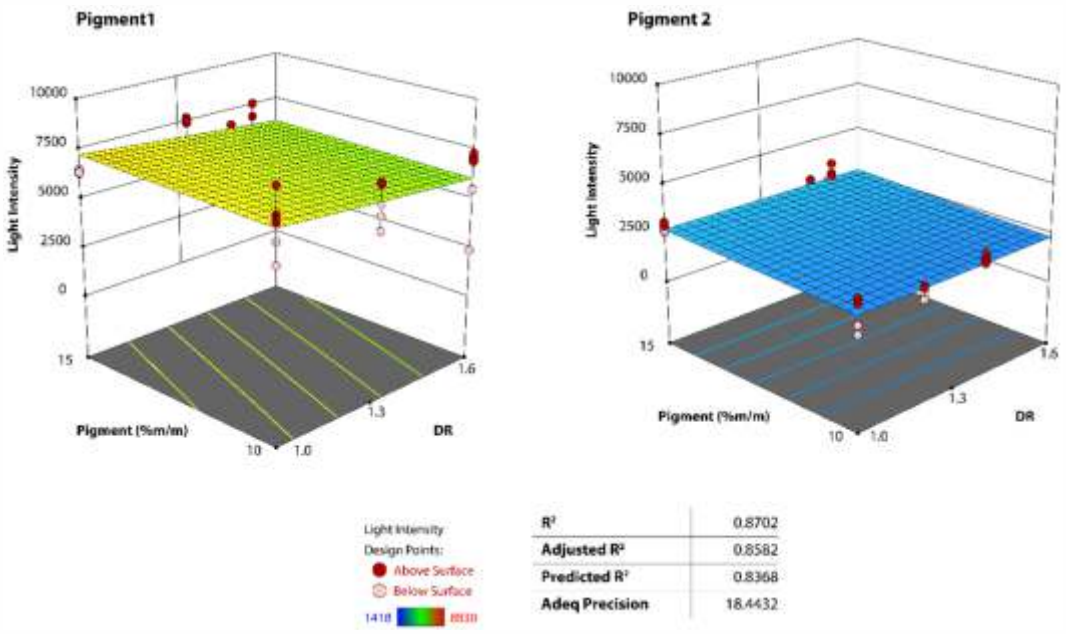

FIGURE 2
RSM plot of Light Intensity, based on Pigment quantity (% w/w) and DR for each pigment.

The study of the processability of phosphorescent pigments proceeded with Pigment 1, since it produced higher values of Light Intensity. The goal was to determine the maximum amount of pigment incorporation, with a stable process, and the maximum DR during processing. The Light Intensity and Tenacity were measured. The results are presented in Figure 3.

Regarding processing limits, a maximum pigment mass of 30 % w/w and a DR of 1.6 were achieved. The maximum value obtained for Light Intensity and Tenacity was 9238 and 0,83 cN/dtex. The new models for Tenacity and Light Intensity were significant, with F-values of 115 and 32, respectively. The individual parameters, Pigment (% w/w) and DR, showed the greatest influence on Tenacity (F-values = 67 and 220, respectively) and Light Intensity (F-value = 82 and 5, respectively). The interaction between these factors was also statistically significant for Tenacity (F-value = 26). As shown in Figure 3, Tenacity decreases with increasing mass of pigment, while the opposite occurs for light intensity, as expected. Regarding DR, Tenacity increases with higher DR values, whereas Light Intensity decreases.

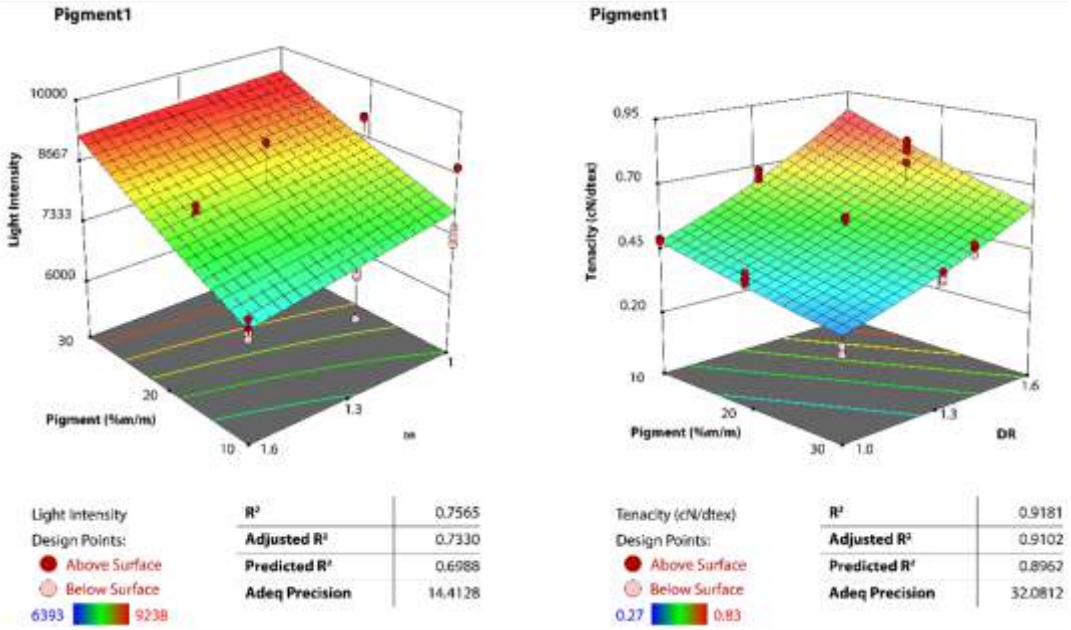

FIGURE 3
Response surface plot of Light Intensity (left) and Tenacity (right) based on Pigment quantity (% w/w) and DR for Pigment 1 (10 to 30 % w/w of Pigment quantity).

CONCLUSIONS

The processability of phosphorescent pigments, using PLA and two different pigments (Pigment 1 and Pigment 2), were studied by melt-spinning, to obtain textile fibres. The influence of both pigments was assessed though the fibres characterization, determining Light Intensity (as an indicator of phosphorescence) and Tenacity.

(i) The study began by incorporating 10% and 15% w/w of each pigment into PLA. Pigment 1 showed better performance regarding Light Intensity, achieving a maximum value of 8830 for 15 % w/w.
(ii) Next, the maximum processing limits for Pigment 1 incorporation were determined. It was possible to incorporate 30 % w/w of pigment and to achieve a DR of 1.6. At this concentration, a maximum Light Intensity of 9238 was achieved.
(iii) Overall, besides the type of pigment, the mass percentage of pigment (% w/w) is the most influential parameter affecting Light Intensity.
(iv) In all reported studies, statistical analysis revealed that the parameters DR and mass percentage of pigment (% w/w), as well as their interaction, significantly impacted Tenacity values.

Values reported in the State-of-the-art refer to 5 % w/w of incorporated pigment. In this study, a maximum of 30 % w/w of Pigment 1 was successfully incorporated, driven by the need to ensure functionality for two-wheel vehicle user safety. The minimum Light Intensity values obtained for 10 %w/w of Pigment 1 and Pigment 2 were 5324 and 2380, respectively. These results are promising compared to those reported by Yan et al. [3], where reported Light Intensity values range between 250 and 500. The average value obtained for Tenacity was 0,55 cN/dtex, which is considerably lower than the average values of 3,01 cN/dtex obtained by Ge *et al.* [2] for PET fibres, suggesting that mechanical properties require significant optimization.

ACKNOWLEDGEMENTS

The present study was developed in the scope of the Project "AM2R - Agenda Mobilizadora para a Inovação Empresarial do Setor das Duas Rodas" [2022-C05i0101-02 | Project nº 15], financed by PRR - Plano de Recuperação e Resiliência under the Next Generation EU from the European Union.

REFERENCES

[1] R. Sharma e N. Bairagi, "The Role of Photoluminescent Pigments in Textiles," Crimson Publishers, pp. 1-4, 2018.

[2] M. Ge, X. Guo e Y. Yan, "Preparation and study on the structure and properties of rare-earth luminescent fibre," Sage Journal, vol. 82, nº 7, 2012.

[3] Y. Yan, Y. Zhu e M. Ge, "Study on the Photochromic Properties of Coloured Luminous Fibres Based on Pa6," Fibres & Textiles in Eastern Europe, vol. 117, nº 3, pp. 38-43, 2016.

DEVELOPMENT OF SELF-REINFORCED COMPOSITES FROM RECYCLED TEXTILE WASTE

Beatriz França[1], Cristina Oliveira[1]; Marta Midão[2]; Cíntia Martins[2]; Helena Silva[3], Pedro Silva[3]
1 CeNTI - Centre for Nanotechnology and Advanced Materials, 2785 Fernando Mesquita St. 4760-034 Vila Nova de Famalicão
2 CITEVE - Technological Center for the Textile ans Clothing Industries of Portugal, 2785 Fernando Mesquita St., 4760-034 Vila Nova de Famalicão
3 TMG Textiles

Self-reinforced composites (SRCs) represent a significant advancement in materials science. These innovative materials, where both the matrix and reinforcement are derived from the same polymer, offer significant advantages, particularly in terms of enhanced fibre-matrix compatibility and improved recyclability. This study focuses on developing SRCs from recycled polyester (rPES) textile waste, aiming to create lightweight, impact-resistant, and fully recyclable composites. The research, conducted under the Two-Wheel Mobilizing Agenda (AM2R) project, and this article details an eco-design approach incorporating recycled textile waste, which involves the use of post-industrial polyester (PES) waste to produce needle-punched nonwoven fabrics (NWFs) and their integration with commercial poly(ethylene terephthalate) (PET) films. SRC plates were developed using hot-pressing, and their morphological and mechanical properties were evaluated. Results indicated that samples with NWF reinforcement exhibited greater consistency in thickness and improved structural homogeneity compared to those with cut-edge reinforcement. Mechanical testing revealed diverse tensile strength and strain percentages, with samples 3 and 6 demonstrating superior performance. The study's findings highlight the promising potential of SRCs developed from recycled PES textile waste for sustainable applications. To further advance this research, future work will focus on optimizing reinforcement distribution and processing techniques to enhance uniformity and performance.

KEYWORDS
SELF-REINFORCED COMPOSITES; POST-INDUSTRIAL WASTE; RECYCLED POLYESTER; SUSTAINABLE COMPOSITES.

INTRODUCTION

Self-reinforced composites (SRCs), also referred to as single-polymer composites (SPCs), represent a distinct class of composite materials in which both the matrix and the reinforcement are composed of the same type of polymer. This configuration provides excellent fibre-matrix interface compatibility and facilitates recycling due to the chemical uniformity of the constituents[1,2]. Initially developed by Capiati and Porter in 1975, SRCs exploit the melting point difference between oriented fibres and a polymeric matrix in polyethylene (PE), resulting in systems with high internal cohesion and favourable mechanical properties[2]. Building on this concept, advanced techniques such as hot compaction, film stacking, and powder impregnation have been established to produce composites characterized by lightweight, excellent impact resistance, and enhanced recyclability-critical features for applications in demanding sectors [1,3]. Given the drive toward environmentally sustainable alternatives, SRCs have gained relevance in industries such as automotive, aerospace, and packaging, where the combination of lightweight materials and recyclability is crucial [3]. Moreover, the use of recycled polymers, such as PES and PET, in the production of SRCs from industrial waste allows for the valorisation of materials that would otherwise be discarded. Incorporating these recycled materials offers an environmentally friendly solution, reduces production costs, and transforms industrial waste into high-performance materials [1,2].

The development of textile composites has been conducted under PPS54, a component of the Two-Wheel Mobilizing Agenda (AM2R) project. This PPS is led by TMG Textiles and co-promoted by CITEVE (Technological Center for the Textile and Clothing Industries of Portugal) and CeNTI (Center for Nanotechnology and Smart

Materials). The project aims to develop functional, interactive, and intelligent clothing solutions, as well as advanced textile composites (vehicle accessories), through the application of multifunctional fibres and textile structures tailored for urban mobility in two-wheel vehicles. Leveraging the synergies among the participating entities, the development of self-reinforced composites (SRCs) has been identified as an innovative and sustainable solution aligned with the project's objectives.

Two distinct R&D approaches have been defined for the development of SRCs. The first approach involves applying textile structures made from bicomponent technical fibres, which are produced through the extrusion of sheath-core fibres combining two polyethylene grades: high-density polyethylene (HDPE) and low-density polyethylene (LDPE). The second approach, focused on eco-design, emphasizes the use of recycled textile waste strategically combined with commercial products. This article highlights the progress and results achieved to date under the second R&D approach, offering a detailed overview of the main advancements made.

MATERIALS AND METHODS

MATERIALS

The industrial partner and leader of the PPS, TMG Textiles, strategically selected a post-industrial waste stream of 100% PES to be recycled (rPES) for the second R&D approach, based on its production consistency and volume. These textile waste materials were recovered at a pre-finishing stage in the textile production process, ensuring minimal contamination. The textile waste was subsequently processed through cutting, mechanical recycling (defibrillation), and the production of needle-punched NWFs using the recycled rPES fibers. This process aimed to evaluate the integration of these materials in various forms into the proposed developments.

For the polymer matrix phase in the SRCs under study, commercial PET films, from DuPont, with a thickness of 100 µm were utilized.

MATERIALS ANALYSIS

TGA (Thermogravimetric analysis) was performed using a TGA 209 F1 Libra equipment from Netzsch. The tests were conducted over a temperature range of 30 °C to 700 °C, with a heating rate of 20 °C/min in a Nitrogen atmosphere. An alumina crucible was used to hold the samples. At least 2 samples of each material were analysed to assess the material degradation curve. This analysis highlights the thermal events of the sample, such as mass loss due to decomposition, dehydration, or volatilization. The goal is to evaluate the composition by quantifying the proportion of fillers or additives in the polymer and to study the decomposition and thermal stability of the materials used.

The recycled staple fibres were characterized following ISO 6889:1981 (n=500) to determine fibre length and length distribution through single-fibre measurements. Additionally, their linear density was assessed using the vibroscope method in accordance with ISO 1973:2021 (n=50). This characterization was essential for optimizing the needle set configuration of the nonwoven machine, as its settings depend on the properties of the working fibers.

SRCS DEVELOPMENT

The SRC plates were developed using a hot-pressing process. The different layers were placed in an aluminum mold, positioned between Teflon sheets to prevent contamination, and then inserted into the press preheated to the working temperature. In the preliminary phase, a mold with a working area of 180 × 95 mm² was used.

A range of working temperatures was defined based on the preliminary characterization of the raw materials, followed by hot-press testing and validation of the parameters. The optimal working temperature was determined by analysing the initial test results, along with the applied force on the press (which can be converted to pressure based on the working area).

SRCS MORPHOLOGICAL ANALYSIS AND MECHANICAL CHARACTERIZATION

Morphological analysis through thickness measurements were made on five points of each sample and the average thickness was considered for discussion. The cross-section area observation was performed to evaluate the reinforcement distribution on the composite and the impregnation. A good impregnation is indicated by a seamless surface on the cross-sectional area, not being possible to distinguish the different layers of materials.

Tensile tests were conducted using a universal mechanical testing machine, model AGX-V50kN from Shimadzu, and a load cell of 50 kN. The tests were performed according to the ISO 527-4 standard, with a crosshead speed of 2 mm/min and a gauge length of 50 mm. At least 6 specimens of each material were tested to evaluate tensile strength and elongation at break.

At a preliminary stage, samples were prepared with dimensions of 75 × 10 mm² due to the limiting size of the final piece (180 × 95 mm²).

This analysis aimed to determine the mechanical properties, including tensile strength, elongation at break, and modulus of elasticity, providing insights into the performance and durability of the materials.

RESULTS AND DISCUSSION

The TGA curves of rPES in its cutted and recycled form, with and without finishing, are presented for comparison in Figure 1. A sample of the commercial PET film was also tested for thermal analysis and the determination of working parameters.

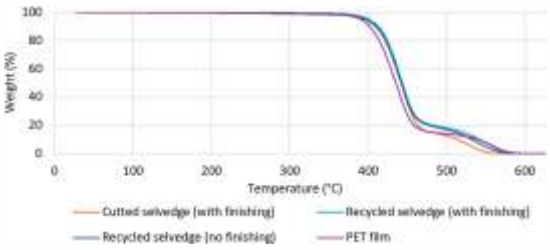

FIGURE 1
Thermogravimetric analysis (TGA) graphs of rPES and commercial PET film.

The average recycled fibre length was 34.7 mm (CV 27.9%) with a mode of 26 mm and a confidence limit of 0.8 mm, while the linear density averaged 2.45 dtex (CV 6.9%) with a 95% confidence limit of 0.05 dtex. This pronounced variability in fibre length, in contrast to the relatively uniform linear density, emphasises the need for precise adjustments to processing parameters in nonwoven production.

In the preliminary phase of the studies, stratifications combining different reinforcement layers, cut edges materials, and needle-punched NWFs with various grammages, along with PET film matrix, were considered (represented in Table 1). The NWFs were produced with fibres obtained from the mechanical recycling of the industrial waste (i.e., cut edges). It was also studied the impact of duplicating polymeric matrix content: samples 4, 5 and 6 represent this study, comparatively with samples 1, 2 and 3, respectively.

The average thickness of the SRC samples was determined to analyse the impact of the reinforcement phase incorporated, namely cut edges and recycled NWF. The statistical analysis of the sample thickness measurements, presented in Table 2, reveals both the variability and consistency across different samples. Understanding these variations is crucial for quality control and ensuring uniformity in applications where precise thickness measurements are essential.

TABLE 2
Average thickness of the SRC fabricated, with standard deviation (S.D.) and coefficient of variation (C.V.).

Thickness		
Mean (mm)	**S.D. (mm)**	**C.V. (%)**
2.420	0.181	7.5
2.020	0.059	2.9
1.678	0.034	2.0
2.328	0.226	9.7
2.024	0.135	6.7
1.872	0.032	1.7
2.090	0.052	2.5
1.994	0.076	3.8
1.790	0.034	1.9

Sample 4 exhibited the highest variability which demonstrates less consistency within the sample, as indicated by its high standard deviation (0.226 mm) and coefficient of variation (9.7%). Conversely, Sample 6 showed the highest consistency in thickness measurements, with the lowest standard deviation (0.032 mm) and coefficient of variation (1.7%), making it the most uniform sample.

On a broad perspective, the statistical data suggest that samples with cut edges reinforcement (samples 1, 4, and 5) tend to present higher variability, while those reinforced with NWF tend to exhibit less variability in thickness (samples 3 and 6).

Tha analyses of the cross-section area were based on a visual observation, following the reference images presented on Table 3.

Considering the cross-section area analyses, sample 6 is the most homogeneous and apparently with good "impregnation" of fibres by the polymeric film, which is coherent with the thickness analyses results.

TABLE 1
Stratification of the SRCs developed.

Sample	1	2	3	4	5	6	7	8	9
Stratification									

Legend: Cutted selvedge; TNT from recycled selvedge; PET film 300 g/m²

TABLE 3
Cross-section images used as a reference for the analysis performed through digital microscopy.

Sample	6	3	9
Cross-section	 Good impregnation		 Bad Impregnation

On samples with cut edges (samples 1, 2, 4, 5, 7, 8 and 9), this reinforcement layer is distinguished on the cross-sectional area. The distribution of reinforcement within these samples is highly heterogeneous, which appears to impact the uniformity (and vice-versa) of the composite's thickness. Additionally, the manual distribution method used to incorporate cut edges, results in lower reproducibility, presenting challenges for its application in an industrial setting. Mechanical properties were tested, and the results are represented in Figure 2.

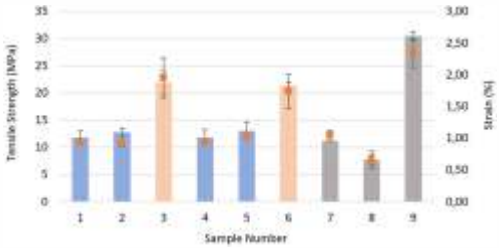

FIGURE 2
Comparison of tensile strength and strain percentage across samples.

Apparently, there is no consistent relationship between tensile strength and strain percentage across the samples. Some samples exhibit both higher tensile strength and higher strain percentages, while others show lower tensile strength and low strain percentages. This diversity highlights the unique mechanical properties of each sample, suggesting that both strength and flexibility can vary independently.

Duplication of polymeric matrix content of the samples 1, 2 and 3 demonstrates little to no effect on the mechanical performance of the samples, when compared with samples 4, 5 and 6.

Sample 9 demonstrates the highest tensile strength and the highest strain percentage, followed by sample 3 and 6.

CONCLUSIONS

In this study, self-reinforced composites (SRCs) developed from PES recycled textile waste were evaluated in preliminary analysis, based on their thickness variability, structural homogeneity, and mechanical properties.

Samples with cut edges reinforcement (samples 1, 4, and 5) exhibited higher variability in thickness, whereas those incorporating needle-punched NWFs derived from recycled cut edges fibres (samples 3 and 6) demonstrated greater consistency. Cross-sectional analysis confirmed that sample 6 possessed the most homogeneous structure and what appears to be a good impregnation, which is consistent with its low variability in thickness. Similar observations were noted for sample 3.

Mechanical testing revealed a diverse range of tensile strength and strain percentages across the samples, with samples 3 and 6, following sample 9, showing the highest mechanical performance. Overall, samples 3 and 6 emerged as the most promising candidates, combining superior structural consistency with enhanced mechanical properties.

Future work should focus on optimizing reinforcement distribution and processing techniques to further improve SRC uniformity and performance. Additionally, subsequent developments will prioritize refining the best stratification method and employing larger moulds to produce SRCs with an expanded working area.

ACKNOWLEDGEMENTS

This work was funded by the PRR - Recovery and Resilience Plan under the European Union's Next Generation EU programme and was carried out as part of the 'AM2R - Mobilising Agenda for Business Innovation in the Two-Wheel Sector' project [2022-C05i0101-02 | Project no. 15].

REFERENCES

[1] Santos, A. (2021). Self-reinforced composites (SRCs). High toughness, low cost, and good recyclability. Journal of Composite Materials, 55(8), 1123-1140.

[2] Gao, Y. (2012). Single-polymer composites and self-reinforced composites (SRCs). Advanced Composite Materials, 21(6), 453-462.

[3] Kmetty, Á., Lendvai, L., & Molnár, K. (2010). Preparation, properties, and applications of self-reinforced polymeric materials (SRPMs). Polymer Composites, 31(4), 721-738.

THE ENVIRONMENTAL VALUE OF WASTEWATERS IN THE TWO-WHEEL INDUSTRY: A CASE STUDY OF CICLO FAPRIL COMPANY

Mariana Santos Gama[1&2], Tiago Teixeira[1&3], Eduardo Ferreira da Silva[1], Carla Patinha[1], Maria Helena Nadais[2], Ana Pupo[4], Flávio Castro Silva[2*]

1 GEOBIOTEC & Departamento de Geociências da Universidade de Aveiro, Campus de Santiago, 3810-193, Aveiro, Portugal
2 CESAM & Departamento de Ambiente e Ordenamento da Universidade de Aveiro, Campus de Santiago, 3810-193, Aveiro, Portugal
3 BIKiNNOV - Bike Value Innovation Center - Association, Rua da Industria, 369, Covão, 3750-792 Águeda, Portugal
4 Ciclo Fapril- Indústrias Metalúrgicas, S.A., Rua Vale do Grou 1378, 3754-908 Águeda, Portugal.

Bicycles are an increasingly popular alternative to motorized transportation and contribute to reduce CO^2 emissions. However, the production of its components generates waste streams that can cause environmental damage, especially because of their high loads of organic matter and metals.

Industrial sludge and wastewater, often toxic and harmful to the environment, could represent a potential source of metals for reintroduction into industrial processes. On the other hand, their high organic content can be further valorised into energy vectors (H^2 and CO^2) through anaerobic treatment processes, thus closing the loop towards a more Circular Economy in the two-wheel industry. This work aims to characterise effluents generated in the two-wheel industry and to address the importance of proper effluent treatment using techniques that minimise environmental impacts.

The Ciclo Fapril company is presented as a case study where effluents have been collected and characterized in the scope of the AM2R project.

KEYWORDS
INDUSTRIAL EFFLUENTS; EFFLUENT CHARACTERIZATION; BICYCLE INDUSTRY.

INTRODUCTION

The increasing number of bicycle users, rapid innovation in industrial production systems, combined with the fact that it is an environmentally friendly means of transport that allows for a reduction in CO^2 emissions and the avoidance of fossil fuels, have made the bicycle a popular solution all over the world (Roy et al., 2019). However, the production of its components is associated with a variety of environmental impacts. In the industrial sphere, these impacts are related to the accumulation of raw materials and waste production, but also to the inefficiency of production processes and waste treatment processes.

Metals such as aluminium (Al), nickel (Ni) or zinc (Zn) used in the production of bicycle components, can reach the liquid effluents generated, damaging public health, the environment and ecosystems (Bitton, 1994; Gray, 2004), especially when emission limits values (ELVs) are not complied with. Other factors contributing to possible non-compliance with the ELVs in wastewater include the high organic load presented by various streams, including oils and greases used in product washing and finishing processes, as well as suspended solids.

Industrial effluents from the manufacturing process of bicycle components vary according to their origin and composition, requiring correct management in order to minimise possible environmental damage. In general, these effluents can be: (a) oily, generated by machining, lubrication and equipment maintenance processes, containing oil, grease and other petroleum derivatives; (b) metal effluents, which commonly arise from processes such as galvanising, painting, anodising and metal surface treatment, and which generally contain heavy metals such as copper (Cu), chromium (Cr), Ni and Zn, (c) paint and varnish effluents, originating from the application of paints and varnishes to parts, which may contain organic solvents, resins and toxic pigments; and finally, (d) cooling water, used to lower the temperature

of parts in processes such as welding or forging, which may contain chemical substances used in water preparation (Pazdzior et al., 2019).

Therefore, it is of utmost importance to implement effective processes for treating industrially generated effluents. This should be done alongside the possibility of valorising some of their components and reusing water in the production process, thus emphasising a sustainable perspective and environmental compliance (Al-Mutair et al., 2024).

Each effluent has a set of characteristics (physical, chemical and biological) that must be considered when testing appropriate treatment strategies. Effluent treatment methods are divided into primary, secondary and tertiary/advanced. Primary treatment removes suspended solids and reduces the organic load, preparing the effluent for the following stages (e.g. sedimentation, flotation, coagulation; Sathya et al., 2022). Secondary treatment uses biological processes (e.g. activated sludge, anaerobic digestion) to remove organic matter and nutrients. Tertiary/advanced treatment removes persistent contaminants through membrane filtration, adsorption with activated carbon and advanced oxidation. The choice of method depends on the characteristics of the effluent to be treated (Woodard, 2001), ensuring that pollutants are removed to meet strict standards, allowing the water to be reused and minimising environmental and human health impacts.

This work aims to provide a preliminary characterisation of the effluents generated in the industrial line for metal parts cleaning and degreasing at the company Ciclo Fapril - Indústrias Metalúrgicas, S.A., addressing improvements in treatment methods and the possibility of valorising components in the effluents produced.

MATERIALS AND METHODS

CICLO FAPRIL COMPANY

Ciclo Fapril - Indústrias Metalúrgicas, S.A. is a company dedicated to producing metal components for various industrial areas, such as the transport industry (parts for cars and bicycles), medical care, and construction, among others. The company uses Al in most of its products. It is dedicated to producing welded metal components, based on sheet metal stamping/machining, tube/wire cutting/bending and turning/machining, focusing on innovation in its products and industrial processes.

The company has an industrial wastewater treatment plant (IWWTP) based on coagulation-flocculation processes. During the treatment, particularly during the filtration stage, sludge is produced, containing appreciable concentrations of various metals and organic matter.

During the process of degreasing and washing metal parts to apply powder paint, effluents are generated such as alkaline degreasing effluent, passivation effluent and pressed sludge. Before being discharged to the IWWTP, the effluents generated are subjected to primary pre-treatment/treatment: degreasing effluent - degreasing and passivation effluent - filtration of iron precipitates. The pre-treated effluent arrives separately by gravity at the IWWTP, where it is separated as follows: acid-concentrated effluent, alkaline concentrated effluent, diluted effluent and reserve effluent. Treatment is then carried out discontinuously in the main reactor using a sequential coagulation, neutralisation and flocculation process. Coagulation-flocculation is a highly effective process for removing microscopic and submicroscopic particles suspended in effluents. This process allows colloidal particles to be transformed into larger particles with greater sedimentation capacity. During coagulation, the suspension or solution is destabilized, i.e. the stability of the system is broken. The coagulant is the chemical compound added to promote this destabilization. Flocculation is the process in which the destabilized particles are induced to form larger aggregates. In this phase, the flocculant is added to facilitate the agglomeration of these particles (Koohestanian et al., 2008). The following products are added to this treatment method: (1) PAC (polyaluminium chloride) coagulant; (2) sulphuric acid; (3) limewater (calcium hydroxide); (4) ST-FLOC flocculant (ST Ibérica). The main purpose of adding sulphuric acid and limewater during the coagulation-flocculation process is to adjust the pH, which is crucial for optimizing the efficiency of the treatment process.

The treated effluent is sent for filtration in a filter press. The filtered water is then subjected to a final pH adjustment and final filtration through quartzite and activated carbon columns. The sludge produced in the filter press is discharged into containers positioned underneath the filter. In support of these operations, the University of Aveiro collaborates closely with Ciclo Fapril, playing a key role in the characterization of waste streams and the development of optimized treatment and recovery strategies, with a focus on both energy and material recovery.

SAMPLING

According to the technical information provided by the company on the production processes, the following streams were identified for the characterisation of liquid effluent and sludge samples at Ciclo Fapril: degreasing effluent 1 (ED1), degreasing effluent 2 (ED2) and pressed sludge. Degreasing effluent 1 results from washing and degreasing aluminium parts, while degreasing effluent 2 is generated from washing and degreasing iron parts. A single representative sample was collected from each of the streams. The liquid samples were transported in 1.5 L plastic bottles, while the sludge was transported in plastic bags and stored in the refrigerator at 4 °C in the Department of Environment and Planning and the Department of Geosciences at the University of Aveiro.

METHODOLOGY

The liquid effluents and solids sampled were characterised by analysing the following physicochemical parameters: liquid effluents - pH, electrical conductivity (EC), total and volatile suspended solids (TSS and VSS, respectively), total chemical oxygen demand (COD), biochemical oxygen demand after five days (BOD^5); sludge - pH, EC, total solids (TS), volatile solids (VS), chemical analysis of major elements, and mineralogy.

The methods and equipment used to analyse the various physicochemical, chemical and mineralogical parameters determined in this work are summarised in Table 1.

Three replicate analyses of each sample were systematically carried out to determine COD, BOD^5, TSS and VSS in the effluent and TS and VS in the sludge.

RESULTS AND DISCUSSION

LIQUID EFFLUENT CHARACTERISATION

Table 2 shows the results of the physicochemical characterisation of the effluent from washing and degreasing metal parts at Ciclo Fapril, as well as comparison with a reference study.

The liquid effluents resulting from the process of washing and degreasing metal parts for the application of powder paint show alkaline pH values (10.3 and 11.6) and high EC values compared to the values of studies carried out on effluents from metallurgical industries located along the Dombivali Industrial Complex in Mumbai, India (Singare and Dhabarde, 2014; Table 2) and at the Hayatabad Industrial Estate (HIE) in Peshawar, Pakistan (Tariq et al., 2006; Table 2). Regarding suspended solids, around 46-48% of total solids are volatile, which could indicate a considerable organic content in the

TABLE 1
Summary of methods and equipment used to analyse the various physicochemical, chemical and mineralogical parameters determined in this work.

	Parameter	Method/method reference	Equipment
Liquid effluents	pH	Direct measurement	pH meter, model HI 9025; HANNA Instruments
	EC	Direct measurement	Conductivity meter, model 1481-50; Cole-Parmer
	COD	5220D*	Spectrophotometer, CODvario
	BOD5	5210D*	Oxitop control equipment
	TSS	2540D*	Oven WTBbinder
	VSS	2540E*	Muffle furnace Carbolite
Sludges	pH	ISO/FDIS 10390:2020	pH meter, model HI 9025; HANNA Instruments
	EC	ISO 11265:1994	Conductivity meter, model 1481-50; Cole-Parmer
	TS	2540G*	Oven WTBbinder
	VS	2540G*	Muffle furnace Carbolite
	Chemical analysis of major elements	Fused beads; X-ray fluorescence (XRF)	Spectrometer AXIOS PW4400/40 FRX-PANalytical
	Mineralogy	X-ray diffraction (XRD)	Diffractometer PANalytical X'Pert Pro

**Standard methods for the examination of water and wastewater (Greenberg et al., 1999)*

TABLE 2
Results of the physicochemical parameters of the liquid effluents.

Parameters	Degreasing effluent 1 (ED1)	Degreasing effluent 2 (ED2)	Tariq *et al.* (2006)*	Singare and Dhabarde (2014)**
pH	10.30	11.60	4.44	48.19-10.30
EC (ɲ$ cm-1)	25900	32300	1920	4949-25067
COD (mg L-1)	9517±74.26	9575±155.80	nd	987-13640
BOD^5 (mg/L-1)	4903±259.27	4219±47.14	340	356-557
TSS (mg L-1)	400±17.32	482±48.05	521	688-1608
VSS (mg L-1)	190±20.00	220±99.88	6400	nd

**Physicochemical properties of effluents discharged by aluminium industries of Hayatabad Industrial Estate (HIE) in Peshawar;*
***Physicochemical properties of effluents discharged by metallurgical industries along the Dombivali Industrial Complex in Mumbai (India); nd - not defined.*

samples. This hypothesis is supported by the BOD^5/COD ratio, which is considered a good proxy for classifying the biodegradability of effluents. This ratio is higher than 0.4 for both samples (ED1=0.52 and ED2=0.44), indicating that these effluents contain a high amount of biodegradable organic matter that could be valorised through biological processes (Esplugas et al., 2004). As effluents resulting from degreasing processes, they are expected to contain organic substances, such as oils and fats, which are susceptible to microbial degradation, giving them a high tendency to biodegrade (Cisterna-Osorio & Arancibia-Ávila, 2019).

SLUDGE CHARACTERISATION

The sludge has an alkaline pH value (8.23), as expected due to the marked presence of CaO in the sample (Figure 1), and an EC value of 4685 uS cm^{-1} as shown in Table 2. The sample studied had 74% total solids, of which 24.5% were volatile (Table 3).

TABLE 3
Results of the physicochemical parameters of the sludges.

Parameters	Sludge
pH	8.23
EC (uS cm^{-1})	4685
TS (%)	74.0
VS (%)	24.5

The major element geochemistry results show that the sludge sample mainly comprises a carbonate component (CaO = 29.6 wt.%; Loss on Ignition (LOI) = 41.3 wt.%; Figure 1), in agreement with the presence of calcite and vaterite in the XRD diffractogram (Figure 2). It also contains appreciable amounts of Al_2O_3 (11.5 wt.%; Figure 1) and P_2O_5 (8.0 wt.%; Fig. 1). The presence of CaO and Al_2O_3 could possibly be related to the addition of calcium hydroxide [$Ca(OH)_2$] and aluminium polychloride (coagulant) during the effluent treatment process at the IWWTP, indicating potential metal recovery.

CONCLUSION

The treatment and recovery of effluents in the two-wheel industry has proved to be essential practices for minimising the environmental impact of the industrial production of bicycle components. The use of wastewater treatment methods and resource recovery strategies by companies linked to the sector not only contributes to compliance with legal and environmental requirements, but also to Circular Economy. Adopting more sustainable practices can reduce operating costs and

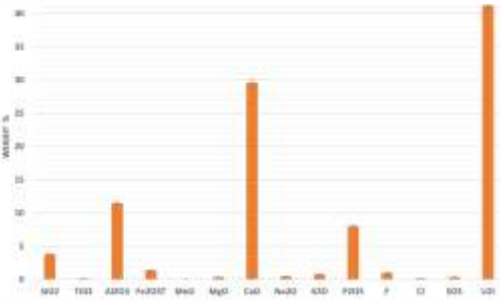

FIGURE 1
Geochemical results of major and minor elements and LOI in industrial sludge.

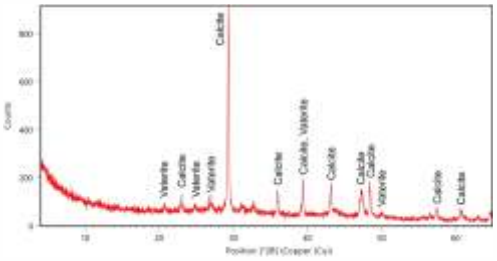

FIGURE 2
XRD patterns of industrial sludge.

generate economic value by transforming waste into valuable resources.

Regarding the effluents generated at Ciclo Fapril, given the high COD concentrations of the effluents studied (above the discharge limits in Portugal - DL 236/98) and the presence of biodegradable organic matter, biological treatments appear to be the first line for this type of effluent, due to their effectiveness, nature and low-cost operation.

Based on the preliminary characterisation carried out in this study, future work should focus on: (a) a more comprehensive physicochemical characterisation and the identification of possible seasonal patterns; (b) the analysis of metals/metalloids in the sludge to assess the potential for metal recovery and valorisation; and (c) the establishment of appropriate treatment schemes based on anaerobic processes to reduce the organic load and valorise its components into energy vectors.

ACKNOWLEDGEMENTS

This study was funded by the "PRR Plano de Recuperação e Resiliência" and by the "Next Generation EU funds at Universidade de Aveiro", through the scope of the Agenda for Business Innovation "AM2R Agenda Mobilizadora para a inovação empresarial do setor das Duas Rodas" (Project nº 15 with the application C 644866475 00000012).

REFERENCES

[1] Al-Mutair, M., Kumar, R., Al-Mur, B.A., Mohamed, O.A., Barakat, M.A. (2024). An overview of metals extraction and recovery from industrial wastewater sludge. The Canadian Journal of Chemical Engineering.

[2] Bitton, G. (1994). Wastewater microbiology. Wiley-Liss, New York.

[3] Cisterna-Osorio, P., Arancibia-Avila, P. (2019). Comparison of biodegradation of fats and oils by activated sludge on experimental and real scales. Water, 11(6), 1286.

[4] DL 236/98 (1998). Decreto-Lei n.º 236/98 de 1 de agosto de 1998. Diário da República, I-Série A, Nº 176, pp. 3676-3722.

[5] Esplugas S., Contreras, S., Ollis D.F, (2004). Engineering Aspects of the Integration of Chemical and Biological Oxidation: Simple Mechanistic Models of Oxidation treatment. Journal of Environmental Engineering, 130: 967-974.

[6] Gray N. (2004). Biology of Wastewater Treatment. Second Edition, Series on Environmental Science and Management, Bell, J.N.B (Ed. Series), Vol. 4, Imperial College Press, London.

[7] Greenberg, A. E., Clesceri, L. S., Eaton, A. D. (1999). Standard methods for the examination of water and wastewater. 20. ed. Baltimore: American Public Health Association, American Water Works Association, Water Environment Federation.

[8] Koohestanian, A., Hosseini, M., Abbasian, Z. (2008). The separation method for removing of colloidal particles from raw water. American-Eurasian Journal of Agricultural & Environmental Sciences, 4(2), 266-273.

[9] Pazdzior, K., Bilieska, L., Ledakowicz, S. (2019). A review of the existing and emerging technologies in the combination of AOPs and biological processes in industrial textile wastewater treatment. Chemical Engineering Journal, 376, 120597.

[10] Roy, P., Miah, M.D., Zafar, M.T. (2019). Environmental impacts of bicycle production in Bangladesh: a cradle-to-grave life cycle assessment approach. SN Applied Sciences 1, 1-16.

[11] Sathya, K., Nagarajan, K., Carlin Geor Malar, G., Rajalakshmi, S., Raja Lakshmi, P. (2022). A comprehensive review on comparison among effluent treatment methods and modern methods of treatment of industrial wastewater effluent from different sources. Applied Water Science 12(4), 70.

[12] Singare, P.U., Dhabarde, S.S. (2014). Pollution discharge scenario of metallurgical industries along Dombivali industrial belt of Mumbai, India. International Letters of Chemistry, Physics and Astronomy, 3, 40-47.

[13] Tariq, M., Ali, M., Shah, Z.J.S.E. (2006). Characteristics of industrial effluents and their possible impacts on quality of underground water. Soil & Environment, 25(1), 64-69.

[14] Woodard, F. (2001). Industrial waste treatment handbook. Elsevier.

PRÉMIO MARIA MANUELA OLIVEIRA

O Prémio Maria Manuela Oliveira foi instituído pela Sociedade Portuguesa de Materiais (SPM) com o objetivo de homenagear o percurso de excelência da Engenheira e Doutora Maria Manuela Oliveira, cuja atividade em investigação, desenvolvimento e promoção da Ciência e Engenharia de Materiais teve um impacto marcante nesta área e na própria SPM, à qual se encontra ligada desde a sua fundação até aos dias de hoje.

Este prémio visa distinguir e reconhecer mulheres que se destacaram num ou mais domínios de atuação da SPM, valorizando o seu contributo científico, técnico e/ou profissional para o avanço da área dos materiais.

Mais do que uma distinção, o prémio pretende também assumir um papel inspirador, promovendo a visibilidade do trabalho desenvolvido por mulheres nesta área e incentivando novas gerações a considerar uma carreira em Ciência e Engenharia de Materiais. O exemplo e o percurso de Maria Manuela Oliveira constituem, assim, uma referência de dedicação, mérito e compromisso com a comunidade científica.

As galardoadas são nomeadas pela Direção da SPM, sendo o prémio atribuído bienalmente, em anos pares, no âmbito das celebrações do Dia Mundial dos Materiais.

https://www.spmateriais.pt/premios/premio-maria-manuela-oliveira

SPM
SOCIEDADE PORTUGUESA de MATERIAIS

SUSTAINABILITY CHALLENGES FOR THE TWO-WHEEL SECTOR: A SCIENTIFIC PERSPECTIVE

Beatriz Triane[1,2], Margarida C. Coelho[2,3,4], Sandra Rafael[5], Pedro Almeida[6], Ana Isabel Miranda[1,2]

1 Centre for Environmental and Marine Studies (CESAM), Campus Universitário de Santiago, 3810-193 Aveiro, Portugal
2 Department of Environment and Planning, University of Aveiro, Campus Universitário de Santiago, 3810-193 Aveiro, Portugal
3 Centre for Mechanical Technology and Automation (TEMA), University of Aveiro, 3810-193 Aveiro, Portugal
4 Intelligent Systems Associate Laboratory (LASI), University of Minho, 4800-058 Guimarães, Portugal
5 Institute of Environment and Development (IDAD), University of Aveiro, 3810-193 Aveiro, Portugal
6 ABIMOTA - National Association of Two-Wheel, Building Hardware, and Furniture Industries and Related Activities of the Represented Sectors, Rua Ramiro Soares de Miranda 133, 3750-866, Águeda, Portugal

The bicycle industry has gained significant attention as a sustainable and healthy mode of transportation, particularly following the COVID-19 pandemic. However, balancing economic growth with sustainability goals remains a challenge, compounded by the lack of consistency in sustainability indicators. This study explores the current state of scientific research on sustainability within the two-wheel industry, analyzing trends, identifying challenges, and highlighting knowledge gaps. The findings reveal that research is predominantly concentrated in countries like China, Taiwan, and the United States, with Italy, Germany, and the United Kingdom leading in Europe. Case studies are prevalent, emphasizing context-specific investigations. The analysis underscores the importance of reducing the environmental impacts of bicycles across their lifecycle, advancing electric bicycle technology, and optimizing management practices. Key challenges include waste generation, supply chain complexities, and the need for circular solutions. The study also highlights gaps, such as the scarcity of targeted sustainability research and inconsistent use of performance indicators, which hinder meaningful comparisons and strategic advancements.

KEYWORDS
BICYCLE INDUSTRY; SUSTAINABILITY; CHALLENGES.

INTRODUCTION

The two-wheeler industry plays a significant role in global mobility. The popularity of bicycles as a sustainable and healthy mode of transportation has increased considerably in recent years, particularly after the COVID-19 pandemic, thus driving the growth and development of this sector [1], [2], [3], [4], [5], [6].

The bicycle industry often faces the challenge of sustainability, balancing economic growth goals with climate action plans [7]. As the industry grows, so does the pressure to align with global sustainability goals, but effectively measuring and assessing sustainable performance remains a complex issue. Measuring sustainable performance still faces challenges, such as the diversity of indicators used and the lack of consistency. This inconsistency hampers the ability to develop a clear and unified approach to sustainability within the industry.

Given these challenges, this study aims to contribute insights toward a more robust and comprehensive sustainability evaluation in the two-wheel industry. By analyzing the existing body of scientific literature on sustainability in this sector, the study aims to identify the industry's primary obstacles to sustainable development. Furthermore, it will explore the existing gaps in knowledge and highlight key research trends that could lead to more effective and standardized sustainability measures within the two-wheel industry.

METHODOLOGY

For this study, a literature review was carried out using open-access papers published in the last 7 years in English in the databases Scopus and Web of Science. Initial searches using the keywords ['bicycle industry' OR 'bike industry'] AND 'sustainable resulted in 316 records. After eliminating duplicates (n=42), a category-based screening of titles and abstracts led to the

exclusion of 188 studies related to physical activity, tourism, physiological and behavioral factors, delivery, and sharing. To maintain a focus on aspects directly related to bicycle production, manufacturing, distribution, use, and its impact as a sustainable mode of transport, a full-text review of the remaining 86 papers was conducted. This review, based on the applied eligibility criteria, resulted in the inclusion of 39 studies. These selected papers were categorized into several key themes to present the findings effectively. This categorization serves multiple purposes critical to the integrity and clarity of the research that highlights the diverse aspects of sustainability within the bicycle industry. These themes include Management and Planning, Waste and Recycling, Electric Bicycles, Life Cycle Assessment (LCA), Technological Innovations, COVID-19, and an Overview of the Bicycle Industry.

RESULTS

Scientific research on the bicycle industry and its relationship with sustainability has grown with a notable focus on countries such as the People's Republic of China (n=11), Taiwan (n=7), and the United States of America (n=6). In Europe (24% of publications), the Netherlands (n=4), Denmark (n=3), Italy (n=3), and Germany (n=3), stand out in the number of publications.

Figure 1 depicts an overview of the distribution of papers based on the results provided, and the seven themes previously mentioned.

The prevalence of case studies in bicycle industry research suggests that researchers are particularly interested in investigating specific and contextualized phenomena, especially in circular economy models, environmental impacts throughout the product life cycle, and the technological advancements and development of electric bicycles.The predominant themes emerging from the analyzed publications can be broadly categorized into three key areas:

(i) Life Cycle Assessment (LCA) - This theme investigates the environmental impacts of bicycles across their entire lifecycle, from raw material extraction and manufacturing processes to usage and eventual disposal or recycling. These studies emphasize the importance of reducing carbon footprints and improving sustainability practices throughout the production chain [8], [9], [10], [11], [12], [13], [14], [15], [16];

(ii) Electric Bicycles - Research in this area highlights the rapid technological advancements in electric bicycles, examining their societal benefits, such as promoting sustainable urban mobility, reducing traffic congestion, and minimizing air pollution. Studies also explore challenges related to battery technology and infrastructure development [17], [18], [19], [20], [21], [22], [23]; and,

(iii) Management and Planning - This theme focuses on the critical role of efficient management and strategic planning in optimizing production processes, reducing waste, and enhancing overall sustainability in the bicycle

FIGURE 1
Number of papers found by subject.

industry. It also addresses supply chain improvements and innovative business models tailored to meet evolving consumer demands [6], [24], [25], [26], [27], [28], [29], [30], [31].

In the past seven years, a few papers have specifically aimed to study and analyze sustainability performance evaluation through indicators in bicycle industries.

In this context, a relevant highlight is a recent paper [6] conducted at a bicycle manufacturing company case study, which examined sustainable practices in the context of Industry 4.0. The study investigated how an industry may use Industry 4.0 concepts (such as automation, big data, and the Internet of Things - IoT) to support sustainable development. The study emphasizes the significance of several actions, including the dedication of top management to sustainability, corporate conduct, community welfare and development, adherence to labor and environmental regulations, and calculated investments in technology.

The main results presented by the authors show that the adoption of 4.0 technologies has made it possible to optimize the use of materials and minimize waste, integrate clean sources into production, reduce the carbon footprint, improve working conditions and employee training, and a competitive advantage as sustainability has become a market differentiator.

CONCLUSION

The bicycle industry faces several key challenges in its pursuit of sustainability. One significant issue is the generation of various types of waste and the associated difficulties in implementing and overseeing effective circular solutions. Managing the lifecycle of materials to minimize waste and maximize reuse remains a persistent obstacle. Additionally, reducing the consumption of raw materials, energy, and pollutant emissions is another pressing challenge. Achieving eco-efficiency and optimizing production processes are critical for creating a more sustainable industry while addressing environmental concerns.

Another major challenge lies in the complexities of supply chain logistics. Issues such as managing stocks, minimizing waste, and addressing shipping costs and their associated environmental impacts are central to reducing the industry's carbon footprint. These interconnected factors highlight the need for streamlined logistics and innovative approaches to mitigate environmental harm.

Despite the progress made in research and practice, notable gaps remain. Specific research focusing on sustainability within the bicycle industry is scarce. This lack of targeted studies limits the development of tailored strategies and solutions. Furthermore, the inconsistency in using sustainability indicators across companies and studies creates difficulties in assessing and comparing performance. Establishing standardized metrics is essential for fostering transparency and enabling meaningful comparisons within the industry.

Following the trend in other manufacturing industries, the sector's modernization will continue with more and more applications of AI and the Internet of Things (IoT), optimizing production, logistics, and maintenance. At the same time, the expansion of electric bicycles is increasingly evident, and advanced technologies will contribute to user safety and more sustainable urban planning.

In this sense, one of the objectives of future work is to address these gaps by developing a specific framework for assessing sustainability in the sector, considering environmental, economic, and social variables. Future research will also analyze sector databases and create standardized methodologies for measuring sustainability indicators.

ACKNOWLEDGMENTS

This work was funded by the PRR - Plano de Recuperação e Resiliência and by the NextGenerationEU funds at Universidade de Aveiro, through the scope of the Agenda for Business Innovation "AM2R - Agenda Mobilizadora para a inovação empresarial do setor das Duas Rodas" (Project no. 15 with the application C644866475 -00000012). The authors would also like to acknowledge the Portuguese Foundation for Science and Technology (FCT)/MCTES for the financial support to CESAM (UIDP/50017/2020+UIDB/50017/2020+ A/P/0094/2020) through national funds. M. C. Coelho thanks to UIDB/00481/2020 (https://doi.org/10.54499/UIDB/00481/2020) and UIDP/00481/2020 Fundação para a Ciência e a Tecnologia; and CENTRO-01-0145-FEDER-022083 - Centro Portugal Regional Operational Programme (Centro2020), under the PORTUGAL 2020 Partnership Agreement, through the European Regional Development Fund.

REFERENCES

[1] Li, Q., Fuerst, F., & Luca, D. (2023). *Do shared E-bikes reduce urban carbon emissions?* J Transp Geogr, 112, 103697. https://doi.org/10.1016/J.JTRANGEO.2023.103697

[2] Buehler, R., & Pucher, J. (2021). COVID-19 *Impacts on Cycling, 2019-2020*. Routledge. https://doi.org/10.1080/01441647.2021.1914900

[3] Nikitas, A., Tsigdinos, S., Karolemeas, C., Kourmpa, E., & Bakogiannis, E. (2021). *Cycling in the era of covid-19: Lessons learnt and best practice policy recommendations for a more bike-centric future.* Sustainability (Switzerland), 13(9). https://doi.org/10.3390/su13094620

[4] Xames, M. D., Shefa, J., & Sarwar, F. (2023). *Bicycle industry as a post-pandemic green recovery driver in an emerging economy: a SWOT analysis*, 30(22), 61511-61522. https://doi.org/10.1007/s11356-022-21985-2

[5] Yang, H., Landes, H., & Chow, J. Y. J. (2024). *A large-scale analytical residential parcel delivery model evaluating greenhouse gas emissions*, COVID-19 impact, and cargo bikes. International Journal of Transportation Science and Technology, 15, 136-154. https://doi.org/10.1016/J.IJTST.2023.08.002

[6] Nirmal, D. D., Gumte, K., & Sohal, A. S. (2025). *Riding towards sustainable development in Industry 4.0: Learnings from a case of the bicycle manufacturing company.* Technol Forecast Soc Change, 212, 123970. https://doi.org/10.1016/J.TECHFORE.2025.123970

[7] Mengistu, A. T., & Panizzolo, R. (2023). *Analysis of indicators used for measuring industrial sustainability: a systematic review.* https://doi.org/10.1007/s10668-021-02053-0

[8] Luo, H., Kou, Z., Zhao, F., & Cai, H. (2019). *Comparative life cycle assessment of station-based and dock-less bike sharing systems*, 146, 180-189. https://doi.org/10.1016/ j.rescorec.2019.03.003

[9] Chen, J., Zhou, D., Zhao, Y., Wu, B., & Wu, T. (2020). *Life cycle carbon dioxide emissions of bike sharing in China: Production, operation, and recycling,* 162. https://doi.org/10.1016/j.resconrec.2020.105011

[10] Chen, W., et al. (2022). *Historical patterns and sustainability implications of worldwide bicycle ownership and use*. Commun Earth Environ, 3(1). https://doi.org/10.1038/s43247-022-00497-4

[11] Liu, W., Liu, H., Liu, W., & Cui, Z. (2021). *Life cycle assessment of power batteries used in electric bicycles in China*. Renewable and Sustainable Energy Reviews, 139. https://doi.org/10.1016/j.rser.2020.110596

[12] Mao, G., et al. (2021). *How can bicycle-sharing have a sustainable future? A research based on life cycle assessment*, 282. https://doi.org/10.1016/j.jclepro.2020.125081

[13] Roy, P., Miah, M. D., & Zafar, M. T. (2019). *Environmental impacts of bicycle production in Bangladesh: a cradle-to-grave life cycle assessment approach.* SN Appl Sci, 1(7). https://doi.org/10.1007/s42452-019-0721-z

[14] Schünemann, J., Finke, S., Severengiz, S., Schelte, N., & Gandhi, S. (2022). *Life Cycle Assessment on Electric Cargo Bikes for the Use-Case of Urban Freight Transportation in Ghana*. In *Procedia CIRP*, Elsevier, pp. 721-726. https://doi.org/10.1016/j.procir.2022.02.120

[15] Tu, J.-C., Luo, S.-C., Huang, P.-C., & Zhang, X.-Y. (2023). *Research on methods and strategies of green design carbon reduction for bicycle industry in Taiwan from perspective of product life cycle.* https://doi.org/10.1007/s10668-023-04131-x

[16] Zhu, Z., & Lu, C. (2023). *Life cycle assessment of shared electric bicycle on greenhouse gas emissions in China.* Science of the Total Environment, 860. https://doi.org/10.1016/j.scitotenv.2022.160546

[17] Calan, C., Sobrino, N., & Vassallo, J. M. (2024). *Understanding Life-Cycle Greenhouse-Gas Emissions of Shared Electric Micro-Mobility: A Systematic Review.* Sustainability, 16(13), 5277. https://doi.org/10.3390/SU16135277

[18] Aono, S., & Bigazzi, A. (2019). *Industry Stakeholder Perspectives on the Adoption of Electric Bicycles in British Columbia*, 2673(5), 1-11. https://doi.org/10.1177/0361198119837158

[19] Apostolou, D. (2020). *Assessing the operation and different refuelling cost scenarios of a fuel cell electric bicycle under low-pressure hydrogen storage*. Int J Hydrogen Energy, 45(43), 23587-23602. https://doi.org/10.1016/ j.ijhydene.2020.06.071

[20] Bucher, D., Buffat, R., Froemelt, A., & Raubal, M. (2019). *Energy and greenhouse gas emission reduction potentials resulting from different commuter electric bicycle adoption scenarios in Switzerland.* Renewable and Sustainable Energy Reviews, 114. https://doi.org/10.1016/j.rser.2019.109298

[21] Koop, C., Grosse Erdmann, J., Koller, J., & Döpper, F. (2021). *Circular Business Models for Remanufacturing in the Electric Bicycle Industry*, 2. https://doi.org/10.3389/frsus.2021.785036

[22] Kumar, R., Pachauri, R. K., Badoni, P., Bharadwaj, D., Mittal, U., & Bisht, A. (2022). *Investigation on parallel hybrid electric bicycle along with issuer management system for mountainous region*. J Clean Prod, 362. https://doi.org/10.1016/j.jclepro.2022.132430

[23] Corti, F., et al. (2024). *A comprehensive review of charging infrastructure for Electric Micromobility Vehicles: Technologies and challenges*. Energy Reports, 12, 545-567. https://doi.org/10.1016/J.EGYR.2024.06.026

[24] Chamberlain, M., et al. (2023). *Development of a bicycle crank arm demonstrator via Industry 4.0 principles for sustainable and cost-effective manufacturing.* Sports Engineering, 26(1). https://doi.org/10.1007/s12283-022-00394-1

[25] Fratocchi, L., & Mayer, J. (2023). *The impact of environmental and social sustainability on the reshoring decision making and implementation process: insights from the bicycle industry.* https://doi.org/10.1007/s12063-023-00372-1

[26] Huang, A., & Badurdeen, F. (2018). *Metrics-based approach to evaluate sustainable manufacturing performance at the production line and plant levels.* J Clean Prod, 192, 462-476. https://doi.org/10.1016/j.jclepro.2018.04.234

[27] Li, J., Chen, C.-W., Wu, C.-H., Hung, H.-C., & Lin, C.-T. (2020). *How do Partners Benefit from IT Use in Supply-Chain Management: An Empirical Study of Taiwan's Bicycle Industry,* 12(7). https://doi.org/10.3390/su12072883

[28] Li, L. R. (2019). *Lean smart manufacturing in Taiwan-Focusing on the bicycle industry.* Journal

of Open Innovation: Technology, Market, and Complexity, 5(4). https://doi.org/10.3390/joitmc5040079

[29] Lin, K.-P., Yu, C.-M., & Chen, K.-S. (2019). *Production data analysis system using novel process capability indices-based circular economy.* Industrial Management and Data Systems, 119(8), 1655-1668. https://doi.org/10.1108/IMDS-03-2019-0166

[30] Shen, C.-Y., Huang, Y.-F., Weng, M.-W., Lai, I.-S., & Huang, H.-F. (2023). *The Role of Industry 4.0 and Circular Economy for Sustainable Operations: The Case of Bike Industry,* 13(10). https://doi.org/10.3390/app13105986

[31] Huang, Y. F., Weng, M. W., Hoang, T. T., & Lai, I. S. (2021). *Circular economy policy of bike industry-exploring the optimal eto component under imperfect production processes system*. In *2021 IEEE International Conference on Social Sciences and Intelligent Management, SSIM 2021.* https://doi.org/10.1109/SSIM49526.2021.9555214

ANA REIS, REPRESENTING THE TECHNICAL-SCIENTIFIC COMMITTEE, PRESENTS THE CONFERENCE'S SPONSORS.

45 ANOS DA SPM

SOCIEDADE PORTUGUESA de **MATERIAIS**

2025 **MATERIAIS 2025,**
XXII Congresso da Sociedade Portuguesa de Materiais, the XIII International Symposium on Materials, and the III Iberian Meeting on Materials Science

2024 **Novo site SPM**

2023 **Rebranding da Marca SPM**

2022 **MATERIAIS 2021,**
11th International Materials Symposium

2021 **40 ANOS da SPM**
Ciclo de conferências on-line sobre "Investigação em Materiais no âmbito das bolsas ERCs»

2020 **1º Prémio Maria Manuela Oliveira**
Seminário Valorização e Mobilização para a Floresta, Instituto Politécnico de Castelo Branco

2019 **MATERIAIS 2019,**
9th International Materials Symposium
(Campus da Caparica)
3º Prémio Carreira e Reconhecimento

2018 **CNMAT- SOCIEMAT CONGRESS MATERIALES 2018 / 1st IBERIAN CONGRESS ON MATERIALS SCIENCE AND TECHNOLOGY,**
(Salamanca, Spain)
FEMS award à melhor tese de mestrado na Europa
(Beatriz Jorge Coelho)
6º ENEM
(FEUP, Porto)
DIA MUNDIAL DOS MATERIAIS 2018
(FEUP, Porto)
3º Seminário Temático
(FCTUC, Coimbra)
SPM na internet - reestruturação do site
Revista da SPM publicada online pela Elsevier

2017 **Presidente da SPM: *Paula Vilarinho*** (U Aveiro)
MATERIAIS 2017,
8th International Materials Symposium
(Universidade de Aveiro)
2º Prémio Carreira e Reconhecimento
Reorganização das Divisões Técnicas
DIA MUNDIAL DOS MATERIAIS 2017
(UBI, Covilhã)
2º Seminário Temático
(U Minho, Guimarães)

2016 **5º ENEM**
(UBI, Covilhã)
DIA MUNDIAL DOS MATERIAIS 2016
(U Minho, Guimarães)
1º Seminário Temático
(Ordem dos Engenheiros, Lisboa)

2015 **Presidente da SPM: *Paula Vilarinho*** (U Aveiro)
MATERIAIS 2015,
7th International Materials Symposium
(FEUP, Porto)
8º Encontro das Divisões da SPM
DIA MUNDIAL DOS MATERIAIS 2015
(Ordem dos Engenheiros, Lisboa)
1º Prémio Carreira e Reconhecimento

2014 **4º ENEM**
(FCT/UNL, Caparica)
7º Encontro das Divisões da SPM
DIA MUNDIAL DOS MATERIAIS 2014
(Aveiro)
SPM na internet - novo site

2013 **Presidente da SPM: *Paula Vilarinho*** (U Aveiro)
MATERIAIS 2013,
6th International Materials Symposium
(FCTUC, Coimbra)
DIA MUNDIAL DOS MATERIAIS 2013
(Ordem dos Engenheiros, Coimbra)
Revista da SPM começa a ser editada pela ELSEVIER

2012 **DIA MUNDIAL DOS MATERIAIS 2012**
(Ordem dos Engenheiros, Lisboa)
Livro "A Vida dos Materiais e os Materiais e a Vida"
(M. Elisabete Almeida)

2011 **Presidente da SPM: *João Bordado*** (IST)
MATERIAIS 2011,
5th International Materials Symposium
(U Minho, Guimarães)
6º Encontro das Divisões da SPM
DIA MUNDIAL DOS MATERIAIS 2011
(FCT/UNL, Caparica)

2010 **3º ENEM**
(IST, Lisboa)
DIA MUNDIAL DOS MATERIAIS 2010
(FEUP, Porto)

2009 **Presidente da SPM: *João Bordado*** (IST)
Revisão dos Estatutos
MATERIAIS 2009,
5th International Materials Symposium
(IST, Lisboa)
5º Encontro das Divisões da SPM
DIA MUNDIAL DOS MATERIAIS 2009
(Ordem dos Engenheiros, Lisboa)
SPM declarada pessoa coletiva de UTILIDADE PÚBLICA
Início da preparação das Páginas Amarelas dos Materiais

2008 **2º ENEM**
(U Minho, Guimarães)
DIA MUNDIAL DOS MATERIAIS 2008
(U Minho, Guimarães)

2007 **Presidente da SPM: *João Bordado*** (IST)
MATERIAIS 2007,
4th International Materials Symposium
(FEUP, Porto)
DIA MUNDIAL DOS MATERIAIS 2007
(IST, Lisboa)

2006 **25 ANOS da SPM**
1º ENEM
(Universidade de Aveiro)
DIA MUNDIAL DOS MATERIAIS 2006
(Universidade de Aveiro)
4º Encontro das Divisões da SPM
Criação da J-SPM

2005 **Presidente da SPM: *Marat Mendes*** (FCT/UNL)
MATERIAIS 2005,
3rd International Materials Symposium
(Universidade de Aveiro)
DIA MUNDIAL DOS MATERIAIS 2005
(IPN, Coimbra)

2004 **3º Encontro das Divisões da SPM**
DIA MUNDIAL DOS MATERIAIS 2004
(FEUP, Porto)

2003 **Presidente da SPM: *Marat Mendes*** (FCT/UNL)
MATERIAIS 2003,
2nd International Materials Symposium
(FCT/UNL, Caparica)
DIA MUNDIAL DOS MATERIAIS 2003 (1ª comemoração)
(Ordem dos Engenheiros, Lisboa)
SPM na internet

2002 **2º Encontro das Divisões da SPM**

2001 **Presidente da SPM: *Manuela Oliveira*** (INETI)
Mudança do Secretariado da SPM para o Campus do INETI
(Lisboa)
MATERIAIS 2001,
1st International Materials Symposium
(FCTUC, Coimbra)
MATERIAIS PARA O NOVO MILÉNIO
- caderno especial, Expresso

2000 **1º Encontro das Divisões da SPM**

1999 **Presidente da SPM: *Francisco Rodrigues*** (INETI)
MATERIAIS'99
(U Minho, Guimarães)
Livro: Inventariação dos Meios Laboratoriais...

1997 **Presidente da SPM: *Luciano Faria*** (IST)
MATERIAIS'97
(CENTIMFE, Marinha Grande)

1995 **Presidente da SPM: *Luciano Faria*** (IST)
MATERIAIS'95
(Universidade de Aveiro)

1994 **Revista da SPM Ciência & Tecnologia dos Materiais**
(2ª série, 1994-2012)

1993 **Presidente da SPM: *Luciano Faria*** (IST)
MATERIAIS'93
(FEUP, Porto)

1991 **Presidente da SPM: *Luciano Faria*** (IST)
MATERIAIS'91
(INETI, Lisboa)

1989 **Presidente da SPM: *Torres Marques*** (FEUP)
MATERIAIS'89
(FCTUC, Coimbra)
Revista da SPM Ciência & Tecnologia dos Materiais
(1ª série, 1989-1992)

1987 **Presidente da SPM: *Antera de Seabra*** (LNEC)
MATERIAIS'87
(U Minho, Braga)

1985 **Presidente da SPM: *Barbedo Magalhães*** (FEUP)
MATERIAIS'85
(Faculdade de Economia, Porto)

1983 **Presidente da SPM: *Pádua Loureiro*** (IST)
MATERIAIS'83
(LNEC, Lisboa)

1981 **Fundação / Escritura**
Presidente da SPM: *Henrique Carvalhinhos* (LNETI)
Secretariado da SPM no Instituto Superior Técnico
(Lisboa)

ENVIRONMENTAL SUSTAINABILITY OF CONVENTIONAL AND ELECTRIC BICYCLES

Paulino Duarte[1], Débora Pons Fiorentin[1], Ramon Carvalho[2], Luís Pires[2], Paula Quinteiro[1]

1 Centre for Environmental and Marine Studies (CESAM), Department of Environment and Planning, University of Aveiro, Campus Universitário de Santiago, 3810-193 Aveiro, Portugal

2 ABIMOTA - National Association of Two-Wheel, Building Hardware, and Furniture Industries and Related Activities of the Represented Sectors, Rua Ramiro Soares de Miranda 133, 3750-866, Águeda, Portugal

The transport sector accounts for around 25 % of the greenhouse gas emissions in the European Union. To reduce these emissions, bicycles are emerging as a sustainable mode of transport, especially in urban areas. However, the environmental performance of different bicycle-use types still lacks research. This review employs a life cycle assessment perspective to analyse how methodological choices influence the environmental impacts of bicycles, i.e., global warming impacts. Results indicate that conventional private bicycles (CPB) have lower impacts than electric private bicycles (EPB). However, when considering the sharing type of use, the conventional shared bicycle (CSB) has higher environmental impacts than the electric shared bicycle (ESB). Future research should i) integrate the environmental evaluation with economic indicators, and ii) explore alternatives to conventional sharing systems to improve the environmental performance of sharing systems.

KEYWORDS

LIFE CYCLE ASSESSMENT; BIKE; ENVIRONMENT PERFORMANCE.

INTRODUCTION

In 2022, the transport sector was responsible for approximately a quarter of the European Union (EU) total greenhouse gas (GHG) emissions [1]. Bicycles represent one of the most sustainable, health-promoting, and efficient modes of transportation. They hold significant potential to contribute to the decarbonization of urban mobility and support the achievement of the EU goal to reduce net GHG emissions by at least 55 % by 2030 compared to 1990 levels and to reach climate neutrality by 2050, as outlined in the European Climate Law and the European declaration on cycling [2-3].

Life Cycle Assessment (LCA) is a methodology for evaluating the environmental impacts of products and systems over their entire life cycle, including production, use, and end-of-life stages [4-5].

The LCA methodology has been applied to evaluate and compare the environmental impacts of bicycles. Bicycles can be classified based on their propulsion mechanism into conventional [6] and electric bicycles [7] but also categorised according to the type of use: i) conventional private bicycle (CPB); ii) conventional shared bicycle (CSB); iii) electric private bicycle (EPB); and iv) electric shared bicycle (ESB).

Some bicycle LCA studies analyse different methodological approaches. For instance, Falgas et al. [8] compared the CPB, CSB, EPB, and ESB, concluding that the CSB has higher environmental impacts than the CPB, EPB and ESB. While [9-12], compared the environmental performance of CPB and EPB, highlighting that EPB has higher environmental impacts. Calan et al. [13] reviewed the environmental impacts of different shared electric micro-mobility modes and compared different ESBs. The review concluded that dockless systems have higher environmental impacts than dock systems.

However, further research is needed to assess the environmental impact of the specific components of bicycles, their assembly, and the end-of-life of bicycle components [9],[14].
This review of LCA-based studies of conventional and electric bicycles advances the current literature by providing a thorough analysis of methodological choices (e.g., functional unit, system boundary, impact assessment method,

etc.), analysing how they affect the global warming (GW) impacts of the categorised bicycle type and highlighting the difference between the bicycle types.

METHODOLOGY

The systematic review used Web of Science and Scopus electronic databases, focusing on papers published in peer-reviewed journals until February 2025. A combination of search terms was considered on the title, abstract, and keywords: "Life cycle assessment" OR "Environmental impact assessment" OR "LCA" OR "Carbon footprint" AND "Bicycle" OR "Bike". A total of 519 papers were identified (314 from Scopus and 251 from Web of Science). The sample was filtered to remove duplicates, articles that did not specifically address the environmental impacts of bicycles, conference papers, opinion papers, articles that were not retrievable, and those not written in English. A final sample of 28 papers was obtained, encompassing 26 case studies, one overview and one review.

RESULTS

In the 26 case study papers, each paper can encompass different scenarios, varying in bicycle types, and types of use, expressed in this review as occurrences. In the sample reviewed, 65 occurrences were identified, 66 % from conventional bicycles and 34 % from electric bicycles.

The definition of functional unit (FU) is crucial for the study's development, as it dictates all the input and output flows. In the sample reviewed, most case study papers (19 out of 26) used the distance travelled by one person over one kilometre (km) as the FU.

Regarding the system boundaries, 92 % of the studies applied the cradle-to-grave approach, which encompasses all life cycle stages from the extraction of raw materials to the end-of-life. The remaining 8 % of the studies applied the cradle-to-user approach, which includes all stages from the extraction of raw materials up to the use stage.

Fig. 1 illustrates the authors' most frequently used keywords, with "Life Cycle Assessment" being the most prevalent, followed by "greenhouse gas emissions," "sustainability," "environmental impact," and "bicycle sharing." These results suggest that the central research theme is the LCA, which focuses on addressing GHG emissions.

Regarding the life cycle inventory, it identifies all the inputs (raw and ancillary materials, and energy) and outputs (mainly the final product, and emission to soil, water, and air). In the sample reviewed, 58 % of the case studies were conducted exclusively based on secondary data, e.g. Ecoinvent database [15]. The remaining 42 % conducted the study based on primary (site-specific data) and secondary data. Several impact assessment methods can be applied to conduct an LCA, in the sample reviewed, ReCiPe was applied in 46 % of the papers, followed by

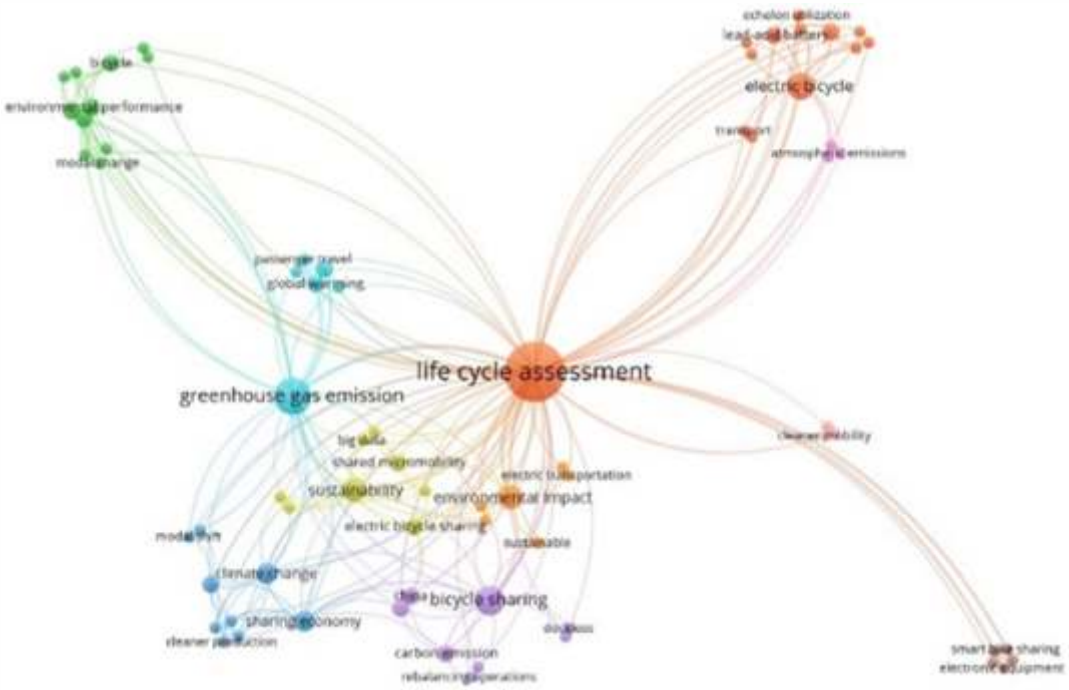

FIGURE 1
Network of authors' keywords.

IPCC (23 %), CML (8 %), and the remaining 23 % applied other impact assessment methods.

The methodological choices presented can influence the GW results of bicycles, as shown in Table 1. The sample reviewed encompasses 55 occurrences, considering the FU of pkm, i.e. GW results expressed in kg CO_2eq/pkm. The occurrences encompass: i) 36 conventional bicycles (12 CPB and 24 CSB); ii) 9 electric bicycles (6 EPB and 3 ESB); and iii) 10 did not specify the type of use.

TABLE 1
Global warming results in different types of bicycle use per FU (one person over one km).

Type of bicycle use	GW (kg CO_2eq/pkm)	References
CSB	0.022 - 0.32	[8], [14-18], [23], [25-29]
ESB	0.058 - 0.15	[13], [16-17]
CPB	0.0015 - 0.017	[8-13], [15], [17], [19], [25-29]
EPB	0.016 - 0.031	[8-12], [17]
Not specified*	0.020 - 0.087	[18], [20-22], [24], [26]

**Refers to case studies that do not specify the type of bicycle use.*

GW results ranged from 0.0015 to 0.32 kg CO_2eq/pkm for conventional bicycles and 0.016 to 0.15 kg CO_2eq/pkm for electric bicycles. Overall, considering the higher GW, private bicycles have a lower environmental impact (0.017 kg CO_2eq/pkm for CPB and 0.031 kg CO_2eq/pkm for EPB) compared to shared bicycles (0.32 kg CO_2eq/pkm for CSB and 0.15 kg CO_2eq/pkm for ESB).

When compared with CPB, EPB presents the worst GW performance, mainly due to the additional electronic components (e.g. printed circuit boards, batteries, motor) used by EPB. Shared-use bicycles (CSB and EBS) presented worse GW than private bicycles (CPB and EPB), which can be mainly attributed to the rebalancing processes and the reduced distance travelled over the bicycle lifespan, which is around 38 % shorter than private use [9], [16]. The oversupply of shared bicycles relative to demand also impacts environmental performance, mainly resulting from their production and less use during their lifespan [14].

CONCLUSION

This review encompasses 26 LCA case studies on bicycles published in peer-reviewed literature. Given the different methodological choices applied, global warming was used to establish comparison as it was the only impact category addressed in all the reviewed publications. The FU was harmonised in some case studies. This work found that shared use of bicycles (CSB and ESB) presented the highest global warming impacts. This work highlights the importance of collecting primary data within the considered system and pursuing consensual impact assessment methods for obtaining comparable environmental results. Further research should be carried out to integrate the environmental assessment with socio-economic indicators, considering the specificities of the different types of bicycle use.

ACKNOWLEDGEMENTS

This study was funded by the "PRR Plano de Recuperação e Resiliência" and by the "Next Generation EU funds at Universidade de Aveiro", through the scope of the Agenda for Business Innovation "AM2R Agenda Mobilizadora para a inovação empresarial do setor das Duas Rodas" (Project nº 15 with the application C 644866475-00000012). This work was funded by national funds through FCT - Fundação para a Ciência e a Tecnologia I.P., under the project CESAM - Centro de Estudos do Ambiente e do Mar, references UID/0017/2025 (doi.org/10.54499/UID/ 50017/ 2025) and LA/P/0094/2020 (doi.org/10.54499/ LA/P/0094/2020) Paula Quinteiro also thanks FCT for the contract 2023.06946. CEECIND, https://doi.org/10.54499/ 2023. 06946. CEECIND/ CP2840/CT0013.

REFERENCES

[1] European Environment Agency (EEA), (2024). Sustainability of Europe's mobility systems. Web report no. 01/2024, Copenhagen, Denmark.

[2] European Commission, (2020). The European climate law. Directorate-General for Communication, Publications Office of the European Union.

[3] European Commission, (2024). European Declaration on Cycling, (C/2024/2377). Communication from the Commission to the European Parliament, the European Council, the Council, the European Economic and Social Committee and the Committee of the Regions.

[4] ISO, (2006). Environmental management - life cycle assessment - principles and frameworks. In: ISO 14040. International Organization for Standardization, Geneva, Switzerland.

[5] ISO, (2006). Environmental management - life cycle assessment - requirements and guidelines. In: ISO 14044. International Organization for Standardization, Geneva, Switzerland.

[6] ISO, (2023). Part 1: Vocabulary, Cycles Safety requirements for bicycles. In: ISO 4210-1. International Organization for Standardization, Geneva, Switzerland.

[7] ISO, (2020). Part 10: Safety requirements for electrically power assisted cycles (EPACs). In: ISO 4210-10. International Organization for Standardization, Geneva, Switzerland.

[8] Felipe-Falgas, P., Madrid-Lopez, C., Marquet, O., (2022). Assessing environmental performance of micromobility using LCA and self-reported modal Change: The case of shared e-bikes, e-scooters, and e-mopeds in Barcelona. Sustainability 14, 4139.

[9] de Bortoli A., (2021). Environmental performance of shared micromobility and personal alternatives using integrated modal LCA. Transportation Research Part D: Transport and Environment 93, 102743.
[10] Montoya-Torres, J., Akizu-Gardoki, O., Iturrondobeitia, M., (2023). Measuring life-cycle carbon emissions of private transportation in urban and rural settings. Sustainable Cities and Society 96, 104658.
[11] Montoya-Torres, J., Akizu-Gardoki, O., Alejandre, C., Iturrondobeitia, M., (2023). Towards sustainable passenger transport: Carbon emission reduction scenarios for a medium-sized city. Journal of Cleaner Production 418, 138149.
[12] Cherry, C.R., Weinert, J.X., Xinmiao, Y., (2008). Comparative environmental impacts of electric bikes in China. Transportation Research Part D: Transport and Environment 14, 281-290.
[13] Calan, C., Sobrino, N., Vassallo, J.M., (2024). Understanding life-cycle greenhouse-gas emissions of shared electric micro-mobility: A systematic review. Sustainability 16(13), 5277.
[14] Sun, S., Wang, Z., Wang, W., (2023). Can free-floating electric bike sharing promote more sustainable urban mobility? Evidence from a life cycle environmental impact assessment. Journal of Cleaner Production 415, 137862.
[15] Wernet, G.; Bauer, C.; Steubing, B.; Reinhard, J.; Moreno-ruiz, E.; Weidema, B., (2016). The Ecoinvent Database Version 3 (Part I): Overview and Methodology. The International Journal of Life Cycle Assessment 3, 1218-1230.
[16] Sun, S., and Ertz, M., (2021). Environmental impact of mutualized mobility: Evidence from a life cycle perspective. Science of The Total Environment, 772, 145014.
[17] Sun, S., Ertz, M., (2022). Can shared micromobility programs reduce greenhouse gas emissions: Evidence from urban transportation big data. Sustainable Cities and Society, 85, 104045.
[18] Huang, Y., Jiang, L., Chen, H., Dave, K., Parry, T., (2022). Comparative life cycle assessment of electric bikes for commuting in the UK. Transportation Research Part D: Transport and Environment, 105, 103213.
[19] Roy, P., Miah, M.D., Zafar, M.T., (2019). Environmental impacts of bicycle production in Bangladesh: a cradle-to-grave life cycle assessment approach. Applied Sciences, 1, 700.
[20] Liu, M., Zhang, K., Liang, Y., Yang, Y., Chen, Z., Liu, W., (2022). Life cycle environmental and economic assessment of electric bicycles with different batteries in China. Transportation Research Part D: Transport and Environment 385, 135715.
[21] Zhu, Z., Lu, C., (2022). Life cycle assessment of shared electric bicycle on greenhouse gas emissions in China. Science of The Total Environment, 860, 160546.
[22] Elliot T, McLaren, S. J., Sims, R., (2018). Potential environmental impacts of electric bicycles replacing other transport modes in Wellington, New Zealand. Sustainable Production and Consumption, 16, 227-236.
[23] Luo, H., Kou, Z., Zhao, F., Cai, H., (2019). Comparative life cycle assessment of station-based and dock-less bike sharing systems. Resources, Conservation and Recycling, 146, 180-189.
[24] D'Almeida, L., Rye, T., Pomponi, F., (2021). Emissions assessment of bike sharing schemes: The case of just eat cycles in Edinburgh, UK. Sustainable Cities and Society, 71, 103012.
[25] Sun, S., Ertz, M., (2022). Can shared micromobility programs reduce greenhouse gas emissions: Evidence from urban transportation big data. Sustainable Cities and Society, 85, 104045.
[26] Wang, Y., Sun, S., (2022). Does large scale free-floating bike sharing really improve the sustainability of urban transportation? Empirical evidence from Beijing. Sustainable Cities and Society 76, 103533.
[27] Sun, S., Ertz, M., (2021). Environmental impact of free-floating bike sharing: From life cycle perspective. Handbook of Solid Waste Management. Springer, 2255-2280.
[28] Sun, S., Wang, Z., Wang, W., (2024). Dockless or docked: Which bike-sharing mode is more environmentally friendly for the city? Current evidence from China's major cities. Cities, 147, 104816.
[29] Sun, S., Wu, Q., & Tian, X. (2022). How does sharing economy advance cleaner production? Evidence from the product life cycle design perspective. Environmental Impact Assessment Review, 99, 107016.

BACTERIAL CULTURE COLLECTION IS A DYNAMIC RESOURCE FOR DRIVING INDUSTRY SUSTAINABILITY

Paula V Morais[1], Miguel Batalha[1], Isabel A.R. Gomes[2], A P. Chung[1]
1 Universidade de Coimbra, Centro de Engenharia Mecânica, Materiais e Processos, ARISE, Departamento de Ciências da Vida, 3000-456 Coimbra, Portugal
2 Sramport, Lda., Rua António Sérgio, Nº 15 3025-041 Pedrulha - Coimbra

In emerging economic models, microorganisms are central elements of development, serving as the basis for bioeconomy products and as essential tools for nature-based solutions. Genome mining and biological databases play a key role in promoting corporate sustainability by enabling the discovery and development of bio-based solutions across a range of sectors, including manufacturing. This work aims to demonstrate the usefulness of performing genome mining in bacteria with phenotypically relevant characteristics to clarify the metabolic pathway(s) and identify opportunities for genetic engineering and biotechnological applications. A comparative genomic analysis of *Diaphorobacter polyhydroxybutyrativorans* B2A2W2 with *D. nitroreducens* SL-205 and *D. aerolatus* 8604S-37 revealed how genome mining of a strain previously considered promising by classical techniques has significantly deepened our understanding of its capabilities. Biological resources collections, such as the University of Coimbra Bacterial Culture Collection are invaluable resources for sustainability in industry, leveraging microbial diversity to support innovative, eco-friendly solutions.

KEYWORDS
UCCCB; BACTERIA; GENOME MINING; PHB GENES.

INTRODUCTION

In recent decades, various ideas and concepts have emerged from academia, industry or political movements to support sustainability transformations, trying to reconcile economic, social and environmental objectives. In these new economic models, microorganisms are central elements of development, being the basis for bioeconomy products, and as essential tools for nature-based solutions [1]. They also provide the resources needed to achieve circularity in the production systems [2], [3].

Since the time of Pasteur, microorganisms have been isolated from natural habitats yet only a small fraction has been preserved globally [4]. To address this limitation, culture collections or microbiological biological resource collections have been established. One of the essential roles of microbial collections such as the University of Coimbra Bacterial Culture Collection - UCCCB, is to make isolated microorganisms available to the research community. Simultaneously, these collections conduct research to characterize and investigate these microorganisms providing valuable tools for industry [5].

Understanding the metabolic and evolutionary patterns of microorganisms has played a pivotal role in the development of several industrial sectors, including healthcare, environment and the production of new materials [6], [7], [8]. Therefore, for the ex-situ conservation of microbial diversity, microbial culture collections remain the most important scientific infrastructure.

In the realm of innovation, the industry relies on culture collections to access patented microorganisms. Microorganisms that are used in patented processes or materials production may be deposited in International Depository Authorities (IDAs) which operate under the Budapest Treaty on the International Recognition of the Deposit of Microorganisms for the Purposes of Patent Procedure. The Portuguese government has recognized the UCCCB as its representative at the World Intellectual Property Organization (WIPO), in Geneva, Switzerland.

Following its goal as a biological resource infrastructure, UCCCB focuses not only on

microbial preservation but is also dedicated to the research and characterization of promising strains for biotechnological applications. Therefore, its research efforts focus on genome analysis and proteomic studies, aiming to identify bioactive molecules and biological markers that can be used in the production of new drugs or in innovative biotechnological processes.

Genome mining involves the use of genomic information to identify biosynthetic pathways of natural products and explore their potential interactions. This process relies heavily on computational technology and bioinformatics tools, using extensive datasets, such as DNA sequences and annotations, available in genomic databases. By applying data mining algorithms, researchers can extract valuable insights that contribute to fields such as medicinal chemistry, including the discovery of novel natural products. The concept of genome mining has emerged as a discipline after whole-genome sequencing of Streptomyces coelicolor which revealed that it encodes far more secondary metabolites than previously anticipated from decades of study [9]. Genome mining can also reveal microbial pathways responsible for the synthesis of biodegradable plastics and the presence of enzymes that degrade these bioplastics [10]. The identification of genes that encode proteins is useful to promote business innovation across different industries including reducing fossil fuel consumption, minimizing waste production and optimizing production processes. This work aims to demonstrate the usefulness of performing genome mining in bacteria with phenotypically relevant characteristics to clarify the metabolic pathway(s) and identify opportunities for genetic engineering and biotechnological applications.

METHODOLOGY

BACTERIAL STRAIN SELECTION

Diaphorobacter polyhydroxybutyrativorans strain B2A2W2, was selected for genome mining. This strain is a gram-negative and facultatively aerobic bacterium, that was isolated from Panasqueira mine tailings in Basin 2 (B2)13 in Reasoner's 2A (R2A) medium (Oxoid) and it is cryopreserved at UCCCB, at -80ºC, in Tryptic Soy Broth with 15% glycerol [11]. Characterization of the strain at the time of its inclusion in the culture collection showed that *D. polyhydroxybutyrativorans* B2A2W2 was able to produce siderophores and degrade poly(3-hydroxybutyrate) (PHB). The genomes of strains *Diaphorobacter nitroreducens* SL-205 and *Diaphorobacter aerolatus* 8604S-37 were obtained from the National Center for Biotechnology Information (NCBI) database (https://www.ncbi.nlm.nih.gov).

GENOME MINING

To identify genes involved in the synthesis, degradation and regulation of bioplastic in bacterial strains from UCCCB culture collection, a set of validated reference genes was selected from the National Center for Biotechnology Information (NCBI) database. This public database is one of the most comprehensive and up-to-date repositories of genetic and protein sequences across all domains of life.

Using a genome mining approach, these reference genes served as query sequences for comparative analysis with BLAST+ [12], a sequence alignment tool, developed by the NCBI, to perform local sequence alignments with private databases. All the bacterial strains included in the UCCCB with an available annotated genome, are compiled in a private database integrated with BLAST+ (Figure 1). Homologous sequences within the genomes of UCCCB bacterial strains were identified and the genes from the *Diaphorobacter* strain B2A2W2, known for its ability to produce PHB biopolymer precursor substances [13], were selected for further analysis.

GENOME VISUALIZATION

To visualize the relative positions of the genes within the genome of the selected bacterial strain, the Microbial Genome Circular Plotter (MGCplotter) was used [14] with default parameters. This software integrates a fast sequence alignment tool (MMseqs2) [15], distinct from BLAST+, to accurately map the locations of the identified genes onto a circular representation of the strain's genome (genes positioning indicated by labels).

Additionally, the alignment of genomes from the three most related bacterial strains (defined by BLAST) was performed using also MGCplotter. The strains considered in this alignment were *Diaphorobacter nitroreducens* SL-205, *Diaphorobacter nitroreducens* B2A2W2 and *Diaphorobacter aerolatus* 8604S-37. A gradient of colors representing the percentage of identity between the selected strains and *Diaphorobacter* B2A2W2 was constructed to enable visual comparison. This strategy enabled an initial insight into whether the identified genes are present in the genomes of the strains.

In addition to gene positioning and sequence alignment, MGCplotter was used to compute and display the genes for several genome chara-

cteristics as 1) genes classification by Clusters of Orthologous Groups (COG) [16] with the functional categories of genes at specific genome positions; 2) the GC skew, highlighting the over- or under-abundance of guanine (G) and cytosine (C) nucleotides; 3) help to determine the location of the origin of replication and assess whether genomic segments are correctly ordered.

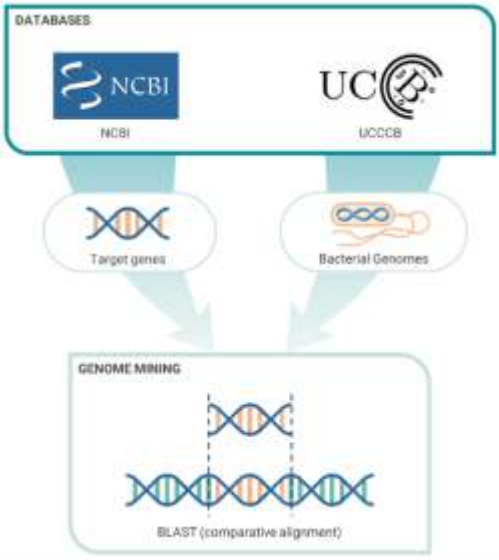

FIGURE 1
Schematic representation of the genome mining approach.

RESULTS

The genome of *Diaphorobacter* B2A2W2 was sequenced by Illumina [17] and the assembled contigs were submitted to the RAST annotation server for subsystem classification and functional annotation [18]. This information was kept private to the UCCCB.

Figure 2 illustrates the results of the bioinformatic analysis of the *Diaphorobacter* B2A2W2 genome alongside two other *Diaphorobacter* strains. The circles in the graph are organized to present different types of information, progressing from the periphery to the center: the genome percentage similarity of the NCBI *Diaphorobacter* strains compared to B2A2W2, the orientation and functional classification of protein-coding sequences, and the nucleotide distortion. In the same direction, the first genome represented is from *Diaphorobacter aerolatus* 8604S-37, the second is from *Diaphorobacter nitroreducens* B2A2W2 and the third one is from *Diaphorobacter nitroreducens* SL-205.

The comparative genomic atlas including strain B2A2W2 reveals a draft genome of approximately 4M nucleotide base pairs. It indicates also that the genome of the strain was not correctly

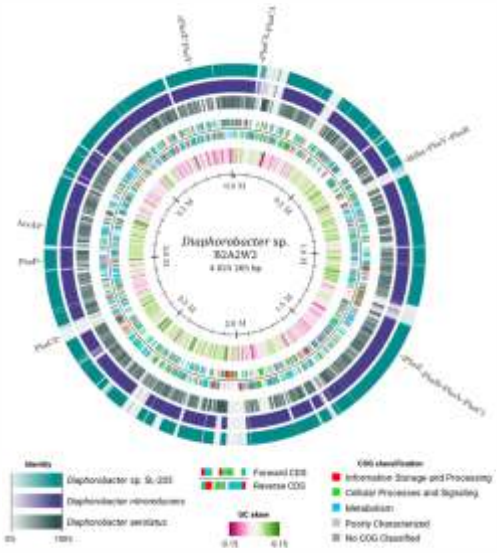

FIGURE 2
Representative atlas of the chromosome of Diaphorobacter sp. B2A2W2. The periphery shows the presence and organization of genes that produce, degrade, and regulate PHAs. The circles on the graph have been grouped to show different information (from the periphery to the centre): the percentage of similarity of Diaphorobacter strains compared to strain B2A2W2, the orientation and functional classification of protein-coding sequences and nucleotide distortion, respectively.

organized before analysis, suggesting potential issues with genome assembly or structural rearrangements. Typically, a well-assembled bacterial genome exhibits a predictable GC skew pattern, with one-half of the genome showing a relative overabundance of Guanine over Cytosine and the other half exhibiting the opposite trend. This expected pattern is absent in the current analysis, highlighting the need for further analysis.

The presence and organization of genes involved in the production and degradation of PHAs, which are bioplastic precursor molecules, are indicated on the periphery of the atlas. The genes identified in the strain genome include *PhaA, PhaB, PhaC, iPhaZ, ePhaZ, PhaY, Bdha, AcsA2, PhaF, and PhbF.* These genes are associated with PHA synthesis *(PhaA, PhaB, PhaC)*, PHA degradation *(iPhaZ, ePhaZ, PhaY, Bdha, AcsA2)* and PHA regulation (*PhaF, PhbF*). This information complements previous studies showing that other strains from the species *D. nitroreducens* have the capacity to degrade poly(3-120 hydroxybutyrate) (PHB) and poly(3-hydroxybutyrate-co-3-hydroxyvalerate) (PHBV) or 121 PHBV, respectively.

CONCLUSION

The bio-based economy is a key sector that stands to benefit from the rapid advancements in scientific discoveries and technological developments. It is characterized as one of the most investment and human-capital-intensive sectors, as well as the fastest-growing, profita-

ble, and flexible innovation sectors. Globally, according to the projections, the bio-based economy is expected to grow by at least 50% by 2030 [19]. A crucial driver of this growth is the use of tools such as genome mining and biological databases, which facilitate sustainable innovation by enabling more efficient use of biological resources. These tools assist companies in rethinking their production processes, promote ecological alternatives and contribute to a reduced environmental impact. Nevertheless, analyses conducted using bioinformatics tools depend on publicly available data, which may be incomplete or contain inaccuracies. Therefore, validating the identified genes through laboratory experiments is essential to confirm their predicted functions.

The present study illustrates how genome mining of a strain that was previously considered interesting significantly enhanced our understanding of its capabilities. Initial classical culture techniques demonstrated that the strain could degrade PHB. However, genomic analysis uncovered the strain's potential to degrade not only PHB but also PHBV. Furthermore, genome analysis identified genes responsible for the production of polyhydroxyalkanoates (PHA). To validate these abilities of the strain, the classical approach would necessitate cultivating the strain under various conditions for extended periods.

The University of Coimbra Bacterial Culture Collection serves as a dynamic resource for driving sustainability in industry. By leveraging microbial diversity, it supports innovative solutions that pave the way for a greener future.

ACKNOWLEDGEMENTS

This work was funded through the PRR - Recovery and Resilience Plan and by the European Funds Next Generation EU, following NOTICE No. 02/C05-i01/2022, Component 5 - Capitalization and Business Innovation - Mobilizing Agendas for Business Innovation, within the scope of the AM2R project - Mobilizing Agenda for business innovation in the Two-Wheel sector (reference 7253).

REFERENCES

[1] A. Rodrigo, Navarro, S. Sankaran, M. J. Dalby, A. Del Campo, and M. Salmeron-Sanchez, "Engineered living biomaterials," Nature Reviews Materials, vol. 6, no. 12, pp. 1175-1190, Aug. 2021, doi: 10.1038/s41578-021-00350-8.

[2] T. Jackson, "Societal transformations for a sustainable economy," Natural Resources Forum, vol. 35, no. 3, pp. 155-164, Aug. 2011, doi: 10.1111/j.1477-8947.2011.01395.x.

[3] E. Loiseau et al., "Green economy and related concepts: An overview," Journal of Cleaner Production, vol. 139, pp. 361-371, Aug. 2016, doi: 10.1016/j.jclepro.2016.08.024.

[4] R. Sharma, Y. Nimonkar, A. Sharma, R. S. Rathore, and O. Prakash, "Concept of Microbial Preservation: Past, present and future," in Soil biology, 2018, pp. 35-54, doi: 10.1007/978-3-319-96971-8_2.

[5] K. Heylen, S. Hoefman, B. Vekeman, J. Peiren, and P. De Vos, "Safeguarding bacterial resources promotes biotechnological innovation," Applied Microbiology and Biotechnology, vol. 94, no. 3, pp. 565-574, Mar. 2012, doi: 10.1007/s00253-011-3797-y.

[6] R. Chaudhary, A. Nawaz, M. Fouillaud, L. Dufossé, I. U. Haq, and H. Mukhtar, "Microbial cell factories: biodiversity, pathway construction, robustness, and industrial applicability," Microbiology Research, vol. 15, no. 1, pp. 247-272, Feb. 2024, doi: 10.3390/microbiolres15010018.

[7] J. M. Laurent et al., "Directed evolution of material-producing microorganisms," Proceedings of the National Academy of Sciences, vol. 121, no. 31, Jul. 2024, doi: 10.1073/pnas.2403585121.

[8] B. H. A. Rehm, "Bacterial polymers: biosynthesis, modifications and applications," Nature Reviews Microbiology, vol. 8, no. 8, pp. 578-592, Jun. 2010, doi: 10.1038/nrmicro2354.

[9] C. Chen, W.-W. Feng, S. Qin, and X.-Q. Zhao, *"Streptomyces xiaopingdaonensis* sp. nov., a novel marine actinomycete isolated from the sediment of Xiaopingdao in Dalian, China," Antonie Van Leeuwenhoek, vol. 107, no. 2, pp. 511-518, Dec. 2014, doi: 10.1007/s10482-014-0347-5.

[10] D.-W. Kim, J.-H. Ahn, and C.-J. Cha, "Biodegradation of plastics: mining of plastic-degrading microorganisms and enzymes using metagenomics approaches," The Journal of Microbiology, vol. 60, no. 10, pp. 969-976, Sep. 2022, doi: 10.1007/s12275-022-2313-7.

[11] B. Rito et al., "Post-measurement compressed calibration for ICP-MS-based metal quantification in mine residues bioleaching," Scientific Reports, vol. 12, no. 1, Sep. 2022, doi: 10.1038/s41598-022-19620-8.

[12] C. Camacho et al., "BLAST+: architecture and applications," BMC Bioinformatics, vol. 10, no. 1, Dec. 2009, doi: 10.1186/1471-2105-10-421.

[13] D. V. Rodrigues, "Exploring biodiversity for natural micro (Bio)-Based polymers biodegradable," Estudo Geral, Feb. 02, 2022. https://hdl.handle.net/10316/98053

[14] Moshi, "GitHub - moshi4/MGCplotter: Microbial Genome Circular plotting tool for comparative genomics using Circos," GitHub. https://github.com/moshi4/MGCplotter

[15]Soedinglab, "GitHub - soedinglab/MMseqs2: MMseqs2: ultra fast and sensitive search and clustering suite," GitHub. https://github.com/soedinglab/MMseqs2

[16] Moshi, "GitHub - moshi4/COGclassifier: A tool for classifying prokaryote protein sequences into COG(Cluster of Orthologous Genes) functional category," GitHub. https://github.com/moshi4/COGclassifier

[17] A. P. Chung, R. Francisco, P. V. Morais, and R. Branco, "Genome mining to unravel potential metabolic pathways linked to gallium bioleaching ability of bacterial mine isolates," Frontiers in Microbiology, vol. 13, Sep. 2022, doi: 10.3389/fmicb.2022.970147.
[18] R. K. Aziz et al., "The RAST Server: Rapid Annotations using Subsystems Technology," BMC Genomics, vol. 9, no. 1, Feb. 2008, doi: 10.1186/1471-2164-9-75.
[19] BIC Consortium, "BIC Strategic Innovation Research Agenda (SIRA)," 2017. [Online]. Available: https://biconsortium.eu/sites/biconsortium.eu/files/publications/BIC_Strategic_Innovation_Research_Agenda_SIRA.pdf. [Accessed: Mar. 1, 2021]

PRÉMIO SPM DE CARREIRA E RECONHECIMENTO

O reconhecimento da excelência na inovação tecnológica e investigação científica na área de Materiais faz parte da missão da Sociedade Portuguesa de Materiais. Para a prossecução deste objectivo foi instituído em 2015 o Prémio SPM de Carreira e Reconhecimento com o intuito de reconhecer, encorajar e promover a excelência nas actividades de ensino, desenvolvimento e investigação, inovação e produção industrial na área dos Materiais em Portugal.

Todos os sócios da SPM devem participar na escolha de nomes para este Prémio.

SPM
SOCIEDADE PORTUGUESA de MATERIAIS

ENHANCING INDUSTRIAL ENERGY EFFICIENCY: WASTE HEAT RECOVERY USING ORGANIC RANKINE CYCLE SYSTEMS

Márcio Santos[1], José Mota[1], Joel Morgado[1], Leandro Ralha[2], José B. Ribeiro[1]
1 Univ Coimbra, ADAI, Department of Mechanical Engineering, Rua Luís Reis Santos, Pólo II, 3030-788 Coimbra, Portugal
2 SRAMPORT Lda., Rua António Sérgio 15, 3025-041, Coimbra, Portugal

The decarbonization of industrial processes is crucial for achieving carbon neutrality by 2050. One of the most effective strategies to reduce energy waste and enhance efficiency is waste heat recovery. This study evaluates the performance of two different Organic Rankine Cycle (ORC) configurations for industrial waste heat recovery, with a particular focus on heat treatment furnaces in the metal industry. Basic ORC and Regenerative ORC were analysed using sixteen low Global Warming Potential and zero Ozone Depletion Potential working fluids. The optimization function targeted exergy efficiency maximization, while thermodynamic efficiency and heat recovery effectiveness were also assessed.

Results indicate that while the inclusion of a recuperator improved thermal efficiency, it had minimal impact on exergy efficiency due to pinch-point limitations. The BORC and RORC configurations exhibited comparable performance. Among the working fluids, R1234yf achieved the highest exergy efficiency. This research highlights the potential of ORC systems for waste heat recovery and suggests that economic feasibility should be considered in future studies to determine the most viable solutions for industrial applications.

KEYWORDS
WASTE HEAT RECOVERY; ORGANIC RANKINE CYCLE (ORC); ENERGY EFFICIENCY; DECARBONIZATION.

INTRODUCTION

The global energy landscape is experiencing increasing demand due to population growth, economic expansion, and higher standards of living. At the same time, the urgent need to reduce greenhouse gas emissions has become crucial in mitigating climate change. Additionally, concerns over energy security, availability, and cost predictability have become major challenges. The energy sector must address these issues by balancing demand growth with environmental sustainability and transitioning toward a secure, decarbonized energy system.

Achieving carbon neutrality by 2050 requires moving away from a fossil fuel-dependent linear economy toward a circular economy based on renewable energy and resource efficiency. Enhancing the penetration of renewables into national energy systems necessitates maximizing energy efficiency across all sectors. One of the key strategies outlined in PNEC 2030 [1] and RNC 2050 [2] involves improving industrial energy efficiency through waste heat recovery and recycling, which have been proven effective in reducing energy losses.

Portugal's geographical conditions allow for the development of a fully decarbonized electricity sector, leveraging hydropower, wind, solar, biomass, and geothermal energy. However, transitioning to renewables is a gradual process requiring technological advancements, particularly in energy-intensive industries, where electrification is often impractical. In such cases, improving industrial energy efficiency remains a priority.

Waste heat, present in both sensible and latent forms, represents unused energy within industrial processes. Traditionally overlooked due to economic and technological constraints, waste heat recovery has gained significance with the increasing emphasis on decarbonization efforts

and technological advancements. According to Eurostat data [3], the EU's industrial sector consumes approximately 1820.73 TWh/year for heat production, with an additional 1400 TWh/year used for space heating, cooling, and electricity consumption. The total waste heat recovery potential in the EU is estimated at 304.13 TWh/year, representing 16.7% of industrial heat consumption and 9.5% of total industrial energy use [4].

Among the most promising technologies for waste heat recovery is the Organic Rankine Cycle (ORC), a variation of the conventional Rankine cycle that uses organic fluids with low boiling points [5]. This characteristic makes ORC systems well-suited for low- and medium-temperature heat sources, such as industrial waste heat, geothermal energy, and biomass. For small-scale applications, i.e., up to 10 MW, ORC technology has demonstrated higher efficiency and better performance than conventional Rankine cycles [6].

METHODOLOGY

This section provides an overview of the main components of the waste heat recovery facility. Figure 1 illustrates the three primary parts of the system. The first component is the heat capture unit, which utilizes a heat exchanger to transfer heat from flue gases to a heat transfer fluid (thermal oil), which then circulates to the ORC circuit. The second component is the ORC circuit, represented in Figure 1 as the basic configuration. However, in this study, two additional configurations will be tested. The third component is the cooling circuit, which is responsible for dissipating heat from the working fluid in the condenser, achieved in this case using a cooling tower.

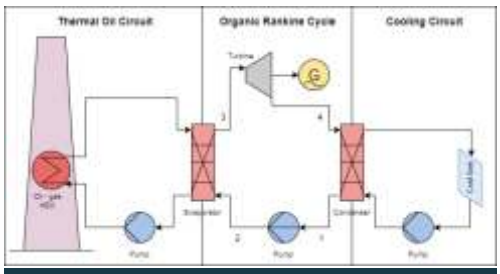

FIGURE 1
Generic schematic of a waste heat recovery system with an Organic Rankine Cycle.

ORGANIC RANKINE CYCLE (ORC)

The first configuration under consideration is the Basic Organic Rankine Cycle (BORC), which operates below the critical temperature and pressure for a given working fluid. The schematic of this system is depicted in Figure 1. In addition to the working fluid circuit, the indirect evaporation ORC includes a supplementary heat transfer fluid (HTF) circuit. The HTF is designed to always remain in a liquid state, ensuring thermodynamic stability and facilitating efficient heat transfer.

In this cycle, the working fluid is pressurized from point 1 to point 2 via a pump. It then enters the heat exchanger (evaporator), where it absorbs heat and transitions to a superheated vapor state at point 3. The vapor is expanded in the expander, reducing its temperature and pressure at point 4, generating mechanical work that is subsequently converted into electricity through a generator. Finally, the fluid enters the condenser, where it releases heat and returns to a liquid state at point 1.
A common enhancement of the ORC is the addition of an intermediate heat exchanger, known as a recuperator, forming the Recuperative Organic Rankine Cycle (RORC). The recuperator recovers residual heat from the expansion process, specifically the transition from superheated vapor to saturated vapor. This configuration enhances thermal efficiency by preheating the working fluid before it enters the evaporator, thereby reducing the additional heat required for vaporization and increasing overall efficiency [7].

THERMAL OIL CIRCUIT

This application involves recovering waste heat from exhaust gases generated by a metal heat treatment furnace, specifically from natural gas combustion. Indirect heating of the working fluid is employed to enhance safety by preventing direct contact between the heat source and the working fluid. Additionally, as waste heat streams often experience fluctuations in both mass flow and temperature, indirect heating is advantageous in stabilizing these variations [8]. However, such fluctuations can still pose challenges for ORC performance, including reduced evaporator effectiveness, instability of the working fluid, and difficulty in maintaining optimal operating conditions. To address these issues, strategies such as thermal energy buffering (e.g., via a thermal oil circuit or heat storage tank), real-time control of working fluid flow rate, or adaptive control of the expander can be implemented to enhance the robustness and responsiveness of the ORC system.

The recovery facility primarily consists of a flue gas recuperator heat exchanger installed in the bypass of the furnace exhaust and a thermal oil transfer loop, which transports thermal energy from the heat source to the ORC module. Figure 2a shows the measured temperature of the

exhaust gases, where the recuperator heat exchanger will be installed. The temperature fluctuates between 100°C and 160°C, with an average value of 130°C, which is used as the heat source temperature for calculations. Figure 2b illustrates the temperature interaction between the exhaust gases, thermal oil, and ORC working fluid, highlighting the irreversibility's associated with the isothermal evaporation stage of the working fluid.

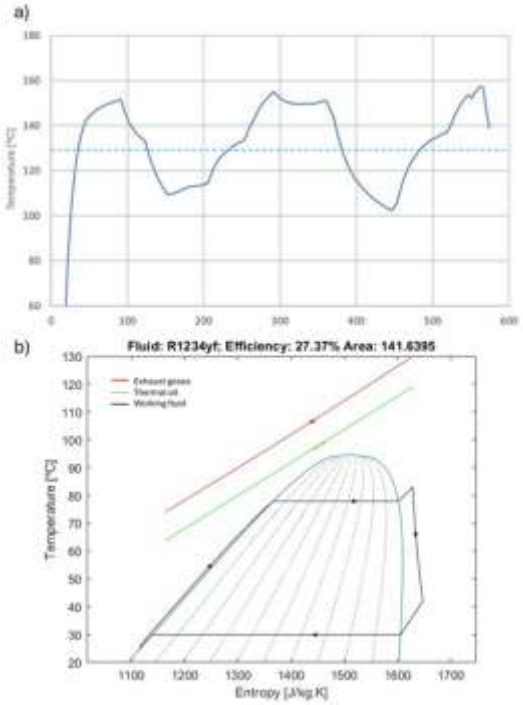

FIGURE 2
a) Heat source temperature profile across time
b) T-s diagram of the RORC for R1234yf.

COOLING CIRCUIT

As is typical for ORC power generation modules, heat dissipation is managed through a cooling tower. This method minimizes the impact of ambient temperature variations compared to air condensers, simplifying system control.

EXERGY EFFICIENCY

For this analysis, a steady-state operation of the power cycle was assumed, with pressure and thermal losses in the heat exchangers considered negligible. The power cycles were modelled using MATLAB and the CoolProp database. This study focuses solely on technical comparisons of the different Rankine-based configurations and does not include economic indicators. To assess ORC performance, thermodynamic efficiency (First Law efficiency) is defined by Equation 1:

$$\eta_{th} = \frac{\dot{W}_{net}}{\dot{Q}_{in,wf}} \quad (1)$$

Where W_{net} represents the net power output (work produced by the expander minus work consumed by the pump), and $Q_{in,wf}$ denotes the thermal power input to the ORC. For waste heat recovery (WHR) applications, thermodynamic efficiency alone is insufficient, as maximizing waste energy utilization is also a goal. Thus, heat recovery efficiency is introduced, as defined by Equation 2:

$$\eta_{hs,u} = \frac{\dot{Q}_{in,wf}}{\dot{m}_{hs}(h_{hs,in} - h_{hs,0})} \quad (2)$$

Where the m_{hs} is the mass flow of the heat source, $h_{hs,in}$ is the specific enthalpy of the heat source at the inlet temperature, and $h_{hs,0}$ is the specific enthalpy at the reference temperature. Exergy efficiency (Second Law efficiency) provides a measure of the amount of mechanical work that can be extracted from the available waste heat. For the same heat source inlet conditions and reference temperature, exergy efficiency is proportional to the product of thermal and heat recovery efficiency, as shown in Equation 3 [9]:

$$\eta_{ex} = \frac{\dot{W}_{net}}{\dot{E}_{in}} = \eta_{th} \cdot \eta_{hs,u} \cdot \frac{(h_{hs,in} - h_{hs,0})}{[(h_{hs,in} - h_{hs,0}) - T_0(s_{hs,in} - s_{hs,0})]} \quad (3)$$

Where T_0 is the reference temperature and $s_{hs,in}$ and $s_{hs,0}$ are the specific entropy values of the heat source at the inlet and reference temperatures, respectively.

For this study, exergy efficiency was selected as the primary performance metric for comparing different configurations and working fluids. The input parameters used in the thermodynamic model are summarized in Table 1, chosen in accordance with typical WHR operating conditions and values adopted in similar studies.

TABLE 1
Inputs set in the thermodynamic mode.

η_{exp} (-)	η_{pump} (-)	$\Delta T_{pp,cd}$ (K)	$\Delta T_{pp,ev}$ (K)	$\Delta T_{pp,reg}$ (K)	T_{cd} (°C)
0.70	0.70	10	10	5	30

WORKING FLUIDS

The selection of working fluids (WF) was based on their global warming potential (GWP) and ozone depletion potential (ODP). The latest generation of fluids should have a GWP lower than 150 and a null ODP. The chosen fluids were selected based on Bahrami et al. work [10] and their availability in the CoolProp open-source library. The full list includes Benzene, Cyclohexane, Cyclopropane, Dimethyl ether, Isopentane, n-Butane, Neopentane, R1233zd(E), R1234yf, R1234ze(E), R1234ze(Z), R1243zf, R1270, R290, R600a, and Toluene.

RESULTS

Two configurations and sixteen working fluids were evaluated for the waste heat temperature

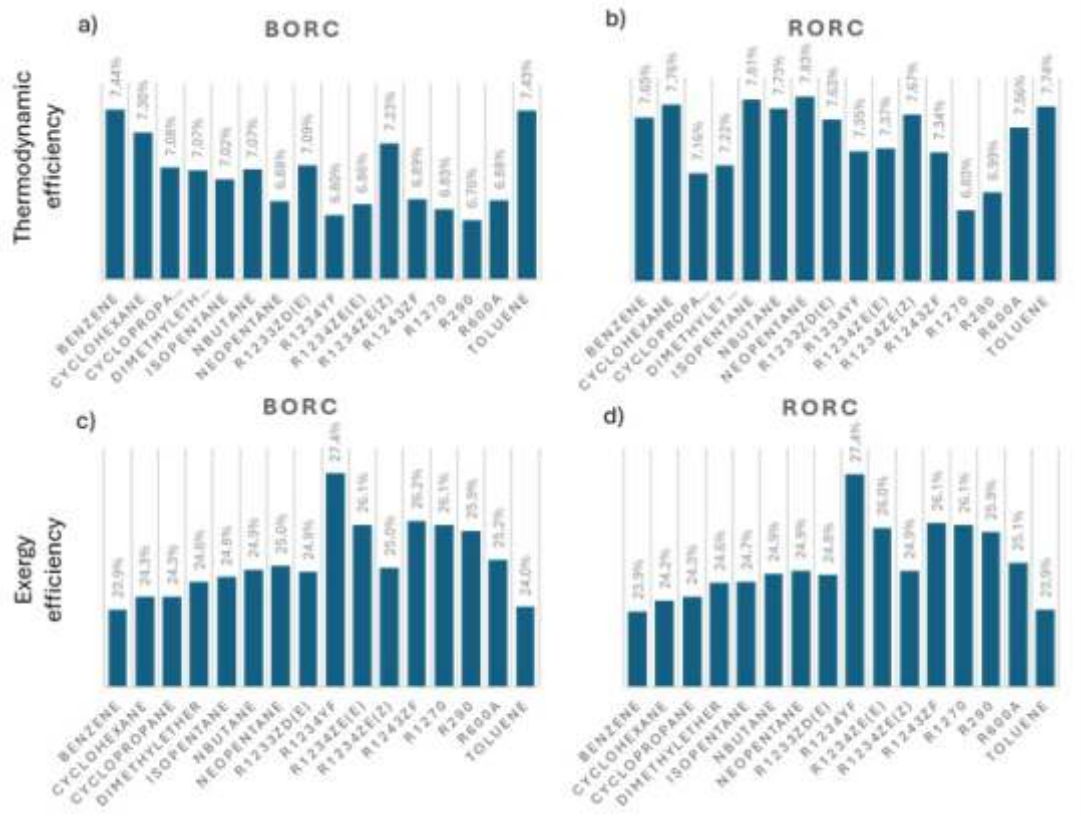

FIGURE 3
Thermodynamic efficiency and exergy efficiency for each configuration and working fluid.

measured at the furnace exit. The optimization function considered in this study was the maximization of the exergy efficiency of the cycle. The BORC and RORC configurations optimization parameter is the evaporation pressure, p_{ev}. Figure 3 illustrates the results of the thermodynamic efficiency hth and the exergy efficiency hex, respectively, for each configuration and working fluid.

One of the primary limitations of the ORC is the irreversibility associated with the isothermal evaporation stage of the working fluid. According to Schuster et al. [11], the temperature mismatch between the working fluid and the heat carrier medium, particularly during the evaporation stage, results in exergy destruction and subsequently increases process irreversibility's, as depicted in Figure 2b.

Regarding the inclusion of a recuperator, the observed gains were minimal, and in some cases, the addition of this heat exchanger had a negative impact on cycle performance. The recuperator raises the inlet temperature of the working fluid in the evaporator, potentially limiting the amount of heat recovered from the heat source due to pinch-point restrictions. Thus, while thermal efficiency increases, heat recovery efficiency declines. Since exergy efficiency is proportional to the product of these two factors, the overall impact may be negligible. Furthermore, from a practical perspective, incorporating a recuperator introduces additional system complexity, increases capital costs, and may require more frequent maintenance due to concerns about fouling or pressure drop. These trade-offs can outweigh the marginal efficiency gains in many industrial settings, especially when operational simplicity and reliability are prioritized.

An interesting observation is that R1234yf yielded the highest exergy efficiency for both BORC and RORC configurations. However, it was not the most thermodynamically efficient fluid. In terms of thermodynamic efficiency, all fluids performed better with the addition of a regenerator when compared to the basic configuration.

CONCLUSION

A comparative analysis was performed for two Rankine-based configurations, testing sixteen working fluids at the measured waste heat temperature from the heat treatment furnace exit. The optimal working fluid for each configuration was selected from a group of sixteen low-GWP and zero-ODP working fluids.
The findings indicate that the incorporation of a recuperator heat exchanger did not result in significant improvements in exergy efficiency.

The BORC and RORC configurations exhibited comparable performance. Additionally, a direct correlation was observed between the critical temperature of the working fluid and the exergy efficiency obtained. If only thermodynamic efficiency were considered, the optimal combination would be a regenerative ORC with n-pentane as the working fluid. However, in terms of exergy efficiency, the preferred combination would be a basic ORC using R1234yf as the working fluid.

This study focused exclusively on technical performance; however, the economic viability of each configuration should not be overlooked. Future research should evaluate the financial feasibility of the various configurations to complement the thermodynamic assessment. Moreover, although the focus was placed on low-GWP and zero-ODP fluids to ensure environmental compliance, future studies could expand the analysis to include fluids with higher GWP but superior thermodynamic properties, especially for applications where environmental regulations are less stringent or where performance under highly variable industrial conditions is critical. This could help extend the applicability of the findings to a broader range of ORC systems.

ACKNOWLEDGEMENT

This research is financed by PRR - Recovery and Resilience Plan and by the Next Generation EU Funds, following NOTICE N.º 02/C05-i01/2022, Component 5 - Capitalization and Business Innovation - Mobilizing Agendas for Business Innovation under the AM2R project "Mobilizing Agenda for business innovation in the Two-Wheel sector" (reference: 7253).

REFERENCES

[1] Direção Geral de Energia e Geologia, Agência Portuguesa do Ambiente, ADENE, and LNEG, "PLANO NACIONAL ENERGIA E CLIMA 2021-2030 (PNEC 2030)," 2019.

[2] Agência portuguesa do ambiente, "ROTEIRO PARA A NEUTRALIDADE CARBÓNICA 2050 (RNC2050)," 2019.

[3] Eurostat, "Final energy consumption by sector,

[4] M. Papapetrou, G. Kosmadakis, A. Cipollina, U. la Commare, and G. Micale, "Industrial waste heat: Estimation of the technically available resource in the EU per industrial sector, temperature level and country," Applied Thermal Engineering, vol. 138, pp. 207-216, Jun. 2018.

[5] Castro Oliveira, M.; Iten, M.; Cruz, P.L.; Monteiro, H. Review on Energy Efficiency Progresses, Technologies and Strategies in the Ceramic Sector Focusing on Waste Heat Recovery. Energies 2020, vol. 13, 6096.

[6] Santos M, Andre J, Mendes R, Ribeiro JB Design and modelling of a small-scale biomass-fueled CHP system based on Rankine technology Energy Procedia 2017, vol. 129, pp 676-683

[7] Santos M, André J, Costa E, Mendes R, Ribeiro J. Design strategy for component and working fluid selection in a domestic micro-CHP ORC boiler. Applied Thermal Engineering 2020, vol. 169, 114945.

[8] Jiménez-Arreola, M., Wieland, C., & Romagnoli, A. Direct vs indirect evaporation in Organic Rankine Cycle (ORC) systems: A comparison of the dynamic behavior for waste heat recovery of engine exhaust. Applied Energy 2019, vol. 242, pp 439-452.

[9] Braimakis, K., Preißinger, M., Brüggemann, D., Karellas, S., & Panopoulos, K. Low grade waste heat recovery with subcritical and supercritical Organic Rankine Cycle based on natural refrigerants and their binary mixtures. Energy 2015, vol. 88, pp 80-92.

[10] Bahrami, M., Pourfayaz, F., & Kasaeian, A. Low global warming potential (GWP) working fluids (WFs) for Organic Rankine Cycle (ORC) applications. Energy Reports 2022, vol. 8, pp. 2976-2988.

[11] Schuster, A., Karellas, S. and Aumann. R., Efficiency optimization potential in supercritical Organic Rankine Cycles, Energy 2010, vol. 35, no. 2, pp. 1033-1039.

SER SÓCIO COLETIVO DA SPM.

VANTAGENS

Participação *com custos reduzidos nas iniciativas da SPM,tais como Cursos técnico-científicos, Conferências, Palestras, Seminários e eventos juntamente organizados com a Ordem dos Engenheiros e Sociedades afins (nacionais e internacionais);*

Divulgação *de atividades, resultados e outras comunicações, tanto na Revista Ciência & Tecnologia dos Materiais, bem como na Newsletter e em eventos realizados pela SPM;*

Identificação *e acesso direto a peritos qualificados para consultoria, estudos, projetos de investigação nas áreas das divisões técnicas nomeadamente: Corrosão e Proteçãode Materiais; Engenharia de Superfícies; Materiais para aEnergia; Materiais Estruturais; Materiais Funcionais; Materiais e Património Cultural; Polímeros e Compósitos; Tecnologia e Processamento de Materiais; entre outras*

Promoção *de formações técnico-científicas em áreas específicas;*

Dinamização *de iniciativas de interesse conjunto em consórcio;*

Acesso *a informação sobre os finalistas ou recém--licenciados na área de Ciência e Engenharia de Materiais e áreas afins;*

Integração *nas diferentes divisões técnicas da Sociedade Portuguesa de Materiais.*

Desconto *de 20% nos valores da publicidade na Revista Ciência & Tecnologia dos Materiais com condições negociáveis.*

Os novos sócios podem considerar o Estatuto do Mecenato, onde se define o regime dos incentivos fiscais no âmbito do mecenato social, ambiental, cultural, científico ou tecnológico e desportivo, para usufruírem de vantagens acrescidas pela sua ligação à SPM.

SPM SOCIEDADE PORTUGUESA de MATERIAIS

CONTACTO

Manuela Oliveira
Tel: 96 5756172

SPM - Apartado 4538
EC Carnide
1511-970 Lisboa

spm@spmateriais.pt
www.spmateriais.pt

DIGITIZATION AND ASSET SUPERVISION USING ULTRA-WIDEBAND (UWB): A TECHNOLOGICAL OVERVIEW FOR WAREHOUSE TRACKING

Bruno Silva[1,2*], Joaquin Dillen[1,2], Rafael Fernandes[1,2], N. Simões[1,2], João M. Faria[1,2], Luis Vilas Boas[1,2], Inês Caetano[3], Luís Cardoso[4], João Borges[1,2], António H. J. Moreira[1,2]

1 2Ai - School of Technology, IPCA, Barcelos, Portugal.
2 LASI - Associate Laboratory of Intelligent System, Guimarães, Portugal.
3 Sistrade - Software Consulting, SA, Porto, Portugal.
4 Miranda & Irmão, LDA, Águeda, Portugal.

*Corresponding author(s). E-mail(s): brsilva@ipca.pt; Contributing authors: jdillen@ipca.pt; rmfernandes@ipca.pt; nsimoes@ipca.pt; jpfaria@ipca.pt; lvilasboas@ipca.pt; ines.caetano@sistrade.pt; lcardoso@miranda.pt; jpbsilva@ipca.pt; amoreira@ipca.pt

Ultra-Wideband (UWB) technology is increasingly crucial in industrial applications for precise real-time asset tracking and spatial awareness in complex environments. UWB offers significant advantages, including high accuracy in distance measurement and resilience in challenging indoor settings, making it ideal for asset supervision systems. This paper outlines the development of a real-time asset location system using UWB technology for indoor environments. The system integrates Qorvo specialized hardware and custom algorithms designed to estimate asset positions with high precision. The approach emphasizes scalability and robustness in real-world industrial scenarios, with a focus on ensuring reliable asset tracking. To conclude, tests were conducted to evaluate system performance and assess the impact of anchor count on accuracy. Although UWB outperforms alternative technologies, its higher costs and infrastructure requirements remain a challenge to widespread adoption.

KEYWORDS
TRACKING; ULTRA-WIDEBAND; INDOOR LOCALIZATION; CALIBRATION.

INTRODUCTION

Digitalization and supervision of assets have become increasingly vital across industries such as logistics, healthcare, and manufacturing. This digital transformation enhances resource management efficiency, leading to significant reductions in operational time and costs. One of the key enablers of this transformation is real-time asset tracking, which offers several advantages, including optimized workflows, faster asset retrieval, and improved inventory management. However, indoor environments present unique challenges for real-time localization due to the limitations of GPS and interference from physical obstacles, such as walls and machinery [1].

Recent technological advancements have positioned Ultra-Wideband (UWB) as a promising solution for precise indoor localization. Unlike GPS, UWB employs short high-bandwidth pulses to measure distances with exceptional accuracy (typically within 10-30 cm). This technology is highly resistant to interference and performs reliably in complex indoor environments, such as warehouses, hospitals, and manufacturing plants. These characteristics make UWB a superior choice for asset tracking, particularly where traditional solutions fall short [2].

To address the growing demand for reliable indoor localization, various radio frequencies (RF), sound waves (ultrasound), and light waves (infrared) technologies have been explored. Among RF-based approaches, Wi-Fi, Bluetooth,

RFID, and UWB are the most widely studied [2], [3], [4], [5]. Wi-Fi is readily available in most buildings and offers a cost-effective localization solution. However, its low accuracy (5-15 meters) makes it unsuitable for applications requiring high precision [5]. Bluetooth Low Energy (BLE) provides a longer range (70-100 meters) and low power consumption, but its accuracy (1-2 meters) remains insufficient for precise tracking [6], [3], [7]. RFID is commonly used for object identification, with passive tags having a limited range (1-2 meters) and active tags offering longer range but lower accuracy compared to UWB [8]. UWB stands out due to its high precision, interference resistance, and low power consumption, making it the preferred choice for real-time indoor asset tracking in complex environments. While UWB offers significant advantages in accuracy and reliability, it comes with higher implementation costs compared to other alternatives. However, for applications that require high-precision tracking, the benefits of UWB justify its adoption.

Various techniques have been developed for indoor positioning systems, each with their own strengths and limitations:

Time of Arrival (ToA): Estimates position based on the time taken for a signal to travel between a tag and an anchor, often used with trilateration algorithms.

Time Difference of Arrival (TDoA): Determines position by calculating the difference in signal arrival times at multiple anchors.

Two-Way Ranging (TWR): Measures the round-trip time of signals, eliminating the need for devices synchronization while maintaining high accuracy and relatively low complexity.

Angle of Arrival (AoA): Uses antenna arrays to determine signal direction, providing precise location estimates but requiring more complex hardware.

Received Signal Strength Indicator (RSSI): Estimates distance based on signal strength, though it is prone to errors due to environmental interference.

For this research, the TWR technique was selected due to its simplicity, accuracy, and lack of complex synchronization requirements. In contrast, RSSI was avoided due to its susceptibility to interference, which could compromise the system's precision.

METHODOLOGY

A real-time localization system based on Ultra-Wideband (UWB) technology consists of several interconnected components that work together to provide accurate position tracking of mobile tags within a predefined space. This section outlines the architecture and roles of key system components, including anchors, tags, and a central server, all integrated to enable precise real-time localization. The system described in this article was developed with the aim of tracking the forks of a forklift, in order to automatically record the storage position of each product in a warehouse. This aims to solve a problem that exists in a company where the warehouse operator forgets to record the position where the products are stored, such a failure results in wasted time searching for the products when they are needed for shipping. Figure 1 shows what is to be achieved by developing this system.

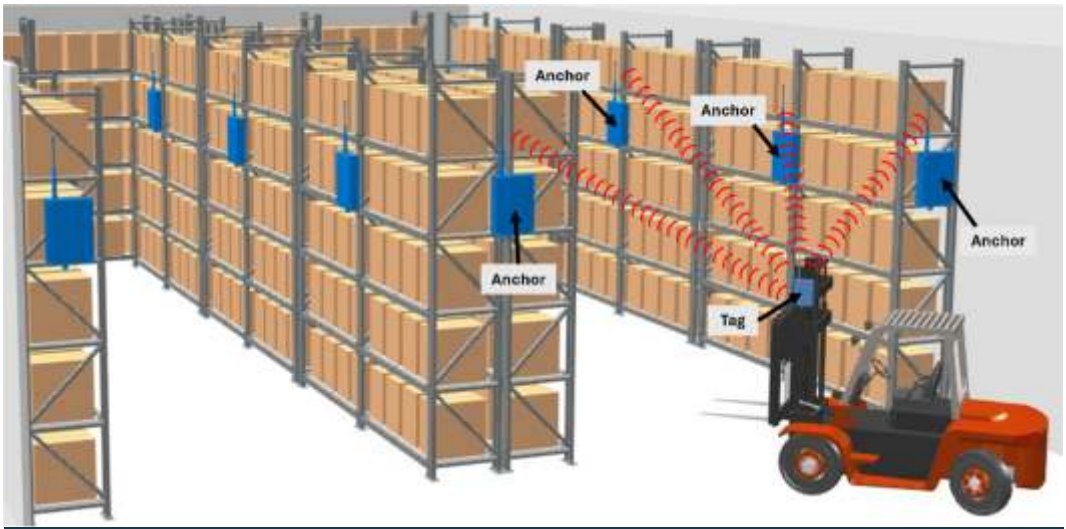

FIGURE 1
Representation of the system installation in a warehouse.

TRACKING SYSTEM ARCHITECTURE

At the core of the system are the anchors, which are stationary devices placed at fixed positions within the monitored area. Unlike other localization systems where anchors perform distance calculations, in this implementation, the anchors only receive requests from the mobile tag and respond with timestamps. Each anchor is equipped with a UWB module and a microcontroller, enabling it to transmit and receive signals, but it does not directly compute distances. The strategic placement of anchors is crucial to ensuring high localization accuracy, as each tag must interact with enough anchors to compute its position precisely. Thus, the anchors were distributed in such a way as to ensure total coverage of the space to be monitored, considering the need to minimize interference and maximize measurement accuracy. To this end, the anchors were positioned in elevated locations, away from physical obstacles such as walls, furniture, or other structural elements that could cause attenuation or unwanted reflections of the UWB signal. The selection of installation points also took into account the main trajectories and circulation areas of the tags, avoiding the placement of anchors in areas with high potential for obstruction. This approach reduces the multipath effect and increases the probability of direct line of sight (LOS) between each tag and the anchors.

Conversely, the tags are mobile devices whose positions need to be tracked in real time. These tags actively send distance measurement requests to the anchors. Upon receiving these requests, the anchors log the request timestamps and reply with the time the request was received and the exact time of their response. The tags then compute the distances to each anchor based on the round-trip time (RTT) of the signals. Once the distances are calculated, the tag forwards them to the central server for position estimation.

The central server functions as the computational core of the system. It receives distance measurements from the tags and determines their precise locations using trilateration algorithms [9]. Additionally, the central server can handle data visualization, integration with external applications, or further processing for tracking and automation systems. Figure 2 shows the overall schematic of implementation.

For accurate localization, the tag must gather distance data from at least three well-placed anchors before forwarding it to the central server. Localization accuracy depends on factors such as anchors placement, measurement

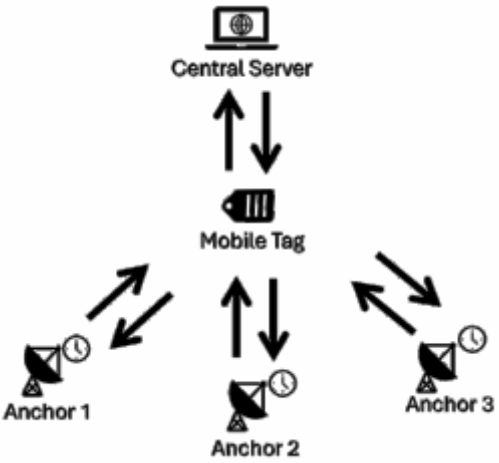

FIGURE 2
Implementation Overview: UWB-based Asset Tracking System.

precision, and environmental conditions like interference from obstacles. Only one tag was used for this system, but the principle of operation is the same for multiple tags.

HARDWARE INTEGRATION

The hardware components play a vital role in ensuring the accuracy and efficiency of the tracking system.

The anchors are equipped with Qorvo DWM3001CDK modules, which provide UWB communication capabilities. The module also contains a microcontroller that manages communication control with the tags, allowing them to take accurate distance measurements.
The mobile tags use Qorvo DWM3000EVB modules for UWB communication, paired with ESP32-WROOM-32D microcontrollers. These microcontrollers manage the tag's communication with the anchors, process the data sent by the anchors, calculating the distance at which each anchor is located, and send these distances to the central server via Wi-Fi communication.
The central server is implemented on a windows 11 computer which processes the data received and estimates the position of the tag.

RESULTS AND DISCUSSION

After completing the implementation of the system presented, two types of tests were carried out: one to assess whether the number of anchors used to estimate the position of the tag influences the accuracy of this estimate and the second test to assess the performance of the system, thus evaluating its accuracy. The results of the tests carried out are presented below.

NUMBER OF ANCHORS EVALUATION

To determine whether the number of anchors used to estimate the position of the tag affects the system's accuracy, tests were conducted

using three randomly selected positions within the traceable space. For each position, 500 samples were collected with configurations employing four, five, six, and seven anchors. The average error of the 500 samples was then analyzed to assess the influence of the number of anchors. Figure 3 illustrates the results for one of the selected positions, with similar findings observed for the other two.

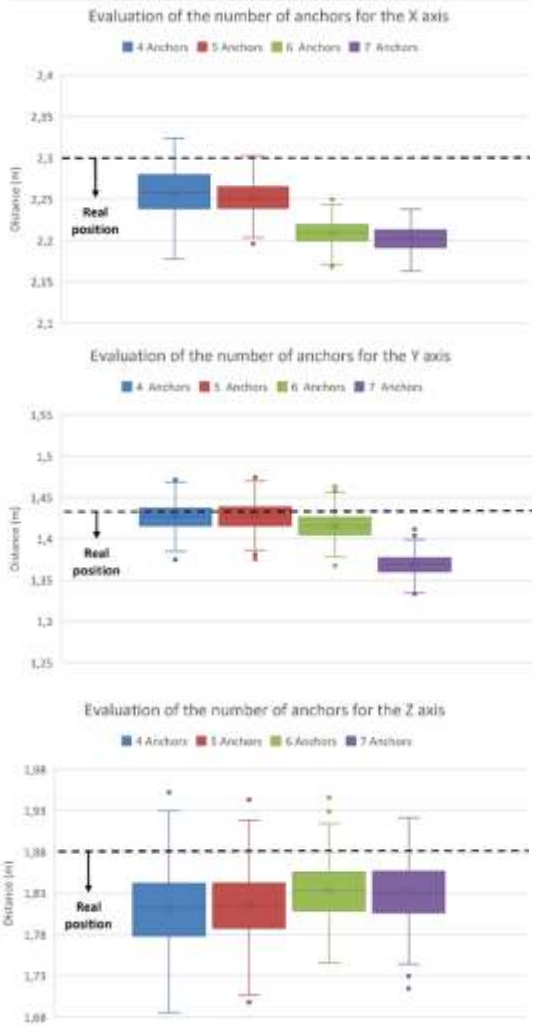

FIGURE 3
Results obtained by taking 500 samples for the position x = 2.30m; y = 1.43m; z = 1.88m.

The tests carried out show that increasing the number of anchors used to estimate the tag's position does not significantly improve the accuracy of the system. On the contrary, it was observed that using a larger number of anchors can, in some cases, reduce the accuracy of the position estimate. This phenomenon may be attributed to the fact that additional anchors tend to be further away from the tag, which can lead to increased measurement errors due to greater signal attenuation, interference, or non-line-of-sight conditions. As a result, distance measurements from these farther anchors are generally less reliable and can introduce additional error into the position estimation process. For this reason, only four anchors were selected for position estimation, prioritizing those that are geographically closest to the tag and offer the best line-of-sight conditions. This approach helps to minimize potential sources of error and ensures a more robust and accurate localization performance.

PERFORMANCE EVALUATION

To evaluate the system performance (system accuracy), a real-time motion tracking system developed and validated by Intel Corporation, called "Intel RealSense Tracking Camera T265", which is considered as ground truth, was used in parallel. With the two systems attached to a support, a trajectory was defined in the laboratory to extract position samples, so that at the end it would be possible to calculate the average error between the two systems, thus allowing an understanding of the accuracy of the developed location system. Figure 4 shows the layout of the laboratory, the position of the anchors and the trajectory taken.

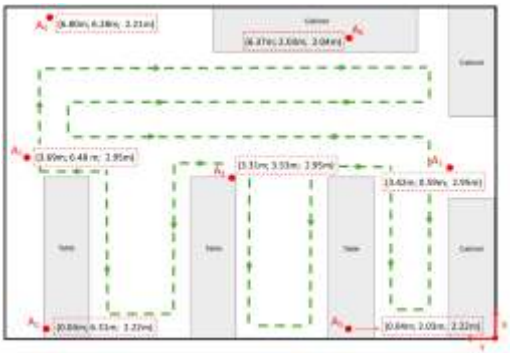

FIGURE 4
Layout of the laboratory, anchors position and trajectory taken.

After performing the trajectory shown in the image above, 31743 sample positions were obtained. With this data, the average error between the two systems was calculated, thus obtaining the accuracy of the system developed. The system developed has an average error of 7.8 cm for the X axis, 11.6 cm for the Y axis and 15.4 cm for the Z axis.

CONCLUSION AND FUTURE WORK

The demand for accurate and efficient location of goods indoors has driven the adoption of various location technologies. This paper presents an overview of a real-time asset tracking system using UWB, demonstrating its superior accuracy, reliability, and robustness to Wi-Fi, Bluetooth, and RFID technologies. The system, which includes anchors, mobile tags, and a

central server, achieves precise location through Two-Way Ranging (TWR) and trilateration, providing positioning accuracy of 5-30 cm. Although UWB outperforms alternative technologies, its higher costs and infrastructure requirements remain a challenge to widespread adoption.

Despite its advantages, limitations such as low vertical accuracy, environmental interference and deployment costs require further optimization. Future research should focus on increasing tracking accuracy by using machine learning models to improve tag position estimation. Integrating UWB with inertial measurement units (IMUs) or computer vision can improve robustness in complex environments. And the use of algorithms to place anchors in optimized locations can reduce infrastructure requirements. Solving these challenges will allow for more cost-effective, scalable and widely adopted UWB-based localization systems, ensuring their role as a key technology in the future of real-time indoor localization.

ACKNOWLEDGEMENTS

This research was funded by the "Agenda Mobilizadora para a inovação empresarial do setor das Duas Rodas (AM2R)" 01/C05-i01/2021 and LASI-LA/P/0104 /2020, co-funded from the "Mobilising Agendas/Alliances for Business Innovation" of the "Next Generation EU" program of Component 5 of the Portuguese Recovery and Resilience Plan (RRP), concerning "Investment and innovation", under the Regulation of the Incentive System for "Mobilising Agendas/Alliances for Business Innovation".

REFERENCES

[1] P. Wu, "Comparison between the Ultra-wide Band based indoor positioning technology and other technologies," in *Journal of Physics: Conference Series*, IOP Publishing Ltd, Feb. 2022. doi: 10.1088/1742-6596/2187/1/012010.

[2] H. Obeidat, W. Shuaieb, O. Obeidat, and R. Abd-Alhameed, "A Review of Indoor Localization Techniques and Wireless Technologies," *Wirel Pers Commun*, vol. 119, no. 1, pp. 289-327, 2021, doi: 10.1007/S11277-021-08209-5/TABLES/4.

[3] P. S. Farahsari, A. Farahzadi, J. Rezazadeh, and A. Bagheri, "A Survey on Indoor Positioning Systems for IoT-Based Applications," *IEEE Internet Things J*, vol. 9, no. 10, pp. 7680-7699, 2022, doi: 10.1109/JIOT.2022.3149048.

[4] M. D. Jovanovic and S. M. Djosic, "Analysis of Indoor Localization Techniques," in *2023 58th International Scientific Conference on Information, Communication and Energy Systems and Technologies*, ICEST 2023 - Proceeding, 2023, pp. 219-222. doi: 10.1109/ICEST58410.2023.10187323.

[5] N. C. Syazwani, N. H. A. Wahab, N. Sunar, S. H. S. Ariffin, K. Y. Wong, and Y. Aun, "Indoor Positioning System: A Review," *Int J Adv Comput Sci Appl*, vol. 13, no. 6, 2022, [Online]. Available: www.ijacsa.thesai.org

[6] F. Zafari, A. Gkelias, and K. K. Leung, "A Survey of Indoor Localization Systems and Technologies," *IEEE Communications Surveys and Tutorials*, vol. 21, no. 3, pp. 2568-2599, 2019, doi: 10.1109/COMST.2019.2911558.

[7] S. G. Leitch and others, "On Indoor Localization Using WiFi, BLE, UWB, and IMU Technologies," *Sensors*, vol. 23, no. 20, 2023, doi: 10.3390/S23208598.

[8] R. Journal, "What Is the Location Accuracy of an RFID System?," 2024. [Online]. Available: https://www.rfidjournal.com/ask-the-experts/what-is-the-location-accuracy-of-an-rfid-system/

[9] "least_squares - SciPy v1.14.1 Manual." Accessed: Sep. 17, 2024. [Online]. Available: https://docs.scipy.org/doc/scipy/reference/generated/scipy.optimize.least_squares.html

VISIBILITY FOR INNOVATION IN MATERIALS

The Portuguese Society of Materials (SPM) plays an active role in disseminating scientific and technological projects, helping to increase the visibility, impact, and value of the results developed in the field of materials. Founded in 1981, SPM positions itself as a strategic link between academia, industry, and society, promoting knowledge and reinforcing the importance of materials in scientific and social development."

COME JOIN US

SPM
SOCIEDADE PORTUGUESA de MATERIAIS

CONTACT

Manuela Oliveira
Tel: 96 5756172

SPM - Apartado 4538
EC Carnide
1511-970 Lisboa

spm@spmateriais.pt
www.spmateriais.pt

ARTIFICIAL VISION SUPERVISOR TO ENHANCE HUMAN ASSEMBLY OPERATIONS

Luís Vilas Boas[1,2], João M. Faria[1,2], N. Simões[1,2], Joaquin Dillen[1,2], Rafael Fernandes[1,2], Bruno Silva[1,2], Inês Caetano[3], Luís Cardoso[4], João Borges[1,2], António H. J. Moreira[1,2]

1 2Ai - School of Technology, IPCA, Barcelos, Portugal.
2 LASI - Associate Laboratory of Intelligent System, Guimarães, Portugal.
3 Sistrade - Software Consulting, SA, Porto, Portugal.
4 Miranda & Irmão, LDA, Águeda, Portugal.

*Corresponding author(s). E-mail(s): lvilasboas@jpca.pt;
Contributing authors: jdillen@ipca.pt; rmfernandes@ipca.pt; brsilva@ipca; nsimoes@ipca.pt; jpfaria@ipca.pt; ines.caetano@sistrade.pt; lcardoso@miranda.pt; jpbsilva@ipca.pt; amoreira@ipca.pt

In the context of Industry 4.0, the increasing demands for flexibility, customization, and efficiency in manufacturing have driven the development of innovative assistance systems to support human operators in complex assembly processes. This work presents vision-based system designed to monitor and improve manual assembly processes in industrial environments. By leveraging an OAK-D Pro PoE camera and a trained YOLO object detection model, the system analyses operational actions in real time, detecting assembly phases, measuring task durations, and identifying errors. A simple Human-Machine Interface (HMI) was developed to provide workers with performance feedback, including Key Performance Indicators (KPIs) such as total assembly time, phase-specific times, and error counts. Experimental tests with multiple operators demonstrated the system's ability to accurately track assembly tasks, identify inefficiencies, and highlight areas for process improvement.

KEYWORDS
INDUSTRY 4.0; DIGITAL MANUFACTURING; ASSEMBLY SYSTEM; KEY PERFORMANCE INDICATORS (KPI).

INTRODUCTION

The success of industrial enterprises in Industry 4.0 is closely tied to their ability to adapt to emerging social, technological, and economic conditions. Key drivers include high flexibility, increased customization, variable production batches, and shorter product life cycles, necessitating a shift to Next Generation Production Systems (NGPSs) [1], [2]. Within these systems, human operators play a pivotal role. As the most adaptable resource in manufacturing, they respond dynamically to complex work conditions[3].

On the shop floor, operators face increased product complexity, accelerated development cycles, and numerous product variants. These factors impact manual operations, making assembly processes more prone to human errors such as delays and defects[4]. Addressing these challenges requires qualification measures at both organizational and technological levels. Such measures aim to equip operators with the tools and skills needed to efficiently perform their tasks while minimizing errors and defects during manufacturing and assembly processes.

Existing assistance systems designed to support manual assembly operations can be broadly categorized into Pick-by-Light and Pick-by-Vision systems. In Pick-by-Light systems, lights are affixed to each component's storage location on the rack, providing visual guidance to operators regarding the specific parts to pick and their quantities[5].

In contrast, Pick-by-Vision systems utilize Human-Machine Interfaces (HMIs) and Augmented Reality (AR) technologies. AR enables the augmentation of the physical world with virtual overlays, offering operators the advantage of receiving virtual instructions directly within their field of view [6], [7].

These systems often employ smart glasses to display the components to be picked, eliminating the need for physical installations on racks and allowing monitoring of larger picking areas with a single device [8]. However, they lack feedback on the correctness of operator actions. Recent advancements focus on marker-less systems leveraging computer vision and depth cameras [9], [10]. These systems aim to evaluate

operator interactions with their surroundings in real-time, enhancing the precision and effectiveness of assembly and manufacturing processes.

Therefore, this paper proposes a Pick-by-Vision hardware/software system that guides and provides real-time feedback through an HMI. By tracking assembly stages, it extracts key performance indicators (KPIs) such as total time, cycle times, phase durations, and errors. This data enables workers to optimize processes, improving efficiency, and reducing mistakes.

METHODOLOGY

A software solution was developed to monitor the assembly process, as shown in Figure 1 (A). It integrates the OAK-D Pro PoE RGB camera for image acquisition, which are then processed by the YOLOv11 Nano model for object detection and KPI computation. The results, including KPIs and processed images, are displayed on an HMI, enabling real-time monitoring and operator interaction during assembly.

The assembly process consists of five stages and involves key objects: a red base, four nuts, a gear, the spider, and four screws. The detection of each stage relies on identifying these objects, allowing the system to track progress and detect errors, such as misplaced components. To ensure accurate detection, a YOLOv11 Nano model was trained using a synthetic dataset of ~50k annotated images, generated via a virtual environment with CAD models. The dataset was divided by assembly stages (5) as shown in Figure 1 (B), and training included a batch size of 32 with data augmentation techniques like flipping, shearing, mosaic augmentation, and color alteration. The trained model achieved high accuracy when tested on real images, with a precision of 0.86, recall of 0.88, and an F1-score of 0.87. By replicating real-world conditions in training, the system can generalize to different assembly processes using corresponding trained models.

EXPERIMENTS

These tests were executed in laboratory environment mimicking industrial conditions, such as variable lights, where 4 individuals were requested to assemble the part, everyone made 5 assembly runs to obtain sufficient and valid data to get credible results. From these assembly runs, it was possible to extract 3 KPI values, these being, the total time for the assembly of the part, the time it takes per phase of the assembly process, and the mistakes that were made during the runs. With this information, it is also possible to determine some resolutions that can be made to improve the process at hand. In addition, a simple HMI was built to communicate with the operator performing the assembly task, presenting the metrics retrieved by the system.

RESULTS

Figure 2 (a) illustrates the evolution of the assembly time of the component as a function of the number of executions/cycles of the

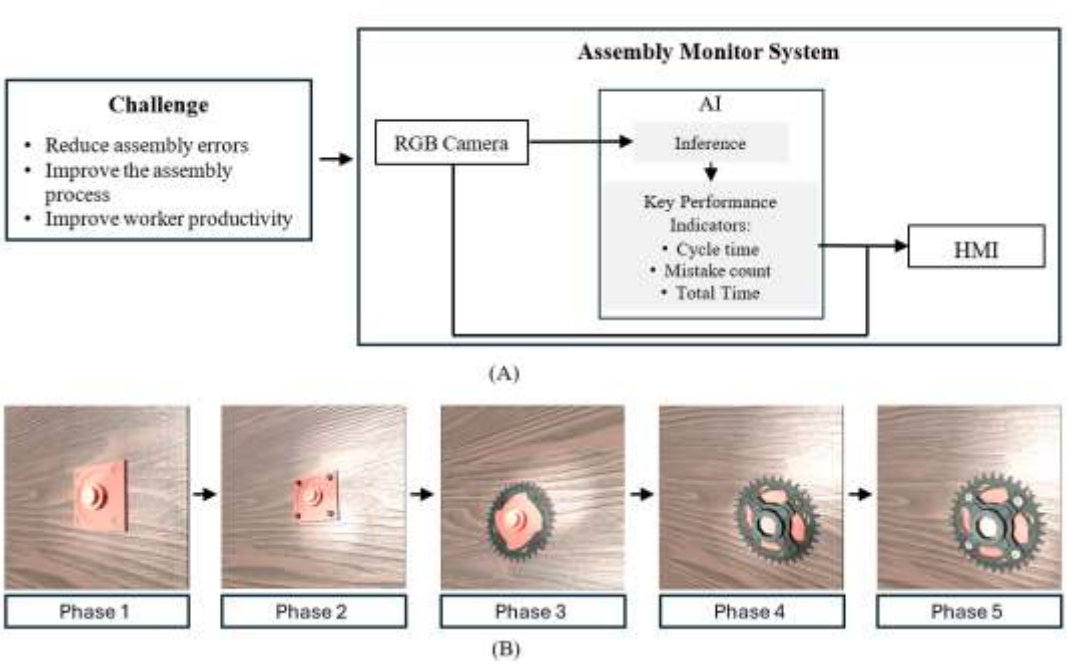

FIGURE 1
Schematic of the designed system for monitoring the assembly process, consisting of a camera, a computer handling AI tasks, and an HMI for operator communication and feedback (A). Additionally, an example of the assembly process is shown, detailing its phases and the correct assembly sequence (B).

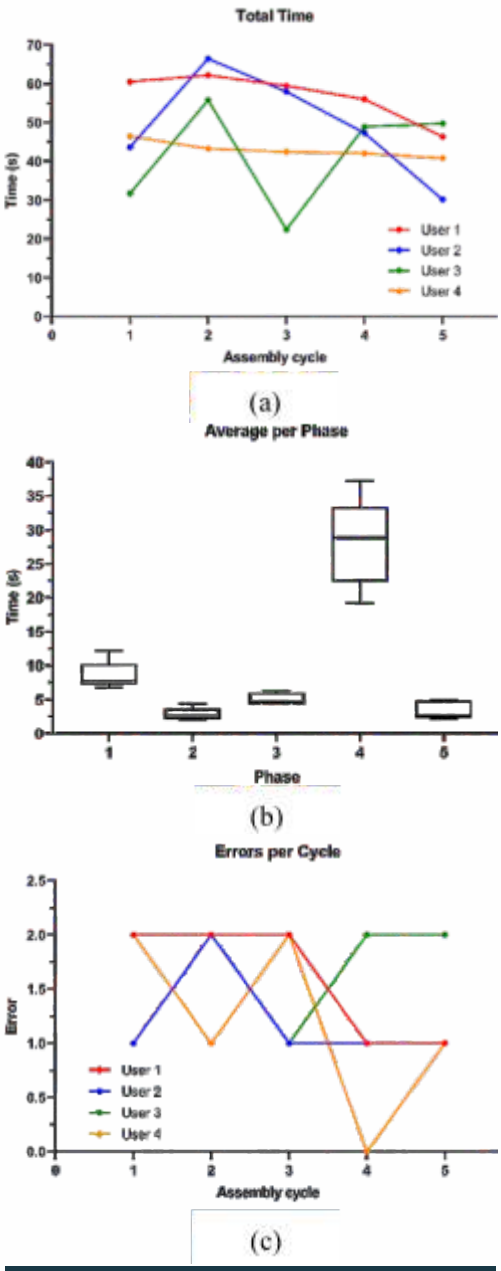

FIGURE 2
Comprehensive analysis of assembly performance: The Graph (a) compares the total time taken by four testers across five assembly cycles.
The graph (b) provides a detailed breakdown of the time spent on each phase of the assembly cycle by a single tester.
The graph (c) highlights the number of errors committed by different testers throughout all test cycles.

process. As expected, a decreasing trend in assembly time is observed as the number of cycles increases, suggesting a learning effect. However, a significant variability in the performance of one of the individuals is noted, characterized by pronounced fluctuations in assembly time. These variations may be associated with difficulties in handling the components or additional time required for screw tightening.

In the next phase of the data analyses, we analyzed the time taken on each phase of the assembly, as shown in Figure 2(b), there are two points on the process that take noticeably more time. Based on the Anova statistical analysis we can see significant differences in assembly times across phases ($F = 58.52$, $p = 5.67e\text{-}09$).

Tukey's post-hoc also test showed phase 4 had significantly higher times than all others (e.g., Phase 1 vs. Phase 4 has a mean difference of 19.5, with a 95% Confidence Interval. In contrast, Phase 1 vs. Phase 2 showed no significant difference. Average times were the highest in Phase 4 (28.06 seconds) and lowest in Phase 2 (2.84 seconds).

Also based in the average values and standard deviation of each phase, phase 4 is the one that presents the greatest deviation from the average (3.83 seconds), presenting itself as the most critical phase and the one with most potential for improvement. If these data were related to a process captured in the industrial environment, phase 4 should be evaluated to reduce time and boost productivity.

The error measuring part of the system that can be evaluated in Figure 2 ©, the colors of the lines present in the graph also correspond to the same lines on the Total time graph in Figure 2 (a) previously mentioned. As should be expected, the number of mistakes committed also correspond to the cycles that take more time to assemble the part, despite this being clear, this may not be true for all assembly processes, because there is one tester (the one that corresponds to the orange line) where this fact is not true.

The HMI built presents all the necessary data, to help the worker and retrieve all the necessary information of the assembly process, as shown in Figure 3.

CONCLUSION

Promising results and valuable insights were obtained from key performance indicators,

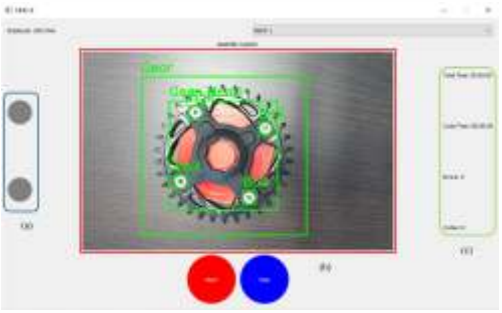

FIGURE 3
Example of the HMI developed, in blue is the alerts in case of occurrence of an error. In red the video feed of the assembly process giving of information of what objects are present, and in green are the KPI metrics that are been retrieved by the system.

particularly in computing essential metrics like cycle times and total assembly times. However, improvements are needed. Enhancing the HMI with clearer error visualization and a more user-friendly design will better assist operators, while increasing the accuracy of the YOLO model is crucial for reducing detection inconsistencies and improving system reliability. Future improvements include refining the model with a more diverse dataset, optimizing real-time performance, and adapting the system to industrial environments, where unforeseen challenges may arise. Additionally, expanding error detection, generalizing key performance metrics across different assemblies and stages, and increasing the number of testers will contribute to more robust and reliable results.

ACKNOWLEDGMENT

This research was carried out in partnership with the companies Sistrade - Software Consulting, SA, SRAM and Miranda & Irmão, Lda, funded by the "Agenda Mobilizadora para a inovação empresarial do setor das Duas Rodas (AM2R)" 01/C05-i01/2021 and LASI-LA/P/0104/2020, co-funded from the "Mobilising Agendas/Alliances for Business Innovation" of the "Next Generation EU" program of Component 5 of the Portuguese Recovery and Resilience Plan (RRP), concerning "Investment and innovation", under the Regulation of the Incentive System for "Mobilising Agendas/Alliances for Business Innovation".

REFERENCES

[1] A. Molina et al., "Next-generation manufacturing systems: Key research issues in developing and integrating reconfigurable and intelligent machines," *Int J Comput Integr Manuf,* vol. 18, no. 7, 2005, doi: 10.1080/09511920500069622.

[2] M. Bortolini, F. G. Galizia, and C. Mora, "Reconfigurable manufacturing systems: Literature review and research trend," 2018. doi: 10.1016/j.jmsy.2018.09.005.

[3] D. Gorecky, M. Khamis, and K. Mura, "Introduction and establishment of virtual training in the factory of the future," *Int J Comput Integr Manuf,* vol. 30, no. 1, 2017, doi: 10.1080/0951192X.2015.1067918.

[4] L. Rodriguez, F. Quint, D. Gorecky, D. Romero, and H. R. Siller, "Developing a Mixed Reality Assistance System Based on Projection Mapping Technology for Manual Operations at Assembly Workstations," *Procedia Comput Sci*, vol. 75, pp. 327-333, Jan. 2015, doi: 10.1016/J.PROCS.2015.12.254.

[5] Å. Fasth-Berglund and J. Stahre, "Cognitive automation strategy for reconfigurable and sustainable assembly systems," *Assembly Automation*, vol. 33, no. 3, 2013, doi: 10.1108/AA-12-2013-036.

[6] Z. Wang et al., "A comprehensive review of augmented reality-based instruction in manual assembly, training and repair," *Robot Comput Integr Manuf*, vol. 78, p. 102407, Dec. 2022, doi: 10.1016/J.RCIM.2022.102407.

[7] M. Eswaran, V. S. S. V. Prasad, M. Hymavathi, and M. V. A. R. Bahubalendruni, "Augmented reality guided autonomous assembly system: A novel framework for assembly sequence input validations and creation of virtual content for AR instructions development," *J Manuf Syst*, vol. 72, pp. 104-121, Feb. 2024, doi: 10.1016/J.JMSY.2023.11.002.

[8] Z. H. Lai, W. Tao, M. C. Leu, and Z. Yin, "Smart augmented reality instructional system for mechanical assembly towards worker-centered intelligent manufacturing," *J Manuf Syst,* vol. 55, pp. 69-81, Apr. 2020, doi: 10.1016/J.JMSY.2020.02.010.

[9] M. A. Zamora-Hernández, J. A. Castro-Vargas, J. Azorin-Lopez, and J. Garcia-Rodriguez, "Deep learning-based visual control assistant for assembly in Industry 4.0," *Comput Ind*, vol. 131, p. 103485, Oct. 2021, doi: 10.1016/J.COMPIND.2021.103485.

[10] E. Kozikowski, N. W. Hartman, and J. D. Camba, "Development and Evaluation of a Computer Vision System for Assembly Bolt Pattern Traceability and Poka-Yoke," in *Volume 2: Manufacturing Processes; Manufacturing Systems*, American Society of Mechanical Engineers, Jun. 2022. doi: 10.1115/MSEC2022-85678.

CHARACTERIZING RFID SIGNAL DISTORTION CAUSED BY MATERIAL INTERFERENCE IN PASSIVE TAG SYSTEMS

Cláudia Pereira[1,2], Joaquin Dillen[1,2*], Luis Vilas Boas[1,2], N. Simões[1,2], Rafael Fernandes[1,2], Bruno Silva[1,2], João M. Faria[1,2], Inês Caetano[3], Luís Cardoso[4], João Borges[1,2], António H. J. Moreira[1,2]

1 2Ai - School of Technology, IPCA, Barcelos, Portugal.
2 LASI - Associate Laboratory of Intelligent System, Guimarães, Portugal.
3 Sistrade - Software Consulting, SA, Porto, Portugal.
4 Miranda & Irmão, LDA, Águeda, Portugal.

*Corresponding author(s). E-mail(s): a13289@alunos.ipca.pt
Contributing authors: jdillen@ipca.pt; lvilasboas@ipca.pt; rmfernandes@ipca.pt; nsimoes@ipca.pt; brsilva@ipca.pt jpfaria@ipca.pt; ines.caetano@sistrade.pt; lcardoso@miranda.pt; jpbsilva@ipca.pt; amoreira@ipca.pt

Passive RFID systems have become essential in various industries for identification, inventory control, and tracking applications. Despite their widespread adoption, RFID tag readability is substantially influenced by the materials surrounding the tags, presenting challenges in diverse operational environments. This study systematically investigates how common industrial and everyday materials, including metals, liquids, and dielectric substances, impact RFID signal propagation and tag detection performance. Through controlled laboratory experiments, we measured signal behavior and tag visibility across multiple trials per material. Results show that while materials like aluminum clearly degraded signal reach and detection rates, others such as iron and water introduced complex signal distortions that resulted in moderate impacts on tag detection. These included effects such as reflection-based amplification and signal absorption. In contrast, acrylic, cardboard, fabric, and wood exhibited minimal signal interference. These findings confirm the presence of distinct material-specific signatures and highlight the usefulness of practical metrics like tag count and RSSI analysis for evaluating RFID signal distortion. The study provides insights for improving RFID system reliability in environments with varied electromagnetic properties.

KEYWORDS
PASSIVE RFID; SIGNAL DISTORTION; MATERIAL INTERFERENCE; ELECTROMAGNETIC INTERFERENCE; TAG DETECTION; SIGNAL PROPAGATION.

INTRODUCTION

Radio Frequency Identification (RFID) has become a fundamental technology for object tracking, inventory control, and automation in both industrial and commercial environments. Passive RFID tags, in particular, offer a low-cost, low-maintenance solution for identification tasks across a wide range of sectors, including supply chain management, manufacturing, and retail. Despite their practical benefits, the performance of RFID systems remains sensitive to environmental conditions, particularly the influence of materials surrounding the tag or obstructing the signal path.

Material-induced interference is a well-documented challenge in RFID deployments. Substances such as metals, liquids, and dense packaging materials can reflect, absorb, or scatter electromagnetic signals, leading to reduced read range, unstable communication, and missed detections. Metals typically reflect signals, causing destructive interference and detuning of the tag antenna. Liquids tend to absorb high-frequency signals, especially in the UHF band, while other materials with varying dielectric properties introduce unpredictable phase shifts and attenuation. These physical interactions have been recognized as critical

barriers to the reliable implementation of RFID systems in complex logistics and production environments [1], [2], [3].

Several studies have proposed strategies to address material interference, ranging from custom antenna designs and shielding techniques to adaptive reader configurations and the use of frequency hopping. With the advent of machine learning and artificial intelligence, new approaches are being explored that aim to characterize the environment and material conditions through signal analysis. Recent research has shown that AI-enhanced RFID systems can improve detection accuracy in dynamic and cluttered settings, particularly in retail and manufacturing scenarios [4], [5]. These developments point toward the possibility of using signal patterns themselves as indicators of the physical context.

In this context, our research investigates whether different materials can be distinguished based on the unique distortions they introduce into RFID signal parameters, namely the Received Signal Strength Indicator (RSSI) and Phase. The central hypothesis of this study is that each material leaves a measurable "signature" on the RFID signal, and that these signatures can be detected, analyzed, and potentially used for material identification. This aligns with broader efforts to improve smart manufacturing through the characterization and prediction of RFID tag behavior in real-world conditions [6].

In this paper, we specialize in analyzing the signal behavior of individual materials. Rather than comparing all materials simultaneously, we focus on profiling one material at a time across multiple trials. This approach allows for a more detailed understanding of signal consistency, interference patterns, and material impact on RFID readability. The results from this single-material analysis form the basis for a future classification framework and provide deeper insight into how materials distort passive RFID signals.

EXPERIMENTAL SETUP AND DATASET

To investigate the impact of different materials on RFID signal behavior, we designed a controlled experiment in which passive UHF RFID tags were exposed to a selected set of materials under repeated and standardized conditions. The objective was to observe how each material influences the Received Signal Strength Indicator (RSSI) and to collect sufficient data to support statistical analysis and potential signal-based material profiling.

EXPERIMENTAL DESIGN

The experiment was structured to evaluate how different materials affect RFID signal strength. A passive UHF RFID system was employed, consisting of a fixed RFID reader and a directional antenna operating under consistent environmental and spatial conditions. The RFID tags remained stationary throughout the experiment, while each material was placed in the center of the setup, positioned between the reader and the tags. This configuration was designed to simulate real-world scenarios involving signal interference and attenuation.

Eight materials were selected for testing: acrylic, water, aluminum, cardboard, iron, wood, fabric, and a control condition labeled "nothing," in which no material was present. These materials were chosen to represent a broad range of electromagnetic properties, including reflectivity, absorption, and dielectric variability, all of which are known to influence RFID system performance [1], [2].

Each material was tested in three independent sessions, referred to as Trial 1 (T1), Trial 2 (T2), and Trial 3 (T3). During each session, the RFID system collected data continuously over a one-minute interval. This protocol was repeated under identical conditions to ensure repeatability and to observe intra-material variability across trials.

DATA COLLECTION

The RFID reader continuously polled for tag responses throughout each trial. Each tag detection was logged along with multiple signal-related attributes. The raw data was recorded in CSV format, with each file corresponding to a specific material and trial. A total of twenty-four files were generated, one for each combination of material and trial.

For each tag read, the following parameters were recorded: the IP address of the RFID reader, the unique Electronic Product Code (EPC) of the tag, the antenna port used, the RSSI value (in dBm), and timestamps indicating the first and last detection events. During preprocessing, additional metadata columns identifying the material and trial were appended to each record.

DATA PREPROCESSING

Data preparation was conducted using Python in the Google Colab platform. All CSV files were loaded from Google Drive, parsed, and merged into a unified dataset to facilitate centralized analysis. The preprocessing pipeline included the removal of formatting artifacts, standardi-

zation of column headers, conversion of timestamp strings to datetime objects, and the elimination of duplicate entries to ensure data quality.

The final dataset included 579,081 entries and was structured to enable per-material analysis, time-series evaluation, and assessment of signal variability. The analysis presented in the following sections focuses primarily on the RSSI data, which serves as the key indicator of signal performance and material-induced distortion in passive RFID systems.

DATASET ANALYSIS

The dataset collected during the experimental trials was analyzed to evaluate the behavior of the RFID signal under different material conditions. The focus of this analysis is the Received Signal Strength Indicator (RSSI), as it serves as the primary indicator of signal quality and material-induced distortion.

RSSI DISTRIBUTION PER MATERIAL

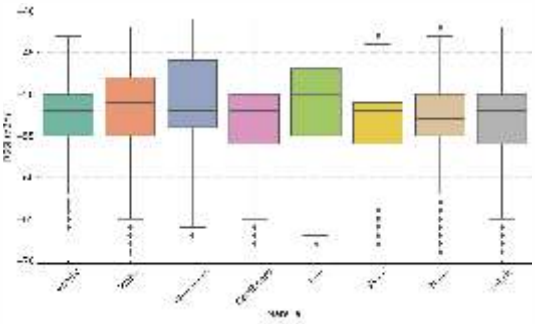

FIGURE 1
RSSI Distribution per material.

The analysis of RSSI distributions across the tested materials reveals clear and measurable differences in signal attenuation behavior. As shown in Figure 1 , the control condition with no obstructing material (None) produced a consistently strong and relatively stable signal, with modest variability and few outliers. While some materials, such as Iron, exhibited higher median RSSI values, these are likely attributable to reflective signal reinforcement rather than genuine signal clarity. The control condition thus establishes a clean baseline for assessing material-induced distortion under ideal conditions.

In contrast, materials such as Aluminum and Water consistently resulted in lower median RSSI values and exhibited wider signal variance. These materials are known for their strong interaction with electromagnetic fields, with aluminum primarily causing reflection and detuning effects, and water absorbing the signal. Both mechanisms degrade signal reliability. Iron, however, showed a relatively high median RSSI, even surpassing the control condition. While this may initially seem inconsistent with classical expectations of metallic attenuation, the elevated RSSI values are consistent with well-documented multipath effects. In such cases, reflected signals from metallic surfaces arrive at the reader with constructive phase alignment, temporarily reinforcing the received power [7]. This effect causes localized signal amplification without enhancing signal clarity or tag readability. Accordingly, the higher RSSI observed for Iron and Aluminum reflects electromagnetic distortion rather than reliable signal transmission, aligning with theoretical models of interference caused by conductive materials.

Materials such as Acrylic, Cardboard, and Wood produced mid-range RSSI values with relatively low variability. These materials are generally considered RFID-friendly due to their low dielectric constants and low levels of signal reflection or absorption. Fabric presented a moderate level of attenuation, likely due to its flexibility and inconsistent density, which may have affected how the signal passed through it during the trial.

The overall distribution patterns support the hypothesis that each material interacts with the RFID signal in a distinct manner. These differences, particularly in median RSSI and spread, serve as the foundation for identifying material-specific signal signatures.

TIME-BASED SIGNAL TRENDS

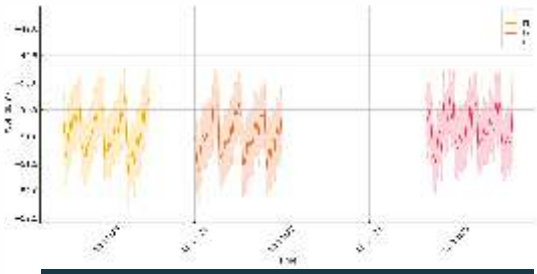

FIGURE 2
RSSI Over time for Aluminium Across Trials T1-T3.

To investigate the temporal characteristics of the RFID signal, RSSI values were plotted over time for selected materials. Figure 2 illustrates the signal behavior for aluminum across Trials 1, 2, and 3. Aluminum was chosen due to its known tendency to interfere strongly with radio signals through reflection and shielding effects.

The plot reveals notable fluctuations in RSSI within each trial. Signal strength varied significantly over short time intervals, with visible dips and spikes occurring even under controlled, static conditions. This suggests that aluminum does not only attenuate the signal but also

introduces instability in signal propagation. The variation observed may be attributed to multipath effects, minor environmental interactions, or internal reflections within the aluminum block itself.

Despite these fluctuations, the three trials show similar overall behavior, reinforcing the consistency of aluminum's impact on the signal. The amplitude and rhythm of the RSSI oscillations appear comparable across trials, which supports the hypothesis that such materials introduce a repeatable yet variable interference pattern.
These time-based trends provide additional insight beyond static signal strength values, revealing how materials may influence signal stability during continuous reading. This information is particularly relevant for applications that rely on real-time or repeated RFID scanning, where not only signal strength, but also its temporal consistency, affects system reliability.

TRIAL CONSISTENCY AND REPRODUCIBILITY

The reproducibility of results across the three trials was assessed by comparing summary statistics for each material. Materials such as acrylic and cardboard demonstrated high consistency between trials. Conversely, materials like fabric and iron exhibited more noticeable shifts in signal strength between sessions.

Although variation was present, the overall shape and range of the RSSI distributions remained consistent for each material, suggesting that while environmental noise may affect individual reads, the material-induced signature is stable across trials.

SIGNAL FEATURE SUMMARY AND SIGNATURE POTENTIAL

To further examine the unique impact of each material on RFID signal behavior, descriptive statistical features were extracted from the RSSI values. These include the mean, standard deviation, minimum, and maximum signal strength per material. The results are presented in Table 1, which highlights the variation in signal characteristics across the tested materials.

The control condition (None) exhibited relatively low signal variability and served as a stable baseline. While its mean RSSI was lower than that of some metallic materials, such as Iron and Aluminum, those stronger signals were accompanied by greater fluctuation and are likely the result of reflective interference rather than genuine signal clarity. In contrast, materials such as Aluminum and Iron demonstrated lower average RSSI values and higher standard deviation, indicating both attenuation and signal instability. Water also caused significant attenuation, though it displayed relatively less variability than metallic materials.

TABLE 1
Signal Summary Per Material (dBm).

Material	Mean RSSI	Standard Deviation	Min RSSI	Max RSSI
Acrylic	- 52.7761	4.155943	-66	-43
Aluminum	-50.9009	5.842091	-67	-41
Cardboard	- 53.1852	4.543199	-68	-42
Fabric	-53.1283	4.528449	-69	-42
Iron	-50.6424	5.936125	-68	-41
None	-53.1069	4.421201	-69	-42
Water	-51.514	5.128941	-69	-42
Wood	-52.9278	4.268933	-68	-43

Materials like Acrylic and Cardboard maintained intermediate mean RSSI values with relatively narrow distributions, suggesting a weaker interaction with the electromagnetic signal. Fabric, while similar in mean RSSI to cardboard, exhibited slightly more variability, which may be attributed to its flexible and non-uniform physical structure.

These signal profiles support the idea that each material imposes a consistent and distinguishable effect on RFID signal strength. The differences in central tendency and dispersion provide a quantitative foundation for identifying materials based on their electromagnetic interaction. This analysis serves as a basis for the machine learning approach that follows, where these features are used to train a classification model capable of predicting the material type from signal observations.

TAG VISIBILITY ANALYSIS BY MATERIAL

To evaluate the effect of different materials on RFID signal propagation, we analyzed the number of unique RFID tags detected during each one-minute trial. This approach offers a straightforward proxy for signal obstruction: materials that attenuate, reflect, or absorb the radio signal tend to reduce the number of tags successfully read.

For each material and trial, we computed the count of distinct tags observed. The results, shown in Figure 3, demonstrate consistent patterns. Materials such as Acrylic, Cardboard, and Wood allowed nearly all 55 tags to be read in every trial, indicating minimal interference. On the other hand, Aluminum led to a clear

reduction in tag visibility, consistent with its known signal reflection and shielding effects. Water caused a moderate decrease in tag detection, likely due to its absorptive interaction with UHF signals. Fabric showed a slight and consistent reduction in the number of tags detected across trials, though its overall performance remained relatively close to that of low-interference materials like Acrylic and Cardboard.

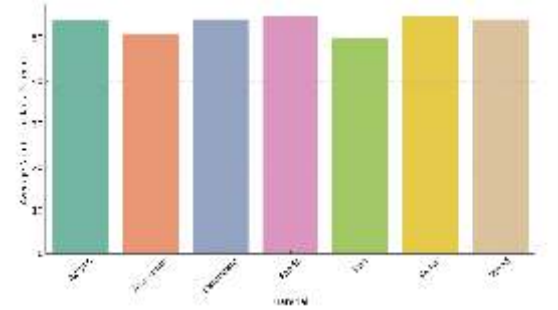

FIGURE 3
Average number of RFID tags detected per material. Signal-blocking materials like Aluminum and Water reduce tag visibility.

These patterns align well with the expected physical properties of the materials: metals and liquids are known to degrade UHF RFID performance through reflection, absorption, or detuning effects, while low-dielectric materials permit more reliable transmission.

This analysis demonstrates that even a simple tag count metric can effectively capture material-induced distortion and provide valuable insight into signal behavior.

RESULTS AND DISCUSSION

The tag count analysis confirms that different materials consistently impact RFID signal behavior in measurable ways. Materials such as Aluminum caused a notable reduction in tag visibility, while Water and Iron introduced signal variability and moderate decreases in detection rates.

These results are consistent with known electromagnetic properties: metals reflect and distort radio signals, while liquids absorb them, both leading to lower detection rates. Conversely, dielectric materials such as plastics and paper-based composites have little effect on UHF RFID propagation.

It is important to note that higher RSSI values observed for some metals, such as Iron, do not necessarily indicate stronger or more reliable signal transmission. These elevated values are often the result of multipath reflections, as previously discussed, and may obscure underlying instability in tag detection.

The ability to differentiate materials based on signal loss alone provides a practical and interpretable metric for system designers. Rather than relying on complex models or sensor fusion, basic visibility metrics may offer enough insight to adjust system parameters or trigger environment-aware behavior.

However, this approach also has limitations. Tag visibility is sensitive not only to material properties but also to environmental factors, tag placement, and reader configuration. Further studies would be required to isolate these variables and enhance the robustness of detection.

CONCLUSION AND FUTURE WORK

This study examined how different materials distort RFID passive tag signals by analyzing variations in tag visibility under controlled conditions. Using a simple metric, the number of tags successfully read per trial, we showed that aluminum consistently reduced signal reach, while water and iron introduced distortion effects that moderately impacted detection reliability. In contrast, materials like acrylic and cardboard allowed for near-complete tag detection. These findings support the idea that each material introduces a measurable signature into the RFID signal environment.

Although this work focused on tag count as a proxy for signal distortion, future research will build on these findings by exploring multi-tag feature aggregation, time-based signal behavior, and advanced classification models. Further investigations will also consider factors such as antenna orientation, reader pow aluminum consistently reduced signal reach, while water and iron introduced distortion effects that moderately impacted detection reliability.

ACKNOWLEDGEMENTS

This research was funded by the "Agenda Mobilizadora para a inovação empresarial do setor das Duas Rodas (AM2R)" 01/C05-i01/2021 and LASI-LA/P/0104 /2020, co-funded from the "Mobilising Agendas/Alliances for Business Innovation" of the "Next Generation EU" program of Component 5 of the Portuguese Recovery and Resilience Plan (RRP), concerning "Investment and innovation", under the Regulation of the Incentive System for "Mobilising Agendas/Alliances for Business Innovation".

REFERENCES

[1] H. Knapp and D. Uckelmann, "Literature review on sources of interference and proposed solutions for RFID installations in complex production and logistics processes in the automotive industry," *International Journal of RF Technologies*, 2022, doi: https://doi.org/10.3233/RFT-210312.

[2] M. Fernandes, J. Rodrigues, P. Saraiva, N. Bonifácio, P. Brochado, and N. B. Carvalho, "Study of Material Interference in a RFID Tag Reading," 2016.

[3] T. T. Electronics, "RFID: The technology making industries smarter." [Online]. Available: https://www.ttelectronics.com/blog/rfid-technology/

[4] Andrea Motroni, M. R. P. Marcos, A. Buffi, and P. Nepa, "Artificial Intelligence enhances Smart RFID Portal for retail," *2022 IEEE International Conference on RFID (RFID)*, 2022, doi: https://doi.org/10.1109/RFID-TA54958.2022.9923995.

[5] M. Lach, F. Rutz, and E. Biebl, "Prediction of UHF-RFID Tag Performance Utilizing Deep Learning Regression," *2022 IEEE 12th International Conference on RFID Technology and Applications (RFID-TA)*, 2022, doi: https://doi.org/10.1109/RFID-TA54958.2022.9923995.

[6] A. Pinto, R. Azevedo, and S. I. Lopes, "Evaluating Maximum Operating Distancein COTS RFID TAGS for SmartManufacturing," 2023, doi: https://doi.org/10.1007/978-3-031-35982-8_3.

[7] "The RF in RFID: UHF RFID in Practice - Daniel Dobkin - Google Libros." Accessed: Jun. 18, 2025. [Online]. Available: https://books.google.pt/books/about/The_RF_in_RFID.html?id=qiEieFBtdd4C&redir_esc=y

A STRUCTURED APPROACH FOR ROBOTIC MANIPULATION OF UNSTRUCTURED BICYCLE CRANKS VIA IMITATION LEARNING

N. Simões[1,2*], Joaquin Dillen[1,2], Rafael Fernandes[1,2], Bruno Silva[1,2], João M. Faria[1,2], Luis Vilas Boas[1,2], Inês Caetano[3], Luís Cardoso[4], João Borges[1,2], António H. J. Moreira[1,2]

1 2Ai - School of Technology, IPCA, Barcelos, Portugal.
2 LASI - Associate Laboratory of Intelligent System, Guimarães, Portugal.
3 Sistrade - Software Consulting, SA, Porto, Portugal.
4 Miranda & Irmão, LDA, Águeda, Portugal.

*Corresponding author(s). E-mail(s): nsimoes@ipca.pt
Contributing authors: jdillen@ipca.pt; rmfernandes@ipca.pt; brsilva@ipca.pt; jpfaria@ipca.pt; lvilasboas@ipca.pt
ines.caetano@sistrade.pt; lcardoso@miranda.pt; jpbsilva@ipca.pt; amoreira@ipca.pt

In recent years, robotics has experienced significant advancements driven by the integration of artificial intelligence and imitation learning techniques. This paper presents a comprehensive methodology for training a robotic system to manipulate unstructured bicycle cranks and place them in predefined positions. The approach combines digital training using high-fidelity simulation with real-world validation. A detailed training pipeline, including demonstration collection, dataset annotation, data augmentation, and iterative fine-tuning, is employed to develop a robust grasping and placement model. Furthermore, domain adaptation techniques are utilized to bridge the simulation-to-real gap. Experimental results in the simulated environment, using a cube as a test object, are compared to preliminary trials with a bicycle crank. The study underscores the potential of imitation learning for flexible industrial robotic manipulation and outlines future work to further enhance system performance and generalization for multiple tasks in shop-floor.

KEYWORDS
IMITATION LEARNING; ROBOTIC MANIPULATION; OBJECT HANDLING.

INTRODUCTION

Recent advances in robotics have been marked by the increasing incorporation of artificial intelligence techniques and imitation learning methods. In industrial applications, where tasks such as object manipulation and component assembly require exceptional precision and flexibility, these developments are particularly critical. Modern robotic systems must not only execute preprogrammed tasks with accuracy but also adapt to dynamic and unstructured environments. As robots become more sophisticated, challenges emerge regarding their ability to generalize and adapt to new scenarios without extensive reprogramming.

Imitation learning has emerged as a promising paradigm to overcome these challenges. By enabling robots to learn complex tasks through human demonstrations, imitation learning reduces the reliance on random exploration, a common drawback in reinforcement learning, and accelerates the overall learning process. Early approaches, such as the DAgger algorithm introduced by Ross et al. [1], were designed to mitigate distributional shifts between training data and real-world execution. More recent methods, including one-shot imitation learning and meta-learning frameworks proposed by Finn et al. [2], have further advanced the field by enabling robots to generalize new tasks from very limited demonstrations. Additionally, the work by Duan et al. [3] reinforces the viability of one-shot imitation learning, offering alternative strategies for rapid skill acquisition.

In object manipulation tasks, several works have contributed to enhancing the robustness and adaptability of imitation learning. Research has underscored the importance of developing implicit visual representations for reconstructing

object shapes, as demonstrated in Visual Imitation Learning of Task-Oriented Object Grasping and Rearrangement [4]. Other studies have integrated tactile sensors to execute delicate grasping actions, as shown in Learning Fine Pinch-Grasp Skills using Tactile Sensing from A Few Real-world Demonstrations [5]. Moreover, wearable systems have been employed to capture human demonstrations more naturally, as described in A Wearable Robotic Hand for Hand-over-Hand Imitation Learning [6]. Advances in multisensory data fusion and the emergence of generalist models, such as the: A Vision-Language-Action Flow Model for General Robot Control [7], further enhance robotic autonomy in industrial contexts. In addition, approaches that incorporate bilateral control have improved the grasping of both soft and rigid objects, as evidenced by Soft and Rigid Object Grasping with Cross-Structure Hand Using Bilateral Control-Based Imitation Learning [8]. Finally, data-efficient strategies for industrial assembly tasks are exemplified by the JUICER framework [9], which reduces the dependency on large training datasets while maintaining high performance.

This research addresses the challenge of grasping unstructured bicycle cranks, a challenge in both industrial and logistics environments. The goal is to develop a system that uses imitation learning to teach a robot to efficiently manipulate these cranks and place them in predefined positions. To achieve this, a structured training pipeline is proposed that includes the collection of demonstrations, annotation of datasets, application of data augmentation, and iterative fine-tuning of the model. In addition, the research combines digital training in simulation with real-world experimentation to validate and refine the solution.

In summary, this work contributes to exploring imitation learning techniques in industrial robotics application by providing a structured and adaptable approach for transferring knowledge from simulated environments to real-world applications. The paper is organized as follows: Section 2 details the methodology, including both digital training and real-world application, while Section 3 presents the conclusions and outlines directions for future research.

METHODOLOGY

This study presents a structured methodology for training a robotic system to manipulate unstructured bicycle cranks and place them in predefined positions. The approach integrates both digital training and real-world, utilizing imitation learning techniques to develop a flexible and robust manipulation model. The methodology is divided into three primary phases: digital training, real-world application, and performance evaluation.

DIGITAL TRAINING AND SIMULATION

The digital training phase is conducted in the Isaac Sim simulator, which provides a realistic and controlled environment for modeling robotic interactions. This phase forms the foundation for training and optimizing the robotic system before real-world deployment.

- **Simulation Environment:** Isaac Sim is used to create high-fidelity scenarios that accurately model the physics of object interactions. To promote robustness and generalization of the trained model, variations in lighting, textures, and physical properties are introduced during simulation.
- **Training Objects:** The training begins with a simple 10 cm^3 cube and progresses to more complex shapes, such as bicycle cranks (20.5 cm in length), to enhance the model's adaptability to different geometries.
- **Scenario Variability:** A total of 4,000 simulation runs include randomized object positions, occlusions, and external disturbances to reflect real-world variability.
- **Domain Randomization:** To improve the model's robustness against real-world inconsistencies, domain randomization is applied in 30% of the simulations. This technique introduces random perturbations in textures, lighting conditions, and friction coefficients, enabling the model to learn invariant features that generalize better to unseen environments.
- **Robotic Arm Configuration:** The setup uses a Franka Emika Panda robotic manipulator equipped with a parallel gripper and an Intel RealSense D435 camera for perception and feedback.

Figure 1 illustrates the experimental setup, including the picking zone (red) and placing zone (green), where the robotic arm performs manipulation tasks.

TRAINING PIPELINE

The training pipeline follows a structured sequence designed to enhance the robot's capability to consistently grasp and position bicycle cranks in varying scenarios. As illustrated in Figure 2, the process comprises four main phases: human teleoperation and data collection, dataset annotation, dataset augmentation, and training and deployment.

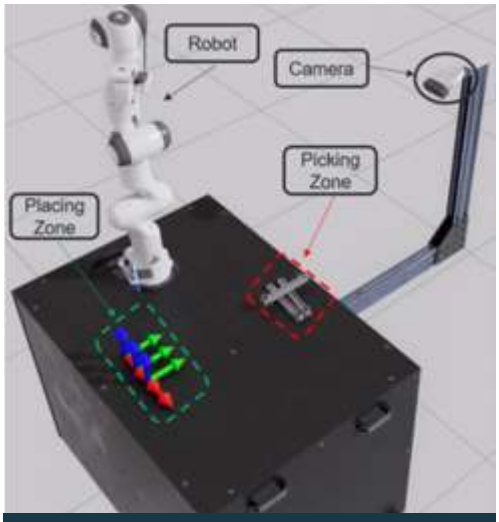

FIGURE 1
Experimental setup illustrating the robotic system used for pick-and-place operations. The picking zone (red) is where objects are initially located, while the placing zone (green) represents the designated target area. The robotic arm performs manipulation tasks, and an external camera captures visual data for perception and model training.

The pipeline begins with human teleoperation, where operators manually control the robotic arm to perform pick-and-place tasks. This phase produces 200-500 demonstration trajectories, each capturing object motion, gripper control, and relevant robot actions across diverse interaction contexts. This dataset introduces behavioral variability, which is essential for robust model generalization.

In the annotation phase, each trajectory is segmented into key stages: grasping, lifting, repositioning, and placing. These labeled segments help the model learn context-dependent behaviors and decision-making patterns.

During dataset augmentation, additional variability is synthetically introduced to increase the robustness of the learning process. Augmentation includes temporal perturbations (e.g., altering action timing slightly), spatial jitter (e.g., minor offsets in object positions or orientations), and sensor noise simulation (e.g., small pixel-level distortions or partial occlusions in depth maps). These transformations simulate real-world inconsistencies, allowing the model to generalize beyond the limited scope of the original demonstrations.

Once augmented, the dataset is expanded further by collecting demonstrations in multiple randomized simulation environments, each initialized with different seeds. This iterative process continues until 4,000 successful task executions are recorded across diverse conditions.

The training phase begins with supervised learning over 200 epochs. Checkpoints are saved every 50 epochs to monitor progress. During training, metrics such as grasp success rate, object placement accuracy, and overall task completion time are logged to track model performance.

Following supervised learning, the model is fine-tuned using reinforcement learning (RL) to improve task performance in dynamic or ambiguous conditions. The RL fine-tuning stage incorporates an actor-critic algorithm that refines the grasping policy through trial and error. The reward function is designed to balance three objectives:

- **Grasp stability:** positive reward for firm, non-slipping grasps.
- **Placement accuracy:** higher reward for precise alignment with the target zone.
- **Execution efficiency:** penalization for excessive time or unnecessary movements.

This multi-objective reward function encourages the robot to develop a policy that is not only effective but also efficient and repeatable under variable conditions. As learning progresses, the reward-weighted optimization leads to improvements in both precision and execution speed, enabling reliable autonomous performance.

Once the model reaches a stable threshold across all metrics, it is deployed to enable autonomous execution of grasping and placement tasks.

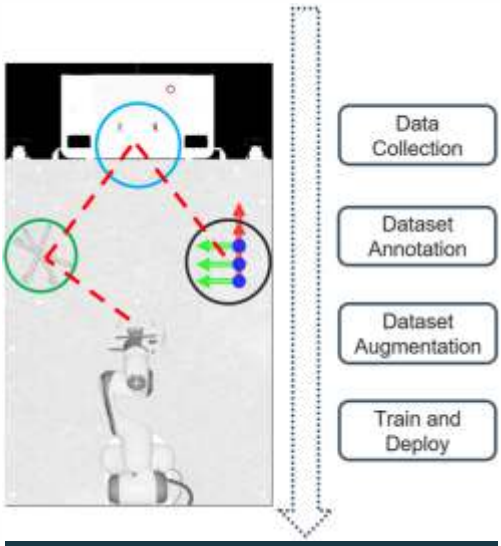

FIGURE 2
Training pipeline for robotic grasping and placement. The left panel shows the robot's motion path: the unstructured picking zone (green), the conification machine (blue), and the placement zone (black). The right panel outlines the four key phases of the training process, from data collection via human teleoperation to autonomous deployment.

Figure 2 illustrates the process, with the left side showing the robot's movement path, including the unstructured picking zone (green), the conification machine (blue), and the placement zone (black). The right side outlines the four training phases, from human teleoperation to autonomous execution. This structured approach ensures a robust manipulation policy capable of handling complex scenarios.

REAL-WORLD APPLICATION

Once the model demonstrates consistent performance in simulation, it is deployed on a physical robotic platform for real-world testing.

- **Physical Setup:** The deployment uses a 7-degree-of-freedom (7-DOF) Franka Emika Panda robotic arm (payload: 3 kg, reach: 855 mm), fitted with a parallel gripper (grip force: 20-70 N, maximum opening: 8 cm) and an integrated vision system for object detection and localization.
- **Task Execution:** The robot performs over 500 grasp-and-place operations involving bicycle cranks under a variety of real-world conditions, including changes in lighting, occlusion, and object positioning. This evaluation phase tests the robustness and adaptability of the trained policy.
- **Sim-to-Real Adaptation:** To account for real-world variations not captured in simulation, such as sensor noise and slight mechanical deviations, additional fine-tuning is performed in approximately 20% of the trials. This helps refine the model's responsiveness and reliability when interacting with unpredictable conditions.
- **Latency Considerations:** The robotic control loop runs at 500 Hz, ensuring rapid and stable low-level actuation. However, the vision system processes at 30 frames per second (FPS), introducing a perception latency of ~33 milliseconds per frame. This temporal gap can affect task execution, particularly during dynamic interactions, such as when the crank is rotating or shifting slightly due to mechanical play. To mitigate this, the system incorporates predictive smoothing and a short action buffer, allowing it to anticipate object motion between frames. Additionally, time synchronization between the control and perception subsystems is optimized to reduce misalignment, ensuring that visual input corresponds closely with the robot's physical actions. This coordination is critical for achieving reliable grasps and precise placements, especially in fast or fine manipulation tasks.

EVALUATION OF METRICS

Figure 3 presents an overview of the model's training behavior across 200 epochs, revealing key indicators of learning progression. In the left panel, the log-likelihood curve increases rapidly during the first 50 epochs before plateauing, indicating that the model learns core representations early and then shifts toward fine-tuning. The right panel shows the training loss decreasing sharply in the initial stages and continuing to decline gradually, suggesting steady improvements in predictive accuracy and model robustness over time. Together, these trends confirm that the learning process is stable and converging as expected.

To evaluate the system's real-world performance, several metrics were tracked. The grasp success rate reached 50% across 4,000 simulation trials. While this result demonstrates basic functionality, it highlights a significant margin for improvement. Failure cases typically involved minor misalignments, particularly in occluded or cluttered scenes, and were more frequent with the irregular geometry of bicycle cranks. These insights underscore the importance of further refinement in perception and trajectory planning.

The average task execution time currently stands at around seven seconds for a complete grasp-and-place cycle. This duration includes object detection, motion planning, and actuation. Further profiling will isolate latency sources in the control and perception loops to support future optimization, especially in scenarios requiring quicker responses.

Positioning accuracy, while generally acceptable in qualitative observations, has not yet been quantified with precise metrics. A detailed assessment is planned using external tracking systems to measure placement deviation and verify sub-centimeter precision. Similarly, the sim-to-real transfer gap is under active evaluation. Initial real-world tests suggest a drop in performance, especially in environments with unstructured lighting or surface inconsistencies. These results indicate the need for further fine-tuning and potentially additional domain adaptation techniques to improve generalization.

Future evaluations will focus on expanding the breadth and depth of testing. This includes scaling real-world trials across diverse conditions to validate robustness, conducting ablation studies to measure the contribution of individual components (such as data augmentation and domain randomization), and analyzing how variations in the reinforcement learning reward function influence task performance. Additional experiments will test the model's ability to generalize new object types with similar geometries, such as wrenches or rods, thereby evaluating its versatility beyond the trained domain.

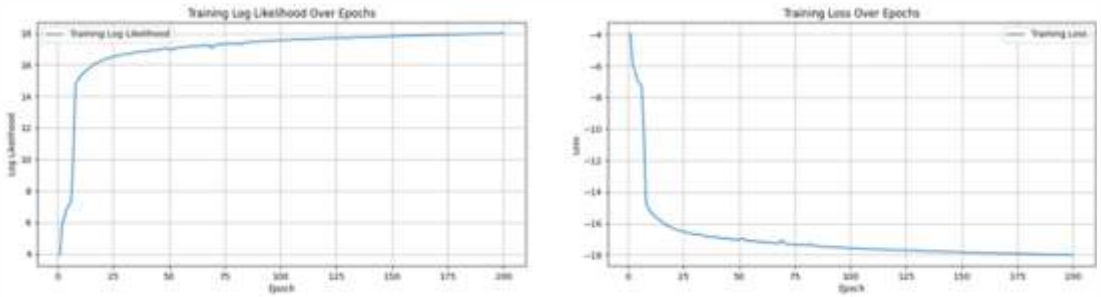

FIGURE 3
Training Performance Metrics Over 200 Epochs. The left panel displays the log-likelihood progression, showing a rapid increase in the initial epochs before stabilizing, indicating improved predictive capability. The right panel illustrates the training loss evolution, which decreases steadily, reflecting enhanced model optimization.

CONCLUSION AND FUTURE WORK

This work presents a structured methodology that combines high-fidelity digital simulation with real-world testing to develop a robust robotic manipulation system. The approach demonstrates the effectiveness of imitation learning, supported by domain randomization and reinforcement fine-tuning, for grasping and placing unstructured objects in semi-structured environments. The training pipeline enabled the robot to learn consistent manipulation behaviors through demonstration and iterative policy refinement.

The integration of domain adaptation strategies and reinforcement learning significantly improved the model's performance in physical deployment, helping bridge the gap between simulation and reality. Preliminary results indicate that training success depends not only on the quantity but also on the quality of demonstrations. Well-executed and consistent demonstrations were associated with improved generalization and execution stability across varied scenarios.

Future work will focus on expanding the dataset by incorporating additional object types and increasing the number of high-quality demonstrations. Planned improvements also include refining domain adaptation methods to reduce the sim-to-real performance gap observed in early evaluations, and integrating force and tactile feedback to enhance grasp robustness. Execution efficiency will also be addressed through control and perception optimization, with the goal of reducing overall task cycle time. These efforts aim to advance the reliability, adaptability, and speed of autonomous robotic manipulation systems for practical deployment.

ACKNOWLEDGEMENTS

This research was funded by the "Agenda Mobilizadora para a inovação empresarial do setor das Duas Rodas (AM2R)" 01/C05-i01/2021 and LASI-LA/P/0104 /2020, co-funded from the "Mobilising Agendas/Alliances for Business Innovation" of the "Next Generation EU" program of Component 5 of the Portuguese Recovery and Resilience Plan (RRP), concerning "Investment and innovation", under the Regulation of the Incentive System for "Mobilising Agendas/Alliances for Business Innovation".

REFERENCES

[1] S. Ross, G. J. Gordon, J. A. Bagnell, and M. Learning, "A Reduction of Imitation Learning and Structured Prediction to No-Regret Online Learning."

[2] C. Finn, T. Yu, T. Zhang, P. Abbeel, and S. Levine, "One-Shot Visual Imitation Learning via Meta-Learning," Sep. 2017, [Online]. Available: http://arxiv.org/abs/1709.04905

[3] Y. Duan et al., "One-Shot Imitation Learning." [Online]. Available: http://bit.ly/nips2017-oneshot.

[4] Y. Cai, J. Gao, C. Pohl, and T. Asfour, "Visual Imitation Learning of Task-Oriented Object Grasping and Rearrangement," Mar. 2024, [Online]. Available: http://arxiv.org/abs/2403.14000

[5] X. Mao et al., "Learning Fine Pinch-Grasp Skills using Tactile Sensing from A Few Real-world Demonstrations," Jul. 2023, [Online]. Available: http://arxiv.org/abs/2307.04619

[6] D. Wei and H. Xu, "A Wearable Robotic Hand for Hand-over-Hand Imitation Learning," Sep. 2023, [Online]. Available: http://arxiv.org/abs/2309.14860

[7] K. Black et al., "? 0?: A Vision-Language-Action Flow Model for General Robot Control." [Online]. Available: https://physicalintelligence. company/blog/pi0

[8] K. Yamane, S. Sakaino, and T. Tsuji, "Soft and Rigid Object Grasping With Cross-Structure Hand Using Bilateral Control-Based Imitation Learning," Nov. 2023, doi: 10.1109/LRA.2023.3335768.

[9] L. Ankile, A. Simeonov, I. Shenfeld, and P. Agrawal, "JUICER: Data-Efficient Imitation Learning for Robotic Assembly," Apr. 2024, [Online]. Available: http://arxiv.org/abs/2404.03729

STRATEGIC PARTNER FOR INNOVATION

With a structured approach and a strong connection to the materials ecosystem, SPM positions itself as a key partner in the dissemination of projects, contributing to the enhancement of knowledge and to Portugal's prominence in the field of materials.

Through its channels and initiatives, SPM ensures effective communication targeted at qualified audiences:

- *Ciência & Tecnologia dos Materiais JournalA technology-focused publication aimed at companies, research centers, and the scientific community.*
- *Digital platformsContinuous dissemination of activities, results, and opportunities.*
- *Technical-scientific events, Conferences, workshops, and seminars that promote knowledge sharing and interaction among stakeholders.*

COME JOIN US

SPM SOCIEDADE PORTUGUESA de MATERIAIS

CONTACT

Manuela Oliveira
Tel: 96 5756172

SPM - Apartado 4538
EC Carnide
1511-970 Lisboa

spm@spmateriais.pt
www.spmateriais.pt

DIGITAL PLATFORMS AND THE COLLABORATIVE ECONOMY IN THE TWO-WHEEL INDUSTRY: OPPORTUNITIES AND CHALLENGES FOR INDUSTRIAL RESOURCE MANAGEMENT

João Fernandes[1], Daniela Herculano[1], Gil Nadais[1], José Aleixo[2], Vital Almeida[3]
1 BIKiNNOV - Bike Value Innovation Center Association, Rua da Indústria, 369, 3750-792, Águeda, Portugal
2 Epedal - Indústria de Componentes Metálicos, SA, Zona Industrial do Bicarenho, 3780-521, Sangalhos, Portugal
3 CicloFapril, SA, Rua do Vale do Grou nº 1378, 3750-064, Águeda, Portugal

This study explores the impact of digital platforms (DP) on resource management in the two-wheel industry, focusing on Portuguese companies. It highlights operational challenges like organizational resistance and data security issues, while also emphasizing opportunities for innovation. Key findings show that DPs can reduce machine idleness, enable raw material sharing, and support sustainability. The proposed collaborative digital ecosystem aims to improve production efficiency, drive innovation, and enhance competitiveness through resource optimization and collaboration, ultimately contributing to sustainable industrial growth.

KEYWORDS
DIGITAL PLATFORMS; COLLABORATIVE ECONOMY; TWO-WHEEL INDUSTRY; DIGITAL TRANSFORMATION; SUSTAINABILITY; RESOURCE OPTIMIZATION; INDUSTRIAL INNOVATION.

INTRODUCTION

Digital transformation and the collaborative economy (CE) drive innovation and sustainability across various sectors, including industry and urban mobility. Portugal stands out in bicycle manufacturing, producing 1.8 million bicycles in 2023, which accounts for 18.6% of EU production [1].

The growing demand for sustainable solutions is fostering new business models, where DPs play a key role in resource optimization and collaboration.

These platforms boost competitiveness by reshaping value chains, promoting resource sharing, and improving operational efficiency. Previous studies [2], [3] highlight the potential of these solutions in optimizing production, improving sustainability, and reducing waste.
This article explores the impact of DPs on the industrial CE, focusing on the two-wheel sector in Portugal. Based on a case study with interviews and observations, the research aims to understand how digitalization can enhance resource management, innovation, and efficiency.

The methodology adopts a mixed approach to identify challenges and opportunities in implementing DPs for optimizing industrial capacity and fostering cooperation. The article includes theoretical foundations, methodology, results, conclusions, and future perspectives.

THEORETICAL FRAMEWORK

The CE and DPs drive industrial digital transformation, enabling new interactions and redefining value chains. In Portugal's two-wheel sector, their integration optimizes resources, reduces waste, and improves efficiency.

CE AND DIGITAL PLATFORMS

The CE is based on resource sharing and decentralized production, enabling better utilization of installed capacity [2]. DPs facilitate

utilization of installed capacity [2]. DPs facilitate this collaboration by connecting different industry stakeholders [3].

In the industrial sector, B2B platforms impact the reconfiguration of value chains by fostering strategic partnerships and increasing production flexibility [4]. One of the main benefits of these platforms is the reduction of operational inefficiencies, such as equipment idleness - a recurring issue in factories, including those analyzed in this study.

Xometry is a B2B DP that connects businesses with suppliers for services like machining and 3D printing. It provides real-time quotes for custom parts, reducing inventory and equipment needs. By linking companies to a broad network of manufacturers, it offers flexibility in supplier choice based on cost, delivery, and quality, optimizing production, and reducing inefficiencies. A similar approach could enhance resource utilization and efficiency in the two-wheel industry.

Additionally, digitalization enhances transparency and traceability, strengthening trust among participants [5]. However, a critical challenge remains data security. The adoption of Non-Disclosure Agreements (NDAs) has been identified as essential for ensuring the protection of sensitive information.

RESEARCH CLUSTERS IN THE CE

The literature identifies five key areas influencing DPs in the CE:

- **Gig Economy and Digital Labor** - Platforms enable flexible workforce allocation, as seen with Uber, where drivers choose their working hours, enhancing labor efficiency [6].
- **Digital Transformation and Platform Economy** - DPs, like Xometry, optimize manufacturing by connecting businesses with a network of suppliers, streamlining operations through real-time data and resource sharing [7].
- **Sharing Economy and Trust** - Trust is essential, as demonstrated by Airbnb, which uses reviews and verification to ensure transparency and reliability between hosts and guests [5].
- **Business Models and DPs** - Platforms like Amazon Web Services allow companies to access third-party resources, reducing entry barriers and fostering innovation through scalable cloud services [8].
- **Platform Capitalism and Collaboration** - Etsy exemplifies how a platform can balance profit with value creation, helping small businesses reach global markets while generating shared benefits [9], [10].

SUSTAINABILITY AND CIRCULAR ECONOMY

Digitalization plays a crucial role in sustainability and the circular economy by reducing waste through the sharing of equipment and surplus raw materials [9].

In the two-wheel industry, optimizing production capacity is a challenge, with companies often facing machine inactivity due to fluctuating demand. A DP could address this by reducing idleness and improving resource utilization. Some companies are already using recyclable materials like aluminum and sustainable plastics, and a collaborative platform could enhance sustainability by promoting resource sharing and circular economy practices across the sector.

FINAL CONSIDERATIONS OF THE LITERATURE REVIEW

DPs can transform the industry by improving efficiency, reducing costs, and promoting sustainability. However, challenges like data security, trust, and cultural adaptation must be addressed for successful adoption. This study, part of WP8 of AM2R, examines the two-wheel sector to assess how these concepts apply to the Portuguese industrial context. The next section outlines the research methodology.

METHODOLOGY

This study uses a qualitative approach, analyzing business cases to understand the impact of DPs on the CE in the two-wheel sector. The research involved technical visits and semi-structured interviews with two representatives from Portuguese industrial companies, each with extensive knowledge of multiple enterprises.

APPROACH AND JUSTIFICATION

A multiple case study approach was used to capture diverse perspectives on adopting DPs for collaborative resource management.
Companies were selected based on their sector significance and digital transformation strategies. Data collection methods included direct observation, document analysis, and interviews with industry professionals, leading to the development of a research matrix to identify challenges and opportunities in implementing a collaborative platform.

ANALYSIS CRITERIA

The analysis was structured around three key dimensions:

- **Operational Challenges** – These included organizational resistance, security, and confidentiality concerns. Interviews focused on undestanding how companies perceive the adoption of DPs, specifically in terms of internal barriers,

such as reluctance to change, as well as concerns regarding data protection and the safeguarding of proprietary information.

- **Collaboration Opportunities** – This dimension examined resource sharing and production efficiency. Interviews explored how companies view the potential for collaborating with other industry players through DPs, including sharing underutilized machinery, surplus materials, and capacity. Discussion points included the expected benefits of greater operational flexibility and cost reduction through such collaborations.
- **Sustainability and Circular Economy** - The interviews delved into how companies are incorporating sustainability practices and the role of DPs in facilitating these efforts. Inter-viewees were asked about their experiences with reducing production waste and optimizing the use of raw materials through digital resources.

The research is ongoing, and the number of companies analyzed will be expanded to reflect the diversity of industrial processes within the sector. The interviews were semi-structured, allowing for a combination of standardized questions and open-ended discussions. This structure enabled the collection of both quantitative data on current practices and qualitative insights into the companies' strategic visions. The following section presents the profile of the studied companies and the main findings.

INDUSTRIAL CONTEXT AND COMPANY PROFILE

PORTUGAL'S ROLE IN THE TWO-WHEEL INDUSTRY

Portugal is a leading bicycle producer in the EU, manufacturing 1.8 million units in 2023, representing 18.6% of the EU's total production, despite a 24% decline in production across Europe [1].

The Águeda region is a key industrial hub, home to companies like Epedal and CicloFapril, which are involved in this research. The growing demand for efficiency has driven companies to explore collaborative solutions, including DPs for capacity management. This article is part of a multi-case study on the sector's industrial capacity, with the first phase involving Epedal and CicloFapril, and the research will expand to include more companies.

PROFILES OF THE STUDIED COMPANIES

Epedal

Founded in 1981 in Sangalhos (Anadia), Epedal produces metal components for the automotive and two-wheel sectors using stamping, tube forming, robotic welding, and assembly.

During the site visit, the interviewee highlighted industrial equipment idleness as a significant challenge, primarily due to the 5-to-6-year production cycles in the automotive industry. The collaborative platform is seen as a potential solution to maximize the utilization of idle machinery and optimize productive resources. However, the company expressed concerns regarding security and confidentiality, emphasizing the need for NDAs to safeguard strategic information.

CicloFapril Group

Established in 1965 in Águeda, CicloFapril Group manufactures metal and plastic components for various industries, including automotive and renewable energy.

The interviewee expressed interest in the DP as a tool for optimizing industrial capacity and sharing surplus raw materials. Advantages were identified in collaborating with the Technology and Innovation Center and the National Association of the Two-Wheel Industry, organizations that could provide services such as prototyping and product testing.

Regarding the platform's membership model, the interviewee suggested that associated companies should have free access for the first two years, while non-associated companies would be required to pay a membership fee.

Both companies acknowledge the benefits of resource sharing and highlight the need for a new capacity-sharing model. The next section examines the barriers and opportunities in implementing this solution.

RESEARCH FINDINGS

The research matrix, developed through observations during site visits and interviews, enabled the identification of challenges, opportunities, and expectations regarding the implementation of a collaborative DP for industrial resource sharing.

OPERATIONAL CHALLENGES AND BARRIERS TO ADOPTION

Three main challenges may hinder the implementation of the platform:

- **Cultural and Organizational Resistance** - Industrial companies tend to be cautious in adopting collaborative models, fearing loss of competitiveness and exposure of strategic data. A possible solution is to start with pilot projects and gradually integrate the platform to build trust and reduce disruption.

· **Security and Confidentiality** – The shared use of resources raises concerns about the protection of industrial information. To address this, companies could use blockchain or encryption for secure data exchange and implement NDAs with role-based access controls to ensure only authorized users access sensitive information.
· **Platform Management Complexity** – Usability is key to adoption. To improve this, the platform should have an intuitive interface, customizable dashboards, and easy navigation for machine reservations. Additionally, offering training and ongoing support can help ease the transition for users unfamiliar with digital tools.

COLLABORATION OPPORTUNITIES AND PLATFORM

Benefits

Despite the challenges, the platform offers strategic benefits, including:

· **Reduction of Machine Idleness** - Enabling machine time rentals to optimize resources and generate additional revenue.
· **Sharing of Raw Materials** – Repurposing surplus materials to reduce waste and lower costs.
· **Efficiency and Sustainability** – Promoting circular economy practices by minimizing the need for new acquisitions and transport, thus enhancing resource efficiency.
· **Integration with Other Entities** – Collaboration with Technology and Innovation Centers and the National Industry Association to offer prototyping, product testing, and certification services.

PROPOSED MODEL FOR THE PLATFORM

The initial model of the platform includes the following key features:

· **Resource Management** – Companies can list available machines with details on their type, capabilities, and availability. A search function will allow users to filter by machine type, location, and availability, ensuring efficient resource sharing.
· **Material Marketplace** – A dedicated space where companies can list surplus raw materials for sale or exchange, specifying material type, quantity, and quality. This feature reduces waste and promotes resource optimization, with real-time inventory tracking ensuring accuracy.
· **Reservation and Payment System** – A user-friendly reservation system with hourly pricing for equipment rentals and a service fee for platform maintenance. Secure payment proces-sing ensures seamless transactions.
· **Security and Confidentiality** – NDAs will be mandatory to protect sensitive data. Advanced encryption protocols will safeguard data storage and transfer, with access controls based on user roles.
· **Progressive Adoption Strategy** – Associated companies receive free access for the first two years, encouraging gradual adoption. Afterward, a tiered subscription model will be introduced based on usage levels.

Additionally, the platform will be scalable, supporting the addition of new companies, machines, and materials, with a cloud-based infrastructure for robust data storage and flexibility to accommodate growing traffic and users.
The findings indicate that a collaborative DP could revolutionize industrial resource management, reducing machine idleness, facilitating the sharing of surplus materials, and optimizing production efficiency. However, challenges such as data security, cultural resistance, and usability must be addressed to ensure successful adoption.

The next section discusses these challenges and how digital strategies, and the CE can help overcome them.

DISCUSSION OF FINDINGS

The research findings show that digitalization and the CE can optimize industrial capacity in the two-wheel sector. The Research Matrix analysis identified both challenges and opportunities in implementing a collaborative DP, providing insights into sustainable business models and digital strategies [2], [3].

The proposed platform addresses two key inefficiencies in the CE [5], [9]:
· Reducing machine idleness to improve equipment utilization.
· Minimizing raw material underutilization through material sharing and waste reduction.

However, the platform's viability depends on three critical factors:
1. Trust between companies – Ensuring transparency and reliability to encourage participation.
2. Information security – Implementing robust data protection measures, including mandatory NDAs.
3. Gradual adoption – Encouraging early participation through incentives for associated companies.

The next section explores how digital strategies and collaborative business models can address these challenges and enhance the platform's

effectiveness.

INTEGRATION WITH THE LITERATURE

The literature review identifies five key research clusters on DPs in the CE [8], [10]:

- **Digital Transformation & Platform Economy** – Digitalization improves production but requires cultural adaptation, as seen in organizational resistance during interviews.
- **Sharing Economy & Trust** – NDAs are crucial for security and confidentiality, ensuring trust in collaboration.
- **Sustainability & Circular Economy** – The platform can reduce waste and promote material reuse, aligning with the UN's 2030 SDGs.
- **DPs & Business Models** – A progressive subscription model, with initial free access for associated companies, encourages adoption.
- **Platform Capitalism & Collaboration** – A balance is needed between resource-sharing and commercial sustainability to prevent excessive commodification.

These insights highlight the role of digital strategies and collaborative business models in overcoming barriers and maximizing opportunities in the two-wheel sector.

IMPLICATIONS FOR THE INDUSTRIAL SECTOR

The adoption of DPs can boost the competitiveness of the industrial sector by reducing costs and strengthening collaboration networks. To ensure successful implementation, it is essential to:

- Establish robust security mechanisms to protect industrial data and ensure confidentiality.
- Implement a progressive membership model that minimizes initial adoption costs to encourage participation.
- Develop an intuitive, user-friendly interface to allow efficient listing, reservation, and management of shared resources.

Additionally, integrating Technology and Innovation Centers and National Industry Associations could expand the platform's value proposition, offering prototyping, certification, and product testing services to enhance industrial efficiency and innovation.

LIMITATIONS AND FUTURE PERSPECTIVES

Despite the valuable insights, there are several limitations to address:

- **Limited sector data** – More research is needed to include a wider range of industrial processes, company sizes, and regions for diverse perspectives on platform adoption.
- **Potential biases** – Self-reported data from interviews may introduce biases. Future research should include quantitative data and external expert opinions to balance these views.
- **Scalability & market acceptance** – The platform will be evaluated with users, applying Lean UX principles to refine usability.
- **Technical & regulatory challenges** – Integration and compliance need alignment with national and EU policies.

Future research will expand company analysis for better representativeness, with a pilot project to assess platform feasibility before full deployment. The platform's approach to resource optimization could also apply to other sectors, such as metal furniture and hardware, promoting cross-industry collaboration and innovation.

FINAL CONCLUSION

This study explored how DPs can enhance efficiency and foster collaboration in the two-wheel sector. The key findings show that collaborative platforms can reduce costs, promote sustainability, and strengthen industry networks, but only if challenges like data security, cultural resistance, and gradual adoption are managed.

The research highlights the potential of DPs to optimize resource use and encourage collaboration, particularly in sectors like metal furniture and hardware, where similar challenges exist. By addressing identified barriers, the platform could improve productivity in the two-wheel industry and serve as a model for other sectors facing similar efficiency and resource optimization needs.

The practical implications extend beyond the two-wheel sector, with the platform potentially driving broader industry collaboration, reducing waste, and enabling sustainable scaling. Future applications could expand the platform's features to meet the needs of different industries, promoting cross-sector innovation.

ACKNOWLEDGEMENTS

This research was carried out in partnership with the companies Epedal, SA, and CicloFapril, SA, funded by the "PRR Plano de Recuperação e Resiliência" and by the "Next Generation EU funds", through the scope of the Agenda for Business Innovation "AM2R Agenda Mobilizadora para a inovação empresarial do setor das Duas Rodas" (Project nº 15 with the application C644866475 00000012).

REFERENCES

[1] Eurostat, "EU production of bicycles down to 9.7 million in 2023." Accessed: Dec. 12, 2024. [Online]. Available: https://ec.europa.eu/eurostat/en/web/products-eurostat-news/w/ddn-20241120-2

[2] V. Ratten, "Digital platforms and transformational entrepreneurship during the COVID-19 crisis," Int J Inf Manage, vol. 72, Oct. 2023, doi: 10.1016/j.ijinfomgt.2022.102534.
[3] M. Drewel, L. Özcan, J. Gausemeier, and R. Dumitrescu, "Platform Patterns—Using Proven Principles to Develop Digital Platforms," Journal of the Knowledge Economy, vol. 12, no. 2, pp. 519–543, Jun. 2021, doi: 10.1007/s13132-021-00772-3.
[4] A. Fortuny-Sicart, M. Pansera, and J. Lloveras, "Directing innovation through confrontation and democratisation: the case of platform cooperativism," J Responsible Innov, vol. 11, no. 1, 2024, doi: 10.1080/23299460.2024.2414512.
[5] M. Möhlmann, "Collaborative consumption: Determinants of satisfaction and the likelihood of using a sharing economy option again," Journal of Consumer Behaviour, vol. 14, no. 3, pp. 193–207, May 2015, doi: 10.1002/cb.1512.
[6] A. Gandini, "Labour process theory and the gig economy," Human Relations, vol. 72, no. 6, pp. 1039–1056, Jun. 2019, doi: 10.1177/0018726718790002.
[7] P. Constantinides, O. Henfridsson, and G. G. Parker, "Platforms and infrastructures in the digital age," Information Systems Research, vol. 29, no. 2, pp. 381–400, Jun. 2018, doi: 10.1287/isre.2018.0794.
[8] G. Zervas, D. Proserpio, and J. W. Byers, "The rise of the sharing economy: Estimating the impact of airbnb on the hotel industry," Journal of Marketing Research, vol. 54, no. 5, pp. 687–705, Oct. 2017, doi: 10.1509/jmr.15.0204.
[9] J. de R. Outomoro and A. Gordo, "From the hype of the sharing economy to the degrowth economy," Athenea Digital, vol. 24, no. 2, 2024, doi: 10.5565/rev/athenea.3352.
[10] S. Vallas and J. B. Schor, "What Do Platforms Do? Understanding the Gig Economy," The Annual Review of Sociology, 2020, doi: 10.1146/annurev-soc-121919.

USING ELECTROCHEMICAL IMPEDANCE SPECTROSCOPY TO DIAGNOSE LITHIUM-ION BATTERY CELLS

Céu Neiva[1], Gustavo Santos[1], Rúben Pedroso[1], Luis Barros[1], João Pedro Cunha[1], Francisco Costa[1], Miguel Gonçalves[1], Inês Matos[1], Bruno Martins[2], Luis Felipe Antunes[2], Paulo Alves[2]

1 CeNTI - Centre the Nano technology and Advanced Materials, Vila Nova de Famalicão, Portugal
2 EDMTECH, Aveiro, Portugal

This study uses Electrochemical Impedance Spectroscopy (EIS) to analyse lithium-ion battery performance under different temperatures and states of charge (SoC). Results show that temperature significantly affects charge transfer efficiency, while SoC influences internal resistance. Higher temperatures improve charge transfer, while lower SoC increases resistance. By fitting impedance data to an equivalent circuit model, key parameters were identified to determine the influence of cell conditions during characterization. These findings are particularly relevant for two-wheeled electric vehicles, where the diagnostic of batteries can be enhanced due to a better understanding of how cell conditions alter characterization results.

KEYWORDS
LITHIUM-ION BATTERIES; EIS; SOFT MOBILITY; ELECTRIC BICYCLES, ELECTROCHEMISTRY; EQUIVALENT CIRCUITS.

INTRODUCTION

Lithium-ion batteries (LIBs) are highly advantageous components for energy storage systems, utilizing electrochemical processes to deliver their functionality. Key characteristics of these systems include high energy density, long life cycles, low self-discharge rates, and minimal memory effect. These attributes justify their widespread use in the market, particularly in portable electronic devices such as smartphones and laptops. However, the mobility sector – encompassing electric vehicles, aircraft, and bicycles – has seen a sharp increase in the adoption of LIBs, driven by efforts to electrify systems and reduce the carbon footprint associated with fossil fuel consumption. Despite the technological maturity of LIBs, ongoing research and development aim to mitigate the negative effects associated with these energy storage systems. One critical area of focus is understanding the mechanisms of degradation and aging in cells, which are highly dependent on operating conditions such as charge and discharge cycles, state of charge, temperature, and other factors [1], [2], [3]. Therefore, it is crucial to develop diagnostic methods capable of gathering as much information as possible about the battery's condition to enhance the interpretation of its state of health. One reason to interpret the effects that different parameters may have on cell characterization in an initial phase (as presented in this paper) is to establish references and baselines. These can later be compared with other stages of their lifecycle, improving diagnostic capabilities at a later stage.

ELECTROCHEMICAL IMPEDANCE SPECTROSCOPY FOR LITHIUM-ION BATTERIES.

Electrochemical Impedance Spectroscopy (EIS) is a technique that enables the study of electrochemical reactions in batteries by measuring the transport and dielectric properties of materials and analysing the characteristics of porous electrodes. Impedance is determined by applying an alternating voltage signal to the cell and measuring its corresponding current response. The applied signal is sinusoidal, which means the current response to this stimulus will consist of a combination of sinusoidal functions [4].

system can be expressed as follows [5]:

$$Z = \frac{v(t)}{i(t)} = Z_0(\cos(\phi) + j\sin(\phi))$$

Equation 1

, where v(t) is the sinusoidal signal of the applied voltage, i(t) is the measured electric current, Z_0 is the absolute value of the impedance (representing the ratio between the amplitudes of the voltage and current signals), and p is the phase difference between the voltage and current signals.

From Equation 1, it can be stated that the impedance spectrum is a complex curve obtained across different frequencies and corresponds to the sum of a real part, referred to as the system's resistance (R), and an imaginary part, referred to as the system's reactance (X)[6]. Using EIS data, a Nyquist plot can be constructed, where the negative of the reactance is plotted on the y-axis, and the resistance is plotted on the x-axis (Figure 1 a).

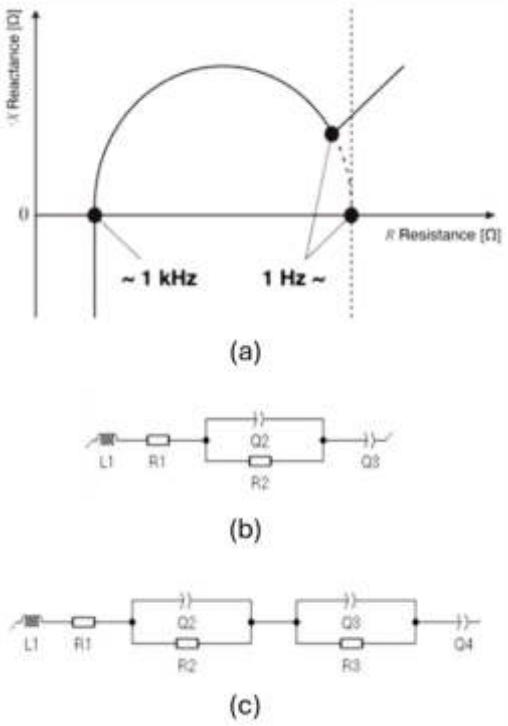

FIGURE 1
(a) Representative Nyquist plot of the EIS for a lithium-ion cell [6]. (b) and (c) Equivalent circuits used as models to determine the parameters from EIS [2], [7].

Typically, the Nyquist plot of a lithium-ion battery consists of two semicircles, which represent the effects occurring at the electrodes. The semicircle for the anode is observed at high frequencies, while the semicircle for the cathode appears at medium frequencies. This response results from the charge transfer effect at the electrodes, which is strongly dependent on the effects associated with the battery's state, it is necessary to consider an equivalent circuit that can fit the obtained spectrum. In Figure 1b and Figure 1c, the circuits considered for representing the effects in lithium-ion batteries are shown. Typically, when considering temperatures close to 20 °C and higher states of charge, a parallel circuit is sufficient to model the effects.
In Table 1, the description of the different components of the equivalent circuit can be observed. For cases of low temperatures and low states of charge, the more complex circuit is used to represent the electrochemical effects at the electrodes.

EXPERIMENTAL WORK

Cells - Commercial lithium-ion cells with NMC chemistry were selected, specifically the Samsung INR21700-50E model. The cells were brand new and were kept under controlled conditions.

State of Charge Control - Four state of charge (SOC) levels were tested: 25%, 50%, 75%, and 100%. In the laboratory, a sourcemeter was used to charge the cells until they were fully charged, and then the desired SOC was reached by discharging the cells.

Cell Temperature Control - Four temperatures between 10° C and 25° C were selected. The choice of this range of temperatures was justified by the need of understanding the EIS response of a cell stored inside a building, to simulate the effect of environment temperature during testing. Using a climatic chamber, the cells were set to the desired temperature and then transported in an insulated container to thermally isolate the cell. Throughout this process, the cell's temperature was recorded using a thermocouple.

Impedance Spectroscopy - Impedance spectra were measured using a potentiostat. The frequency range from 0.1 Hz to 100 kHz was selected for the impedance measurements. During the measurement the temperature of the cell was controlled through the previously mentioned thermocouple. The test seemed to generate heat which increased the temperature of the cell by 1 degree during all measurements. So, it was considered the temperature at the start of the measurement with one degree of uncertainty as the testing temperature.

Determination of equivalent circuit - Using the impedance values, a fitting was done to determine the best parameters that can be used to assemble the equivalent circuit model of the cell

TABLE 1
Description of the components used in the equivalent circuits as models for the cells [2], [7].

Component	Parameter	Associated Effect	Impedance
L	Inductance resulting from wiring and connections	Dependent on the cables and connectors used	$j\omega L$
R0	Ohmic or internal resistance	Dependent on the conductivity of the electrolyte (ion transport)	R_0
R1	Charge transfer resistance	Associated with the charge transfer occurring at the electrodes	R_1
Q1	Electrode capacitance	Related to the accumulation of charges at the electrodes	$\frac{1}{(j\omega)^{\alpha}Q_1}$
W	Warburg impedance	Related to the diffusion of ions in the electrodes	$\frac{1}{(2j\omega)^{0.5}W}$

for each set of conditions. Because the focus was in the negative part of the reactance the fitting dismisses the inductive part to reduce variables.

Considering conditions of temperature above 10° C and state of charges superior to 25%, one assumes to be possible to use the simplest equivalent circuit to model the cells, therefore the expression used when fitting the parameters should be:

$$Z(\omega) = j\omega L + R_0 + \frac{R_1}{1 + R_1(j\omega)^{\alpha}Q_1} + \frac{1}{(2j\omega)^{0.5}W}$$

Equation 2

Every parameter presented in Equation 2 is described in Table 1, except for a. This value is associated with the electrode capacity, which is normally described as a constant phase element (CPE), this means that it is not represented as a perfect capacitor. This constant phase a can be between 0 and 1, where the first one represents a perfect resistance and the last one the perfect capacitor. When the value is 0.5 it usually is associated with the Warburg impedance.

RESULTS AND DISCUSSION

After performing EIS under different ambient conditions, it was possible to construct the graphs in Figure 3, which illustrate the effect of these conditions on the impedance spectrum. At first glance the presence of a semicircle was evident in every Nyquist plot, which is expected from [2].

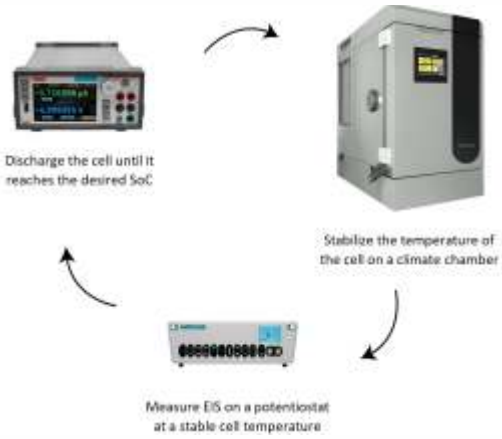

FIGURE 2
Schematic of the methodology adopted for the study.

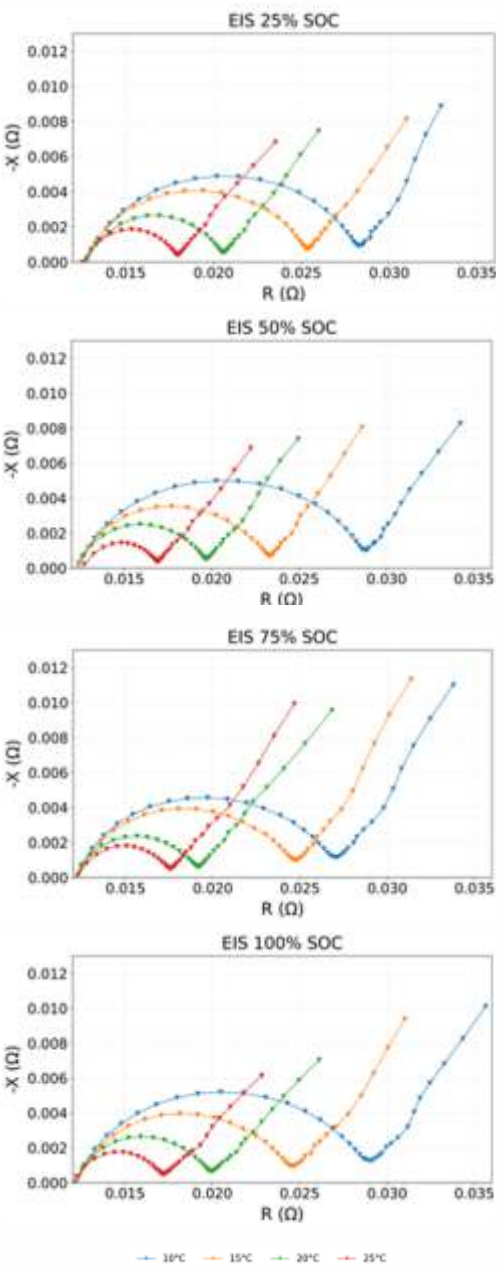

FIGURE 3
EIS Nyquists for the different states of charge and temperatures.

Secondly, the values of Resistance and Reactance do not seem to vary much between the different SOC. This could mean that the SOC does not affect the electrochemical processes involved in the cell operation. On the other hand, the temperature of the cell seems to change the Nyquist plots. The resistance and decreasing temperature, subsequently increasing charge transfer resistance and therefore overall battery impedance [10].

Through fitting of the impedance spectra, the relationship between the fitting parameters and the testing conditions was analysed.

Figure 4 illustrates the variations in the fitting parameter values across all tested temperatures and states of charge (SoC).

The internal resistance of the cell shows minimal variation with temperature, although it tends to decrease at higher states of charge (SoC). The charge transfer resistance decreases as temperature increases, with no noticeable dependency on SoC. Electrode capacitance exhibits a clear dependence on temperature, decreasing as the temperature rises, while showing little variation with SoC. The phase value remains consistently above 0.7 for these cells and increases with temperature; at higher temperatures, it closely resembles the behaviour of an ideal capacitor. The Warburg constant ranges between 300 and 475 for these cells, slightly increasing with temperature but decreasing for SoC levels above 50%. Notably, the data for 100% SoC shows some deviation from the general trends observed for other states of charge.

CONCLUSION

This study provided valuable insights into the importance of using electrochemical impedance spectroscopy as a method for analysing electrochemical systems, particularly in lithium-ion batteries. These electrochemical systems, according to previous works, are highly dependent on the external conditions in which they are exposed. In this study, virgin cells were

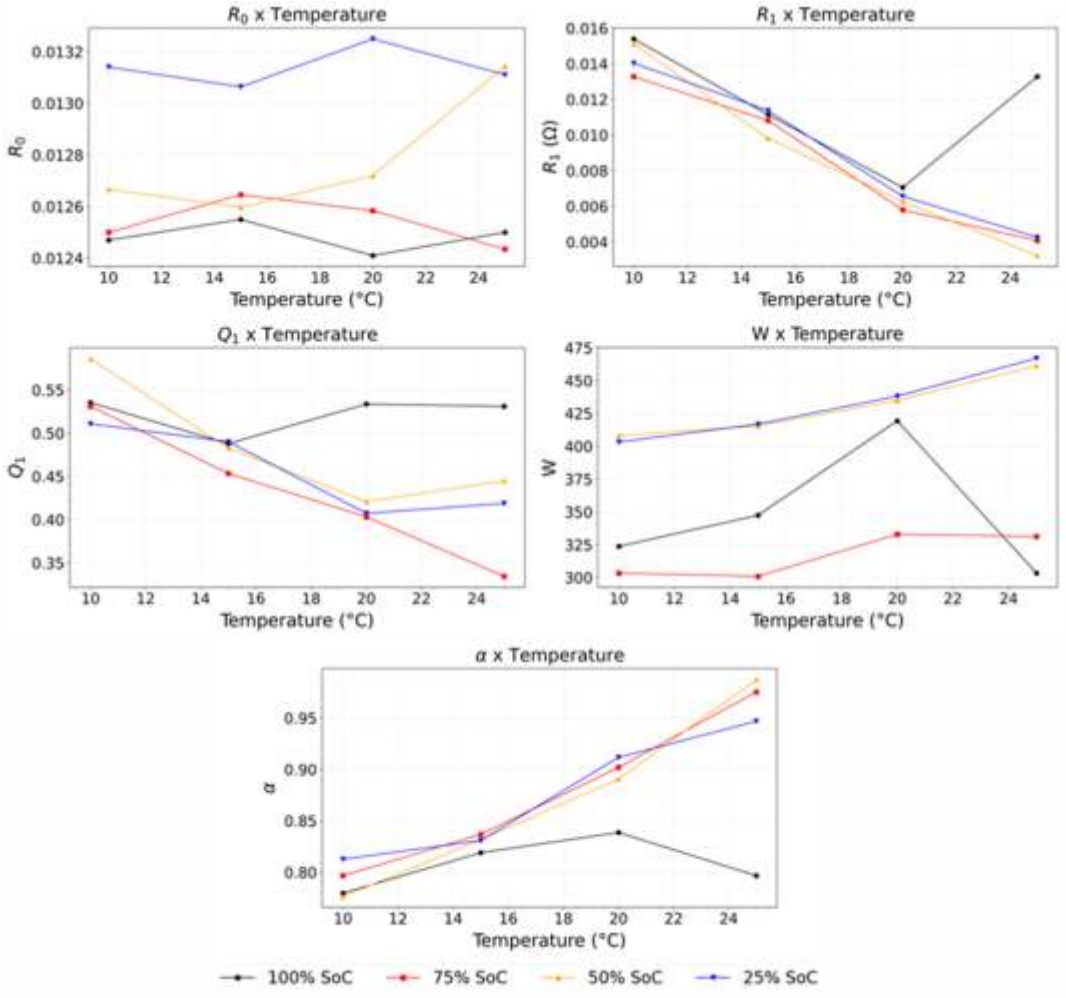

FIGURE 4
Fitting parameters obtained for the different testing conditions.

tested as a case study, while carefully considering their state of charge and the range of temperatures they may experience.

The state-of-the-art review identified some methods for analysing lithium-ion batteries with NMC chemistry. For this study, the simplest equivalent circuit model was selected to minimize variables and provide a focused approach for evaluating new, unused cells. The resistances in these equivalent circuits are directly linked to energy dissipation during cell operation. Minimizing these resistances is critical, especially for commercial cylindrical cells, where typical values are in the range of tens of milliohms, as demonstrated by the results of this work. Lower resistances diminish the cell's inherent heating during normal operation, reducing its degradation therefore increasing its lifespan. Temperature significantly impacts the efficiency of charge transfer at the electrodes, with higher temperatures enhancing the transfer coefficient. Conversely, the SoC influences the internal resistance of the cell, which increases as the cell approaches a depleted state. These results suggest that a restricted voltage operating window might be beneficial for long term cycling of the cell.

Further insights into these phenomena could be obtained from improving on this study through higher sampling, both in terms of number of samples and number of cells with different chemistry, providing a more faithful view of the reality of the temperature's impact on internal resistance. Furthermore, maintaining a constant temperature by performing the measurements inside a climatic chamber instead of requiring an insulated container will allow more certainty in the findings.

This work emphasizes the importance of controlling cell conditions for accurate characterization. Reporting and quantifying these effects help establish a solid foundation for developing reliable battery diagnostics. One good example of application could be the determination of the state-of-health of batteries in two-wheeled vehicles which are more susceptible to atmospheric conditions, such as temperature variations, than those in automobiles. This study can contribute to the determination of how temperature affects battery durability under adverse thermal conditions.

ACKNOWLEDGMENTS

The present study was developed in the scope of the Project "AM2R - Agenda Mobilizadora para a Inovação Empresarial do Setor das Duas Rodas" 02/C05-i01.01/2022.PC644866475-00000012 | Project nº 15], financed by RRP - Recovery and Resilience Planunder the Next Generation EU from the European Union.

REFERENCES

[1] Y. Guo, J. Cai, Y. Liao, J. Hu, and X. Zhou, "Insight into fast charging/discharging aging mechanism and degradation-safety analytics of 18650 lithium-ion batteries," *J Energy Storage*, vol. 72, p. 108331, Nov. 2023, doi: 10.1016/j.est.2023.108331.

[2] R. Gopalakrishnan *et al.*, "Electrochemical impedance spectroscopy characterization and parameterization of lithium nickel manganese cobalt oxide pouch cells: dependency analysis of temperature and state of charge," *Ionics (Kiel)*, vol. 25, no. 1, pp. 111–123, Jan. 2019, doi: 10.1007/s11581-018-2595-2.

[3] P. Iurilli, C. Brivio, and V. Wood, "On the use of electrochemical impedance spectroscopy to characterize and model the aging phenomena of lithium-ion batteries: a critical review," *J Power Sources*, vol. 505, p. 229860, Sep. 2021, doi: 10.1016/j.jpowsour.2021.229860.

[4] H. S. Magar, R. Y. A. Hassan, and A. Mulchandani, "Electrochemical Impedance Spectroscopy (EIS): Principles, Construction, and Biosensing Applications.," *Sensors (Basel)*, vol. 21, no. 19, Oct. 2021, doi: 10.3390/s21196578.

[5] Gamry Instruments, "Basics of electrochemical impedance spectroscopy." Accessed: Sep. 23, 2024. [Online]. Available: https://www.gamry.com/application-notes/EIS/basics-of-electrochemical-impedance-spectroscopy/

[6] HIOKI, "Nyquist plot for impedance measurement of lithium-ion batteries." Accessed: Sep. 23, 2024. [Online]. Available: https://www.hioki.com/in-en/learning/electricity/nyquist.html

[7] W. Choi, H.-C. Shin, J. M. Kim, J.-Y. Choi, and W.-S. Yoon, "Modeling and Applications of Electrochemical Impedance Spectroscopy (EIS) for Lithium-ion Batteries," *Journal of Electrochemical Science and Technology*, vol. 11, no. 1, pp. 1–13, Feb. 2020, doi: 10.33961/jecst.2019.00528.

[8] Y. Guo *et al.*, "Determination of the tortuosity and contact resistances in thick graphite anodes via electrochemical impedance spectroscopy," *J Power Sources*, vol. 569, p. 233003, Jun. 2023, doi: 10.1016/j.jpowsour.2023.233003.

[9] S. Ma *et al.*, "Temperature effect and thermal impact in lithium-ion batteries: A review," *Progress in Natural Science: Materials International*, vol. 28, no. 6, pp. 653–666, Dec. 2018, doi: 10.1016/j.pnsc.2018.11.002.

[10] S. S. Zhang, K. Xu, and T. R. Jow, "The low temperature performance of Li-ion batteries," *J Power Sources*, vol. 115, no. 1, pp. 137–140, Mar. 2003, doi: 10.1016/S0378-7753(02)00618-3.

TAKE PART IN THE NEXT EDITION

Ciência & Tecnologia dos Materiais invites:

COMPANIES to showcase innovative products, technologies, and solutions
RESEARCH GROUPS to present projects, results, and emerging areas
INSTITUTIONS and CONSORTIA to promote initiatives and strategic agendas.
Possibility of thematic editions dedicated to specific areas.

*If you are interested in participating in the next edition of the **Ciência & Tecnologia dos Materiais Journal**, either through editorial collaboration and/or commercial presence, please contact us.*

comunicacao@spmateriais.pt

SPM SOCIEDADE PORTUGUESA de MATERIAIS

CONTACT
Manuela Oliveira
Tel: 96 5756172

SPM - Apartado 4538
EC Carnide
1511-970 Lisboa

spm@spmateriais.pt
www.spmateriais.pt

ANA ISABEL BENTO

1 | Biography

Ana Isabel Bento holds a Bachelor's and Master's in Industrial Engineering and Management from the University of Coimbra. She is pursuing a PhD in Industrial Engineering and Management and is a research fellow on the AM2R project. More recently, she began her career as an Invited Assistant Professor, teaching Introduction to Management. Her primary research interests include Logistics, Supply Chain Management and Operations Management.

2 | What motivated you to pursue a PhD?

My first exposure to research occurred during the development of my Master's thesis. During that period, I realized that research, even in the context of a dissertation, required two fundamental characteristics: curiosity and critical thinking. With the guidance of my supervisor, Professor Luís Miguel Ferreira, I honed these skills, and the decision to pursue a PhD came almost naturally. Several factors drove the decision to do a PhD. Firstly, the possibility of deepening my knowledge in a specific field of study (in this case, logistics), as well as the chance to contribute to advancing knowledge with real-world impact. Additionally, I saw the PhD as a means to enhance career opportunities. Dealing with more complex challenges, working more autonomously, and collaborating with other researchers opens doors not only to more conventional paths - such as teaching, research, and academic management positions - but also to challenging roles in industry.

3 | Can you briefly explain the topic of your PhD and its impact on the Two-Wheel sector?

The focus of my PhD is on logistics triads. A logistics triad consists of three actors (supplier - Logistics Service Provider (LSP) - buyer), along with the relationships established between them. Within this context, I study governance mechanisms, which can be formal (such as contracts), relational (trust, commitment, satisfaction, etc.), and virtual (a combination of formal and relational governance mechanisms based on IT tools), and how these should be applied to maintain and strengthen relationships. Additionally, since the LSP is a central player, I explore the dynamic capabilities this actor must possess to ensure the proper functioning of the triad and offer an adequate service portfolio.

Although the topic is broad, as logistics triads exist in any supply chain, it is particularly relevant for the Two-Wheel sector in Portugal. The sector has grown rapidly in recent years, due to environmental concerns and social distancing guidelines during the pandemic. However, the sector currently faces significant challenges, such as the adoption of electric bicycles, which require additional attention in production, transportation, and warehousing. Portugal is the largest producer of bicycles in the EU, yet companies belonging to the sector, despite being geographically close, have limited connectivity with each other. Furthermore, over 60% of companies outsource logistics operations, primarily low-value-added activities, such as transportation. In this context, studying logistics triads, particularly the role of the LSP is crucial to promoting a more connected sector and a more agile and resilient supply chain.

4 | What would you like to do after completing your PhD?

After completing my PhD, I would like to continue my academic career. However, I have not ruled out the possibility of applying my knowledge in consulting, particularly in multinational companies.

5 | Do you use any vehicle from the two-wheel sector ? If so, what purpose ?

I do not use vehicles from the Two-Wheel sector, although I consider cycling an excellent leisure activity.

BEATRIZ TRIANE

1 | Biography

My name is Beatriz Triane, and I am a Brazilian graduate in Geography from the State University of Rio de Janeiro and a Master of Science in Environmental Studies at the Federal University of Rio de Janeiro. I have almost 10 years of experience with environmental licensing, impact assessment, and environmental program design and implementation for electricity transmission projects. This experience blessed me with some insights into the corporate sector.

2 | What motivated you to pursue a PhD?

After a decade of working, I needed to step back and dedicate myself to further academic studies and developing new knowledge. This desire for intellectual growth brought me to Portugal to embark on a new career phase.

When choosing the Doctoral Program at the University of Aveiro, I considered the course's innovative approach, the institution's reputation, and the city's quality of life. I was eager to expand my energy and climate change knowledge-topics I consider crucial in today's global context.

3 | Can you briefly explain the topic of your PhD and its impact on the Two-Wheel sector?

In my PhD research, I aim to develop a sustainability framework through an integrated indicator capable of assessing and improving the sustainable performance of the two-wheel industry. The goal is to provide a practical tool that helps companies and policymakers make more sustainable decisions, promoting innovation and efficiency in the sector.

My research can lead to more sustainable practices in the industry, encouraging cleaner production processes, more efficient material use, and a reduced carbon footprint. Implementing this framework could help the sector comply with increasingly strict environmental regulations, enhance its competitiveness in the global market, and accelerate the transition to more eco-friendly mobility solutions.

4 | What would you like to do after completing your PhD?

After completing my PhD, I intend to continue working on sustainability in academia and the corporate sector. I believe that scientific research conducted in educational institutions should have real applications in society, improving quality of life and reducing the impact of human activities on the planet.

5 | Do you use any vehicle from the two-wheel sector ? If so, for what purpose ?

Unfortunately, I rarely use two-wheel vehicles, mainly due to the lack of proper infrastructure where I live now, such as bike lanes and safe spaces for this type of transportation. If better conditions were available, I would use soft mobility to commute to the university, daily activities, and leisure.

JOSÉ DAVID CASTRO

1 | Biography

I'm José Castro, and currently, I'm coursing my last year at UC for my PhD in mechanical engineering. I'm from Colombia and have a bachelor's and master's in mechanical engineering. Before admission to UC, I worked as a service customer and project engineer for the HVAC industry for 5 years (MAYEKAWA MYCOM) and as a lecturer in two universities (Colombian universities) for 2.5 years. I have also received two grants for the ON-Surf and KERAMOS projects. I received an FCT doctoral grant during the 2020/2021 academic period. During my PhD, I have published 17 papers in indexed journals, 9 of them from my doctoral thesis, 1 European patent, 1 provisional Portuguese patent (from my thesis), several oral contributions and posters at international conferences and was part of the organising committee of 1 international conference (FEMS Junior EUROMAT 2022).

2 | What motivated you to pursue a PhD?

Since childhood, I've been curious about how the world works, and I desire to improve people's lives through my knowledge and experience. A PhD aligns with my desires, allowing me to add more capabilities to use science as an advancing tool for the world's sake.

3 | Can you briefly explain the topic of your PhD and its impact on the Two-Wheel sector?

My PhD topic is to develop a multifunctional advanced coating that gathers anticorrosion, antibiofouling, and reliable mechanical properties. The original objective application was to provide a solution in this line for small components for ships with a harsh working regime (exposure to moving seawater, several environmental conditions and biological agents), being one of the most challenging engineering applications. However, partial results of my work demonstrated a potential material for bike chains as ZrN-based coating by DCMS, which possesses reliable mechanical properties, good tribological performance, and a good-looking aspect desirable for this application.

4 | What would you like to do after completing your PhD?

After completing my PhD, I would like to follow in research, focusing on improving corrosion resistance in some specialised engineering components and green energy production. Additionally, I would like to collaborate with the industry to apply my advanced coatings knowledge to real working applications, solve possible problems, improve existing products, or develop new ones.

5 | Do you use any vehicle from the two-wheel sector ? If so, for what purpose ?

Currently, I use a bicycle for leisure and physical conditioning.

MARIANA PINTO

1 | Biography

My name is Mariana Pinto, I am 25 years old and I was born in São João da Madeira, a city with strong industrial ties, where I still live today and where I studied from elementary to high school. In addition, I practiced rhythmic gymnastics for 6 years at the Associação Desportiva Sanjoanense, and I am part of the local volunteer bank, promoted by the Associação de Jovens Ecos Urbanos.

My university career began with the integrated Master's degree in Metallurgical and Materials Engineering, at the Faculty of Engineering of the University of Porto, currently divided into Bachelor's and Master's Degrees in Materials Engineering. This path ended with a research grant under the AARM 4.0 project (High Strength Steels in Metalworking), co-promoted by the Martifer group, which gave rise to my dissertation: "Evaluation and Metallurgical Characterization of Welded Joints of High Strength Structural Steels".

After completing the master's degree, specializing in metallurgy, I had the opportunity to start a professional internship at DURIT, in Albergaria-a-Velha, already aiming to do a PhD in an industrial environment.

2 | What motivated you to pursue a PhD?

Doing a PhD was never part of my plans, at least in the short term, but it was always like a very distant dream. However, due to the strong encouragement of several professors and following the example of Doctor Pedro Pereira (former student of FEUP), I decided to start my PhD earlier, right after completing my master's degree.

The opportunity to carry out my PhD in an industrial environment, at DURIT, was undoubtedly determinant for my decision-making, supported by the recent experience in the research field in a project (AARM 4.0) with a strong industrial connection.

In short, I dare to update the popular saying "better late than never" to "better sooner than never".

3 | Can you briefly explain the topic of your PhD and its impact on the Two-Wheel sector?

My research focuses on the development of new binder compositions for industrial hardmetal grades for wear resistance and metal forming applications.

Although it is not part of bicycles, hardmetal is essential in the manufacturing process of their various metallic components, such as the transmission chain links. The high hardness, wear resistance, and high dimensional accuracy make hardmetals an effective material for steel-forming tools.

The goal of my PhD is to develop new hardmetal compositions, with a high content of alternative binders, with improved properties, namely the wear resistance and the response to fatigue. Simultaneously, this project aims to reduce the dependence on cobalt, which remains the most common binder and is considered a critical raw material. Fundamentally, this work aims to create more reliable and durable metal forming dies, and therefore more sustainable, thus promoting innovation in the soft mobility sector.

4 | What would you like to do after completing your PhD?

Although I am not sure at the moment, after completing my PhD I would like to continue working directly with the industry in the field of Materials Engineering, which I have always been passionate about.

I also hope to be able to achieve all my professional goals in Portugal, where I believe there is enormous potential for innovation in materials and manufacturing processes.

5 | Do you use any vehicle from the two-wheel sector ? If so, for what purpose ?

I currently don't use any, most of my trips are made by car and for shorter trips I prefer to walk, since I don't feel safe enough to circulate on the existing bike lanes. As for sports, I only use exercise bikes, at the gym or at home, especially during the 2020 confinement, in which it was my main way to stay active.

PAULINO DUARTE

1 | Biography

My name is Paulino Duarte. I was born on July 14, 1991, in the village of São Pedro, in the municipality of Figueira da Foz. My academic journey (mandatory education) began and was completed in the city of Anadia, where I lived most of my life. I started higher education at the University of Coimbra in 2012, where I completed my master's degree in physical geography - environment, and spatial planning. In 2023, the opportunity arose to begin my PhD in environmental science and engineering at the University of Aveiro. I am currently developing a project to assess the environmental impact of bicycles using the life cycle assessment methodology. Currently, on the professional level, I work for the municipality of Porto.

2 | What motivated you to pursue a PhD?

My motivation to start a PhD stems from my love for learning and studying. After taking a break of approximately seven years from academic life, I felt that I needed to complete one of the most significant challenges of my life, the final step in higher education. In 2023 I decided it was the right time to take on this challenge. I see the PhD as an opportunity to enhance my academic and professional skills while contributing to academia through my research. Since I began my journey in higher education, earning a PhD has always been a personal goal, and I can confidently say that I am fulfilling a dream.

3 | Can you briefly explain your PhD topic and its impact on the Two-Wheel sector?

My PhD goal is to analyse the environmental impact of conventional and electric bicycles using the life cycle assessment methodology. It also seeks to conduct a socio-economic analysis of bicycle use in urban areas. The expected impact on the two-wheeler sector is to understand the impact of bicycle production in Portugal, identifying which components and stages have the highest environmental impact. Additionally, the socio-economic study and analysis aims to increase the acceptance levels of bicycle usage.

4 | What would you like to do after completing your PhD?

After completing my PhD, I intend to return to the municipality of Porto and contribute to the development and improvement of the cycling network, as well as to consider policies to promote bicycle use within the city.

5 | Do you use any vehicle from the two-wheel sector ? If so, what purpose ?

I own two bicycles-one for mountain biking and another for road cycling. I frequently cycle with friends on weekends, combining leisure with physical activity.

TIAGO TEIXEIRA

1 | Biography

My name is Tiago Teixeira. I was born in Portugal, in a small village surrounded by nature, and from an early age, I realised that Earth sciences could play an important role in my life. My academic background is mainly focused on Geosciences but also includes some aspects of Biology, through the degrees I pursued at the University of Aveiro and at the Faculty of Sciences of the University of Porto. In recent years, my work has been centred on environmental geochemistry, with a focus on sustainability and the search for innovative solutions to minimise environmental impacts. I am currently pursuing a PhD focused on the treatment and valorisation of industrial effluents, aiming to develop more efficient and sustainable approaches for better industrial waste management.

2 | What motivated you to pursue a PhD?

The decision to pursue a PhD stemmed from my desire to go beyond the knowledge I had acquired, and to make a more significant impact in the field of environmental sustainability. I have always been highly self-taught and eager to delve into challenging topics, and my current work allows me to explore new techniques and innovative approaches. Moreover, collaborating with the industry through BIKiNNOV provides a unique opportunity to bridge science with real-world societal challenges, enabling the search for more effective and sustainable solutions for an ever-growing industrial sector that is a benchmark in our country. I believe that this interaction between academia and the industrial sector is essential to transforming knowledge into practical innovation, contributing to a more environmentally responsible future.

3 | Can you briefly explain the topic of your PhD and its impact on the Two-Wheel sector?

My PhD focuses on the treatment and valorisation of industrial effluents from the production of bicycle components. The goal is to develop innovative and sustainable solutions that not only reduce the environmental impact of these wastes but also transform them into by-products with potential for reuse in the industry. In a sector where sustainability and process efficiency are increasingly valued, this research contributes to fostering a circular economy within the two-wheeled industry.

4 | What would you like to do after completing your PhD?

After completing my PhD, I would like to see some of the ideas currently being developed put into practice, as well as feel that I have contributed to strengthening a healthy partnership between academic research and industry. Additionally, I aspire to explore opportunities that allow me to continue learning and developing new techniques, whether through applied research, collaboration with companies in the sector, or even the creation of new projects that can play a relevant role in the transition to a more environmentally friendly industry.

5 | Do you use any vehicle from the two-wheel sector ? If so, for what purpose ?

I have been a bicycle user since I was young. In the past, I practiced cycling sports, but nowadays, I mainly use my bicycle for leisure, taking advantage of the benefits of a city like Aveiro, which offers a good network of bike lanes and cycling routes surrounded by nature. During the summer, I also use my bicycle for some trips between home and university, making my journeys more enjoyable and sustainable.

FROM PORTUGAL BIKE VALUE TO BIKINNOV: THE GROWTH OF THE TWO-WHEEL CLUSTER

Gil Nadais[1]
1 BIKiNNOV - Bike Value Innovation Center Association, Rua da Indústria, 369, Covão, 3750-792, Águeda, Portugal
E-mail: geral@bikinnov.pt

Portugal has established itself as one of the leading bicycle producers in Europe, driven by the success of Portugal Bike Value (PBV), an initiative that has promoted the national industry beyond its borders. However, the sector's growth required a transition towards a model more focused on innovation and technological development. This led to the creation of BIKINNOV, a Technology and Innovation Center aimed at positioning Portugal not only as a manufacturer but also as a leader in the design and development of innovative solutions for sustainable mobility.

BIKINNOV addresses strategic challenges such as the need for technological infrastructure, the commitment to sustainability and digitalization, the development of human resources, and the internationalization of the sector. This initiative represents a paradigm shift for the Portuguese industry, fostering the evolution from an OEM (Original Equipment Manufacturer) model to ODM (Original Design Manufacturer) and OBM (Original Brand Manufacturer) models, ensuring the country's competitiveness in a rapidly transforming global market.

The future of sustainable mobility relies on increasingly efficient and integrated solutions, and BIKINNOV positions itself as a driving force of this revolution, ensuring that Portugal remains at the forefront of innovation in the two-wheel sector.

KEYWORDS
BICYCLE INDUSTRY; INNOVATION; SUSTAINABLE MOBILITY; PORTUGAL BIKE VALUE; BIKINNOV; TECHNOLOGICAL DEVELOPMENT; DIGITALIZATION.

INTRODUCTION

In recent years, Portugal has solidified its position as one of the leading bicycle producers in Europe. Portugal Bike Value (PBV), a project that evolved into an international brand, played a crucial role in this growth, placing the national industry in the spotlight and promoting its manufacturing capabilities beyond borders. However, the sector's evolution required more than large-scale production; it became imperative to advance towards a knowledge- and innovation-based model. In this context, BIKINNOV emerged - a Technology and Innovation Center that embodies the ambition of industry players to transform Portugal from a mere manufacturer into a leader in technological development within the two-wheel industry.

THE SUCCESS OF PORTUGAL BIKE VALUE

Portugal Bike Value was launched as a strategy to enhance and promote the national bicycle industry, leveraging its existing production capacity and the growing demand for sustainable mobility solutions. Led by ABIMOTA, the national association representing the sector, this initiative enabled Portugal to achieve significant milestones, including becoming the leading bicycle producer in Europe, experiencing exponential growth in exports, and gaining recognition as a benchmark for quality and efficiency.

However, as the industry evolved, reliance on a business model based solely on OEM (Original Equipment Manufacturer) production became a limiting factor. Portuguese companies needed to position themselves at higher levels of the value chain, actively contributing to the design and development of innovative products. Thus, while Portugal Bike Value fulfilled its initial mission, it also made clear that the next step was to strengthen the sector's Research and Development (R&D) capabilities.

THE TRANSITION TO BIKINNOV

BIKINNOV emerges as a response to this necessity. More than just a new name, it represents a structural and strategic shift. The objective is to enable Portugal to transition from a predominantly OEM (Original Equipment Manufacturer) model to ODM (Original Design Manufacturer) and, eventually, OBM (Original Brand Manufacturer). In other words, the goal is not only to manufacture bicycles but also to develop new concepts, technologies, and products that will define the future of sustainable mobility.

The creation of BIKINNOV was driven by several key factors:

a) Need for Technological Infrastructure - Portugal's two-wheel industry had already demonstrated strong production capabilities but lacked dedicated research and development centers. BIKINNOV addresses this gap by establishing state-of-the-art laboratories to test new materials, industrial processes, and emerging technologies.

b) Focus on Sustainability and Digitalization - The sector faces challenges such as transitioning to more sustainable materials and integrating digitalization into the production chain. BIKINNOV is structured with a cross-cutting approach, ensuring that innovation and environmental responsibility go hand in hand.

c) Capacity Building and Knowledge Transfer - The new center acts as a catalyst for knowledge, promoting the training of highly skilled human resources and facilitating technological transfer between universities, research centers, and the industry.

d) Strengthening International Presence - With the support of international networks, BIKINNOV positions itself as a global player in two-wheel mobility innovation, integrating strategic partnerships and contributing to the definition of international technical standards.

BIKINNOV was born from the industry itself, resulting from the union of 35 founding companies, later joined by 16 additional entities, bringing the total to 51 members. This initiative arose from the collective efforts of companies in the sector that, recognizing the importance of innovation and technological development, sought support from the Portuguese Cycling Federation, technology centers, educational and research institutions, industry associations, and municipal councils. With such a diverse membership base, BIKINNOV has become a solid and representative ecosystem, fostering cooperation between business and non-business entities and consolidating an environment conducive to the sustainable growth of Portugal's bicycle industry.

THE TRANSFORMATION OF THE NATIONAL INDUSTRY

The significance of BIKINNOV goes beyond technological innovation; it represents a paradigm shift in the positioning of the national industry, transitioning from a subcontracting role to a leadership position in the design and development of new solutions. This transition does not occur in isolation – it requires the mobilization of resources, strategic financing, and a cultural shift within companies, fostering the recognition of Research and Development (R&D) as a key value driver.

Portugal has been establishing itself as a country with unique expertise in the sector, a result of decades of specialization. However, global competition necessitates the continuous enhancement of both production and technological capabilities. BIKINNOV aligns with this dynamic by providing national companies with access to cutting-edge infrastructure and frontier knowledge, ensuring that Portugal remains competitive in a rapidly evolving industry.

Furthermore, BIKINNOV promotes collaboration across different industrial sectors, fostering synergies between the mobility industry, advanced materials, digitalization, and artificial intelligence. This integrated approach will enable the development of innovative solutions that address the demands of future mobility.

ELECTRIFICATION OF MOBILITY AND ITS IMPACT ON THE TWO-WHEEL SECTOR

The electrification of mobility is one of the most significant transformations in the transport sector, driven by the need to reduce emissions, improve energy efficiency, and meet new urban demands. The growth of electric mobility has been supported by stricter environmental regulations, technological advancements in energy storage, and government incentives favoring more sustainable transport solutions. In the two-wheel sector, this evolution is redefining the concept of mobility and positioning Portugal as a hub for innovation and development.

Urban challenges such as congestion, pollution, and fossil fuel dependency are increasingly pressing issues. Electric bicycles (e-bikes) have emerged as an efficient alternative, enabling fast and accessible travel with a reduced environmental impact. According to a Deloitte study commissioned by BIKINNOV, e-Cargo Bikes

could replace up to 50% of short-distance commercial trips, promoting more efficient urban logistics. This trend reflects a structural shift in mobility patterns, where electrification is becoming essential for a more sustainable transportation model.

Several factors are driving this change. Public policies have been a key catalyst, offering subsidies and tax incentives for the purchase of electric bicycles. At the same time, the expansion of dedicated cycling infrastructure and charging stations has facilitated the integration of e-bikes into urban ecosystems. Changing consumer habits have also contributed to this growth, with increased adoption of shared and flexible mobility solutions, reflecting a growing commitment to sustainability and transport efficiency.

Technological innovation has been a crucial factor in the adoption of electric bicycles. Advances in lithium-ion batteries have significantly increased range and reduced charging times, making these vehicles more competitive. Additionally, digitalization and connectivity have enhanced the user experience, with IoT sensors enabling real-time monitoring of bicycle performance and pre-dictive maintenance. These improvements have led to the diversification of business models, driven by the increasing adoption of electrification.

The two-wheel sector has witnessed a rise in electric bicycles for shared mobility and urban logistics. Last-mile delivery companies have heavily invested in e-Cargo Bike fleets, leveraging their efficiency, low operational costs, and environmental advantages to optimize delivery services. According to Deloitte forecasts, the global e-Cargo Bike market is expected to grow by 7.6% annually until 2030, with Europe accounting for 34% of this market. Portugal, with its strong industrial cluster, has a strategic opportunity to position itself as a key player in this expanding sector.

Despite the opportunities generated by electrification, certain challenges remain. Supporting infrastructure is still insufficient, with a need for more charging points and adapted cycling lanes. Regulatory frameworks also pose an obstacle, as the lack of uniform standards for e-Cargo Bikes can hinder their integration into urban ecosystems. Another challenge is the high initial purchase cost, which, despite long-term benefits, remains a barrier for many consumers and businesses.

BIKINNOV plays a key role in this transformation, acting as a driver of innovation in the two-wheel sector. The center focuses on Research and Development (R&D), fostering collaboration between industry, universities, and research centers to develop more efficient and competitive products. Moreover, its efforts to internationalize the Portuguese industry contribute to consolidating the country's position as a European leader in sustainable mobility.

Electrification of mobility is not just a trend, but a necessity in addressing environmental and urban challenges of the 21st century. Portugal has the opportunity to leverage its expertise in the two-wheel sector and strengthen its position in the transition towards more efficient, accessible, and eco-friendly mobility. The success of this transformation will depend on continued investment in innovation, infrastructure, and public policies that encourage the adoption of electric and sustainable solutions. If these conditions are met, Portugal can establish itself as a global reference in electric and sustainable mobility, securing a competitive position in a rapidly evolving global market.

THE FUTURE OF SUSTAINABLE MOBILITY

Sustainable mobility has become a central theme in urban and environmental development policies. The European Union has set ambitious targets for reducing the carbon footprint and transitioning to more eco-friendly transport solutions. In this context, the bicycle plays a strategic role, not only as an efficient means of transportation but also as a viable solution to urban mobility challenges.

The rise of electric bicycles (e-bikes) exemplifies the sector's evolution and its ability to adapt to new consumer demands. The integration of smart technologies, such as performance sensors, connectivity, and energy optimization, reinforces the importance of digitalization in mobility. BIKINNOV positions itself as a driving force behind these transformations, supporting research and the implementation of new solutions that make bicycles increasingly efficient and seamlessly integrated into urban ecosystems.

CONCLUSION: A NEW CHAPTER FOR THE PORTUGUESE INDUSTRY

The transition from Portugal Bike Value to BIKINNOV represents the maturity of the sector. The path forward is now clear: investing in R&D, strengthening companies' capacity to develop proprietary products, and consolidating Portugal as a center of excellence in sustainable mobility innovation.

If Portugal Bike Value demonstrated to the world that Portugal is a leader in bicycle manufacturing, BIKiNNOV is here to prove that this success can be expanded through innovation, ensuring a future where the country not only follows industry trends but also defines them. The revolution of Portugal's two-wheel industry has already begun – and BIKiNNOV is at the heart of this transformation.

The challenge now is to ensure that this transition is supported by an ecosystem conducive to innovation. This requires:

- Strengthening collaboration between companies and academic institutions,
- Public policies that encourage research and development, and
- A continuous commitment to excellence.

If these conditions are met, Portugal will not only maintain its leadership position in bicycle production but also establish itself as a global benchmark for innovation in sustainable mobility.

THE PORTUGUESE TWO-WHEELER INDUSTRY: A CORNERSTONE OF EUROPE'S MOBILITY FUTURE

The European two-wheeler sector has undergone a significant transformation over the past decade, driven by the demand for sustainable transport solutions, technological innovation, and changing consumer preferences. At the heart of this evolution lies Portugal, an increasingly vital player in the production, assembly, and export of bicycles, e-bikes, and motorcycles within Europe.

PORTUGAL'S ROLE IN THE EUROPEAN TWO-WHEEL MARKET

Portugal has established itself as a manufacturing powerhouse in the European two-wheeler industry, particularly in the cycling segment. Portugal is the largest producer of bicycles in the European Union, a status achieved through strategic investments in production capacity, automation, and sustainable manufacturing processes.

The country's success can be attributed to its robust industrial base, skilled workforce, and commitment to innovation. The Agueda region, often referred to as the "Bike Valley" of Europe, has become a hub for two-wheeler production, housing major industry players and fostering a dynamic ecosystem of suppliers, component manufacturers, and research institutions.

The Portuguese two-wheeler industry is not only meeting domestic demand but also playing a crucial role in strengthening Europe's supply chain. With increasing concerns over global supply chain disruptions, Portugal's capacity to produce high-quality two-wheelers domestically has provided brands with a reliable alternative.

INNOVATION AND SUSTAINABILITY: DRIVING THE INDUSTRY FORWARD

Innovation is central to Portugal's success in the two-wheeler sector. The industry is embracing new technologies, from lightweight materials to the new innovation testing centre BIKiNNOV and modern machineries in industrial processes. The integration of these innovations has enabled Portuguese manufacturers to compete on a global scale while contributing to Europe's push for sustainable mobility solutions.

Sustainability is another key pillar of Portugal's two-wheeler industry. Many manufacturers have adopted eco-friendly production processes, including the use of recycled materials, energy-efficient facilities, and reduced carbon footprints. This aligns with the European Union's Green Deal objectives and strengthens

the industry's appeal among environmentally conscious consumers.

Furthermore, the growth of the electric bicycle market has been a game-changer for Portugal's two-wheeler industry. E-bikes have surged in popularity across Europe as consumers seek convenient, low-emission transport options. Portuguese manufacturers have been quick to adapt to this trend, investing in the development and production of electric bicycles.

THE ROLE OF CONEBI IN SUPPORTING THE SECTOR

The Confederation of the European Bicycle Industry (CONEBI) has played a role in supporting and advocating for the growth of the cycling sector in Europe. As a key Industry association, CONEBI works to ensure that policies and regulations are conducive to the development of the industry, promoting investments in sustainable mobility and manufacturing.

Portugal benefits from CONEBI's efforts in several ways. Firstly, the organization's advocacy for pro-cycling policies at the European level has helped drive demand for bicycles and e-bikes, directly boosting the Portuguese industry. Secondly, CONEBI facilitates collaboration between different stakeholders, including manufacturers, policymakers, and research institutions, creating opportunities for knowledge-sharing and industry growth.

At the EU level, moreover, fair trade policies that protect European manufacturers from unfair competition and market distortions have been crucial in ensuring that Portuguese producers can thrive in an increasingly competitive global market.

The Crucial Role of EU Regulations

CONEBI is actively involved in advocating for EU regulations that have a considerable impact on the cycling industry. Some of the key areas of regulatory focus include:

- **Personal Mobility Devices (PMD) and Safety Regulations:** To ensure consumer confidence, CONEBI is working on safety requirements across EU member states, reducing the risk of unsafe products flooding the market. Moreover, with the rise of electric e-kick steps and other personal mobility devices, CONEBI is working to ensure clear and fair regulations that support innovation while prioritizing safety and sustainability, marking a substantial cleavage between Pedal Assist E-Bikes and passive mobility, open throttle vehicles and devices. Finally,
- **Battery Regulations:** Given the growing importance of e-bikes, battery safety, recycling, and environmental impact are major topics. CONEBI is advocating for EU requirements that are industrially feasible and appropriate in terms of consumer-safety.
- **Ecodesign Forum:** Sustainable product design is crucial for the future of the industry. CONEBI's involvement in the Ecodesign Forum aims at ensuring that bicycles, e-bikes, parts & accessories will have the right framework requirements to comply with European sustainability goals, promoting durability, reparability, and lower environmental impact.
  These regulations not only enhance the sustainability of the industry but also strengthen Portugal's position as a leading manufacturer within Europe by ensuring that production aligns with high environmental and safety standards.

CHALLENGES AND FUTURE OUTLOOK

Despite its impressive growth, the Portuguese two-wheeler industry faces challenges that must be addressed to maintain its upward trajectory. Rising international raw material costs, for example, are a possible obstacle to the industry's long-term full growth.

Additionally, while Portugal's industrial capabilities are strong, further investment in research and development will be crucial to maintaining its competitive edge. Strengthening collaboration between the industry and academic institutions could foster more technological breakthroughs and enhance production efficiency.

Looking ahead, Portugal is well-positioned to play an even greater role in shaping the future of Europe's two-wheeler sector. By continuing to innovate, investing in sustainability, and leveraging support from organizations like CONEBI, Portugal can solidify its reputation as a key player in the global mobility revolution.

CONCLUSION

The Portuguese two-wheeler industry has become an integral part of Europe's mobility landscape, contributing significantly to economic growth, technological advancement, and sustainability efforts. As demand for bicycles and e-bikes continues to rise, Portugal's role in meeting this demand is more relevant than ever. With continued support from industry associations like CONEBI and a commitment to innovation and sustainability, Portugal is not only securing its place as a leading manufacturer but also shaping the future of two-wheeled mobility in Europe and beyond.

Former CONEBI President
Massimo Panzeri

"AM2R WILL TRANSFORM THE TWO-WHEEL SECTOR AND ESTABLISH PORTUGAL AS A LEADER IN SUSTAINABLE MOBILITY"

Pedro Araújo, CEO of Polisport Plásticos S.A., leader of the AM2R consortium, reveals the ambitious objectives of the Mobilizing Agenda for Business Innovation in the Two-Wheel Sector (AM2R). The initiative aims to drive innovation, promote sustainable mobility, and make Portugal a center of excellence in the production of bicycles and electric motorcycles, with a focus on creating skilled jobs and enhancing industrial autonomy. With 65 new products and a projected turnover of 336 million euros by 2027, AM2R is shaping the future of the two-wheel sector in Portugal.

What are the main objectives of AM2R, and how does the agenda aim to transform the two-wheel sector in Portugal?

The main objective of AM2R is to drive innovation in the two-wheel sector in Portugal. To achieve this, we are developing 65 new products, including bicycles and electric motorcycles, promoting sustainable mobility by replacing traditional delivery vehicles and reducing CO_2 emissions, noise, and urban congestion.

We aim to empower the national industry to produce all the necessary components, ensuring the country's industrial autonomy, creating the first 100% Portuguese bicycle, and reducing dependence on the Asian market.

Additionally, we are strengthening the connection between businesses and the scientific-technological system, fostering research and development to increase the sector's competitiveness and resilience.

How did Polisport Plásticos become the leader of the AM2R consortium?

Polisport Plásticos was chosen to lead the AM2R consortium due to its leadership position and uniqueness in the two-wheel sector. With 46 years of market experience, a solid international presence, and a continuous commitment to innovation, the Polisport Group has a solid foundation and significant strength in this sector.

The company is capable of coordinating the efforts of the efforts of 42 co-promoters, including 34 companies, 8 entities from the Scientific and Technological System and an Association, thanks to its ability to integrate and drive strategic partnerships.

With a unique business model, Polisport plays a crucial role in the two-wheel cluster. Its broad business scope, combined with the group's solidity and the portfolio of 'Made in Europe' brands, reinforces its position as a leader and reference in this market.

PEDRO ARAÚJO
CEO of Polisport Plásticos S.A.

What have been the main challenges and responsibilities of leading such a diverse consortium?

The main challenges and responsibilities of leading such a diverse consortium mainly involve defending the common objectives of the Agenda, ensuring that the individual needs of each member, including IAPMEI and government entities, are respected. This requires continuous coordination and effective communication, with the responsibility to maintain cohesion among all parties involved while keeping the focus on achieving the objectives and deadlines.

Effective management of collaboration between multiple entities, each with its own organizational culture and objectives, requires systematic effort and dedication, especially from the Executive Committee of the Agenda. In this context, ABIMOTA and its team play a fundamental role in strategic coordination, facilitating communication, and ensuring that collaboration between participants occurs efficiently and aligned with the consortium's objectives. Clear communication and knowledge sharing are crucial factors for the success of the initiative.

MAIN EXPECTED RESULTS OF AM2R

What are the main expected results of AM2R by 2026?

The main expected results of AM2R by 2026 include the completion and launch of 65 new products, such as accessories, bicycles, electric motorcycles, and cargo bikes, with the aim of revolutionizing individual, family, and service mobility.

Additionally, it is expected that 1,114 jobs will be created, of which 238 are high-skilled positions, helping retain talent in Portugal.

The consortium also aims to achieve a turnover of 336 million euros, with an export rate of 73%, corresponding to 245.28 million euros in international sales.

How do you assess the collaboration between the consortium companies and the Non-business Entities of the Research and Innovation System ?

The collaboration between the consortium companies and the Non-business Entities of the Research and Innovation System has been very positive, creating important synergies and promoting knowledge sharing. This collaboration has driven innovation, resulting in advanced and competitive solutions for the market.

The interaction between the parties has strengthened the ability to respond to sector demands, especially in global trends for sustainable mobility. Moreover, it allows for the capture and retention of talent from universities for the two-wheel industry, providing an excellent opportunity to bridge that gap.

It is crucial that companies, industries, and universities grow closer, with internships, consulting, and systematic collaboration-not isolated and occasional. This flexibility and proximity are essential for the continuous success of the sector.

How would you assess the "Sustainable Mobility Future, from Portugal to the World" technical-scientific conference, held on December 10-11, at the Leixões Cruise Terminal?

The technical-scientific conference was a great success. The event was highly attended, bringing together experts, researchers, and professionals from the sector, creating a dynamic and comprehensive space to discuss the challenges and opportunities in sustainable mobility.

The presence of people genuinely interested in the topics elevated the quality of the debates, highlighting the importance of technological innovation and environmental sustainability as drivers of development.

During the conference, the latest innovations and ongoing projects were presented, reinforcing Portugal's role as a leader in sustainable mobility, making it a key moment on the agenda.

How important is this collaboration between companies and scientific entities for driving innovation and advancing the development of the sector?

Collaboration between companies and scientific entities is essential for developing innovative solutions that address real market needs. This partnership allows for the sharing of resources, knowledge, and experiences, accelerating the innovation process and strengthening both the sector's and the country's competitiveness.

Creating business synergies and strengthening clusters, like Portugal Bike Value, is crucial to maintain and expand Portugal's leadership in bicycle production. However, it is essential to highlight the importance of this brand, as well as the valuable contribution of initiatives like ABIMOTA and the BIKiNNOV Lab. These initiatives, which involve academia, technical expertise, and research, are fundamental for positioning the sector as an international benchmark.

KEY RESULTS EXPECTED FROM AM2R BY 2025

What are your expectations for the future of the two-wheeler sector in Portugal once the AM2R project is completed?

Our expectations are very positive. We believe that the country will establish itself as a leader in the production of accessories, bicycles, and electric motorcycles, with a complete and independent value chain, reinforcing 'Made in Europe' and promoting the decentralization of Asian production.

We also expect a significant increase in exports, which will further solidify Portugal's presence in international markets. Additionally, we are confident that the continued collaboration between companies and scientific entities will remain and be strengthened, which is essential for promoting a culture of constant innovation in the sector. One of the main goals is to retain qualified resources in Portugal, preventing early migration abroad.

This project is strategic for the country, creating skilled jobs, promoting innovation, and strengthening Portugal's leadership position in the sector.

ABIMOTA

ABIMOTA - Associação Nacional das Indústrias de Duas Rodas, Ferragens, Mobiliário e Atividades Complementares dos Setores Representados is a non-profit association and a single point of reference, at national level. It provides high-value-added services in close cooperation with its members and clients.

Development of a Sustainability Standard

A new sustainability standard is currently being developed, based on a single dynamic indicator capable of comprehensively assessing the environmental performance of the Two-Wheel Industry. This indicator will aggregate externalities and impacts, as well as their associated costs.

ABIMOTA owns the brands **Portugal Bike Value**, **Portugal Building Hardware**, and **Portugal Metal Furniture**, supporting the international growth and competitiveness of the sectors it represents.

Our Services

- **Legal Support**
- **Technical Consulting**
- **Training**
- **Industry Support**
- **Laboratory Standardization**
- **Environment and Sustainability**
- **Quality Management**
- **Energy**
- **Internationalization**
- **Thermography**

PORTUGAL BIKE VALUE by ABIMOTA

PORTUGAL BUILDING HARDWARE by ABIMOTA

PORTUGAL METAL FURNITURE by ABIMOTA

PRR Plano de Recuperação e Resiliência
REPÚBLICA PORTUGUESA
Financiado pela União Europeia NextGenerationEU

GIL NADAIS
Secretary-General of ABIMOTA

"AM2R WILL POSITION PORTUGAL AS A CENTER OF EXCELLENCE IN THE TWO-WHEEL SECTOR"

Gil Nadais, Secretary-General of ABIMOTA, outlines the objectives and challenges of the Mobilizing Agenda for the Two-Wheel Sector (AM2R), emphasizing the importance of innovation and sustainability to transform Portugal into a global leader and reduce dependency on the Asian market.

What are the main objectives of the Mobilizing Agenda for the Two-Wheel Sector (AM2R), and how is the National Association of Two-Wheel Industries, Hardware, Furniture, and Related Activities (ABIMOTA) contributing to achieving them?
The AM2R's central objectives are to transform the national production profile, establish a new specialization alignment in the two-wheeled sector, and increase the competitiveness of Portuguese companies. ABIMOTA is responsible for the international promotion of the consortium and, simultaneously, for coordinating AM2R by delegation of powers and functions from the consortium leader.

What is ABIMOTA's role as the coordinator of AM2R?
As mentioned, ABIMOTA coordinates AM2R by delegation of powers, ensuring the effective implementation of the agenda's objectives. Our mission is to guarantee that AM2R's goals, which aim to consolidate the connection between the business fabric and the scientific-technological system, are fully achieved. We drive innovation through R&D projects, facilitating the creation of disruptive solutions, and ensuring that innovations are rapidly valued and industrialized, strengthening the sector's competitiveness and promoting the internationalization of their solutions.

What are the main challenges ABIMOTA has faced in coordinating AM2R?
Coordinating AM2R involves significant challenges due to the large number of partners. The biggest challenge has been coordinating partners from different areas of activity and interests, which requires constant communication and rigorous management. Additionally, ensuring the meeting of deadlines and

efficient use of financial resources, given the complexity of technological innovations, is an ongoing challenge. Another obstacle is the limitation on direct commercial relationships between consortium members, which, while necessary to avoid conflicts of interest, may hinder the spirit of quick and direct collaboration, which is essential for the development of innovative solutions. However, ABIMOTA has managed to overcome these challenges through disciplined management and the commitment of partners who are aligned with the Agenda's objectives.

> ***"Once AM2R is completed, Portuguese companies will become more competitive,offering a differentiated range of products with higher added value, which will enhanceour presence in the global market."***

OPPORTUNITIES AND ECONOMIC IMPACT OF AM2R

What are the biggest opportunities the Agenda offers for the two-wheeler sector in Portugal?
AM2R provides a unique opportunity to position Portugal as a center of excellence in the two-wheeler sector by creating an innovation ecosystem based on disruptive products, processes, and services. The Agenda aims not only to increase the international competitiveness of the sector but also to reduce dependence on the Asian market. Focusing on sustainability, digitalization, and innovation, AM2R strengthens Portugal's position in the global market and drives the sector's development both nationally and internationally.

What is the expected impact of AM2R on the regional and national economy?
AM2R is expected to generate a business volume of 336 million euros by 2027, with an export rate of 73%. This growth will reflect the enormous internationalization potential of the solutions developed, while also contributing to increasing competitiveness and reducing dependence on imports, especially from Asia. The agenda will also strengthen the sector's capacity and create highly specialized jobs, promoting economic sustainability within the national business fabric.
AM2R will further foster the transfer of knowledge and the sector's capacity building, contributing to sustainable growth and the creation of value within the national business fabric.

JOB CREATION AND SECTOR CAPACITY BUILDING

How is the agenda contributing to job creation and skills development in the sector?
AM2R is having a direct impact on job creation by driving new initiatives and expanding the operations of companies in the sector. The agenda is also promoting skills development by encouraging continuous training, the creation of new curricula, and the sharing of knowledge between companies and universities. The creation of new PPS (Products, Processes, and Services), and the sector's ability to produce a 100% Portuguese bicycle, will increase qualifications and specialized employment. The development of these innovations will allow the industry to reduce dependence on external suppliers and increase national capacity, with strong prospects for economic and export growth.

> ***"ABIMOTA has played a strategic role in promoting the two-wheeled sector, with initiatives such as 'Portugal Bike Value,' positioning the country as a leader in innovation and sustainable mobility."***

How does the agenda intend to increase exports and reduce dependence on the Asian market?
AM2R is boosting the competitiveness of companies in the two-wheeler sector by developing innovative solutions that meet the needs of the international market. The creation of 65 new PPS has strong export potential, contributing to market diversification and reducing dependence on Asian suppliers. The Agenda aims to promote independence from the Asian market by enabling Portuguese companies to produce essential components, allowing for the creation of a 100% Portuguese bicycle. With an export forecast of 73% by 2027, AM2R is strengthening Portugal's position in the global market, positioning it as a leader in advanced and sustainable solutions in the two-wheeler sector.

THE FUTURE OF THE TWO-WHEELER SECTOR IN PORTUGAL

What are your expectations for the two-wheeler sector in Portugal once the AM2R initiative has been fully implemented?
Once AM2R is completed, the expectations for the future of the two-wheeler sector in Portugal are

extremely positive. The agenda will provide a solid foundation of technological innovation and sustainability, enabling companies in the sector to be more competitive in the global market. The solutions developed under AM2R, particularly the creation of new products, processes, and services, will position Portuguese companies with a differentiated and higher value-added offering. We expect substantial growth in exports, reinforcing the sector's international presence. Additionally, the skills development and capacity building driven by AM2R will create qualified jobs, contributing to the modernization and strengthening of the national economy. Independence from the Asian market, achieved through the national ability to produce all the necessary components for a 100% Portuguese bicycle, will be another key milestone, ensuring the sector's autonomy and sustainability.

How does ABIMOTA intend to continue supporting innovation and the development of the two-wheeler sector in the future?
ABIMOTA will continue to support innovation and the development of the two-wheeler sector by maintaining the creation of strategic partnerships with companies, research centers, and academic institutions as one of its main priorities. We will strengthen the encouragement of research and development (R&D) to ensure that companies in the sector continue to innovate and improve their processes. Facilitating access to funding for innovative projects will also be a priority. A clear example of our commitment to innovation is BIKiNNOV - Bike Value Innovation Center - Association, which aims to promote the development of advanced technological solutions in the two-wheeler sector. Our mission is to continually strengthen collaboration between all stakeholders in the sector, ensuring that companies are prepared to face future challenges with a solid foundation in technology, sustainability, and innovation.

> ***"Extending the execution deadline for the mobilizing agendas would be essential to ensure the full realization of the export potential of the innovations developed."***

INTERNATIONAL PROMOTION: ABIMOTA'S ROLE

What has been ABIMOTA's role in promoting the two-wheeler sector in Portugal?
ABIMOTA has played a strategic role in promoting the two-wheeler sector in Portugal. We have maintained a constant presence at international fairs, giving Portuguese companies greater visibility and contributing to the sector's global competitiveness. A significant example of this promotion is Portugal Bike Value, an ABIMOTA initiative aimed at positioning Portugal as a center of excellence in production and innovation in the two-wheeler sector. Portugal Bike Value highlights the Portugal brand at international fairs, promoting the innovative solutions of national companies and consolidating the country's image as a leader in sustainable mobility. This promotion is crucial to strengthen exports, attract new investments, and establish strategic partnerships, thus contributing to the growth and competitiveness of the sector.

How do you evaluate the impact of the technical-scientific conference "The Future of Sustainable Mobility: From Portugal to the World," held in December 2024 at the Porto de Leixões Cruise Terminal?
The conference was a great success and an excellent opportunity to discuss the future of sustainable mobility and Portugal's role in this context. We brought together experts, companies, and scientific institutions who shared knowledge, presented innovations, and strengthened strategic partnerships. The feedback from participants was extremely positive, highlighting the relevance of the discussions for the advancement of the two-wheeler sector and for positioning Portugal as a leader in sustainable mobility solutions. The conference also facilitated the exchange of experiences and identification of new paths for the development and internationalization of the sector, which will have a direct and positive impact on the future of companies and the global competitiveness of the sector.

1. New e-bikes for the high-end segment and cargo bikes on display at the entrance of the Leixões Cruise Terminal building.
2. The conference secretariat was efficiently managed by the students of Escola Superior de Tecnologia e Gestão de Águeda (ESTGA)'s Secretarial and Business Communication course.
3. Distribution of AM2R tote bags to participants.
4. Participants had the opportunity to explore the various prototypes developed within the framework of the Agenda.
5. The exhibited products and services captured the interest of the participants.
6. Bicycle nipples for spokes, which will be produced for the first time in Portugal.
7. The conference introduced new products developed by consortium members.
8. Pedro Araújo from Polisport Plásticos, leader of the AM2R Consortium, at the opening of the conference.
9. Gil Nadais from ABIMOTA presented AM2R.
10. Ana Reis from INEGI shared the key figures and results related to Research and Development (R&D) within the Agenda.
11. "This is one of the agendas whose success is already recognized by many," stated the Secretary of State for Planning and Regional Development, Hélder Reis, at the opening of the conference.
13. Frames for e-cargo bikes & long tail e-bikes, and full-suspension carbon e-bike frames for high-end models.






PATROCINADORES
centi
ineqi

SESSÃO DE ABERTURA
HÉLDER
REIS
SECRETÁRIO DE ESTADO DO PLANEAMENTO
E DESENVOLVIMENTO REGIONAL




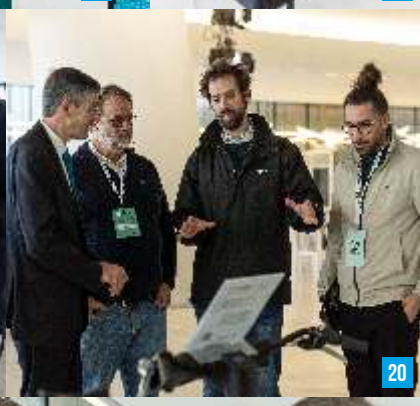


27. PPS from POLISPORT PLÁSTICOS.
28. Isabel Gomes from SRAMPORT with the PPS "New Transmission Components for Bicycles".
29. PPS "Motor Bracket - light electric mobility".
30. Participants had the opportunity to learn about the products and services being developed in AM2R.
31. Detail of the "Long John" cargo bike.
32. New e-bikes for the high-end segment and conventional and electric bicycles with new configurations.
33. Manuel Marsílio (CONEBI), Gil Nadais (ABIMOTA), Diogo Fula (BATPOWER), and Miguel Araújo (MOBINOV).
34. The event was attended by over two hundred participants.
36. Roundtable on Metals and Surface Treatments in the Mobility Sector, moderated by João Paulo Dias from Instituto Pedro Nunes.
37. Eduardo Bianchi de Aguiar (TRIANGLE'S) and Isabel Gomes (SRAMPORT).
39. At the end of each panel, participants had the opportunity to ask questions to the speakers.
40. César Coutinho introduced BIKiNNOV - Bike Value Innovation Center.
41. Collaborative innovation / perspectives and challenges of a technology and innovation center.
42. Sharing experiences from the user's perspective.
43. Presentations on the theme "Metals and Surface Treatments in the Mobility Sector".

















44. Manuel Marsílio, Pedro Araújo, and Eduardo Bianchi de Aguiar.
45. Hubs by RODI.
46. César Coutinho, representing BIKiNNOV, presented the new facilities of the CTI.
47. Paulo Alves from EDMTECH on module and pack assembly and BMS development.
48. Various conference speakers presented the technical-scientific developments of the Agenda.
49. During coffee breaks, participants were invited to visit the exhibition of demonstrators and posters from consortium entities.
50. Paula Quinteiro's presentation on Life Cycle, in the panel "Sustainability: Challenges and Opportunities in the Two-Wheeled Sector".
51. Apresentations on Sustainability.
52. José Baranda Ribeiro from UC on energy efficiency in production processes.
53. Ramon Carvalho presented the status of the development of the Sustainability Framework.
55. Roundtables involved ENESII and companies.
56. The challenges of digitization and logistics were the topic of one of the many roundtables.
57. The synergies between ENESII and the industry were one of the many topics discussed.
58. The event organizing team.
59. The poster "Cemented and Nitrided Steels for Bicycle Freehub Gears" was voted the best of the conference.

DIVISÕES TÉCNICAS

Representam importantes Áreas do conhecimento e desenvolvimento em Ciência e Tecnologia de Materiais, proporcionando aos membros ações no seio das várias comunidades profissionais específicas, reuniões técnico-científicas e recursos, oportunidades de educação, de participação e formação de redes e plataformas e divulgação nas respetivas áreas do conhecimento.

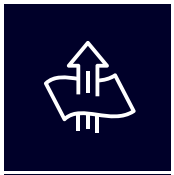

CORROSÃO E PROTEÇÃO DE MATERIAIS,

*coordenada por **Teresa Diamantino** (LNEG) **Isabel Tissot** (Universidade Nova de Lisboa), contempla conhecimento e a atividade no domínio da Corrosão e Proteção de Materiais.*

ENGENHARIA DE SUPERFÍCIES,

*coordenada por **Fábio Ferreira** (FCTUC) **Cláudia Lopes** (TEMA, Universidade de Aveiro), agrega: Eletroquímica de Materiais, Tratamentos Térmicos e Engenharia de Superfícies, Tribologia e áreas afins Materiais.*

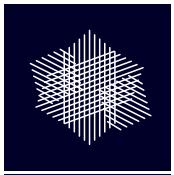

MATERIAIS ESTRUTURAIS,

*coordenada por **Ana Reis** (FEUP), **Rui L. Amaral** (INEGI/FEUP), **Tiago Silva** (INEGI/FEUP), tem como principal missão o estudo, desenvolvimento e aplicação de materiais utilizados em estruturas que exigem elevada resistência mecânica, durabilidade e desempenho em condições extremas. Estes materiais são fundamentais para setores como a construção civil, indústria automóvel, aeroespacial, naval e energética.*

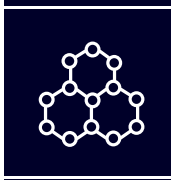

MATERIAIS FUNCIONAIS,

*coordenada por **Diana Gaspar** (CENIMAT-UNL) **Vítor Sencadas** (DEMaC-UA), abrange áreas de Nanotecnologias e Biomateriais, Materiais para a Eletrónica, Optoeletrónica e Dispositivos Médicos.*

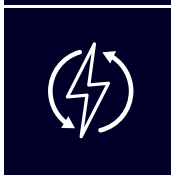

MATERIAIS PARA A ENERGIA,

*coordenada por **Filipe Neves** (LNEG) **Jennifer Teixeira** (INL), agrega: Materiais a serem usados em aplicações energéticas de conversão, armazenamento e para o aumento de eficiência energética de vários processos.*

POLÍMEROS E COMPÓSITOS,

*coordenada por **Jorge Coelho** (FCTUC), **A. Torres Marques** (FEUP), **J. C. Bordado** (IST e UTIS), A. Correia Diogo (IST), agrega: termoplásticos, elastómeros, termoendurecíveis, polímeros funcionais e respectivos sistemas compósitos.*

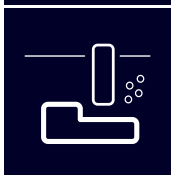

TECNOLOGIA E PROCESSAMENTO DE MATERIAIS,

*coordenada por **Abílio de Jesus** (FEUP), **Hélder Puga** (UM) e **Pedro Rosa** (IST) tem como principal objetivo contribuir para a dinamização da investigação e disseminação em tecnologias de produção de componentes mecânicos num enquadramento de constante evolução dos materiais e consideração pela sustentabilidade ambiental e social.*

J-SPM,

*coordenada por I**nês Prata, Bernardo Ribeiro, João Miranda** e **Fábio Brandão** integra os sócios da SPM com menos de 35 anos e tem como principal objetivo representar os pontos de vista, as necessidades e expectativas dos sócios jovens.*

COMUNICAÇÃO E DIVULGAÇÃO,

*Coordenada por **Paula Vilarinho** (U Aveiro), conta com a colaboração de **Manuela Oliveira** e **Joana Sousa** foi criada em julho de 2019, pretende ser o veículo da SPM por excelência, através do qual se dará mais voz à área de Materiais.*

MATERIAIS E PATRIMÓNIO CULTURAL,

*Coordenada por **João Pedro Veiga** e **Márcia Vilarigues** foi criada na Assembleia Geral da SPM de dezembro de 2022, tendo como objetivo ser um fórum dinâmico na promoção e divulgação do conhecimento aa área dos materiais do património cultural. Através da dinamização de ações para o público em geral e especializado, assim como para empresas que operam no sector e instituições de Ensino que oferecem formação na área, seja através de palestras, workshops, conferências, exposições ou notícias, pretende-se incentivar novos estudos e uma melhor compreensão do papel desempenhado pelos materiais no património cultural.*

PERITOS

A SPM disponibiliza no seu site uma lista de peritos que pode consultar se necessitar de apoio, colaboração ou serviço.

JUNTE-SE A ESTA LISTA!

- Abílio de Jesus
- Abílio Manuel Pereira da Silva
- Adriana Cavaco
- Aida Beatriz Vieira Moreira
- Albano Cavaleiro
- Alice Tavares
- André Ferreira Costa Vieira
- Andrei Kholkin
- Andreia Ruivo
- Andreia F. Sousa
- Ana Cabral
- Ana Rosanete Lourenço Reis
- Ana Sofia Figueira Ramos
- António José Vilela Pontes
- António Paulo Cerqueira Duarte
- António Torres Marques
- Artur Jorge dos Santos Mateus
- Bruno Araújo de Almeida
- Carlos Manuel da Fonseca Dias
- Carlos Miguel Marto
- Celeste Pereira
- Clara Rodrigues Pereira
- Cláudia Lopes
- Cláudia Ranito
- Edmundo Manuel Tavares Marques
- Fernando de Almeida Costa Oliveira
- Frederico Calheiros Maia
- Georgina Miranda
- Guilherme Nuno Carvalho
- Hugo Águas
- Inês Rondão
- João Alexandre Costa Gomes da Peixinha
- João Carlos Velosa Pereira
- João C.C. Abrantes
- João Pedro Nunes Pereira
- João Pedro Oliveira
- João Salvador Fernandes
- Joana Filipa dos Santos Teixeira
- Jingzhong Xiao
- José Cruz Oliveira
- José David Castro Castro
- José Luís de Sousa Amorim do Vale Quaresma
- José Manuel Antelo
- Jorge Fernando Jordão Coelho
- Jorge Lino Alves
- José Manuel Monteiro da Costa
- José Ramiro Afonso Fernandes
- Luís Gil
- Luís Manuel Lopes de Carvalho
- Maria de Fátima Reis Vaz
- Maria do Carmo Henriques Lança
- Mariana Sofia Peixoto Fernandes
- Manuel João Mendes
- Martinho Oliveira
- Nuno Ferreira
- Paulo Mourão
- Pedro A.R. Rosa
- Pedro Barquinha
- Pedro Salomé
- Penka Girginova
- Regina Santos
- Rosa Marat Mendes
- Sónia Simões
- Susana França de Sá
- Teresa Leonor Ribeiro Cardoso Martins Morgado
- Teresa Monteiro
- Vanessa Cardoso
- Virgínia Infante
- Vitor Sencadas
- Zohra Benzarti

Para mais informações consulte o nosso site:
http://www.spmateriais.pt/socios/bolsa-de-peritos

SÓCIOS COLETIVOS

- AIMMAP
- ALMASCIENCE COLAB
- AMORIM CORK COMPOSITES
- C5LAB - SUSTAINABLE CONSTRUCTION MATERIALS ASSOCIATION
- CATIM
- CELOPLÁS - PLÁSTICOS P/A INDÚSTRIA, S.A.
- CEMMPRE - UNIVERSIDADE DE COIMBRA
- CENIMAT - UNL NOVA.ID.FCT
  ASSOCIACAO PARA A INOVACAO
- CENTI - CENTRE FOR NANOTECHNOLOGY AND SMART MATERIALS
- CHEMITEK - QUIMICA AVANÇADA, S.A
- CIN - CORPORAÇÃO INDUSTRIAL DO NORTE, S.A.
- CIRES
- CODEPLAS - ENGª DE PEÇAS PLÁSTICAS, S.A.
- COFICAB PORTUGAL
- CTCV
- DIAS DE SOUSA - INSTRUMENTAÇÃO ANALÍTICA E CIENTÍFICA S.A.

SÓCIOS COLETIVOS

	DIRECÇÃO DE NAVIOS
DURIT	DURIT
eurogalva	EUROGALVA
U.PORTO FEUP FACULDADE DE ENGENHARIA UNIVERSIDADE DO PORTO	FEUP
Filsat	FILSAT EQUIPAMENTOS MÉDICO-CIENTÍFICOS, LDA
gravimeta Equipamentos para Laboratório	GRAVIMETA-EQUIPAMENTOS PARA LABORATORIO,LDA
ictpol	ICTPOL
I.L.C.	ILC - INSTRUMENTOS LABORATÓRIO E CIENTÍFICOS, LDA
IMMAS	IMMAS INSTITUTO DE MATERIAIS, MANUTENÇÃO, AMBIENTE E SEGURANÇA
inegi driving science & innovation	INEGI
INL	INL
ISEP INSTITUTO SUPERIOR DE ENGENHARIA DO PORTO	INSTITUTO SUPERIOR DE ENGENHARIA DO PORTO
IPN	IPN
Leica	LEICA - APARELHOS ÓPTICOS DE PRECISÃO, S.A.
LISNAVE ESTALEIROS NAVAIS, S.A.	LISNAVE ESTALEIROS NAVAIS SA
MASILVA WE ARE CORK	M A SILVA CORTIÇAS LDA

SÓCIOS COLETIVOS

- M.T.BRANDÃO
- MEDBONE
- PALBIT,SA
- PARALAB, SA
- PIEP ASSOCIAÇÃO
  PÓLO DE INOVAÇÃO EM ENGENHARIA DE POLÍMEROS
- PLASTIFA - PLÁSTICOS TÉCNICOS, LDA
- RELACRE
- REPSOL POLÍMEROS, UNIPESSOAL, LDA
- SMALLMATEK
- SRAMPORT
- UBI
- ULTRAPRECISÃO LDA
- UNIVERSIDADE DE AVEIRO/CICECO
- VISTA ALEGRE ATLANTIS SA

AM2R CONSORTIUM

Polisport
Hydro
SANTIAGO & TAVARES, LDA
ABIMOTA
IBÉRICA INDÚSTRIA DE COMPONENTES METÁLICOS, S.A
SisTrade
AJ Maias
incycles bike group
SRAM
Bike Valley Services
inegi driving science & innovation
TMG TEXTILES
BICIWAY
INTERBIKE OEM FACTORY
TRIANGLE'S
BIKiNNOV / bikevalueinnovationcenter association
IPCA INSTITUTO POLITÉCNICO DO CÁVADO E DO AVE
RUN REGIONAL UNIVERSITY NETWORK EUROPEAN UNIVERSITY
universidade de aveiro theoria poiesis praxis
CARBONTEAM
light mobie
1290 UNIVERSIDADE D COIMBRA
castros
santos
wavecom
centi
mhsi
CF CICLO FAPRIL Metal works.
MIKRALTEK PERFIS TÉCNICOS E DE PRECISÃO
citeve TEXTILE TECHNOLOGY
Miranda The European Bike Fundamentals.
DURIT METALDURO
Polinter plastics
edmtech
Rangel LOGISTICS SOLUTIONS
Europa Coatings
DECATHLON
FABCAST YOUR ALUMINIUM PART
RODI industries
fig plásticos
sangal E-bike Manufacturing, Lda.

SPM
SOCIEDADE PORTUGUESA de MATERIAIS

CONTACTOS

www.spmateriais.pt
comunicacao@spmateriais.pt
965 756 172